

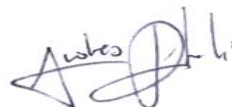
UNIVERSITÀ VITA-SALUTE SAN RAFFAELE

**CORSO DI DOTTORATO DI RICERCA INTERNAZIONALE
IN MEDICINA MOLECOLARE**

Curriculum in Cellular and Molecular biology

Precise characterization
of hemogenic endothelial cells
during human hematopoietic development

DoS: Dr. Andrea Ditadi



Second Supervisor: Dr. David Wilkinson

Tesi di DOTTORATO DI RICERCA di Rebecca Scarfò

Matr. 013833

Ciclo di dottorato XXXIV

SSD: BIO/13

Anno Accademico 2020/2021

CONSULTAZIONE TESI DI DOTTORATO DI RICERCA

La sottoscritta

Nome/Name: Rebecca Cognome/Surname: Scarfò

n° matr./Id number: 013833

nata a /Place of Birth: Tortona (AL)

il (Date of Birth) 05/08/1993

/autore della tesi di Dottorato di Ricerca dal titolo /author of the PhD thesis entitled:
Precise characterization of hemogenic endothelial cells during human hematopoietic
development

NON AUTORIZZA/ DOES NOT AUTHORIZE

La consultabilità della tesi non è autorizzata per 12 mesi a partire dalla data di conseguimento del titolo e precisamente dal 08/04/2022 al 08/04/2023 poiché:

The Consultation of the thesis is not allowed for 12 months from the PhD thesis date, specifically from 16/04/2021 to 16/04/2022 because:

X l'intera ricerca o parti di essa sono potenzialmente soggette a brevettabilità/ The whole project or part of it might be subject to patentability;

la tesi è finanziata da enti esterni che vantano dei diritti su di esse e sulla loro ci sono parti di tesi che sono già state sottoposte a un editore o sono in attesa di pubblicazione/ Parts of the thesis have already been submitted to a publisher or are in press;

la tesi è finanziata da enti esterni che vantano dei diritti su di esse e sulla loro pubblicazione/ the thesis project is financed by external bodies that have rights over it and on its publication.

È fatto divieto di riprodurre, in tutto o in parte, quanto in essa contenuto /It is not allowed to copy, in whole or in part, the data and the contents of the thesis

Data 15/03/2022

Firma



Declaration

This thesis has been composed by myself and has not been used in any previous application for a degree. Throughout the text I use both 'I' and 'We' interchangeably. All the results presented here were obtained by myself, except for:

1) Isolation, immuno-staining analysis of YS and AGM isolated from CS13 human embryos processing and RNA sequencing of ACE⁺ and ACE^{neg} cells derived from CS13 human embryos, (Results, Paragraph 3.1, Figure 18a, 19, 20), were performed in collaboration with Dr. Manuela Tavian, Inserm, Strasbourg, France.

2) Single-cell RNA sequencing of mesodermal populations isolated at day 3 of WNT-dependent hematopoietic differentiation and murine xenografts experiments (Appendix to main result (I), Paragraph 7.1, Figure 34, 37) were performed in collaboration with Dr. Christopher Sturgeon, Icahn School of Medicine at Mount Sinai, New York.

Fair Use Disclaimer: the figures used in the introduction of this thesis are under fair use as defined under section 107 of the US Copyright Act of 1976 and according to Italian Law n. 68 of April 9th, 2003 «Attuazione della direttiva 2001/29/CE sull'armonizzazione di taluni aspetti del diritto d'autore e dei diritti connessi nella società dell'informazione». All rights and credit go directly to their rightful owners. No copyright infringement is intended.

All sources of information are acknowledged by means of reference.

Abstract

During embryonic development, blood cells emerge from a subset of specialized endothelial cells, named hemogenic endothelium (HE), via a process known as endothelial-to-hematopoietic transition (EHT). HE represents a heterogeneous population found in various anatomical sites, including the yolk sac (YS) and the aorta-gonad-mesonephros (AGM). It comprises cells that differ in developmental potential, thus defining distinct hematopoietic programs. Despite the endothelial descendancy of blood cells is well established, the identity of HE is still debated. A more thorough characterization of HE is therefore essential to guide the efforts to derive this population from human pluripotent stem cells (hPSCs), a critical step to generate therapeutic blood products *in vitro*. However, current known markers used to isolate HE are insufficient as they also enrich associated arterial cells. To identify specific human HE markers, we performed transcriptomic analysis of 4-5-week-old human embryos, a developmental stage characterized by active EHT. We identified *FCGR2B* encoding for the Fc receptor CD32, previously associated with other specialized endothelia, as enriched gene in the ACE⁺CD34⁺ population that contains HE. Functional *ex vivo* analyses confirmed that multilineage hematopoietic potential is highly enriched in CD32⁺ endothelial cells isolated from the AGM and YS of human embryos. In addition, CD32 emerged as selective marker for hPSC-derived HE across different hematopoietic programs. Remarkably, our analyses showed that CD32 specificity for cells with hemogenic potential is superior to other known HE markers in hPSC-derived hematopoietic cultures. These findings provide a simple method for isolating HE from human embryos and hPSCs, allowing its molecular characterization as well as the efficient generation of hematopoietic cells *in vitro*.

Table of contents

Table of contents	1
Acronyms and abbreviations	4
List of figures and tables.....	8
1. Introduction	11
1.1 Functional assays to evaluate the potential of hematopoietic stem and progenitor cells	13
1.2 The mesodermal origin of the hematopoietic system	15
1.3 Extra-embryonic hematopoiesis.....	16
1.3.1 Primitive wave.....	16
1.3.2 The erythro-myeloid progenitor wave.....	17
1.4 Intra-embryonic hematopoiesis	18
1.4.1 A note on HSC-independent lymphopoiesis	21
1.5 The cellular origin of hematopoiesis: the hemangioblast	24
1.6 The cellular origin of hematopoiesis: the hemogenic endothelium.....	26
1.6.1 The endothelial to hematopoietic transition	28
1.6.2 The heterogeneity of the HE during embryonic development	32
1.7 Molecular regulators involved in the EHT	35
1.8 Signaling pathways involved in EHT: Notch.....	42
1.9 Signaling pathways involved in EHT: Retinoic Acid	48
1.10 Immuno-phenotypical identification of the HE	52
1.10.1 Runx1+ 23.....	53
1.10.2 Ly6A.....	53

1.10.3 CD44	55
1.10.4 Lyve1	56
1.10.5 ACE	57
1.11 Modeling human hematopoiesis in a dish.....	58
2. Aim of the work	64
3. Results	65
3.1 CD32 is differentially expressed in human embryonic endothelial cells with hemogenic potential65	
3.2 CD32 distinguishes a population with hemogenic fate in CS13 human embryos	70
3.3 CD32 is expressed in hPSC-derived HE	75
3.4 CD32 ⁺ DLL4 ^{neg} cells generate erythroid and myeloid progenitors.....	77
3.5 CD32 ⁺ DLL4 ^{neg} cells are enriched for NK lymphoid progenitors in WNT-independent hematopoietic culture	79
3.6 CD32 ⁺ DLL4 ^{neg} cells give rise to NK and T lymphoid progenitors in WNT-dependent hematopoietic culture	81
3.7 Clonal analysis of CD32 ⁺ DLL4 ^{neg} hemogenic potential	82
3.8 Evaluating CD32 as HE marker in mouse.....	86
4. Discussion.....	89
5. Materials and methods	98
5.1 Human embryonic tissues	98
5.2 Immunohistochemistry and immunofluorescence	98
5.3 RNA sequencing data analysis	99
5.3.1 Public single-cell RNA-seq datasets visualization.....	100
5.4 Murine embryonic fibroblasts	100

5.5 Human embryonic stem cells	101
5.6 Hematopoietic differentiation.....	101
5.6.1 Aldefluor assay	102
5.6.2 Mesoderm isolation and RA treatment.....	102
5.7 OP9DLL4 or OP9DLL1 co-culture for T and NK lineage differentiation.....	102
5.8 T- and NK lineage differentiation	103
5.9 Colony forming cell assay	104
5.10 Multilineage clonal assay	104
5.11 Mouse embryonic tissues.....	105
5.12 Murine xenografts	105
5.13 Multilineage assay from murine samples.....	106
5.14 Gene expression analysis by quantitative real-time PCR	106
5.15 Cell staining, flow cytometry and cell sorting.....	106
5.16 Ethical statement.....	107
5.17 Table 1: Antibodies list	108
6 Appendix to main results (I).....	109
6.1 Mesodermal activation of RA pathway triggers a distinct WNT-dependent hematopoietic wave from hPSCs	109
7. Appendix to main results (II)	118
7.1 Immuno-phenotypic EMPs display lymphoid potential in E9.5 murine YS	118
8. References	122

Acronyms and abbreviations

Angiotensinogen (AGT)

Aorta-gonad mesonephros (AGM)

Burst-forming units-erythroid (BFU-E)

Blast colony formic cell (BL-CFC)

Bone morphogenic protein (BMP)

Bone marrow (BM)

Brachiury (Bry)

Carnegie Stage (CS)

Central nervous system (CNS)

Chromatin immuno-precipitation (ChIP)

Colony-forming cell (CFC)

Colony-forming unit-erythroid (CFU-E)

Colony-forming unit-granulocytes (CFU-G)

Colony-forming unit-granulocytes/macrophages (CFU-GM)

Colony-forming unit-megakaryocytes (CFU-Mk)

Colony-forming unit-granulocytes, erythrocytes, macrophages, megakaryocytes (CFU-GEMM)

Cyclic guanosine monophosphate (cGMP)

Days post coitum (dpc)

Differentially expressed genes (DEGs)

Dorsal aorta (DA)

Embryo equivalent (e.e.)

Embryonic day (E)

Embyo equivalent (e.e.)

Endothelium (E)

Endothelial nitric oxide synthetase (eNOS)

Endothelial-to-hematopoietic transition (EHT)

Erythro-myeloid progenitor (EMP)

Fetal liver (FL)

Fibroblast growth factor (FGF)

Fluorescence minus one (FMO)

Galactosidase (gal)

Gene ontology (GO)

Gene Set Enrichment Analysis (GSEA)

Glycogen synthase kinase 3 (GSK3)

Green fluorescent protein (GFP)

Hematopoietic stem cell (HSC)

Hematopoietic stem and progenitor cell (HSPC)

Hemogenic endothelium (HE)

Hours post fertilization (h.p.f.)

HSC precursor (Pre-Hsc)

Human embryonic stem cell (hESC)

Immunoglobulin type (?) G (IgG)

Intra-aortic hematopoietic clusters (IAHCs)

Kilobase (kb)

Kit-ligand (Kitl)

Liver sinusoidal endothelial cells (LSEC)

Lymphoid tissue inducer cell (LTi)

Lymphoid-primed multipotent progenitor (LMPP)

Molecular Signatures Database (MSigDB)

Mouse embryonic stem cell (mESC)

Natural killer lymphoid cell (NK)

Nitric oxide (NO)

Notch intracellular domain (NICD)

Para-aortic splanchnopleura (P-Sp)

Primitive streak (PS)

Renin (REN)

Renin-angiotensin system (RAS)

Retinoic Acid (RA)

single cells RNA sequencing (scRNA seq)

Spleen colony forming cell (CFU-S)

SRY-related HMG-box (SOX)

T cell acute leukemia gene 1 (Tal1)

Tumor necrosis factor alpha (TNF α)

Tumor necrosis factor receptor (Tnfr2)

Umbilical artery (UA)

Vascular endothelial growth factor receptor 2 (VEGFR2/KDR)

VE-cadherin (VE-cad)

Vitelline artery (VA)

Yolk sac (YS)

List of figures and tables

Figure 1 – Different models of hematopoietic hierarchy	11
Figure 2 – Patterning of mesoderm during gastrulation.....	16
Figure 3 – Dynamics of hematopoietic development in the murine embryo.....	19
Figure 4- The aortic region of the AGM, vitelline and umbilical arteries have HSC activity at E10.5	21
Figure 5 – The hematopoietic development in mouse, human and zebrafish embryos	24
Figure 6 – The hemangioblast development in vitro and in vivo	26
Figure 7 – Hematopoietic cells originate from the HE during zebrafish embryonic development	29
Figure 8 - Hematopoietic cells originate from the HE during murine embryonic development	30
Figure 9 – The HE and hemangioblast models	32
Figure 10 – Three-dimensional mapping of hematopoietic clusters in the mouse embryo	35
Figure 11 – The gene regulatory network in the HE.....	40
Figure 12 – The Notch pathway	44
Figure 13 - Formation of IAHCs involves Notch signaling.....	46
Figure 14 – RA signaling pathway	50
Figure 15 – Raldh2-mediated RA synthesis is essential for HSC emergence from the AGM.....	51
Figure 16 – Scheme of in vitro hematopoietic differentiation from hPSCs	61
Figure 17 - CD34 ⁺ CD43 ^{neg} CD73 ^{neg} CD184 ^{neg} cells show HE potential from hPSCs	63

Figure 18 – ACE tracks RUNX1 ⁺ cells in the AGM of CS13 human embryos but does not enrich hPSC-derived HE	66
Figure 19 – ACE-expressing cells enrich the expression of arterial and hematopoietic genes.....	67
Figure 20 – Top 10 differentially expressed genes on HEC versus EC.....	69
Figure 21 – CD32 is expressed in extra- and intra-embryonic hematopoietic sites of CS13 human embryos	70
Figure 22 – Flow cytometry analysis of CD32 expression in CS13 human embryo .	71
Figure 23 – CD32 ^{+/neg} endothelial populations show lymphoid potential in ex vivo cultures.....	73
Figure 24 – CD32 ⁺ endothelial cells display clonogenic potential	75
Figure 25 – CD32 is expressed within the hPSC-derived WNT-dependent or WNT-independent CD34 ⁺ CD43 ^{neg} CD184 ^{neg} CD73 ^{neg} DLL4 ^{neg} population.	76
Figure 26 – hPSC-derived CD32 ⁺ endothelial cells give rise to erythroid and myeloid progenitors	78
Figure 27 – hPSC-derived CD32 ⁺ endothelial cells give rise to NK lymphoid progenitors in WNT-independent hematopoietic cultures.....	80
Figure 28 – hPSC-derived CD32 ⁺ endothelial cells give rise to NK and T lymphoid progenitors in WNT-dependent hematopoietic cultures	82
Figure 29 – Quantification of the frequency of HE cells within hPSC-derived CD32 ⁺ endothelial population	84
Figure 30 – Analysis of CD44 as hPSC-derived HE marker.....	86
Figure 31 – Fc _γ 3 is expressed in endothelial populations of E6.5-E9.5 mouse embryos	86
Figure 32 - Evaluating CD16/32 as HE marker in mouse embryos.....	88
Figure 33 – WNT-dependent CD184 ⁺ mesoderm shows ALDH activity.....	111

Figure 34 – scRNA-seq analysis of WNT-independent and WNT-dependent cultures at day 3 of differentiation	112
Figure 35 – CD184 ^{+/neg} mesodermal populations generate CD34 ⁺ CD43 ^{neg} endothelial cells	113
Figure 36 – RA-treatment of CD184 ⁺ mesoderm allows the emergence of RAd hemogenic potential.....	114
Figure 37 – RA signaling activation at mesodermal level generates CD34 ⁺ cells with engrafting potential	115
Figure 38 – Modulation of TGFβ, Notch and AHR signaling pathways influence ALDH activity within WNT-dependent CD184 ⁺ mesoderm.	117
Figure 39 – YS E9.5 Kit ⁺ CD41 ⁺ CD16/32 ⁺ SCA1 ^{neg} (EMP) cells display erythroid, myeloid, and T-lymphoid potential	119
Figure 40 – Clonal analysis of T lymphoid potential within E9.5 KIT ⁺ CD41 ⁺ CD16/32 ⁺ SCA1 ^{neg} population	121

1. Introduction

The term hematopoiesis refers to the production of blood cells and in particular the process through which hematopoietic stem cells (HSCs) originate a wide repertoire of specialized blood cells that support the needs of the body through life. For instance, platelets regulate homeostasis, erythrocytes oxygenate the tissues, innate and adaptive immune cells protect the body from attacks by exogenous pathogens. In adult mammals, hematopoiesis occurs in the bone marrow (BM) where HSCs reside and undergo the processes of self-renewal and differentiation supplying blood cells throughout life.

For long time, the generation of blood cells from HSCs has been reported to follow a rigid hierarchical model (Kondo *et al*, 1997; Akashi *et al*, 2000). At the top, limited numbers of HSCs self-renew or differentiate in response to environmental cues. Their differentiation gives rise to committed hematopoietic progenitors with progressively reduced potential that will ultimately generate uni-lineage progenitors following a series of dual decisions (Figure 1 a). However, evidence obtained by more advanced technologies, as lineage tracing and single-cell transcriptomics, point to a continuum of differentiation, a more plastic model able to adapt to the changing needs of blood demand (Laurenti & Göttgens, 2018; Baron & Oudenaarden, 2019) (Figure 1 b).

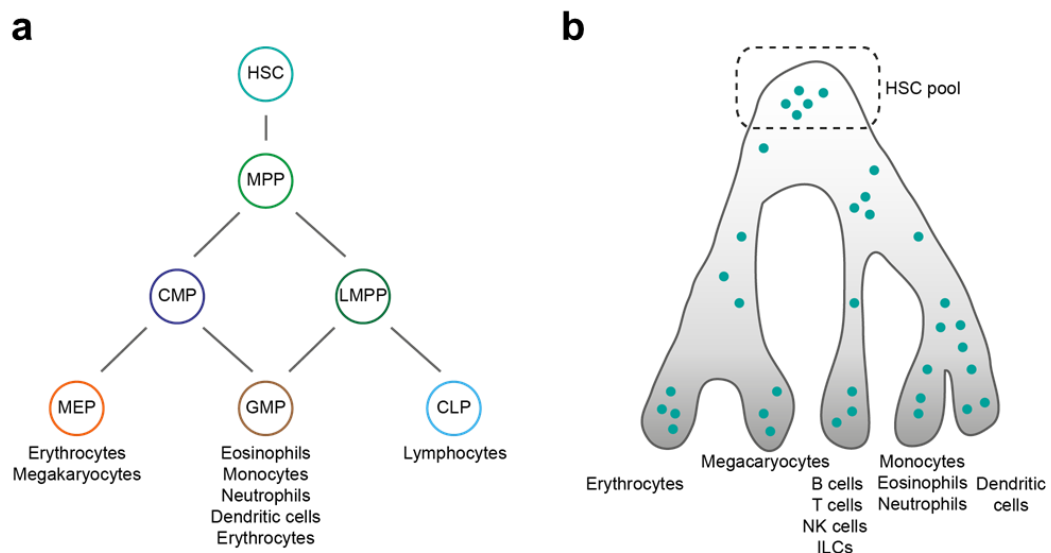


Figure 1 – Different models of hematopoietic hierarchy

a) Classical tree-like organization of hematopoiesis. HSCs at the top give rise to the different hematopoietic progenitors with progressively reduced potential (from the top: multipotent progenitors (MPP); common myeloid progenitors (CMP) and lymphoid-myeloid primed progenitors (LMPP), megakaryocyte-erythrocyte progenitors (MEP), granulocyte-macrophage progenitors (GMP), common lymphoid progenitors (CLP)) b) Recent single cell-transcriptomic analysis and lineage tracing pointed out a continuum of differentiation from the HSC pool. Each green dot represents a single cell and its position along the differentiation trajectory. The figure was re-drawn from (Laurenti & Göttgens, 2018).

Because of their features, especially the extraordinary regenerative capacity, HSCs represent a successfully established therapy for patients with different hematopoietic disorders including BM failures. However, the limited availability of immunologically matched donors and the frequent immune rejection of transplanted cells impair the success of allogenic HSC transplants. On the other hand, the possibility to perform autologous transplantation of HSCs may overcome this issue.

In this context, the advent of induced pluripotent stem cells (iPSCs) technology made the employment of autologous HSCs *ex vivo* as a more concrete possibility for the treatment congenital BM disorders, albeit still unsuccessful. Indeed, the generation of engrafting HSCs from human pluripotent stem cells (hPSCs) remains elusive. Only the enforced overexpression of a specific set of transcription factors led to HSC generation *in vitro* (Sugimura *et al*, 2017). However, many of the transcription factors overexpressed are proto-oncogenes that might lead to malignant transformations making them unsafe for clinical use. A safer approach would be recapitulating the stepwise specification of HSC from hPSCs *in vitro* as it occurs during embryonic development, mirroring what evolution has shaped as an efficient process.

To this extent, *in vivo* studies, mainly performed on zebrafish and mouse models, have provided extensive knowledge about the mechanisms of HSC emergence (Mikkola & Orkin, 2006; Paik & Zon, 2010; Costa *et al*, 2012; Ditadi *et al*, 2016; Ivanovs *et al*, 2017; Bruijn & Dzierzak, 2017), which by large have turned out to be conserved across species. Moreover, these models pointed out the complexity of blood cells development in the embryo, that is not limited to HSCs but includes several HSC-independent hematopoietic progenitors that emerge during embryonic development and persist in the adult contributing to the homeostasis and protection of our body. The structural complexity and the functional heterogeneity of the hematopoietic system during embryonic development will be the main topic of the next paragraphs with particular attention on the cellular origin of hematopoietic

cells. Mouse and zebrafish models will be taken as reference to dissect the hematopoietic development since similar processes appear conserved in humans.

1.1 Functional assays to evaluate the potential of hematopoietic stem and progenitor cells

Before introducing how the hematopoietic development is structured, I will briefly describe the functional assays that have been, and to some extents still are, used to identify HSCs or other hematopoietic progenitors.

In 1950s-1960s, two major assays to study the potential of hematopoietic stem and progenitor cells were developed: the *in vitro* culture of BM hematopoietic cells based on semi-solid media supplemented with cytokines to monitor the hematopoietic potential (Bradley & Metcalf, 1966), and the *in vivo* transplantation into irradiated recipients (FORD *et al*, 1956; MCCULLOCH & TILL, 1960; Szilvassy *et al*, 1990). Till and McCulloch firstly described spleen colony forming cells (CFU-s) as a functional assay to quantify the proliferative and the lineage potential of multipotent hematopoietic stem and progenitor cells (HSPCs). In fact, murine HSPCs form multilineage hematopoietic colonies in the spleen of transplanted irradiated animals and a single CFU-s can produce more CFU-s (MCCULLOCH & TILL, 1960; Siminovitch *et al*, 1963). Despite these assays have been subsequently modified and refined, they set the gold standard for define the HSCs biology.

By definition, HSCs are characterized by unlimited self-renewal and multilineage differentiation ability (Osawa *et al*, 1996). These intrinsic characteristics distinguish HSCs from all the other hematopoietic progenitors generated through embryonic development. Therefore, functional HSCs are defined as cells that can contribute to long term (greater than 16 weeks) multilineage hematopoiesis when transplanted into immune-compromised (usually conditioned *via* irradiation) mice (primary recipients). A more stringent definition of HSCs requires that the BM isolated from primary recipients allows long term multilineage reconstitution of irradiated secondary recipients. At present, the combination of primary and secondary transplants into adult recipient constitutes the gold-standard assay to test HSC functionality. However, it is worth to note that adult and embryonic HSCs show a different repopulation potential. In fact, adult BM-derived HSCs repopulate adult recipients at higher frequency than neonatal recipients, while early embryonic HSCs

better reconstitute neonatal recipients (Yoder & Hiatt, 1997; Arora *et al*, 2014). This is likely due to differences between the adult and neonatal BM niche, with the latter providing a more suitable environment to complete the full maturation of embryonic HSCs. In addition, the lack of engrafting potential of embryonic HSCs in adult recipients might be mediated by host-derived NK response that targets the embryonic cells that mildly express major histocompatibility complex (MHC) class I on their surface (Ozato *et al*, 1985; Jaffe *et al*, 1991; Cumano *et al*, 2001). Alternatively, early embryonic HSCs can be further coaxed to progress into their maturation *via ex vivo* cocultures prior to *in vivo* transplantation, thus bypassing the requirement of neonatal recipients (Cumano *et al*, 2001).

In addition to *in vivo* assays, *in vitro* systems are used to qualitatively identify the lineage potential of HSPCs. Although they do not allow the detection of functional HSCs (that strictly relies on *in vivo* transplantation experiments), I will introduce the colony-forming cell (CFC) assay to provide a complete picture of the assays commonly used measure the frequency and the lineage potential of hematopoietic progenitors *in vitro*. The CFC assay consists of culturing a given tissue or cell population in a semi-solid methylcellulose-based media that supports the growth of single hematopoietic clones. CFCs mostly consist of uni-lineage colonies as burst-forming units-erythroid (BFU-E), immature precursor of colony-forming units-erythroid (CFU-E), CFU-granulocytes (CFU-G), CFU-macrophages (CFU-M), CFU-megakaryocytes (CFU-Mk) and CFU-granulocytes/macrophages (CFU-GM). While bi-lineage CFCs can be also observed, real multipotent CFCs composed by CFU-granulocytes, erythroid, macrophages and megakaryocytes (CFU-GEMM) are rare.

Despite CFC assay can also be used to assess the lymphoid potential *in vitro* (Lacaud *et al*, 1998), specialized co-culture systems are preferred since allow a more reliable, simple and efficient evaluation of lymphoid-specific lineages. The *in vitro* lymphoid culture methods will be extensively treated in the section 1.4.1: "A note on HSC-independent lymphopoiesis".

Having in mind the assays to evaluate the potential of hematopoietic progenitors and HSCs, we can move forward to dissect the embryonic hematopoietic development.

1.2 The mesodermal origin of the hematopoietic system

In mammalian and non-mammalian vertebrates, the first steps of hematopoietic commitment can be traced back to gastrulation, the process through which an embryo at blastula stage exits the pluripotency and establishes the basis for the future body plan (Sadler & Langman, 2004). During this process, the epiblast, a thin sheet of primitive ectodermal cells, gives rise to three embryonic layers (mesoderm, endoderm and ectoderm) from which all the tissues of the embryo proper originate. In the mouse, by embryonic day (E) 6 the epiblast cells converge into the posterior pole of the embryo to form the primitive streak (PS) (Figure 2 a). Epiblast cells ingress the PS and undergo an epithelial-mesenchymal transition (EMT) to form mesodermal and endodermal lineages. The site and the time of ingression of epiblast cells into the PS determines their fate. For instance, the first mesodermal progenitors enter in the most posterior part of the PS and then form the yolk sac (YS) extra-embryonic mesoderm (Kinder *et al*, 1999) (Figure 2 b). Here, part of these cells will differentiate into YS blood islands where the first hematopoietic cells originate (Lawson *et al*, 1991). On the other hand, epiblast cells that migrate into the middle region form the splanchnic or lateral plate mesoderm, which will generate intra-embryonic regions such as the aorta-gonad mesonephros (AGM) in which other hematopoietic progenitors, including HSCs, will emerge (Medvinsky *et al*, 1993; Medvinsky & Dzierzak, 1996; Bruijn *et al*, 2000).

Therefore, during embryonic development multiple hematopoietic waves originate blood cells both outside (Palis *et al*, 1999; Lux *et al*, 2008; Bertrand & Traver, 2009; Frame *et al*, 2016) and inside the embryo (Bruijn *et al*, 2000; Bertrand *et al*, 2008, 2005, 2010a; Boisset *et al*, 2010; Kissa & Herbomel, 2010). Temporally, the onset of the extra-embryonic hematopoietic program in the YS precedes that of intra-embryonic hematopoiesis. This spatial and temporal distinction translates into the exposure of mesodermal cells to different signaling hubs. Consequently, distinct hematopoietic waves yield hematopoietic progenitors with different function and potential. We will now cover more specifically the different hematopoietic output of the different ingression of epiblast cells through the PS and the successive migration to different locations.

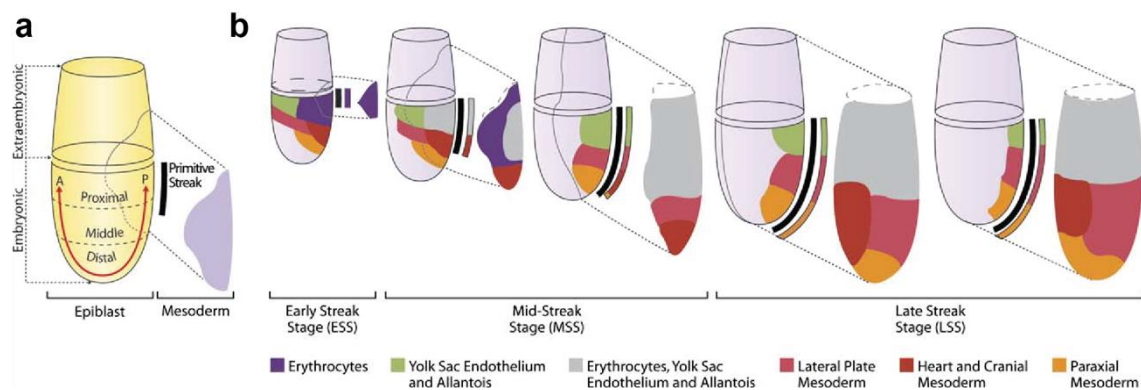


Figure 2 – Patterning of mesoderm during gastrulation

From (Baron, 2005), *Experimental Hematology*, 2005. a) In early post-implantation embryo, the reciprocal signaling between embryonic and extraembryonic lineages allows morphogenic changes and the establishment of the anterior-posterior axis (A-P, red arrow). Mesoderm is generated from the primitive streak (PS, black bar) in the posterior epiblast. b) Fate maps showing the location of mesodermal progenitors during development: epiblast (purple), PS (black bar), mesodermal layers (different fate corresponds to a different color). Mesodermal cells migrate posteriorly to contribute to extra-embryonic hematopoiesis. More anterior regions of the PS generate the embryonic mesoderm, migrating laterally and distally.

1.3 Extra-embryonic hematopoiesis

1.3.1 Primitive wave

The first wave of hematopoiesis occurs right after mesodermal cells migrate through the posterior PS (at E6.5-E7.0 in mouse, day 20-21 in human) to form the extra-embryonic region of the YS (Figure 3). The hematopoietic cells are closely associated with vascular endothelial cells in the YS, forming cell aggregates known as YS blood islands. YS blood islands generate megakaryocytes, macrophages and erythrocytes while are devoid of lymphoid and HSC potential (Palis *et al*, 1999; Tober *et al*, 2006, 2008; Squarzoni *et al*, 2014; Palis, 2017) (Figure 3). The defining lineage of this program is represented by erythroid cells. These cells are nucleated and mostly express embryonic globin and some fetal globin. These globin types show an increased oxygen affinity compared to adult globin-types, necessary to offer the oxygen supply to the growing embryo before the onset of the circulation (around E8.25) (Palis *et al*, 1995; Fraser *et al*, 2006; McGrath & Palis, 2008). This first wave of YS erythroid cells was defined as “primitive”, based on their size and nucleation typical of erythrocytes of birds, fish, and reptiles (Palis, 2014). However, in mammals, primitive erythroblasts undergo a tardive enucleation between E12.5 and

E16.5, generating mature primitive red blood cells that persist in the circulation as late as five days after birth (Kingsley *et al*, 2004).

While primitive erythrocytes endure only shortly after birth, macrophages from the primitive hematopoietic wave contribute to the life-long adult hematopoietic compartment as tissue resident macrophages. In fact, *in vivo* fate mapping analysis revealed that microglial cells, a population of tissue resident macrophages of the adult central nervous system (CNS), derive from primitive macrophage progenitors that arise early in murine development and persist in the adult brain (Ginhoux *et al*, 2010). These primitive macrophages emerge before E8 in the YS blood islands (Takahashi *et al*, 1989). After the onset of the circulation at E8.5, primitive macrophages colonize different tissues including the brain in which they differentiate into microglia (Naito *et al*, 1990). Another distinguishing characteristic of these cells is their distinct signaling requirement. In fact, their development is not affected by KIT ligand (KITL) deficiency, which is required for the proliferation and survival of hematopoietic progenitors generated during later hematopoietic waves (Azzoni *et al*, 2018). Remarkably, the embryonic origin of microglia is conserved across different species including zebrafish (Herbomel *et al*, 2001) and avians (Cuadros *et al*, 1993).

1.3.2 The erythro-myeloid progenitor wave

Right after the first wave of primitive hematopoiesis, a second hematopoietic program originates in the YS around E8.5 and comprises erythro-myeloid progenitors (EMP) (Figure 3). Despite an erythro-myeloid-restricted potential was initially ascribed to EMPs, Dege and colleagues have recently shown that these progenitors also display lymphoid potential, giving rise to natural killer (NK) cells (Dege *et al*, 2020). This characteristic distinguishes them from primitive progenitors that are devoid of lymphoid potential. In addition, unlike primitive progenitors, EMPs differentiate into a broader type of myeloid cells, giving rise to macrophages, granulocytes as well as monocytes (Palis *et al*, 1999). Moreover, EMPs generate erythrocytes that express fetal and adult-type of globin and persist through late fetal and peri-natal life (McGrath *et al*, 2011). For this reason, EMPs have been historically described as belonging to *definitive* hematopoiesis (Palis, 2014) to distinguish them from *primitive* erythrocytes that mainly express embryonic globins (Palis *et al*, 1995). However, this definition is misleading, since definitive progenitors would also include HSCs, that, however, do not emerge from the EMP hematopoietic wave. In fact, EMPs

lack long-term engrafting capacity associated to HSCs (McGrath *et al*, 2015). To avoid any confusion, I will refer to this second extra-embryonic hematopoietic program as "EMP wave" while the *definitive* term will be used only to indicate the HSC-dependent hematopoietic wave.

EMPs can be isolated thanks to the expression of a peculiar cell surface marker signature that distinguishes them from HSC-derived and primitive progenitors. In fact, McGrath and colleagues defined E9.5 EMPs by KIT⁺CD41⁺CD16/32⁺SCA1^{neg} cell-surface expression. While CD41 and KIT are ubiquitous hematopoietic markers, CD16/32 is not expressed neither on primitive progenitors nor on HSCs (McGrath *et al*, 2015). The latter are instead characterized by SCA1 (LY6a) expression (Chen *et al*, 2011a), among other markers. Despite the differences in molecular cell surface markers, EMPs and HSCs also differ in the molecular signaling required in the specification of either cell type (*i.e.*, Notch signaling) (Bertrand *et al*, 2010b), subject that will be next discuss in this thesis.

As EMPs arise in the YS concomitantly to the establishment of the circulation, the possibility to specifically isolate YS-derived EMPs allowed to characterize them in detail (McGrath *et al*, 2015). At E10.5 EMPs are detected throughout the peripheral blood and mostly in the fetal liver (FL), the principal site of hematopoietic colonization during embryonic development. Circulating EMPs are detected until E14.5, albeit at low level, suggesting they support the hematopoietic homeostasis before and after the emergence of HSCs that will be discussed in the next paragraphs.

1.4 Intra-embryonic hematopoiesis

While the first two programs of hematopoietic development occur extra-embryonically and give rise to hematopoietic progenitors, the third hematopoietic wave occurs within intra-embryonic hematopoietic sites where the first multilineage, self-renewing HSCs and hematopoietic progenitors emerges.

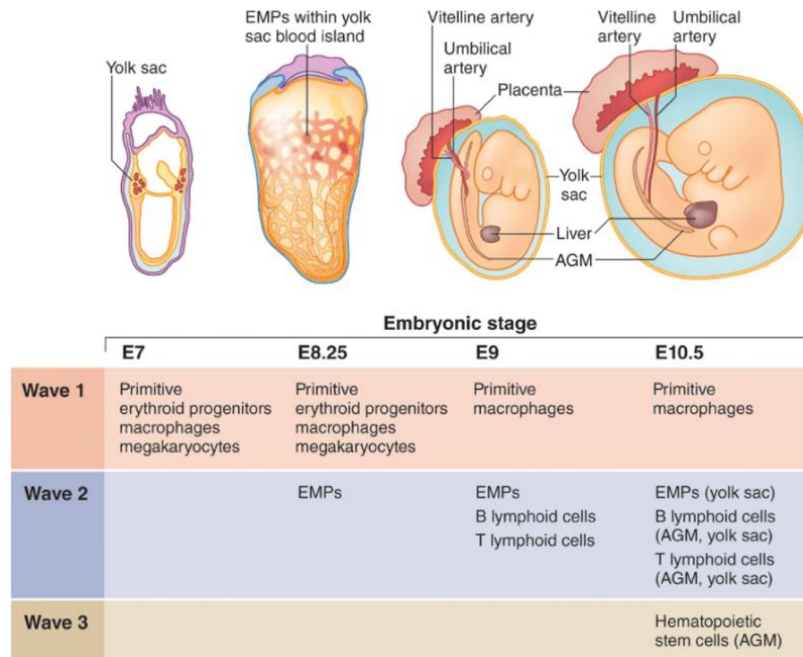


Figure 3 – Dynamics of hematopoietic development in the murine embryo

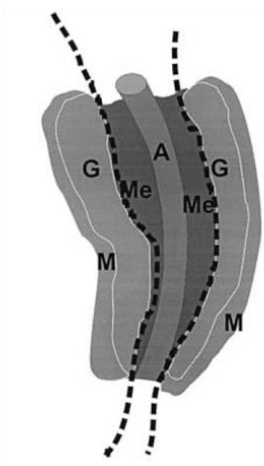
From Yoder *et al*, *Nature Biotechnology*, 2014. *Stages of hematopoietic development. Hematopoiesis starts in the YS with the generation of primitive hematopoietic progenitors (E7). A second wave of extra-embryonic hematopoiesis initially generates erythro-myeloid progenitors (EMPs). Secondly, lymphoid progenitors emerge both in the yolk sac (YS) and in the aorta-gonad-mesonephros (AGM), around E9. Simultaneously to the second wave, the third wave of hematopoiesis generates HSCs at E10.5 in the AGM, umbilical and vitelline arteries and placenta. Finally, HSCs seed the FL that results in a reservoir of hematopoiesis until late gestation when HSCs are mobilized and migrate to the BM. Together with HSC-derived hematopoietic progenitors, also the previous waves contribute to the adult hematopoietic compartment.*

The first HSC arises in the aorta-gonad-mesonephros (AGM) region at E10.5 in mouse embryos (Dieterlen-Lievre, 1975; Medvinsky *et al*, 1993; Müller *et al*, 1994; Medvinsky & Dzierzak, 1996; Bruijn *et al*, 2002) (Figure 3). The Dzierzak group firstly identified the intra-embryonic origin of HSCs by evaluating CFU-s potential of the embryo body from E9.5-E11 murine embryos. The CFU-s potential peaks at 11 days post coitum (dpc) in the axial area of the embryo that includes the AGM while YS and FL show very low CFU-s numbers at similar stage (Medvinsky *et al*, 1993). More precisely, the sub-dissection of the AGM showed that HSCs are initially confined to the dorsal aorta (DA), not emerging from other regions as urogenital ridges (Bruijn *et al*, 2000) (Figure 4 a, b). However, at similar stages other embryonic sites harbor HSC activity: the vitelline artery (VA) that is fused with the DA and connected to the FL, the umbilical arteries (UA) that connect the embryo proper to the placenta (Bruijn

et al, 2000) (Figure 4 c) and the placenta (Gekas *et al*, 2005; Ottersbach & Dzierzak, 2005). Among them, the AGM is the mostly characterized site of HSC emergence while the placental origin of HSCs is still debated. In particular, whether the placenta represents a site for the *de novo* HSC generation or for the homing of HSC generated in other anatomical regions (Gordon-Keylock *et al*, 2013). The picture is complicated by the fact that circulation spreads HSCs generated in different intra-embryonic sites towards other hematopoietic tissues and mostly to the FL which represents the HSC reservoir during mid-gestation stages. For this reason, circulation-deficient (*Ncx1*^{-/-}) murine embryos are useful to study the specific origin of hematopoietic cells (Wakimoto *et al*, 2000; Koushik *et al*, 2001). These embryos bear a null mutation in the *Ncx* gene that encodes for the cardiac Na⁺/Ca²⁺ exchanger. The mutation causes embryonic lethality by E10.5 due to lack of functional heartbeat, circulation and HSC development (Wakimoto *et al*, 2000; Koushik *et al*, 2001). Indeed, blood flow has been shown to be essential for HSC generation (Rhodes *et al*, 2008; Lux *et al*, 2008; North *et al*, 2009; Adamo *et al*, 2009). Therefore, other assays are required to shed the light on the placental origin of HSC.

Eventually, at E17, HSCs start to migrate towards the BM (Christensen *et al*, 2004), the ultimate colonization site of HSCs. Here, HSCs acquire a quiescent state that is maintained in homeostatic conditions (Wilson *et al*, 2008) and will support life-long blood cell production.

a



b**Table I.** HSC activity in directly transplanted and cultured E11 and E12 aorta and UGR

Tissue	Embryo equivalent	No. of mice repopulated/total transplanted ^a	
		E11	E12
Aorta ^c	1	7/17	17/29
	0.3	4/15	1/6
UGR	4.3 ^d	0/3	
	1	0/10	5/26
	0.3	0/9	0/4
AGM	1	7/8	7/9
	0.3	1/6	1/2

^aOnly mice with $\geq 10\%$ donor repopulation in the peripheral blood at 4–9 months after transfer were independent experiments.

^cAorta region: includes surrounding mesenchyme.

^dAn average of 4.3 e.e. were transplanted in two experiments (range 4–5).

c

Tissue	Embryo equivalent	No. of mice repopulated/total transplanted ^a	
		E10.5	E11.5
Vitelline/umbilical	2.5–5	4/35 ^b	
	3		3/7
	1		3/8
	0.3		1/3
	0.1		
AGM	2.5–3	1/12	
	1		4/6
	0.3		3/6
	0.1		1/3
Liver ^c	3	0/3	2/2
	1		2/6
	0.3		1/2

^aWith one exception (see below), only mice with $\geq 10\%$ donor repopulation at 4–7 months after transfer were included as positive. Data are from a total of 12 independent experiments.

^bOne mouse transplanted with 5 e.e. of umbilical arteries was engrafted at high levels (100%) at 3 months post-transplantation, but died before the >4 month bleed could be performed.

^cLiver was used in these experiments as a positive control and thus is not mentioned in the text of the Results.

Figure 4- The aortic region of the AGM, vitelline and umbilical arteries have HSC activity at E10.5

Adapted from de Bruijn *et al*, *The EMBO Journal*, 2000. a) Schematic plot of E11 and E12 AGM dissection along the dotted lines. Aorta (A) and mesenchyme (Me) are separated from the urogenital ridges (G) that include the developing gonads and pro/mesonephroi (M). b) Table showing the results of the direct transplantation of 1 or 0.3 embryo equivalents (e.e.) of E11 aorta and mesenchyme or UGR in irradiated recipients. Engrafting samples were detected by peripheral blood analysis after 4–9 months. c) Table showing the results of the direct transplantation of 2.5–5 e.e. of E10.5 or E11.5 vitelline/umbilical arteries, AGM and liver (positive control) in irradiated recipients. Engrafting samples were detected by peripheral blood analysis after 4–7 months.

1.4.1 A note on HSC-independent lymphopoiesis

The establishment of lymphoid potential has been historically associated to the emergence of HSC. For this reason, in the attempt to find the site of HSC development, lymphoid potential has been extensively characterized within extra- or intra-embryonic hematopoietic sites (Cumano *et al*, 1996, 2001; Kennedy *et al*,

2012). Functional studies to assess lymphoid potential of specific embryonic tissues have been mostly performed *in vitro* by coculturing on stromal cell lines as OP9.

OP9 stromal cells derive from the bone marrow (BM) of OP/OP mice that lack the macrophage-colony stimulating factor (M-CSF) (Yoshida *et al*, 1990). As such, OP9 cells do not support myeloid cell development and expansion, but rather sustain the early stages of lymphopoiesis (Yoshida *et al*, 1990). In addition, the overexpression of Notch ligand DLL1 or DLL4 promotes T cell at the expense of B cell differentiation (Schmitt *et al*, 2004; Holmes & Zúñiga-Pflücker, 2009). Before OP9 became the “elected” cell line to test lymphoid potential, other stromal cell lines have been used, such as S17 stromal cells which extensively support B-lymphopoiesis and myelopoiesis (Collins & Dorshkind, 1987).

To investigate the lymphoid potential of specific embryonic regions, Cumano and coworkers isolated YS and paraaortic splanchnopleura (P-Sp, from which AGM will derive at later stages of development) tissues that were then cocultured as *ex vivo* explants on S17 stromal cells in a cytokine-supplemented medium. They observed that before the establishment of the circulation, E7.5-E8.5 YS explants lack lymphoid potential whereas P-Sp at the same stages generates both multipotent myeloid and lymphoid progenitors *ex vivo*. However, these embryonic hematopoietic cells could not reconstitute adult wild-type recipients (Cumano *et al*, 1996). To favor the emergence and engraftment of lymphoid progenitors, the same group performed similar experiment transplanting YS or P-Sp derived cells into irradiated Rag2^{neg/neg} and Rag2^{γc^{neg/neg}} immunocompromised recipients. Both models lack a mature lymphoid compartment, and the latter fails to develop NK cells that may target MHC class I-low embryonic donor cells. In detail, isolated E7.5-E8.5 YS and P-Sp were cultured for 4 days *ex vivo* without the support of stromal cells or exogenous growth factors and then transplanted into irradiated recipients. YS explants display short term myeloid reconstitution but lack lymphoid potential and long term multilineage reconstitution *in vivo*. On the other hand, the P-Sp explants provide long term multilineage engrafting (including B and T lymphoid cells), suggesting the P-Sp as site of HSC emergence and not the YS (Cumano *et al*, 2001). These and other experiments (Nishikawa *et al*, 1998b) suggest the possibility that lymphoid potential exist before and independently from HSC emergence. Nevertheless, the temporal and anatomical identification of lymphoid potential remained controversial and particularly confounded by the onset of circulation.

To shed the light on this, the study of hematopoietic development in *Ncx1*-deficient embryos was critical. Despite the lack of HCSs, these embryos preserve early waves of hematopoietic development, confirming the existence of a HSC-independent hematopoiesis (Fraser *et al*, 2002; McGrath *et al*, 2015; Lux *et al*, 2008). Taking advantage of this model, Yoder group demonstrated that E9.5 YS and P-Sp give rise HSC-independent B and T lymphocytes that can also be transplanted and used for adoptive transfer (Yoshimoto *et al*, 2011, 2012). Interestingly, lineage tracing experiments have shown that embryonic-derived lymphocytes persist in the adult hematopoietic system where they represent the first-line defense against non-self-pathogens in peripheral tissues (Haas *et al*, 2012; Gentek *et al*, 2018; Sandrock *et al*, 2018). Recent studies in zebrafish further support the existence of a HSC-independent lymphoid potential (Tian *et al*, 2017). Despite the emergence of early embryonic lymphoid potential is generally accepted, the ontogeny of early embryonic lymphocytes is still under discussion. Indeed, major studies of the field support the existence of an immuno-restricted progenitor with lymphoid potential (Böiers *et al*, 2013) or of a transient fetal-restricted HSC (Beaudin *et al*, 2016; Kristiansen *et al*, 2016; Elsaid *et al*, 2020). Nevertheless, these data support the onset of specialized lymphoid progenitors within extra- and intra-embryonic tissues before the emergence of HSC.

In conclusion different overlapping hematopoietic waves generate hematopoietic progenitors and stem cells that, thanks to the blood flow, migrate into different anatomical locations and to the FL, where they proliferate and expand before colonizing other hematopoietic tissues where they remain throughout life. A summary of the different anatomical sites and timing of hematopoietic development in the mostly characterized model organisms is depicted in Figure 5. The rarity of these populations in early development and their frequent overlapping potential hampers the complete characterization and dissection of HSC-independent and -dependent programs. In the attempt to resolve the heterogeneity of hematopoietic development, the cellular origin of HSPCs and the mechanisms involved in cellular fate acquisition will be discussed in the next paragraphs.

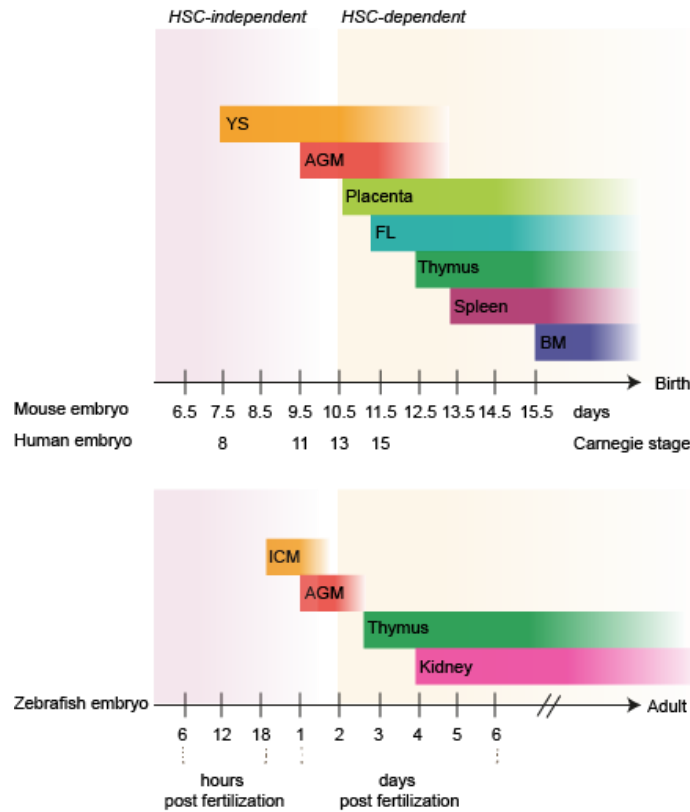


Figure 5 – The hematopoietic development in mouse, human and zebrafish embryos

The graph shows a schematic representation of the time and location of hematopoietic development in mouse, human and zebrafish embryos. In mouse and human embryos, the time of development is depicted in days. Hours (6-18) and days (1-6) post fertilization are reported for zebrafish development. YS, yolk sac; AGM, aorta-gonad-mesonephros; FL, fetal liver; BM, bone marrow; ICM, intermediate cell mass; DA, dorsal aorta. Light red and yellow backgrounds indicate the switch from HSC-independent and -dependent hematopoiesis.

1.5 The cellular origin of hematopoiesis: the hemangioblast

As mentioned, the onset of the hematopoietic system begins during gastrulation when the mesodermal layer derives several cellular lineages including hematopoietic endothelial cells. For long time, the common mesodermal source of hematopoietic and endothelial cells prompted the idea of a common progenitor for both lineages defined as "hemangioblast". In 1932, Murray coined the word "hemangioblast" starting from a similar concept introduced more than a decade before (Sabin, 1920), to define the cell of origin of the endothelial and hematopoietic cells observed in the YS blood islands (Murray, 1932). Murray hypothesized the existence of cells with bi-lineage potential able to give rise to both blood and endothelial cells. Later, Choi and colleagues observed that differentiating mouse embryonic stem cells (mESCs)

contain a unique population that, when placed in methylcellulose in presence of vascular endothelial growth factor (VEGF), gave rise to blast colony forming cells (BL-CFCs) (Choi *et al*, 1998). These BL-CFCs could be individually coaxed to generate both hematopoietic and endothelial cells at the clonal level *in vitro* (Figure 6). Therefore, BL-CFCs were thought to represent the *in vitro* confirmation of the existence of the hemangioblast.

Some years later, the same group showed the presence of the hemangioblast as a bipotent progenitor in gastrulating mouse embryos (Huber *et al*, 2004). In detail, they isolated cells from E7.0-E7.5 embryos, containing both the presumptive YS and embryo proper, and they cultured them *ex vivo* in presence of hematopoietic and vascular cytokines. After few days in culture, single embryo-derived colonies generated both adherent cells, expressing endothelial and smooth muscle markers, and non-adherent cells, expressing hematopoietic genes. The embryo-derived colonies resemble the BL-CFCs derived from mESCs *in vitro* (Figure 6), thus confirming their existence *in vivo*. They both originate myeloid and erythroid cells, the latter expressing embryonic and/or adult type globin. Moreover, they showed that embryo-derived hemangioblasts differentiate from cells expressing the mesodermal markers Brachyury (Bry) (Willison, 1990) and the vascular endothelial growth factor receptor 2 (VEGFR2 or KDR) (Motoike *et al*, 2003) and mainly emerge from the posterior PS in a narrow developmental window. Therefore, they proposed the hemangioblasts as a transient population *in vivo*, that peaks at the late streak/early neural plate stage, and rapidly differentiate into lineage restricted progenitors migrating towards other regions as the YS.

However, the hemangioblasts origin of hematopoiesis is still controversial. Indeed, *in vivo* clonal lineage tracing studies showed that most YS blood island clones contained either hematopoietic or vascular cells and only few bilineage clones (Padrón-Barthe *et al*, 2014; Kinder *et al*, 1999; Vogeli *et al*, 2006). It must be pointed out that these studies are not formally disputing the existence of the hemangioblast, as they are only proving that the blood islands are not clonal. Nevertheless, they suggest that the hemangioblast represents a subset of mesodermal cells, possibly with a restricted potential.

Alternatively, it cannot be excluded that transient and highly dynamic hemangioblasts are the precursors of the entire YS hematopoiesis and

vasculogenesis. A set of more thorough temporal-specific lineage tracing experiments are needed to clarify this point.

In parallel, an interesting speculation saw the hemangioblasts as capable to migrate towards the P-Sp/AGM region and behave as precursor of intra-embryonic hematopoiesis. However, the current data lean towards a model in which hematopoietic cells emerge from a specialized endothelial population, the hemogenic endothelium (HE), rather than developing directly from the hemangioblast. The endothelial origin of blood cells will be developed in detail in the next paragraph.

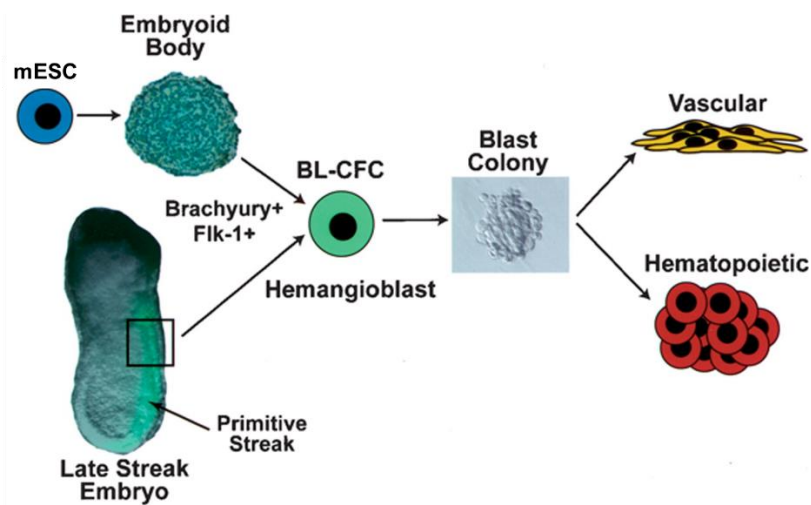


Figure 6 – The hemangioblast development in vitro and in vivo

From Gordon Keller, *Genes & Development*, 2005. Murine embryonic stem cells (mESC) and posterior primitive streak cells generate Brachyury/Flk1-expressing cells with blast colony forming cell (BL-CFC) potential. The derived blast colonies contain both vascular and hematopoietic cells.

1.6 The cellular origin of hematopoiesis: the hemogenic endothelium

The first evidence that challenged the hemangioblast origin of hematopoiesis, at least intra-embryonically, derives from experiments performed in avian embryos. Indeed, cells arising from the DA, in the AGM region, and from the VA/UA, appear as clusters budding from the endothelial cells lining the lumen of the vessel (Dantschakoff, 1908; Turpen *et al*, 1981; Garcia-Porrero *et al*, 1995; Tavian *et al*, 1996; Walmsley *et al*, 2002; Jaffredo *et al*, 2003). Jaffredo and colleagues took advantage of the specific binding of acetylated low-density lipoproteins (LDL) on endothelial cells to label these cells in the embryo and evaluate the endothelial origin of blood. They injected

fluorescent LDL (Ac-DiI-LDL) into the heart of embryos at specific developmental stages, so that the endothelial layer of the aorta lacked the expression of the pan-hematopoietic marker CD45 at the time of injection. After 24 hours, they dissected the embryo and observed that the newly formed intra-aortic hematopoietic clusters (IAHCs) were labelled with Ac-DiI-LDL. Thus, IAHCs emerge from a population that could uptake LDL, likely the endothelial layer of the DA. Newly formed hematopoietic cells within IAHCs express the pan-hematopoietic marker CD45 and retain the DiI labeling, confirming that hematopoietic cells are budding from the endothelial layer (Jaffredo *et al*, 1998).

A similar experiment performed in E10 murine embryos showed that endothelial CD31- and CD34-expressing cells retain Ac-DiI-LDL over time. The hematopoietic cells emerging from DiI⁺ endothelium share the same labeling with endothelial cells. However, they will progressively lose the DiI-labeling while maintaining hematopoietic-specific markers (Sugiyama *et al*, 2003). The evidence that emerging hematopoietic cells co-express endothelial (*i.e.* CD34, CD31, VE-Cad) and hematopoietic markers on their surface was observed in different organisms as well as the loss of the endothelial-like signature as they fully mature (Tavian *et al*, 1996, 1999; Wood *et al*, 1997; Labastie *et al*, 1998; Nishikawa *et al*, 1998a, 1998b; Fraser *et al*, 2002, 2003; Kim *et al*, 2005; Taoudi *et al*, 2005).

The endothelial ontogeny of hematopoietic cells was next proposed by the experiments of Nishikawa and coworkers (Nishikawa *et al*, 1998b). The authors isolated the endothelial population from the caudal part of E9.5 embryos (that includes the AGM region), by the expression the endothelial-specific marker VE-Cadherin (VE-Cad, CD144) (Breier *et al*, 1996). The *ex vivo* co-culture of isolated cells on OP9 stroma allowed the emergence of hematopoietic cells. Notably, the authors got rid of any emerging hematopoietic cells by the exclusion CD45⁺ cells and CD45^{neg}Ter119⁺ mature erythroid cells whereas they isolated endothelial cells.

Nevertheless, for years, the origin of hematopoietic cells remained controversial with opposite hypothesis regarding an endothelial (North *et al*, 1999; Bruijn *et al*, 2002) and/or a mesenchymal origin of hematopoiesis (Bertrand *et al*, 2005). In particular, the latter was proposed by the observation of sub-aortic mesenchymal cells that express hematopoietic markers. These cells would include

HSC precursors that will migrate through the endothelium and bud into the lumen of the aorta to form IAHCs.

Eventually, the progress of cell-fate studies ultimately acknowledged the endothelial origin of hematopoietic cells. In 2008, Zovein and colleagues used Cre-mediated recombination driven by *VE-Cad* expression to mark endothelial cells at specific developmental stages (Zovein *et al*, 2008). They induced VE-cad mediated β -galactosidase labeling at E9.5 using a tamoxifen-inducible *VE-cad-CreERT2* (Monvoisin *et al*, 2006) transgenic mouse crossed to a *ROSAR* (R26R) line (Soriano, 1999). At the time of hematopoietic activity in the AGM (E9.5-E12.5), *VE-cad* derived cells are present in both the endothelium of the DA and the associated hematopoietic cells. *VE-cad*-derived cells were capable to give rise to adult hematopoiesis, generating hematopoietic cells in BM, spleen, thymus one year after the induction (Zovein *et al*, 2008). Therefore, *VE-cad*-derived derived populations likely include HSCs.

1.6.1 The endothelial to hematopoietic transition

After the identification of the endothelial ontogeny of hematopoietic cells, the process through which endothelial cells become hematopoietic (endothelial-to-hematopoietic transition, EHT) was characterized in detail. In 2010, three groups showed for the first time live imaging movies of the EHT occurring *in vivo* in either mouse (Boisset *et al*, 2010) or zebrafish embryos (Bertrand *et al*, 2010a; Kissa & Herbomel, 2010). Due to their intrinsic transparency, the latter are particularly useful to study morphogenesis by live microscopy. In zebrafish embryos, *cmyb* and *CD41* expression was used to track the emergence of blood cells that occurs in the DA around 28-48 hours post fertilization (h.p.f) (that corresponds to E9.5-E11.5 in mouse, as shown in Figure 5) (Bertrand *et al*, 2008). On the contrary, *Lmo2* and *kdr1* (*Kdr* in mouse) are highly expressed on endothelial cells (Yamaguchi *et al*, 1993; Millauer *et al*, 1993; Yamada *et al*, 2000) and therefore were exploited as endothelial markers.

Bertrand and colleagues applied confocal-based microscopy on double transgenic zebrafish models (*cmyb:eGFP;kdr1:memCherry*) and showed that hematopoietic *cmyb:eGFP*⁺ cells emerge directly from *kdr1:memCherry*⁺ endothelial cells in the ventral wall of the DA at 30-38 h.p.f. (Figure 7 a-d) (Bertrand *et al*, 2010a). As the transition occurs, HE undergoes morphological changes to allow the detachment of the developing hematopoietic cell from the neighbor endothelium. In

the meantime, HE acquires hematopoietic specific markers while maintaining the endothelial ones (*i.e. cmyb:eGFP⁺kdrl:memCherry⁺*). Once the transition is completed, the hematopoietic cell lose the expression of endothelial markers retaining only the hematopoietic ones (*i.e. cmyb:eGFP⁺kdrl:memCherry^{neg}*) (Figure 7 c, d).

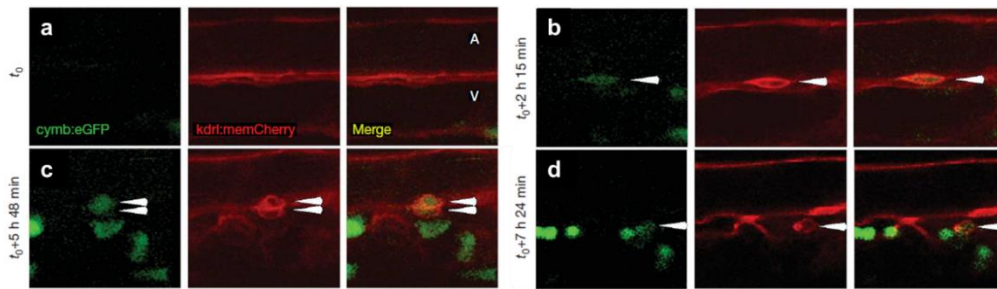


Figure 7 – Hematopoietic cells originate from the HE during zebrafish embryonic development
 From Bertrand et al, Nature, 2010. a-d) Four sequences of a time lapse-imaging of zebrafish embryo at 30-38 h.p.f.. Double transgenic zebrafish embryos (*cmyb:eGFP, kdrl:memCherry*) document the emergence of hematopoietic cells (*cmyb⁺* in green) from the hemogenic endothelium (*kdrl⁺*, in red).

Similar evidence in zebrafish embryos has been reported by Kissa and Herbomel (Kissa & Herbomel, 2010). In this study, they took advantage of a different double transgenic model, *Lmo2:Dsred;CD41:GFP* to follow the development of the DA from 23 to 100 h.p.f. and the emergence of hematopoietic cells. Between 30 to 37 h.p.f., the diameter of the DA increases accompanied by an extensive rearrangement of the aortic endothelium. In particular, endothelial *Lmo2:Dsred⁺* cells migrate from the lateral or dorsal wall to the floor of the DA. After this complex reorganization, hematopoietic cells start to emerge, specifically from the floor of the DA (*Lmo2:Dsred⁺;CD41:GFP⁺*). After 52 h.p.f., EHT events become rarer until 60 h.p.f., when they are not anymore detected in the AGM.

As in zebrafish, the EHT was examined in murine embryos by live imaging. Since murine embryos are not as transparent as zebrafish ones, Boisset and colleagues imaged thick transverse sections of non-fixed mouse embryos to maintain the integrity of the aortic architecture (Boisset et al, 2010). The authors used two different murine transgenic models to track the generation of hematopoietic cells from the DA at E10.5. In particular, they used *Ly-6a-GFP* transgene to mark functional HSCs as shown by de Bruijn and coworkers in 2002 (Bruijn et al, 2002).

On the other hand, they used *CD41-YFP* to follow the emergence of hematopoietic cells, including HSCs (Corbel & Salaün, 2002; Mikkola *et al*, 2003; Eilken *et al*, 2009). They observed that *Ly-6a-GFP*⁺ cells emerge from the endothelial layer of the ventral wall of the DA (*CD31*⁺*Ly-6a-GFP*^{neg}) (Figure 8 a-c) and co-express other known hematopoietic markers, (*i.e.* C-KIT (Sánchez *et al*, 1996), CD41) as well as endothelial ones (*i.e.* CD31 and CD34) (Figure 8 d, e). Similarly, *CD41-YFP*⁺ hematopoietic cells bud from the *CD31*⁺*CD41*^{neg} endothelium, expressing both endothelial (CD31) and hematopoietic markers on their surface (CD41, C-KIT) (Boisset *et al*, 2010).

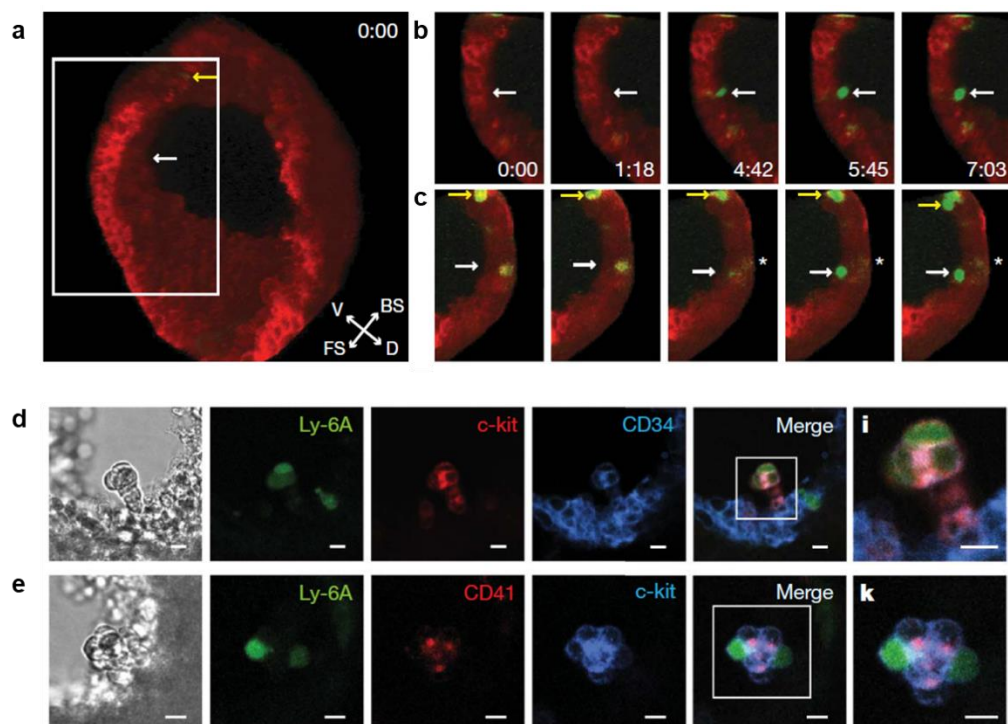


Figure 8 - Hematopoietic cells originate from the HE during murine embryonic development

From and Boisset *et al*, *Nature*, 2010. a-c) Three-dimensional reconstruction of time-lapse confocal imaging of the DA of E10 *Ly6a-GFP* mouse embryonic slices. Orientation scheme is indicated in a), bottom right: V, ventral; D, dorsal; BS, back side; FS frontal side. The squared white box in a) is zoomed in b), FS and c) BS. The endothelial layers were immuno-stained with *CD31* (red). Hematopoietic *GFP*⁺ cells emerge from the *CD31*⁺ endothelial layer as shown by white and yellow arrows in f,g).

In summary, imaging experiments in zebrafish and murine embryos support the model in which intra-embryonic hematopoietic cells directly emerge from the HE of the DA (Figure 9 a). Similarly, extra-embryonic hematopoietic progenitors, as YS-derived EMPs, emerge via a HE intermediate (McGrath *et al*, 2015; Frame *et al*,

2016). In fact, lineage tracing studies proved that E7.5-E9 4OHT induction in *VE-Cad-CreERT^{+/neg}; Rosa^{tdT}* mice selectively labels YS HE and its hematopoietic progeny (Zovein *et al*, 2008; Gentek *et al*, 2018), definitely proving the HE origin of the second hematopoietic program.

Despite the hematopoietic activity during EMP and intra-embryonic programs has been associated to HE, the origin of primitive hematopoiesis is still discussed. Padrón-Barthe and coworkers suggest that the first wave of primitive hematopoiesis develops directly from a mesodermal precursor, already specified before the PS stage, independently from the HE and EHT (Padrón-Barthe *et al*, 2014). On the contrary, RNA sequencing analysis at single-cell level of E6.5-E8.5 murine embryos showed that primitive erythroid cells pass through subclusters of hemato-endothelial progenitors at a different molecular state from ones typical of the EMP wave (Pijuan-Sala *et al*, 2019). Thus, the specification of the primitive program might differ from the following. This view could be linked to the hemangioblast model, suggesting that a specific mesodermal population gives rise to progenitors with endothelial and primitive hematopoietic potential.

Despite the hemangioblast and HE models for the origin of blood cells appears distinct, they could fit in the same scenario. Lancrin and colleagues proposed that the hemangioblast originates extra-embryonic hematopoietic cells through a HE intermediate (Lancrin *et al*, 2009) (Figure 9 b). In fact, the hemangioblast shares with the HE the expression of endothelial markers (Choi *et al*, 1998; Kennedy *et al*, 2006; Huber *et al*, 2004) as well as the ability to uptake AcLDL (Choi *et al*, 1998). However, the hemangioblast is strictly biased towards the endothelial and hematopoietic fate *in vivo* (Padrón-Barthe *et al*, 2014; Ueno & Weissman, 2006) and has a multipotent nature *in vitro* (Choi *et al*, 1998; Huber *et al*, 2004) while the HE is clonally committed to hematopoiesis (Swiers *et al*, 2013; Ditadi *et al*, 2015). Therefore, we might encounter a semantic paradox according to how the HE is specifically defined. In fact, also the hemangioblast might be considered as HE as it shares endothelial-like features and generates hematopoietic cells together with other cellular types. Strictly relying on the definition of HE as a population of cells that clonally generate hematopoietic progeny, primitive hematopoiesis might not derive from a "strictly-defined" HE, but a different one. As single-cell transcriptomic analysis suggests (Pijuan-Sala *et al*, 2019), the molecular characteristic of the population of origin of hematopoietic cells might change as development progresses,

accompanied by differences in hematopoietic potential. Furthermore, the plasticity and dynamicity of development might hamper the through dissection of hematopoiesis, especially during early stages of development characterized by massive reorganizations and structural changes.

In this context, we believe that the selective molecular identification of the HE population across the different programs is necessary to dissect and characterize its contribution to hematopoietic development.

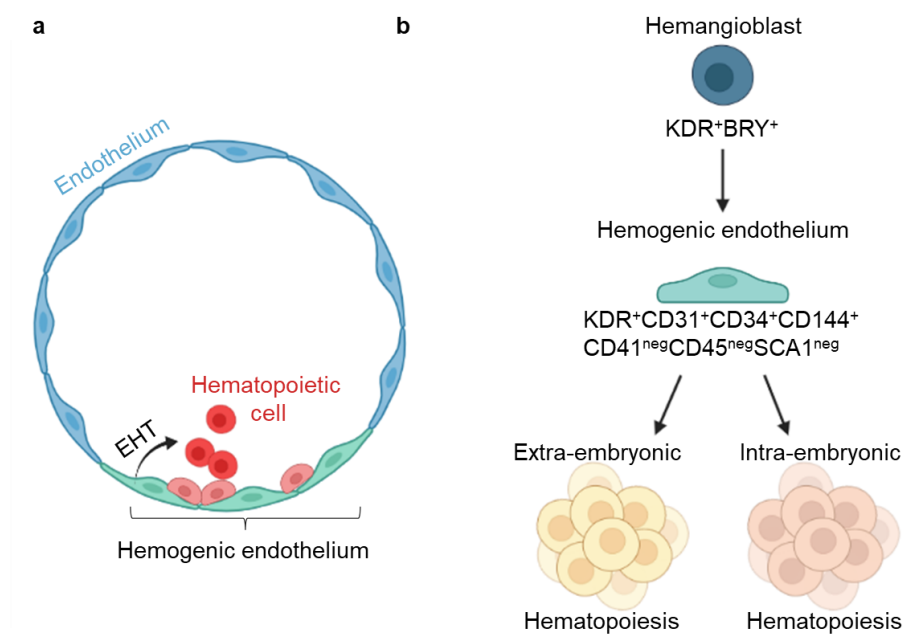


Figure 9 – The HE and hemangioblast models

a) HE model: hemogenic endothelium (in green) localized in the ventral wall of the DA undergoes endothelial to hematopoietic transition (EHT) and generates hematopoietic cells (in light and dark red) budding into the lumen of the DA in mouse. Endothelial cells are depicted in blue. b) Hemangioblast model: KDR^+BRY^+ hemangioblast precursor differentiate into hemogenic endothelial cells that generate intra- and extra-embryonic hematopoietic progenitors.

1.6.2 The heterogeneity of the HE during embryonic development

Despite the controversial origin of the primitive cells, the HE origin of hematopoietic progenitors from the EMP and intra-embryonic hematopoietic waves has been extensively demonstrated. However, while the generation of blood cells share a common EHT process, the emerging hematopoietic cells are heterogeneous in terms of potential. The differences in hematopoietic output can be tracked already at the

level of the HE. HE isolated at different time and/or from different locations displays distinct potential. As an example, while the E8.5 YS HE lacks lymphoid potential, the HE population isolated from the same region 24h later (E9.5) generates a robust lymphoid output (Nishikawa *et al*, 1998b; Yoshimoto *et al*, 2011; Dege *et al*, 2020). In addition, lymphoid potential was identified in HE from E9.5 P-Sp, apparently suggesting that E9.5 YS and P-Sp share a HE with similar potential at this stage (Cumano *et al*, 1996; Nishikawa *et al*, 1998b; Cumano *et al*, 2001; Yoshimoto *et al*, 2011). However, these two HE are rather different, as they give rise to specific subsets of cells within the same lineage.

An example of this is represented by lymphoid tissue inducer cells (LTi), the first members of innate lymphoid cells (ILC). By using *VE-Cad* inducible transgenic murine models (Zovein *et al*, 2008), Simic and colleagues observed the *VE-Cad* labeling induced at E8.5-E9.5 marks peripheral and FL lymphoid tissue inducer cells (LTi) (Simic *et al*, 2020). However, later induction failed to trace the same lineage. To address spatio-temporal heterogeneity of HE, they set to determine the intra- or extra-embryonic origin of LTi. For this, they used a *Cxcr4-CreERT^{+/-}; Rosa^{tdT}* model to specifically label intra-embryonic HE, excluding the YS endothelium that does not express *Cxcr4* (McGrath *et al*, 1999). Coherently, the E8.5-E9.5 induction in this model does not label cells in the YS but in the embryo proper, including LTi demonstrating the intra-embryonic restricted origin of this lymphoid progenitors.

A further proof of the heterogeneity of HE is suggested by the evidence that hematopoietic progenitors emerge (Yokomizo & Dzierzak, 2010; Yoshimoto *et al*, 2011; Simic *et al*, 2020) before the onset of the first functional HSC within the same intra-embryonic regions (Medvinsky *et al*, 1993; Medvinsky & Dzierzak, 1996; Bruijn *et al*, 2000, 2002). Notably, limiting dilution analysis in adult recipients revealed that only 2-3 engrafting HSCs are present in the E10.5-E11.5 embryo (Müller *et al*, 1994; Medvinsky & Dzierzak, 1996; Kumaravelu *et al*, 2002). However, as discussed, early embryonic samples difficultly repopulate adult wild-type recipients while immunodeficient models and neonates are more permissive. For instance, E9 P-Sp can long-term, multi-lineage reconstitute immunocompromised neonates (Peeters *et al*, 2005). However, it needs further *ex vivo* maturation to engraft in adult immunodeficient mice but it is still not sufficient to allow the engrafting in wild-type adults (Cumano *et al*, 1996, 2001). Repopulating studies in wild-type or *Rag2^{γC}neg/neg* neonates estimated an average of 2 HSCs precursors at early E10. The number

increases to 12 at E10.5 (Boisset *et al*, 2015). On the contrary, more than 500 IAHCs (*i.e.* CKIT⁺CD31⁺) are present at the same stage, spanning between the DA, UA and VA (Yokomizo & Dzierzak, 2010) (Figure 10 a). Concomitantly to the migration of hematopoietic cells into the FL at E11.5, the number of aortic hematopoietic clusters decreases (Yokomizo & Dzierzak, 2010; Rybtsov *et al*, 2016) (Figure 10 b) while the number of functional HSCs increases to 66 at the same stage (Kumaravelu *et al*, 2002). Since early-stage HSC are slowly cycling (Batsivari *et al*, 2017), the discrepancy on embryonic HSC number between E10.5 to E11.5 is hardly explained even considering that HSC-competent HE is already present at earlier stages but need further maturation to develop functional HSCs (Taoudi *et al*, 2008; Rybtsov *et al*, 2011, 2014; Boisset *et al*, 2015). In addition, the presence of immature HSC-competent HE would not justify the discrepancy between IAHCs and HSC numbers within intra-embryonic hematopoietic regions at similar stages (Boisset *et al*, 2015).

The evidence that both transient, HSC-independent hematopoietic progenitors and HSCs are concomitantly generated from the intra-embryonic HE (Zovein *et al*, 2008; Chen *et al*, 2009; Yokomizo & Dzierzak, 2010; Boisset *et al*, 2015; Rybtsov *et al*, 2016), raises arguments about the heterogeneity of the HE. In fact, intrinsic properties of the HE may drive the differences in lineage potential of the hematopoietic cells generated throughout embryonic development. Moreover, the supportive environment of the niche might affect the hematopoietic emergence from the HE.

In agreement with the latter hypothesis, only the HE located in the ventral part of the DA originates engrafting HSCs. On the other hand, the dorsal wall of the DA cannot multilineage reconstitute irradiated recipients (Taoudi & Medvinsky, 2007). In the attempt to understand the differences between the two domains of the DA, Medvinsky and other groups analyzed the factors specifically polarized in the ventral domain. Among them, BMPER (negative regulator of the bone morphogenic protein, BMP) and secreted endothelin1 emerged as important regulator of HSC development *in vivo* (Crosse *et al*, 2020; McGarvey *et al*, 2017). Therefore, non-cell-autonomous factors secreted by other cells than HE, influence the EHT. Moreover, spatial transcriptomic analysis of dorsal revealed that TGF β and nitric oxide (NO)-stimulated genes are enriched in the ventral domain of the DA suggesting that the activation of specific signaling pathways might be implicated in HSC emergence and

might drive the heterogeneity of HE (Crosse *et al*, 2020; Monteiro *et al*, 2016; Adamo *et al*, 2009; North *et al*, 2009).

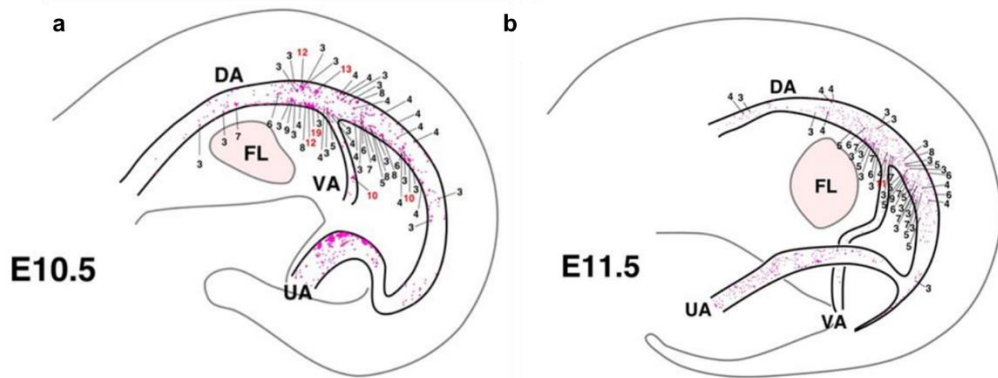


Figure 10 – Three-dimensional mapping of hematopoietic clusters in the mouse embryo

From Yokomizo and Dzierzak, *Development*, 2010. Distribution of *c-Kit*⁺ cells (pink dots) in the aorta of E10.5 a) and E11.5 b) mouse embryos. Numbers indicate the cellular size of the clusters. Dorsal aorta (DA), umbilical artery (UA), vitelline artery (VA).

In conclusion, the hemogenic activity of endothelium is tightly regulated in space and time. The HE gives rise to hematopoietic cells with distinct potential according to the developmental stage and the location. To dissect the heterogeneity of the HE, understanding whether the HE shows a different molecular identity across the hematopoietic programs is primarily important. Thus, molecular regulators and signaling pathways have been extensively interrogated to dissect their involvement in the transition from HE to hematopoiesis and will be discussed in the next paragraphs.

1.7 Molecular regulators involved in the EHT

Several studies have been performed to dissect the mechanisms of hematopoietic cell emergence. Indeed, shedding the light on the molecular characteristics that define the HE from other endothelial cells, is fundamental to accurately recapitulate the hematopoietic development. In particular, the transcription factor RUNX1, a member of the family of RUNX proteins (RUNX1, 2, 3 in mammals) distinguishes the HE from non-hemogenic endothelial cells.

RUNX proteins were initially discovered in the fly while identifying mutations that affect development (Nüsslein-Volhard & Wieschaus, 1980). The mutation in *runt* gene, encoding for a transcriptional regulator involved in several developmental processes in *Drosophila*, causes defects in pre-segmentation patterning, resulting in the formation of runted embryos. Instead, the human *RUNX1* was initially identified as *AML1* due to its association to acute myeloid leukemia (Miyoshi *et al*, 1991). However, the high homology with *runt* (DAGA *et al*, 1992) changed the family name to runt-related proteins or RUNX. Differently from the fly, the role of *RUNX1* remained unknown for few years. Molecular cloning and protein purification unraveled the role of *RUNX1* as heterodimeric transcriptional factor (Kamachi *et al*, 1990; Ogawa *et al*, 1993; Wang *et al*, 1993) in complex with a non-DNA-binding partner, the core binding factor β (CBF β).

The deletion of *Runx1* or *CBF β* affects the different hematopoietic programs (Wang *et al*, 1996a, 1996b; Okuda *et al*, 1996; Sasaki *et al*, 1996; Niki *et al*, 1997; Cai *et al*, 2000). For years, *Runx1* was believed to be dispensable for primitive hematopoiesis (Okuda *et al*, 1996; North *et al*, 1999). However, while primitive progenitors still emerge in *Runx1*-deficient models, primitive erythrocytes display an immature phenotype (Yokomizo *et al*, 2008) and the frequency of primitive macrophages (Lacaud *et al*, 2002; Frame *et al*, 2016) and megakaryocytes (Potts *et al*, 2014) is reduced. On the contrary, the absence of *Runx1* causes major defects later in development. *Runx1* knock-out or silencing completely blocks the EHT and the generation blood cells from all the hematopoietic waves but the primitive (North *et al*, 1999; Yokomizo *et al*, 2001; North *et al*, 2002; Chen *et al*, 2009; Boisset *et al*, 2010; Bertrand *et al*, 2010a; Kissa & Herbomel, 2010; Tober *et al*, 2013; Padrón-Barthe *et al*, 2014; Eliades *et al*, 2016; Frame *et al*, 2016). The requirement of *Runx1* in the emergence of the hematopoietic cells from the HE and not of primitive progenitors further suggests that the latter do not derive from a proper HE but from a different population of cells with endothelial characteristics.

The crucial role of *Runx1* in the EHT is confirmed by its conditional deletion in *VE-Cad-* or *Tie2-*expressing cells that impairs the emergence of functional HSCs, intra- and extra- hematopoietic progenitor cells inducing embryonic lethality at mid-gestation with severe FL anemia (Li *et al*, 2006; Chen *et al*, 2009). These experiments confirmed that endothelial *Runx1* expression is required for the EHT possibly cell-autonomously and regulates the development of HSC and hematopoietic progenitors.

However, *VE-Cad* and *Tie2* expression is not restricted to endothelial and HE populations as these markers are observed in emerging hematopoietic clusters as well. Therefore, Chen and colleagues investigated the requirement of *Runx1* using *Runx1^{flox/flox};Vav1-Cre* transgenic model. *Vav1* is selectively expressed on committed hematopoietic cells but not during the EHT (Ogilvy *et al*, 1999; Stadtfeld & Graf, 2004). *Vav1*-mediated *Runx1*-deletion allows the emergence of HSC and hematopoietic progenitors that are detected as circulating cells in the FL of E11.5 murine embryos. Similarly, the knock-out of *Runx1* in adult mice mildly affects the hematopoietic compartment and the animals survive without major defects (Ichikawa *et al*, 2004; Gowney *et al*, 2005). Therefore, *Runx1* is a master regulator of hematopoietic development, but it is largely dispensable at later stages, once hematopoietic progenitors and stem cells are formed (Ichikawa *et al*, 2004; Gowney *et al*, 2005; Chen *et al*, 2009).

Coherently with the master role in hematopoietic development, *Runx1* expression is detected within the major hematopoietic sites, following the trend of the different programs. Indeed, in mouse *Runx1* is expressed from E7.5 to E10.5. From E8.5 onwards, the expression declines in the YS and starts to emerge inside the embryo in the VA and in the ventral floor of the paired DA. At E10.5, *Runx1* expression extends to the FL, VA, UA. At this stage, *Runx1* expression is not limited to endothelial cells but spreads to the emerging hematopoietic clusters, the aortic mesenchyme and few mesonephros cells (North *et al*, 1999; Daane & Downs, 2011; North *et al*, 2002; Bee *et al*, 2009a, 2009b). Concomitantly to the end of intra-embryonic HE activity and hematopoietic cell emergence (by E14.5), endothelial *Runx1* expression within intra-embryonic hematopoietic sites disappears (North *et al*, 1999; Yokomizo & Dzierzak, 2010). In summary, *Runx1* expression in endothelial cells anticipates the emergence of blood and is restricted to time and locations of the EHT (North *et al*, 1999).

The crucial developmental role of *Runx1* is confirmed by its highly conservation among vertebrates (North *et al*, 1999; Ciau-Uitz *et al*, 2000; Burns *et al*, 2002; Kalev-Zylinska *et al*, 2002; Bollerot *et al*, 2005; Gering & Patient, 2005). Two alternative promoters dictate the transcriptional expression of *Runx1*: the distal promoter P1 and the proximal P2. The alternative transcription generates a distal and a proximal *Runx1* transcript that differ in the 5'- untranslated regions (UTR) and N-terminal coding sequence. The two transcripts are translated in two proteins: the

distal isoform RUNX1c and the proximal RUNX1b (Pozner *et al*, 2000; Fujita *et al*, 2001). In addition, alternative splicing of the two transcripts originates further Runx1 isoforms (Bae *et al*, 1994; Tsuji & Noda, 2000; Telfer & Rothenberg, 2001; Bee *et al*, 2009b). However, the transcriptional differences do not confer any reported distinct properties in RUNX1b and RUNX1c proteins (Fujita *et al*, 2001; Challen & Goodell, 2010). Nevertheless, the transcription from either one or the other promoter appears to regulate the expression level and the time of *Runx1* expression. P2 promoter activity is dominant during the first stages of hematopoietic development while the P1 is predominantly expressed during FL and BM hematopoiesis in mouse (Bee *et al*, 2009b, 2010; Fujita *et al*, 2001; Sroczynska *et al*, 2009). Despite the two promoters regulate *Runx1* expression in time and dosage during mammalian embryonic development, they do not regulate its tissue-specific expression (Bee *et al*, 2009a) that, in turn, is regulated by upstream enhancers (Nottingham *et al*, 2007; Ng *et al*, 2010) further controlled by the finely orchestrated activity of other pivotal transcription factors (Figure 11).

The core transcription factors involved in the regulation of *Runx1* are GATA2, FLI1 and TAL1 (T cell acute leukemia gene 1, also known as SCL) (Robb *et al*, 1995; Nottingham *et al*, 2007; Pimanda *et al*, 2007; Ng *et al*, 2010) that will be described below. In addition, the regulatory network is fueled by a positive feedback mechanism that ensures their expression in embryonic tissues controlling hematopoietic cells emergence (Pimanda *et al*, 2007).

The transcription factor **GATA2** plays an essential role in embryonic development. *Gata2*-deficient embryos prematurely die at E10-E11 displaying severe anemia, brain hemorrhages and defects in hematopoietic development including the lack of HSCs (Tsai *et al*, 1994; Minegishi *et al*, 1999; Pater *et al*, 2013), similarly to *Runx1*-null embryos (Wang *et al*, 1996a). The analysis of mouse chimaeras obtained by the injection of *Gata2* knock-out mESCs into wild-type blastocysts showed a dramatic impairment in hematopoietic stem and progenitor cells pool at early embryonic stages (Tsai *et al*, 1994). A similar phenotype is observed in *Gata2* heterozygous mutant embryos (Tsai *et al*, 1994) that shows reduced frequency of HSPCs, HE cells and IAHCs (Ling *et al*, 2004; Khandekar *et al*, 2007; Pater *et al*, 2013). In addition, *Gata2* levels and dynamicity influence different stages of EHT (Eich *et al*, 2018) and its expression modulates EHT, HSC emergence and activity (Ling *et al*, 2004; Pater *et al*, 2013)). Given the crucial role of GATA2 in embryonic

hematopoietic development, its expression is tightly regulated for instance by Notch signaling that is highly involved in hematopoietic development, as it will be further discussed (paragraph 1.8) (Robert-Moreno *et al*, 2005; Robert-Moreno *et al*, 2008). The role of GATA2 in hematopoietic development is mediated by the regulation *Runx1* expression as suggested by *Runx1*- and *Gata2*-deficient phenotype and experiments performed in zebrafish and murine embryos (Gao *et al*, 2013; Butko *et al*, 2015).

Gata2 expression is upstream regulated by one of the earliest recognized markers involved in hematopoietic development, **FLI1**. FLI1 is expressed in dorsal lateral plate mesoderm (Walmsley *et al*, 2002), endothelial cells and hematopoietic clusters (Brown *et al*, 2000; Hart *et al*, 2000). The knock-out of *Fli1* induces a similar phenotype to *Runx1*-deficiency albeit at lower level (Wang *et al*, 1996b; Hart *et al*, 2000; Spyropoulos *et al*, 2000; Gao *et al*, 2013).

Finally, the role of **SCL** in the regulation of *Runx1* expression in endothelium is less defined. SCL is one of the first pro-hematopoietic transcription factor expressed during embryonic development. In fact, at mesodermal level, SCL controls the transcriptional network to favor hematopoietic *versus* cardiac fate (Van Handel *et al*, 2012; Org *et al*, 2015). Its master role in hematopoietic development is confirmed by the effect of its genetic disruption that causes early embryonic lethality at E9.5 with complete abrogation of hematopoietic development including the primitive compartment, mildly affected in *Runx1*-null embryos (Robb *et al*, 1995; Porcher *et al*, 1996; D'Souza *et al*, 2005; Lancrin *et al*, 2009). In addition, *Tal1*-deficient mESCs fail to generate the HE population *in vitro*, stage in which *Runx1* is required (Lancrin *et al*, 2009; D'Souza *et al*, 2005). Therefore, *Tal1*-deficiency blocks the hematopoietic development before the requirement of *Runx1*. However, *Tal1* deletion in *Tie2*-expressing endothelial cells shows a modest effect on hematopoiesis. This suggests a compensatory effect mediated by TAL1-related proteins, as LYL1 (Schlaeger *et al*, 2005), that mitigate *Tal1*-deficiency regulating *Runx1* expression in endothelial cells (Giroux *et al*, 2007).

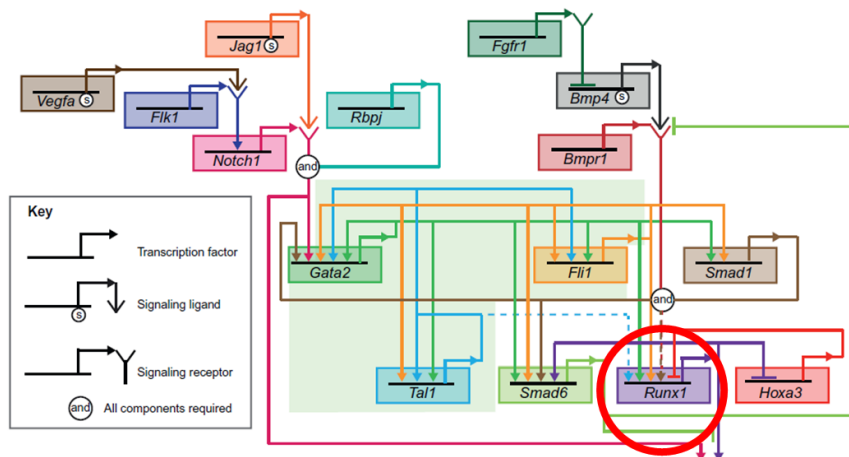


Figure 11 – The gene regulatory network in the HE

Adapted from Tober, Maijenburg, Speck, *Current topics in developmental biology*, 2016. The legend for the gene regulatory symbols used are highlighted in the bottom left box. The shaded green panel in the center highlights the interconnected gene regulatory network of *Gata2*, *Fli1*, *Tal1* (Pimanda et al, 2007). The dotted lines indicate presumed interaction, not yet demonstrated.

In addition to RUNX1 and its upstream regulatory network, also downstream targets are implicated in HE specification and EHT process. Two of them are ***Gfi1*** and ***Gfi1b*** that code for zinc finger transcriptional repressors. GFI1 and GFI1b downregulate endothelial-specific genes in the HE such as *VE-Cad*, *Pecam1* and *Endoglin*. However, other endothelial genes as *Cd34*, *Kdr* and *Tie2* remain unaffected (Lancrin et al, 2012). In absence of *Runx1*, the overexpression of *Gfi* favors the upregulation of genes involved in hematopoiesis such as *Myb* and *Lmo2* as well as endothelial to hematopoietic-like morphological changes. However, the enforced expression does not rescue the emergence of any functional HSC and hematopoietic progenitor cells in *Runx1*-deficient embryos. On the other hand, *Gfi1* and *Gfi1b* deficiency permits the emergence of hematopoietic cells, yet they fail to circulate and maintain the expression of endothelial-specific genes as *Sox7*, *Tie2*, *VE-cad* and *Flk1* (Lancrin et al, 2012).

Together with the aforementioned transcription factors, a complex and vast network of upstream and downstream RUNX1-related proteins modulates the hematopoietic development and influences the fate of hemogenic endothelial cells, in particular around the EHT stage.

For instance, another family of transcription factors involved in the EHT is SRY-related HMG-box (SOX) and, among its member, **SOX17** is the most studied. The analysis of *Sox17*-GFP reporter mice showed that it is expressed between E9.5-E11.5 in VE-Cad⁺ endothelial cells and emerging hematopoietic clusters lining the lumen of the DA in the AGM region (Clarke *et al*, 2013; Kim *et al*, 2007). The deletion of *Sox17* in endothelial cells using *VE-Cad-Cre* or *Tie2-Cre;Sox17^{flox/flox}* transgenic mice, affects arterial development, vascular remodeling and intra-embryonic hematopoiesis (Clarke *et al*, 2013). These embryos lack functional HSCs and die prematurely by E12.5 (Clarke *et al*, 2013; Kim *et al*, 2007). However, its requirement seems to be temporally restricted. In fact, the conditional knock-out of *Sox17* in E9.5 VE-Cad expressing cells *in vivo* does not affect the emergence of IAHCs, that maintain the physiological expression of RUNX1 and GATA2 in AGM endothelial cells (Lizama *et al*, 2015). On the contrary, the expression of Notch-related genes decreases, in agreement with the role of SOX17 in the positive regulation of Notch pathway (Corada *et al*, 2013), mainly involved in arterial specification (Lawson *et al*, 2001; Zhong *et al*, 2001; Lawson *et al*, 2002; Gering & Patient, 2005). AGM explant culture experiments suggested a possible role of SOX17 as negative regulator of EHT (Lizama *et al*, 2015). Indeed, the deletion of *Sox17* in *VE-Cad* -expressing cells of AGM explants isolated at E9.5 and E11, increased the frequency of hematopoietic cells and upregulated the expression of genes involved in the EHT while Notch-related genes decreased. This suggests that endothelial SOX17 is needed (whether cell-autonomously or not is not clear) before E9.5 for HSC development, but it dispensable thereafter. In addition, different groups report a contrasting effect of *Sox17* over-expression *in vitro*. In one case, it has been implicated in the expansion of a population able to generate hematopoietic cells while downregulating endothelial markers (Clarke *et al*, 2013; Nakajima-Takagi *et al*, 2013). In another, *Sox17* gain of function has a detrimental effect on hematopoietic cell survival (Serrano *et al*, 2010). Therefore, the implication of SOX17 in intra-embryonic hematopoiesis and hemogenic endothelial specification is not clear. However, *in vitro* chromatin immunoprecipitation experiments (ChIP) and functional validations, report a reciprocal regulation of *Sox17*, *Runx1* and *Notch* that may be critical in the fine-tuned regulation of hemogenic and non-hemogenic fate of endothelial cells (Clarke *et al*, 2013; Lizama *et al*, 2015). In addition, SOX17 is linked to homeobox genes A (*HOXA*) expression (Jung *et al*, 2021) that, in turn, is determinant to HSC identity and function (Dou *et al*, 2016; Ng *et al*, 2016).

Interestingly, **HOXA3** promotes endothelial rather than hematopoietic fate during embryonic development. In fact, *HoxA3* and *Runx1* expression are mutually exclusive in the embryo. At E8.5, *Runx1* marks HE of the YS while *HoxA3* is highly expressed in the endothelium of the DA where the hematopoiesis has not started yet. From E9.5, ventral cells of the DA begin to express *Runx1* and lose *HoxA3* expression. Their reciprocal regulation is mediated by HOXA3 binding at *Runx1* proximal promoter P2, inhibiting its transcription (Iacovino *et al*, 2011). Therefore, not only specific regulators are involved in determining the hemogenic potential of the endothelium, but also the mutual inhibition of pro-endothelial and pro-hematopoietic factors regulate the hematopoietic fate.

In conclusion, the expression of the master regulator of the hematopoietic development, *Runx1*, is regulated at multiple levels by transcription factors broadly expressed in endothelial cells. The gene regulatory network upstream of *Runx1* involves other molecular regulators and integrates with the signaling pathways activated during different stages development (Figure 11).

1.8 Signaling pathways involved in EHT: Notch

In the previous paragraph, we have briefly mentioned the role of Notch pathway in controlling the EHT, regulating a transcriptional network upstream to *Runx1* expression (Figure 11). Throughout this section, I will present in more details the Notch-mediated orchestration of embryonic hematopoietic development.

The Notch pathway was first identified in genetic experiments in *Drosophila*. The X-linked mutation caused notched wings to heterozygous female and the peculiar phenotype gave the name to the pathway (Morgan, 1917).

The Notch family consists of four Notch receptors (NOTCH1-4) and five different ligands (specifically, three Delta-like ligands, DLL1, 3, 4 and two Jagged ligands, JAG1, 2). The activation of Notch signaling is mediated by the binding of a single transmembrane Notch receptor to one of its ligands, located on adjacent cells. The binding triggers two sequential proteolytic cleavages of the receptor that result in the release of the intracellular part of the Notch receptor (or Notch intracellular domain, NICD) mediated by a multiprotein complex with γ -Secretase activity (Edbauer *et al*, 2003; Okochi *et al*, 2002). NICD eventually translocates into the

nucleus (Struhl & Adachi, 1998; Schroeter *et al*, 1998) where it binds the nuclear transcription factor RBPJ κ (also known as CSL) whose activity is otherwise repressed by the association of a co-repressor complex (Kao *et al*, 1998). NICD binding to RBPJ κ displaces the co-repressor complex and triggers the recruitment of the co-activator Mastermind (Mam) on the promoter of target genes (Wu *et al*, 2000; Fryer *et al*, 2002; Yatim *et al*, 2012). RBPJ κ activates the transcription of Notch-responsive genes and orchestrates the feedback loop mechanisms that regulates Notch signaling (Heitzler *et al*, 1996; Timmerman *et al*, 2004) (Figure 12 a). Most of the Notch effects is mediated by the activation of *Hes* or *Hes*-related, *Hrt*, family of genes. HES and HRT proteins are basic helix-loop-helix (bHLH) factors that generally act as transcriptional repressors (Iso *et al*, 2003).

The Notch pathway is well-conserved among species and regulates several developmental processes mediating cell-to-cell interactions between neighboring cells (Lai, 2004). Two different models have been proposed to explain the role of Notch in controlling cell-fate decision: the lateral inhibition and the lateral induction model (Figure 12 b). In the former, the initial population of cells express similar levels of Notch ligands and receptors. However, the upregulation of DLL-like ligand expression in one cell and the consequent NICD cleavage, activates Notch targets as *Hes/Hrt* that inhibit the Notch ligand expression by a negative feedback loop mechanism. This process favors the differentiation of the neighboring cells and the acquisition of a "salt and pepper" phenotype. In fact, receiver cells will expose low level of DLL-like ligands compared to DLL-expressing sender cells (Figure 12 b, upper panel). On the opposite, in the lateral induction model the ligand expressing cells (JAG-like) induce the Notch activity in adjacent cells. The NICD release allows the transcription of target genes that include *Jag* ligands. In this model, the positive feedback loop mechanism favors a homogeneous differentiation pattern between sender and receiver cells (Figure 12 b, lower panel). Despite these two models are useful to explain some of the Notch roles during development, it is not always obvious to define how Notch regulates a given developmental process and to ascribe its effect to one of these models.

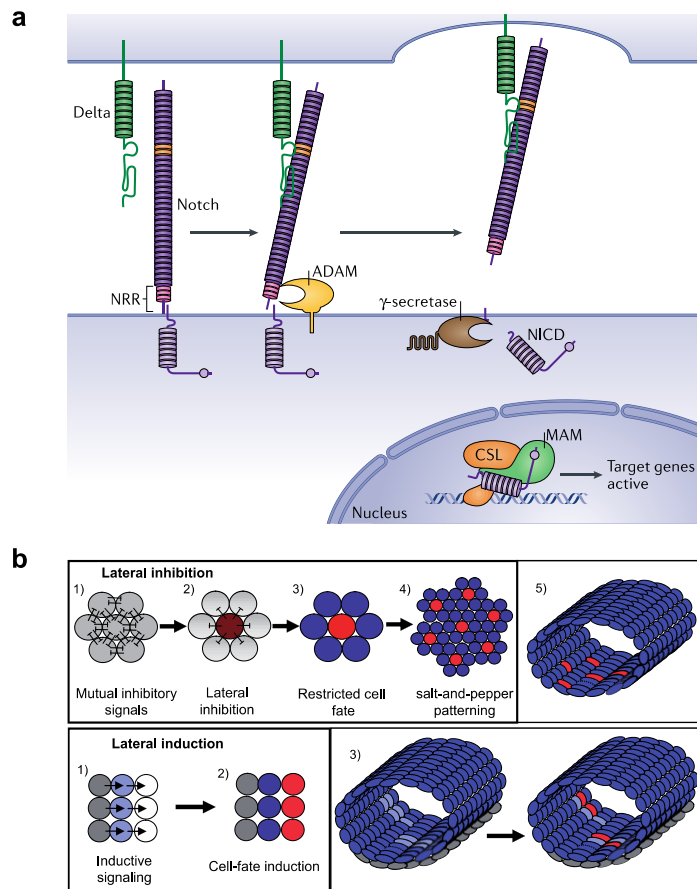


Figure 12 – The Notch pathway

From Bray, *Nature Reviews*, 2006 (upper panel, a) and Bigas *et al*, *International Journal of Developmental Biology*, 2010 (lower panel, b). a) Binding of the Notch ligand (i.e., Delta ligand in green) on one cell to the Notch receptor (purple) on another, results in two proteolytic cleavages of the receptor. ADAM10 or TACE (TNF- α -converting enzyme; also known as ADAM17) metalloprotease (yellow) mediate the first cleavage, the γ -secretase complex the second (brown). The proteolytic cleavages release the Notch intracellular domain (Nid), which enters the nucleus and interacts with the DNA-binding CSL also known as RBPJ (orange). The binding recruits the co-activator Mastermind (Mam; green) to activate the transcription of target genes. On the other hand, the co-repressors (Co-R; blue and grey) are released. b) Upper panel, lateral inhibition model. The negative feedback loop (1, 2) mediated by Notch activation in receiver cells favors a salt and pepper phenotype (3, 4). Receiver cells express low ligands on their surface while sender cells express them and the two cell types differentiate (5). Lower panels, lateral induction model: the positive feedback loop activated (1, 2) by Notch in receiver cells favors the acquisition of a homogeneous pattern between sender and receiver cells (3).

The Notch pathway is primarily involved in vascular development, particularly in artery specification (Krebs *et al*, 2000; Lawson *et al*, 2001; Zhong *et al*, 2001; Lawson *et al*, 2002; Gering & Patient, 2005). In addition, Notch directly regulates also hematopoietic development. The first *in vivo* evidence that Notch pathway is involved in hematopoietic development came from the study of *Notch1*-null murine

embryos (Kumano *et al*, 2003). E9.5 P-Sp of *Notch1^{neg/neg}* embryos lack HSCs, while, at the same stage, YS hematopoiesis remains unaffected (Kumano *et al*, 2003). In addition, mutant and wild-type embryos show a similar frequency of CD34⁺CKIT⁺ progenitors in the endothelium. Therefore, the lack of Notch signaling results in an impaired commitment specifically in HSC generation and not HSC-independent progenitors, and, as such, Notch-dependency has been used since as a defining feature of HSC-competent HE. Chromatin immunoprecipitation (ChIP) assays showed that NOTCH1 intracellular domain specifically binds to *Gata2* promoter through two functional RBPJ κ binding sites. In fact, this interaction is lost in *Rbpjk* mutant embryos that show a phenotype similar to *Notch1*-deficiency with premature embryonic death, severe intra-embryonic hematopoietic defects but intact extra-embryonic hematopoiesis (Robert-Moreno *et al*, 2005). Therefore, Notch-mediated control of *Gata2* justifies the defective hematopoietic development observed in *Notch1*-null embryos (paragraph.1.7). The role of Notch1 in intra-embryonic hematopoietic development is supported by the expression of *Notch1* in the aorta between E9.5 and E10.5. On the other hand, *Notch2* and *3* are not expressed in E9.5-E10.5 DA whereas *Notch4* is expressed within arterial cells of the DA but not at the level of hematopoietic clusters (Robert-Moreno *et al*, 2005; Robert-Moreno *et al*, 2008). *Notch2*, *Notch3* or *Notch4* mutant embryos do not show hematopoietic but vascular defects (Joutel *et al*, 1996; Krebs *et al*, 2000; McCright *et al*, 2001; Kumano *et al*, 2003).

The analysis of Notch ligands revealed that JAG2, DLL1 and DLL3 are not involved in the Notch-dependent effect on intra-embryonic hematopoietic development. Indeed, the lack of *Jag2* that is heterogeneously expressed in the DA, does not impair the intra-embryonic hematopoiesis at E10.5 (Robert-Moreno *et al*, 2008). *Dll1* and *Dll3* ligands are not detected in the emerging IAHCs and aortic endothelial cells of mid-gestation murine embryos (Robert-Moreno *et al*, 2005; Robert-Moreno *et al*, 2008). On the contrary, similarly to *Notch1* and *Rbpjk* -deficient embryos, the analysis of JAG1 and DLL4 ligands confirmed the involvement of Notch signaling in intra-embryonic hematopoietic development.

JAG1 expression is mostly restricted to endothelial cells underlining the emerging hematopoietic clusters in the E10.5 AGM (Robert-Moreno *et al*, 2005; Robert-Moreno *et al*, 2008). *Jag1*-mutant embryos show several angiogenic defects and prematurely day around E10.5 (Xue *et al*, 1999a). As in *Notch1* mutant (Kumano

et al, 2003), intra-embryonic hematopoietic development is defective while YS progenitors remain unaffected (Robert-Moreno *et al*, 2005; Robert-Moreno *et al*, 2008).

Dll4^{neg/neg} embryos die at E9.5 with major vasculogenic defects and a complete loss of arterial identity (Krebs *et al*, 2004). In the DA, DLL4 is mostly expressed on aortic endothelial cells but shows a heterogeneous expression within IAHCs at mid-gestation (Robert-Moreno *et al*, 2005; Robert-Moreno *et al*, 2008). DLL4 is preferably expressed within small clusters while only few cells of larger IAHCs express DLL4. This suggests a role of DLL4 in regulating phases of IAHC growth. Indeed, blockage of DLL4 with monoclonal antibodies increases the number of cells incorporated into the IAHCs without affecting the total number of clusters at E10.5, as observed by whole mount immunostaining (Porcheri *et al*, 2020). Porcheri and colleagues proposed a model in which DLL4-mediated Notch signaling does not affect neither the generation nor the cell fate of IAHCs while it regulates the recruitment of new cells into hematopoietic clusters (Figure 13). In fact, the inhibition of DLL4-mediated signaling does not affect the multilineage engrafting potential neither the transcriptomic identity of E10.5 IAHCs. However, the frequency of hematopoietic $KIT^+CD45^+CD31^+$ cells increased compared to untreated samples.

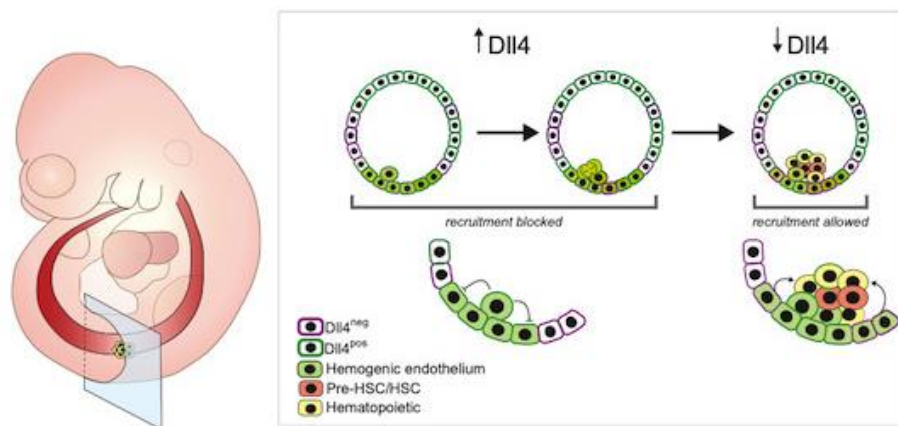


Figure 13 - Formation of IAHCs involves Notch signaling

From Porcheri *et al*, *EMBO journal*, 2020. Scheme highlighting the formation of hematopoietic cell clusters in the aorta of E10.5 mouse embryos. Nascent clusters are proliferative, monoclonal, and express high level of Notch ligand DLL4. The reduced DLL4-mediated Notch signaling increases the size of the clusters that become polyclonal via recruitment of neighboring endothelial cells.

In summary, the two Notch ligands JAG1 and DLL4 appear primarily involved in intra-embryonic hematopoietic development. The two ligands show specific spatial expression pattern. In addition, they are known to be involved with opposite function in other biological processes as angiogenesis. Benedito and colleagues showed that JAG1 counteracts DLL4-Notch interactions in non-cell-autonomous way and regulates the sprouting of endothelial cells in response to proangiogenic factors as VEGF. In this model, high level of JAG1 efficiently antagonize the more potent DLL4 ligand present on neighbor cells thanks to post-translational modifications on Notch receptor mediated by Fringe glycosyltransferases (Brückner *et al*, 2000; Benedito *et al*, 2009). Translating this observation to intra-embryonic hematopoietic development, the balance between DLL4 ligand expressed in IAHCs and JAG1 on underlining aortic endothelial cells might act as determinant regulator of the EHT. In addition, the functional Notch activation on IAHCs might downregulate the expression of pro-angiogenic VEGF receptors (VEGFR) as VEGFR2 and VEGFR3 (Suchting *et al*, 2007; Hellström *et al*, 2007; Tammela *et al*, 2008) in favor of a hematopoietic-like signature, mediated by Notch-dependent transcriptional activation of *Gata2*, *Scf* and *Runx1* (Robert-Moreno *et al*, 2005; Burns *et al*, 2005; Robert-Moreno *et al*, 2008). Other studies report that co-expression of Delta-like and Jagged ligands on the same cell triggers a mechanism known as *cis*-inhibition that prevents signaling activation through E3 ubiquitin ligases-mediated endocytosis in a cell-autonomous way (Glittenberg *et al*, 2006). Therefore, alternative mechanisms might regulate the complex role of Notch signaling in hematopoietic development, also possibly including the effect of non-canonical activation of Notch signaling (Lakhan & Rathinam, 2021).

The coupling of impaired arterial identity and intra-embryonic hematopoietic development in mouse embryos with defective Notch signaling (Xue *et al*, 1999b; Krebs *et al*, 2004; Robert-Moreno *et al*, 2005; Robert-Moreno *et al*, 2008), raises the question of whether proper arterial specification is required cell-autonomously for intra-embryonic hematopoietic development. In fact, intra-embryonic definitive hematopoiesis is closely associated to arteries (Bruijn *et al*, 2000) and most, if not all, arterial-defective mutants show severe EHT impairment. However, the lineage relationships between arterial and hemogenic endothelium have not been completely elucidated yet. For instance, in zebrafish embryos hematopoietic cells can emerge in the AGM region from cells that do not express the arterial marker EphrinB2 (EfnB2) after transient Notch activation by induction of NICD transgenic expression (Burns *et al*, 2005). Similar results have been reported also in murine embryos with arteriovenous malformations (Urness *et al*, 2000; Lawson *et al*, 2001, 2002).

Therefore, it seems possible that hematopoietic cells can emerge in absence of arterial markers expression. However, the hematopoietic output has not been tested for HSC potential in these cases. In addition, it is not clear whether cells lacking EfnB2 expression maintain the arterial specification. New single-cell resolution fate studies are needed to dissect the ontogeny of HE, or better, of the different heterogeneous HE populations present intra-embryonically. This will also allow to determine the exact role of the Notch pathway in both arterial specification and hematopoietic development. Indeed, different Notch signals might be required during aorta development in mid-gestation embryos. A possible model might include that HSC-independent intra-embryonic hematopoiesis requires Notch signaling to develop but not immuno-phenotypical arterial cells to emerge (Ditadi *et al*, 2015). On the other hand, HSC-fate of intra-embryonic HE would require both the activation of Notch signaling and correct Notch-dependent arterial specification. Therefore, the Notch signals deriving from different combinations of Notch receptor-ligand coupling on neighboring cells might be the crucial regulator of HSC-competent and non-competent HE.

In conclusion, the regulation of Notch signaling activation in HE and/or surrounding arterial endothelial cells at specific stage of the EHT controls the hematopoietic development. Notch ligand expression might serve to spatio-temporally compartmentalize Notch signaling activity and integrate Notch signaling into a molecular network that orchestrates the transition of HE to hematopoiesis.

1.9 Signaling pathways involved in EHT: Retinoic Acid

Another signaling pathways widely involved in embryonic development is retinoic acid (RA) signaling. Retinoic acid or all-*trans*-retinoic acid (ATRA) is the biologically active metabolite of vitamin A1 or all-*trans*-retinol (ROH). ATRA is required for the activation of RA signaling by the binding to retinoic acid receptor (RAR α , β or γ) that forms heterodimers with the rexinoid receptor (RXR α , β or γ) and binds the DNA on RA responsive element (RARE) to trigger the transcriptional activation of target genes. Among target genes, RA activates the expression of *Cyp26a1-c1* that encodes for cytochrome P450 family 26 (CYP26) enzymes. CYP26 enzymes mediate the metabolism of RA in the cytoplasm. Therefore, the RA activation coordinates a negative feedback loop mechanism mediated by CYP26 enzymes that regulate RA

signaling activation, fine-tuning autocrine and paracrine RA-mediated effects (reviewed in (Niederreither & Dollé, 2008) (Figure 14).

RA is produced from retinoids, most commonly from retinol (ROH), through a series of oxidative reactions. During embryonic development of placental species, the main source of retinoids is diet or maternal transfer (Niederreither & Dollé, 2008). Circulating ROH is bound to the retinol-binding-protein 4 (RBP4) and uptaken by target cells (Kawaguchi *et al*, 2007). ROH is then oxidized to retinaldehyde by cytosolic alcohol dehydrogenases (ADH) or retinol dehydrogenases (RDH). During embryonic development, RDH10 is mainly responsible of ROH oxidation to retinaldehyde, and, in its absence, murine embryos survive until E13 (Sandell *et al*, 2007). Retinaldehyde is further oxidated to RA by retinaldehyde dehydrogenases (RALDH1, 2, 3), each of which is functional at specific spatio-temporal stages throughout embryogenesis. RALDH2 is the first retinaldehyde dehydrogenases expressed in murine embryonic tissues as PS, mesoderm and visceral endoderm (Niederreither *et al*, 1997) and it is the most active RALDH up to mid-gestation stage (Niederreither *et al*, 1997; White *et al*, 2007; Wingert *et al*, 2007). In fact, murine embryos lacking *Raldh2* display abnormal vascular development and die around E10 (Niederreither *et al*, 1999; Lai *et al*, 2003; Bohnsack *et al*, 2004) even before *Rdh10*-deficient models, highlighting the redundancy of ADH enzymes and the specificity of RALDH2 activity in hematopoietic and vascular development. In fact, *Raldh1*- or *Raldh3*- null embryos do not show major hemato-vascular defects (Niederreither *et al*, 1999; Goldie *et al*, 2008). On the other hand, *Raldh2*-null embryos die before the emergence of HSC and show impaired extra-embryonic EMP-wave but not in primitive hematopoiesis (Goldie *et al*, 2008; Jong *et al*, 2010; Chanda *et al*, 2013).

Given the prominent hematopoietic defect caused by *Raldh2*-deficiency, Chanda and colleagues evaluated whether RA signaling might be involved in the establishment of intra-embryonic hematopoiesis. In particular, they took advantage of a non-immunological fluorescent system (Aldefluor, StemCell Technologies) to evaluate the presence of RA-active signaling within intra-embryonic hematopoietic sites. In detail, Aldefluor assay allows the detection of active aldehyde dehydrogenases (ALDHs, thus including RALDHs) within the cells. A fluorescent, diffusible substrate is converted to a negatively charged product by active ALDHs present within the cells. The intra-cellular accumulation of the negatively charged product allows the increase of fluorescence, detectable by flow cytometry. Therefore,

the assay allows the detection of active aldehyde dehydrogenases into a specific cellular population. The authors observed that AA4.1⁺CD144⁺CD45⁺ emerging HSPCs within the E11.5 AGM display ALDH activity and mainly express *Raldh2* (Figure 15 a). By engrafting experiments, the authors confirmed that functional HSCs are restricted to AA4.1⁺CD144⁺CD45⁺ALDH⁺ population in E11.5 AGM whereas AA4.1⁺CD144⁺CD45⁺ALDH^{neg} counterpart is devoid of long term multilineage reconstitution in immunocompromised recipients (Figure 15 b). However, both fractions generate hematopoietic progenitors *in vitro*, albeit the AA4.1⁺CD144⁺CD45⁺ALDH⁺ show a reduced frequency (Figure 15 c). This evidence supports the hypothesis that ALDH activity and RA signaling distinguish the HSC-dependent from the HSC-independent intra-embryonic hematopoiesis.

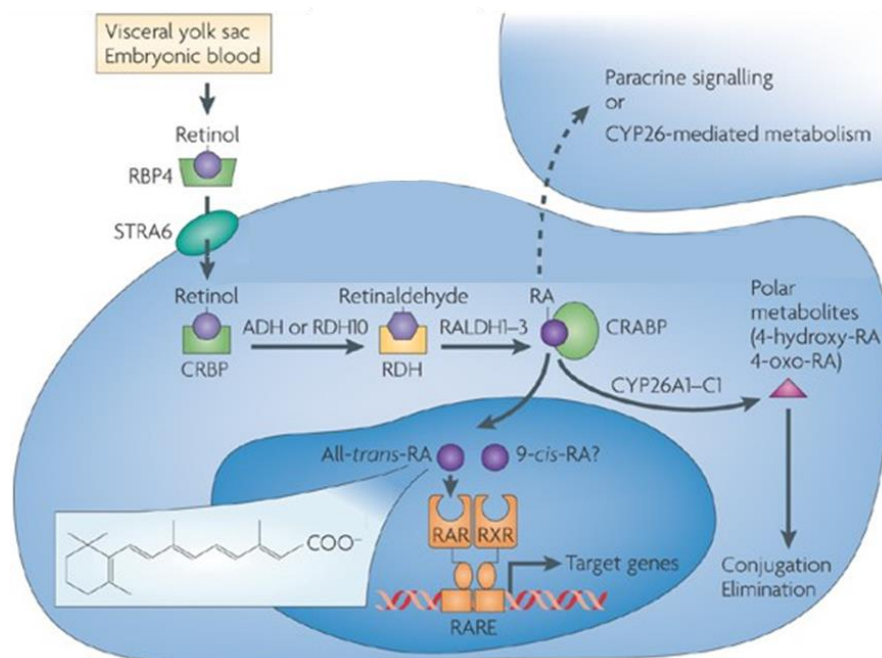


Figure 14 – RA signaling pathway

Adapted from Niederreither and Dollé, *Nature Reviews Genetics*, 2008. The scheme represents the process of retinoic acid (RA) synthesis in placental species. Retinol uptake occurs by retinol binding protein 4 (RBP4). The receptor protein stimulated by retinoic acid (STRA6) transfers retinol intracellularly where is bound by cellular retinol binding proteins (CRBPs). Once in the cytosol, retinaldehydes, mainly retinal dehydrogenase 10 (RDH10, that belong to the family of alcohol dehydrogenases, ADHs), oxidates retinol to retinaldehyde. Next, retinaldehyde dehydrogenases (RALDH1-3) generate retinoic acid (RA) that is bound by cellular retinoic acid bind proteins (CRABPs) that facilitate its nuclear translocation. In the nucleus, RA binds to RA receptors (RARs) and retinoid X receptors (RXRs) and activates the transcription of target genes that own RA-response element (RARE). All-trans-RA is the principal *in vivo* RAR ligand. The 9-cis-RA stereoisomer is the *in vitro* ligand of RXR while its presence *in vivo* is discussed. Cytochrome P450 26 (CYP26) metabolizes RA to 4-hydroxy-RA and 4-oxo-RA that will be further degraded and eliminated. RA acts as autocrine and paracrine factor (dashed arrow).

To address the requirement of RA signaling activation during HSC development, the authors used the *Raldh2^{flox/flox};VE-Cad-Cre* murine model in which *Raldh2* Cre-mediated deletion is driven by *VE-Cadherin* promoter. Transplantation of E11.5 AGM derived from mutant embryos dramatically reduces the long-term engraftment potential in immunocompromised recipients (Figure 15 d). To confirm the positive role of RA signaling in HE maturation and HSC emergence, the authors isolated AA4.1⁺CD144⁺ endothelial cells from E10.5 or E11.5 AGM and cultured them *ex vivo* with ATRA, a pan-RAR agonist or a specific agonist for each of the RAR. After 8 hours of treatment, the authors transplanted the cells at limiting dilution into immunocompromised recipients and assessed the engraftment after 16 weeks. Their results highlight the prominent role of RAR α -mediated signaling in increasing the frequency of HSCs. In fact, the treatment of E10.5 *Raldh2^{fl/fl};VE-Cad-Cre* -derived cells with the RAR α agonist AM580 rescues the emergence of functional HSCs in the embryo. In conclusion, RA signaling is a key regulatory pathway in the formation of the HE and its transition to HSC fate. Hence, RA-dependency is another defining characteristic of HSC-competent HE. However, the role of RA for the specification of the HE lineage has not been tested yet.

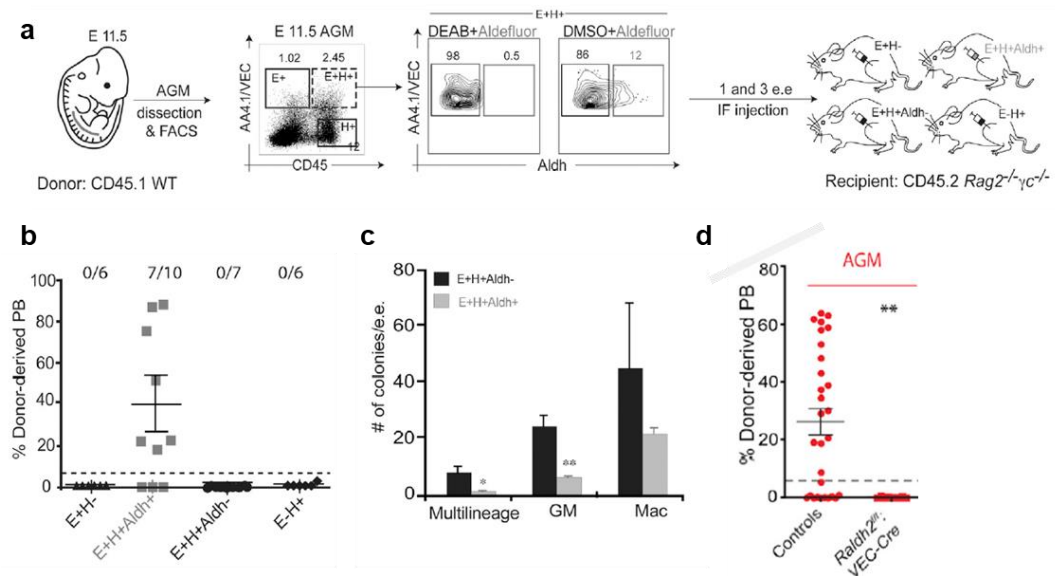


Figure 15 – *Raldh2*-mediated RA synthesis is essential for HSC emergence from the AGM

From Chanda et al, *Cell*, 2013. a) Scheme of the experimental layout: E11.5 AGM was isolated and dissected. Three population were isolated by facs analysis: AA4.1⁺/VEC-CD45⁺ (E+H+) and AA4.1⁺/VEC+CD45⁻ (E+H-) and AA4.1⁺/VEC+CD45⁺ population (E+H+, highlighted by the black dashed rectangle). The latter was analyzed to detect ALDH activity by Aldefluor assay. The Aldefluor positive (E+H+Aldh⁺) and negative (E+H+Aldh⁻) fraction were isolated

and transplanted at 1 embryo equivalent (e. e.) intra-femur (IF) in adult irradiated recipients. E+H- and E-H+ were similarly transplanted. Cells treated with the aldehyde dehydrogenase inhibitor DEAB (DEAB+Aldefluor) were used as negative control. b) Engraftment potential of the transplanted populations: E+H- solid triangle, E+H+Aldh+ solid square, E+H+Aldh- solid circle, E-H+ solid diamond. c) Methylcellulose-based CFC assay to measure the progenitor frequency of E+H+Aldh- (black bar) and E+H+Aldh+ (grey bar). Asterisks indicate the significant difference (* $p < 0.05$, t test). d) Transplantation of E11.5 AGM cells isolated from *Raldh2^{flox/flox};VE-Cad-Cre* or control embryos. The graph shows the frequency of mice engrafted with more than 5% of donor-derived cells.

1.10 Immuno-phenotypical identification of the HE

As we discussed in the previous paragraphs, understanding the mechanisms at the basis of EHT is fundamental to dissect the heterogeneity of hematopoietic development and characterize the generation of different blood cell types, including HSCs. Indeed, a faithful understanding of embryonic development would allow the recapitulation of hematopoiesis *in vitro*, leading to the generation of HSCs from hPSCs that, thus far, have been elusive. To accomplish this, we believe that a crucial step would be to dissect the heterogeneity of HE during embryogenesis. Indeed, the selective identification of the population of origin of the different blood cells within the various hematopoietic waves might reveal program-specific mechanisms that characterize the fate of HE.

Despite the numerous studies and transcriptomic analyses (Swiers *et al*, 2013; Kartalaei *et al*, 2015; Zhou *et al*, 2016; Baron *et al*, 2018; Oatley *et al*, 2020), a specific and selective molecular identification of the HE remains elusive. In fact, before starting the hematopoietic transition, HE shows a phenotypic profile identical to endothelial cells (*i.e.* expression of FLK1/KDR, VE-Cad, CD34) and do not express hematopoietic markers (*i.e.* CD45, CKIT, CD41, Ter119, GFI1b) (Fraser *et al*, 2002; Oberlin *et al*, 2002; Hirai *et al*, 2003; Swiers *et al*, 2013; Zhou *et al*, 2016; Baron *et al*, 2018; Nishikawa *et al*, 1998b). The common immuno-phenotypical identity of hemogenic and non-hemogenic endothelium and the rarity of the former population precludes the effective isolation and study of HE. For instance, at E10.5, only 1 out of 43/49 putative HE cell gives rise to blood cells in the AGM and 1 out of 108 generates endothelial progeny using the same molecular characterization (Swiers *et al*, 2013; Gao *et al*, 2018). Therefore, while enriching the HE, current markers also include a population of cells that will differentiate towards non-hematopoietic lineages and cannot be defined as selective HE markers. The available and most reliable markers to enrich the HE population will be described in the following sub-paragraphs.

1.10.1 *Runx1*+ 23

A valid candidate to distinguish hemogenic from non-hemogenic endothelium murine hematopoietic development, is the *Runx1* +23 enhancer located in the intronic region 23.5 kb downstream to the transcriptional start codon (ATG) of *Runx1* (Nottingham *et al*, 2007; Bee *et al*, 2009a; Ng *et al*, 2010; Swiers *et al*, 2013). The *Runx1* +23 enhancer-reporter mice recapitulate the endogenous *Runx1* expression within sites of hematopoietic development (Nottingham *et al*, 2007; Swiers *et al*, 2013). The advantage of *Runx1* +23 transgenic model is that enhancer expression precedes that of *Runx1*, labeling the endothelial cells with a hemogenic fate early during embryonic development (Swiers *et al*, 2013) and avoiding non-hemogenic endothelial cells or mesenchymal cells in the DA that, on the contrary, are labeled by other *Runx1* reporters (North *et al*, 1999). In fact, *Runx1* +23 reporter marks the hemogenic population already at E9.5 in the P-Sp when 1 out of 540 *Runx1* +23-expressing cells has hematopoietic progeny and 8 out of 540 originate endothelial cells. The frequency of hematopoietic progeny increases to 11 out of 539 marked cells at E10.5 in the AGM whereas the endothelial decreases to 5 out of 539. However, no hemogenic endothelial cells is present in the *Runx1* +23 reporter negative fraction. Hence, while all HE cells can be labeled with the *Runx1* +23 reporter, tracking *Runx1* +23 enhancer does not selectively enrich the HE population as it comprises a broad population devoid of hematopoietic fate. Therefore, *Runx1* +23 enhancer-reporter population cannot be defined as a pure HE. Nevertheless, this model has been useful to dissect the developmental window of HE specification that occurs between E8.5 and E10.5 (Swiers *et al*, 2013). In addition, the system allows to study the dynamics of the HE and to evaluate the regulators upstream to *Runx1* transcriptional activation, dissecting the transcriptional factors involved in the EHT (Nottingham *et al*, 2007). In conclusion, the study of the regulation of *Runx1* transcription through *Runx1* +23 enhancer is critical to dissect HE specification, but *Runx1* +23 enhancer activity alone cannot be used as a reliable HE marker.

1.10.2 *Ly6A*

Ly6a encodes the cell-surface protein SCA1 that selectively distinguishes HSCs located in the murine FL or BM (Spangrude *et al*, 1988; Ikuta & Weissman, 1992; Li & Johnson, 1995; Kim *et al*, 2006). Moreover, SCA1 expression characterizes functional HSCs emerging from the DA in the developing murine embryo

(CD31⁺CKIT⁺SCA1⁺) and distinguishes them from emerging hematopoietic progenitor cells devoid of engrafting potential, negative for its expression (Bruijn *et al*, 2002; McGrath *et al*, 2015; Kartalaei *et al*, 2015).

To characterize *Ly6a* expression during murine embryonic development, Dzierzak group established a *Ly6A-GFP* murine model (Bruijn *et al*, 2000). As the endogenous protein, the authors observed the reporter expression on hematopoietic cells within IAHCs at E10.5. In addition, transgenic *Ly6a-GFP* expression defines a subpopulation of endothelial cells (CD31⁺GFP⁺) within the endothelial layer lining the E10.5-E11 AGM. Notably, CD31⁺GFP⁺ cells show an upregulation of genes involved in the EHT (*i.e.* *Runx1*, *Sox18*, *Sox17*, *Sox7*, *Gfi1*, *Notch1*, *Notch4*) compared to CD31⁺GFP^{neg} endothelial cells. Clear proof of the hemogenic fate of GFP⁺ endothelial cells came from live imaging analysis of E10.5 AGM in which *Ly6A-GFP* expression distinguishes the CD31⁺ endothelium that will transition to hematopoiesis (Boisset *et al*, 2010).

Ly6A-GFP is not detected intra-embryonically before E9.5 and it is never detected in the YS. The lack of *Ly6A-GFP* within extra-embryonic HE can be considered as additional evidence of the heterogeneity of the HE. In fact, while both EMP and intra-embryonic EHT depends on RUNX1 expression at HE level (Paragraph 1.7), the emergence of EMP progenitors or HSC can be uncoupled by *Ly6a* expression. By means of *CBFβ*-deficient murine embryos that show dramatic impairment in hematopoietic development (Wang *et al*, 1996b), Chen and colleagues showed that the ectopic over-expression of *GFP/CBFβ* transgene driven by the promoter of the endothelial gene *Tie2* (Miller *et al*, 2002) rescues the formation of EMPs but it is not sufficient to HSC emergence (Chen *et al*, 2011a). On the contrary *Ly6a*-mediated *GFP/CBFβ* expression restores HSCs formation while not supporting EMP emergence. In conclusion, the formation of hematopoietic progenitors with different potential from the HE might rely on similar mechanisms but can be distinguished by specific marker expression. In this context, *Ly6a* distinguishes HSC-competent HE and does not equally characterize the extra-embryonic HE that gives rise to EMPs.

Despite *Ly6a-GFP* reliably tracks HSC-competent HE, the SCA1 endogenous cell-surface protein is not equally reliable or even detectable, not allowing a similar flow cytometric-based isolation of the HE (or either HSCs). Differently from the two endogenous copies of *Ly6a* gene, the transgenic mice have six *Ly6a* extra copies,

thus creating a more intense and detectable signal by flow cytometry. Moreover, the complex post-translational modifications required for the cell-surface localization of SCA1, are skipped in the transgenic LY6A-GFP form, that is quickly detectable in the cytoplasm right after being translated. Therefore, a specific immuno-phenotypic identity of the HE based on SCA1 expression is only available by using transgenic models. However, *Ly6a* expression has been evaluated during murine development and not studied in other vertebrate models. In addition, unfortunately, the human ortholog of murine SCA1 has not been identified yet.

1.10.3 CD44

Recently, Oatley and coworkers identified CD44 as a marker that distinguishes a sub-population of VE-CAD⁺Kit^{neg} cells primed to the hematopoietic transition in E9.5, E10 and E11 AGM (Oatley *et al*, 2020). They observed that CD44 expression distinguishes four sub-populations within VE-CAD⁺ cells: CD44^{neg}, CD44^{low}Kit^{neg}, CD44^{low}Kit^{pos}, CD44^{high}. While the latter two populations identified cells already committed to hematopoiesis, CD44^{neg}, CD44^{low}Kit^{neg} cells characterize the endothelial cells lining the lumen of the DA. To test the hemogenic capacity, they isolated CD44^{neg} CD44^{low}Kit^{neg} cells and co-cultured them *ex vivo* on OP9 co-culture system. They observed that hematopoietic potential segregated uniquely to the CD44^{low}Kit^{neg} fraction. In addition, the application of a CD44 blocking antibody that prevents the interaction with its ligand, the hyaluronan, impairs the budding of hematopoietic cells. Likewise, blocking CD44 interaction with hyaluronan during mESC-derived hematopoietic differentiation *in vitro*, impairs the frequency of CD144^{neg}CD41⁺ committed hematopoietic progenitors while increasing those of endothelial cells. Similar effect has been showed using hyaluronidase, that catalyzes the degradation of hyaluronan, and methylumbelliferone that blocks hyaluronan synthesis. In conclusion, Lancrin group showed that CD44 is useful marker to enrich HE population in VE-CAD⁺ cells derived from the AGM of E10-E11 murine embryos. Moreover, CD44 acts as regulator of the EHT since preventing its binding with hyaluronan affects blood cell formation. However, CD44 also labels emerging hematopoietic cells and non-hemogenic arterial cells in murine AGM.

CD44 has been also characterized as HE marker during human intra-embryonic hematopoiesis. In fact, CD44 is expressed in IAHCs and the underlying endothelium of human embryonic DA at 32 days, Carnegie Stage (CS) 13, that

corresponds to E10.5 of murine development (Watt *et al*, 2000). Moreover, Zeng and colleagues analyzed the single-cell transcriptomic differences of CD34⁺CD235a^{neg}CD45^{neg}CD44^{+/neg} endothelial population at similar developmental stage. They observed that the CD44⁺ fraction includes all the *Runx1* expressing cells (Zeng *et al*, 2019). Although no functional assay has been performed, transcriptomic data parallel the studies performed on mouse embryos, placing CD44 as promising marker of the HE during intra-embryonic hematopoietic development. Nevertheless, CD44 is widely expressed on vascular endothelial cells and it is broadly implicated with endothelial cell functions in human and mouse (Griffioen *et al*, 1997; Nandi *et al*, 2000; Cao *et al*, 2006; Flynn *et al*, 2013). In particular, most of aortic endothelial cells in human and murine AGM express CD44 at the time of EHT (Watt *et al*, 2000; Oatley *et al*, 2020). Therefore, CD44 alone might enrich but not selectively distinguish a rare population as the HE.

1.10.4 Lyve1

In 2016, Lee and colleagues identified Lymphatic vessel hyaluronan receptor-1 (Lyve1) as marker of YS and vitelline vessels' endothelial cells (Lee *et al*, 2016). Already at E7.5 a sub-population of Tie2⁺CD31⁺ endothelium express LYVE1. Using *Lyve1-Cre;Rosa^{mT/mG}* fluorescent reporter mice, the authors lineage-traced *Lyve1* expressing cells by *GFP* expression after Cre-mediated recombination. They observed that the majority of E8.5-E9.5 YS and vitelline vessels endothelium is marked by *Lyve1-Cre* whereas DA and placenta endothelium is not. Despite YS endothelium is largely traced by *Lyve1*, not all the YS-derived hematopoietic progenitors originate from *Lyve1*-expressing endothelial cells. In fact, erythrocytes from the first, primitive hematopoietic wave do not derive from *Lyve1*-expressing endothelial cells. Nevertheless, the majority of E9.5 YS EMPs and CD41⁺cKit⁺ hematopoietic progenitors from the second extra-embryonic hematopoietic wave do. As previously reported (McGrath *et al*, 2015), erythroid progenitors from the second extra-embryonic hematopoietic wave colonize the FL to complete their differentiation and support the embryonic needs before the establishment of the HSC-dependent erythropoiesis. Indeed, *Lyve1-Cre* labeled YS-derived erythroid progenitors contribute to FL erythropoiesis before being replaced by HSCs after E13.5. Moreover, the authors reported the presence of a subset of *bona fide* HSCs in E11.5-E16.5 FL, possibly arising from *Lyve1*-expressing cells in the VA. However, the authors do not show any functional and precise immuno-phenotypic characterization of the HSC

pool. In conclusion, *Lyve1* expression marks a population of YS endothelial cells that includes the HE with EMP fate. However, the authors miss to thoroughly characterize the ontogeny of other YS hematopoietic progenitors as lymphoid progenitors, know to derive from E9.0 YS endothelium (Yoshimoto *et al*, 2011). Therefore, *Lyve1*-expressing endothelial cells in the YS might not track the totality of HE population. In addition, *Lyve1* expression has not been characterized during hematopoietic development of other vertebrate models.

1.10.5 ACE

Angiotensin converting enzyme (ACE) has been reported to track aortic endothelial cells and IAHCs of 4-week human embryos (Jokubaitis *et al*, 2008). In detail, the authors observed that the cell surface monoclonal antibody BB9 that tracks ACE expression, labels CD34⁻ and CD144-expressing cells within the ventral domain of the DA. Isolated BB9⁺ cells from the AGM of 28 day-old human embryos generates hematopoietic cells *ex vivo*, whereas BB9^{neg} cells not (Jokubaitis *et al*, 2008). Moreover, a subset of CD34⁺CD45⁺ emerging hematopoietic cells from the DA express BB9 at similar stages, suggesting they originated from BB9⁺ HE (Jokubaitis *et al*, 2008). Similarly, endothelial cells lining the lumen of the DA and the emerging IAHCs of E9.5-E10.5 mouse embryos express ACE. In particular, the ACE⁺ endothelial fraction (CD144⁺ACE⁺CD41^{neg}CD45^{neg}TER119^{neg}) within the E10.5 AGM shows robust erythro-myeloid colonies *ex vivo* while the corresponding ACE^{neg} counterpart is depleted of hematopoietic potential (Fadlullah *et al*, 2021).

Notably, ACE expression is not restricted to intra-embryonic hematopoietic sites. Indeed, YS endothelial cells express ACE in E9 mouse embryos, suggesting it may also track extra-embryonic hemogenic precursors (Julien *et al*, 2021). Given the expression of ACE within hematopoietic sites, Julien and colleague interrogated its function during hematopoietic development.

The physiological role of ACE is the regulation of blood pressure and homeostasis of fluid by acting in the renin-angiotensin system (RAS). In RAS, Angiotensinogen (AGT) is cleaved by renin (REN) into angiotensin I. ACE catalyzes angiotensin I cleavage into its active form, the angiotensin II. Thus, angiotensin II can bind to the receptors AT1 or AT2 and exerts its function (Bernstein & Berk, 1993). By *ex vivo* culture of E9 murine P-Sp, the stimulation of RAS increases hematopoietic

cells emergence while antagonizing the pathway has an opposite effect (Julien *et al*, 2021). Therefore, ACE might be considered not only as conserved marker of endothelial cells with hemogenic potential, but recent data suggest it has a function in hematopoietic cells emergence.

1.11 Modeling human hematopoiesis in a dish

Embryonic hematopoietic development is mainly conserved in mammals. Despite extensive studies shed light on this process in different model organisms, our knowledge of human hematopoiesis is still limited. In fact, human embryos are rare, and their manipulation is limited by ethical constraints. In this scenario, pluripotent stem cells (PSCs) represent a powerful tool to wide our understanding of human hematopoiesis. In fact, mESCs- and human PSCs (hPSCs)- derived *in vitro* differentiation can effectively recapitulate hematopoietic development *in vivo*, paralleling similar mechanisms and signaling observed in model organisms (Keller, 2005; Ackermann *et al*, 2015).

Currently, the most used hPSC-based hematopoietic differentiation systems rely on serum-free 2-dimension (2D) or 3D cultures (embryoid body, EB). hPSC co-culture on stromal cells in medium containing serum is a less diffused model of hematopoietic differentiation. However, the *in vitro* hPSC-based hematopoietic differentiation recapitulates the whole spectrum of hematopoietic progenitors *in vivo* excluding HSCs. The induction of different hematopoietic programs is achieved by an orchestrated activation/inactivation of multiple signaling pathways at specific stages that allows to reproduce in a dish the events that take place during embryonic development. Despite many published protocols report a successful recapitulation of human hematopoietic development *in vitro*, an extensive evaluation of all of them is beyond the scope of this thesis. Therefore, I will only introduce the hPSC-based differentiation methods adopted during the work of this thesis. In particular, the differentiation method is based serum- stroma-free EB culture that allows the specific and reproducible modulation of signaling pathways fundamental for extra- or intra-embryonic hematopoiesis (Figure 16 a, b).

The first step towards the recapitulation of embryonic hematopoiesis is mimicking the gastrulation process, in particular the formation of the PS, fundamental for the mesoderm induction. Different mesodermal lineages (*i.e.*

posterior or lateral plate mesoderm) selectively contribute to the different hematopoietic waves. Analyses of the signaling pathways required for the specification of either mesodermal types, led to the identification of bone morphogenic protein (BMP), fibroblast growth factor (FGF), Activin/Nodal and WNT- β catenin as fundamental signals contributing to mesoderm induction and patterning, coherently with previous studies performed in murine embryos (Chadwick *et al*, 2003; Kennedy *et al*, 2006; Schier & Shen, 2000; Pick *et al*, 2007; Nostro *et al*, 2008; Wang & Nakayama, 2009; Yu *et al*, 2011). The relevance of mesodermal patterning is in line with the existing signaling polarization of the developing embryos. In the posterior part of the PS, where the hematopoietic mesoderm is formed, the Activin-Nodal signaling is particularly active. Emerging mesodermal cells that migrate anteriorly are exposed at Wnt inhibitors secreted by endodermal cells (Sadler & Langman, 2004; Ditadi *et al*, 2016). These cells will then colonize the extra-embryonic YS and generate YS blood islands that give rise to the first hematopoietic cells (Palis *et al*, 1999). On the other hand, mesoderm that will give rise to intra-embryonic hematopoietic progenitors will migrate through a ventral-posterior axis with limited Wnt and Activin-Nodal signaling activation (Sadler & Langman, 2004; Ditadi *et al*, 2016).

To recapitulate WNT-dependent, extra-embryonic-like hematopoietic progenitors from hPSCs, the initial mesodermal induction by BMP4 is followed by the activation of Activin-Nodal signaling (Kennedy *et al*, 2012) and the inhibition Wnt- β catenin signaling (*i.e.* by using the WNT antagonist IWP2) (Sturgeon *et al*, 2014). This results in the specification of extra-embryonic-like mesoderm characterized by the expression of the mesodermal marker KDR and the cell surface protein glycoprotein a (CD235a) (Sturgeon *et al*, 2014). After the mesodermal specification and patterning, 3-4 days after the initiation of the differentiation from hPSCs, the specification of endothelial and hematopoietic lineages occurs by addition of VEGF and bFGF. At day 6 of differentiation, the culture is supplemented with pro-hematopoietic cytokines (SCF, IL11, IL6, IGF1, EPO). At this stage, the cells already express endothelial markers as CD34 and VE-CAD. In addition, WNT-independent primitive hematopoietic progenitors start to emerge, distinguished by the acquisition of the early hematopoietic marker CD43. At day 8 of differentiation, CD34⁺CD43^{neg} progenitors with endothelial-like features include the HE population. Notably, CD34⁺CD43^{neg} progenitors emerging within this wave do not express *HOXA* genes whose expression is restricted to the endothelial and hematopoietic cells arising from intra-embryonic hematopoietic waves (Ng *et al*, 2016; Dou *et al*, 2016).

CD34⁺CD43^{neg} cells will undergo EHT to generate myeloid progenitors, ϵ - and γ -globin-expressing erythroid progenitors and NK progenitors whereas they are devoid of T lymphoid potential (Sturgeon *et al*, 2014; Dege *et al*, 2020). Such phenotype is coherent with EMPs emerging from the YS during murine development (McGrath *et al*, 2015).

On the other hand, the induction of WNT-dependent intra-embryonic-like hematopoiesis relies on time-dependent activation of Wnt signaling after BMP4-mediated mesodermal induction. Wnt signaling activation through the addition of WNT agonist CHIR990201 to the culture, in the absence of Activin-Nodal signaling, shifts the differentiation towards WNT-dependent- intra-embryonic like-hematopoietic progenitors (Ditadi & Sturgeon, 2016; Ditadi *et al*, 2015; Sturgeon *et al*, 2014).

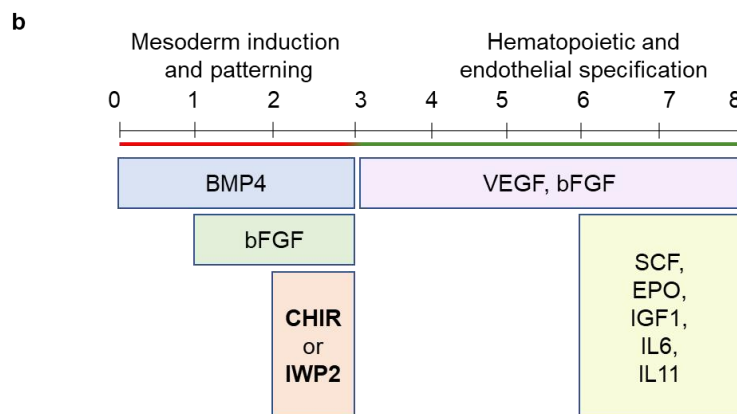
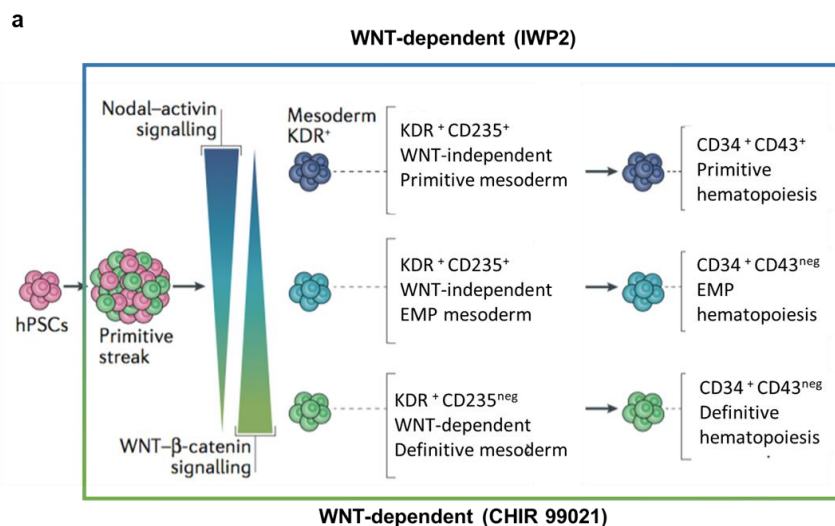


Figure 16 – Scheme of *in vitro* hematopoietic differentiation from hPSCs

a) Adapted from Ditadi *et al*, Nature reviews, 2016. Representative scheme of hematopoietic differentiation from hPSCs. After the induction of the primitive streak the modulation of Nodal/Activin and WNT signaling allows the formation of WNT-independent-extra-embryonic-like mesoderm (KDR^+CD235^+) or of WNT-dependent-intra-embryonic-like mesoderm (KDR^+CD235^{neg}). From the respective mesoderm, primitive, EMP or definitive-like hematopoietic progenitors arise. b) Schematic representation of time-specific cytokines manipulation to recapitulate extra- or intra-embryonic like hematopoietic programs from hPSCs. For the first two days of differentiation, BMP4 signaling favors the differentiation of hPSCs to a PS-like state. At day 2, the mesoderm is patterned towards WNT-independent extra-embryonic-like hematopoietic culture, using the WNT antagonist IWP2 or towards WNT-dependent intra-embryonic-like hematopoietic culture, using the WNT agonist CHIR 99021. At day 4, the mesoderm is specified, and further culture support the endothelial (VEGF and bFGF) and hematopoietic (SCF, EPO, IL11, IL6, IGF1) specification. At day 8, the HE population is specified and originates hematopoietic progenitors typical of the different hematopoietic waves.

Importantly, the mesodermal population that will give rise to intra-embryonic-like hematopoietic progenitors can be distinguished by $KDR^+CD235a^{neg}$ immunophenotype. Thus, both extra- and intra-embryonic hematopoietic programs are defined early in development, distinguished by opposite Wnt-dependency during mesodermal formation. The following steps of differentiation are in common for both hematopoietic programs. At day 8 of differentiation $CD34^+CD43^{neg}$ cells include the HE population and is marked by *HOXA* genes expression, hallmark of intra-embryonic HSPCs (Ng *et al*, 2016; Dou *et al*, 2016). To generate multilineage erythroid, myeloid, T and NK lymphoid progenitors, $CD34^+CD43^{neg}$ progenitors rely on Notch signaling (Ditadi *et al*, 2015), characteristic feature of the intra-embryonic hematopoiesis (Kumano *et al*, 2003; Robert-Moreno *et al*, 2005; Robert-Moreno *et al*, 2008; Porcheri *et al*, 2020). In fact, Notch signaling manipulation *in vivo and ex vivo* affects HSCs emergence (Bigas & Espinosa, 2012).

Despite hPSC-derived WNT-dependent differentiation recapitulates fundamental aspects of intra-embryonic hematopoiesis, the physiological generation of transplantable HSCs from WNT-dependent HE has been unsuccessful. Nevertheless, the enforced overexpression of seven hematopoietic transcription factors (*ERG*, *HOXA5*, *HOXA9*, *HOXA10*, *LCOR*, *RUNX1* and *SPI1*) allows the HSC emergence from hPSC-derived, WNT-dependent HE (Sugimura *et al*, 2017) obtained with the protocol we described (Ditadi *et al*, 2015). Although this approach is not translatable to the clinics since involves the over-expression of proto-oncogenic factors, it proves that the hPSC-based *in vitro* platform we employ might be prone to generate HSCs upon additional manipulations. Nevertheless, the lack of a selective immunophenotypical identification of the HE during human embryonic development,

hampers the identification of the molecular mechanisms specifically required to the emergence HSC-fated HE. Indeed, at day 8, CD34⁺CD43^{neg} cells include three different sub-populations of endothelial cells that can be identified by CD184 and CD73 expression (Ditadi *et al*, 2015; Sturgeon *et al*, 2014). The CD34⁺CD43^{neg}CD184⁺CD73^{mid} population shows arterial-like features, and it is devoid of any hematopoietic potential. Similarly, CD34⁺CD43^{neg}CD184^{neg}CD73^{high} has no hematopoietic potential but shows venous-like features. On the contrary, the isolation of the CD34⁺CD43^{neg}CD184^{neg}CD73^{neg} fraction shows an enrichment in HE with multipotent hematopoietic potential (from WNT-dependent mesoderm) or EMP potential (from WNT-independent mesoderm) (Figure 17). This fraction shows endothelial-like feature as the ability to attach on Matrigel-coated cell-culture dish (Arnautova & Kleinman, 2010). In addition, these cells undergo EHT and give rise to RUNX1⁺CD45⁺ hematopoietic cells (Ditadi *et al*, 2015; Ditadi & Sturgeon, 2016). Single cell analysis performed in WNT-dependent hematopoietic cultures showed that 1 out of 38 CD34⁺CD43^{neg}CD184^{neg}CD73^{neg} cell generates hematopoietic progeny and 1 out of 5 generates endothelial cells in WNT-dependent intra-embryonic-like hematopoietic cultures. In addition, the CD34⁺CD43^{neg}CD184^{neg}CD73^{neg}DLL4^{neg} fraction further enriches the HE population. In fact, in this case 1 out of 4 CD34⁺CD43^{neg}CD184^{neg}CD73^{neg}DLL4^{neg} generate hematopoietic cells while 1 out of 9 endothelial lineages. Notably, endothelial and hematopoietic potential never derive from the same cell as previously described *in vivo* (Swiers *et al*, 2013).

Differently from what we observed, another group showed that hPSC-derived RUNX1⁺ hemogenic progenitors are instead associated with the DLL4⁺ fraction of CD144⁺CD43^{neg}CD73^{neg} endothelial cells (Uenishi *et al*, 2018). It is important to note that Uenishi and colleagues do not discriminate among the different hematopoietic programs so it is difficult to assess the origin of such HE population. Nevertheless, further experiments are needed to evaluate whether CD34⁺CD43^{neg}CD184^{neg}CD73^{neg}DLL4^{neg} cells obtained through our WNT -dependent or -independent hematopoietic cultures, transit to a DLL4⁺ state while undergoing the EHT. This might imply the requirement of a Notch-mediated arterialization during the EHT in one and/or the other hematopoietic program.

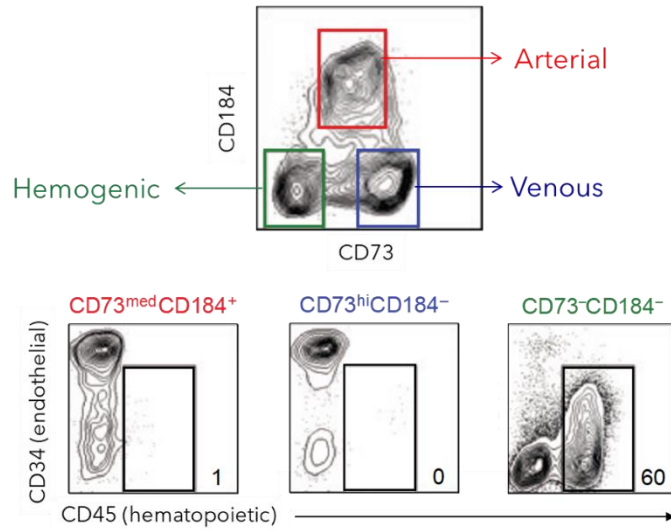


Figure 17 - $CD34^+CD43^{neg}CD73^{neg}CD184^{neg}$ cells show HE potential from hPSCs

Representative plot of the endothelial populations obtained at day 8 of WNT-dependent differentiation from hPSCs. $CD73^{med}CD184^+$ fraction (red) expresses arterial markers and has no hemogenic potential. $CD73^{hi}CD184^{neg}$ fraction (blue) expresses venous markers and has no hemogenic potential. $CD73^{hi}CD184^{neg}$ fraction (green) does not express neither arterial nor venous marker but has hemogenic potential.

In conclusion, our established hPSC-based *in vitro* system faithfully recapitulates HSC-independent-, extra-embryonic- and intra-embryonic-like hematopoietic development by modulating signaling pathways involved in the specification of either one or the other program (Ditadi & Sturgeon, 2016; Ditadi *et al*, 2015; Sturgeon *et al*, 2014). However, current markers available both *in vivo* and *in vitro* do not allow the selective identification of human HE population, precluding its study and the definition of the mechanisms involved in the determination of specific hematopoietic fates.

We believe that dissecting the heterogeneity of HE would shed the light on the mechanisms of blood development, setting the basis for the *in vitro* generation of HSCs. In addition, further manipulation of signaling pathways known to be involved in hematopoietic development *in vivo*, such as the RA signaling (Chanda *et al*, 2013), might be essential to allow the emergence of HSC-competent HE. The generation of HSCs *in vitro* as well as an efficient production of specific blood cell types from patient-derived iPSCs would represent an important milestone for the treatment of several hematological disorders and for the deep understanding of specific pathological mechanisms through PSC-based disease modeling.

2. Aim of the work

During embryonic development, hematopoietic cells originate from a specialized endothelial layer, the hemogenic endothelium (HE), throughout a tightly regulated process, the endothelial to hematopoietic transition (EHT). Despite the endothelial descendancy of blood cells is well established, the HE is a very transient and heterogeneous population, whose identity is still unknown. The lack of selective markers identifying HE makes its precise isolation and characterization difficult, especially in the human, where hematopoietic sites are not easily accessible.

Throughout this work, we propose to identify a selective immuno-phenotype of the HE. The specific isolation and tracing of HE cells will allow us to study their contribution to hematopoietic embryonic development. To accomplish this, we will perform transcriptomic analysis on human embryos at typical stage of hematopoietic development. The candidate HE population will be functionally validated by *ex vivo* analysis of human embryonic samples. In addition, we will parallel the findings obtained on human embryos using an *in vitro* human pluripotent stem cell (hPSC)-based hematopoietic differentiation. The concordance of our *ex vivo* and *in vitro* results will further support the hPSC-based *in vitro* differentiation as a powerful tool to recapitulate and dissect human embryonic development.

In conclusion, the project will offer the opportunity to dissect the heterogeneity of HE during human embryonic development. In addition, we believe that our results will help to understand the mechanisms involved in the emergence of hematopoietic progenitor cells and/or HSCs both *in vivo* and *in vitro*, offering broad future applications in clinical therapeutics and disease modeling studies.

3. Results

3.1 CD32 is differentially expressed in human embryonic endothelial cells with hemogenic potential

The HE is a specialized endothelial population that shares cell surface markers with non-hemogenic endothelial cells (*i.e.*, CD34, CD144 (Kabrun *et al*, 1997; Oberlin *et al*, 2002; Nishikawa *et al*, 1998a)). During the transition to hematopoiesis, the HE progressively loses the endothelial markers to acquire a committed hematopoietic identity (*i.e.* CD45, CD43) (Eilken *et al*, 2009). The specification of the hematopoietic fate in HE is accompanied by the expression of specific transcription factors (*i.e.* RUNX1, SCL, GATA2) that distinguish these cells from the other endothelial cells. However, the expression of these transcription factors is maintained by emerging and committed hematopoietic cells and identify other cellular types within hematopoietic sites (*i.e.* also sub-aortic mesenchymal cells express *Runx1* (North *et al*, 1999; Nottingham *et al*, 2007)). Therefore, they cannot be used to uniquely identify the HE. Since the HE is a transient and rare population characterized by impressive heterogeneity, the lack of a selective identification prevents the characterization of the mechanisms driving the transition to blood as well as the identification of the functional heterogeneity observed across the different hematopoietic waves.

In order identify a specific immuno-phenotype of the HE, we established a collaboration with Manuela Tavian's lab at Inserm, Strasbourg, France. The work of Manuela Tavian has been pivotal to study human embryonic hematopoietic development and to identify ACE (BBA clone, see Introduction, paragraph 1.10.5) as marker of human embryonic CD34⁺ cells with hemogenic potential (CD34⁺ACE⁺CD45^{neg}) (Jokubaitis *et al*, 2008). In detail, ACE expression in the P-sP starts between 23 and 26 days of gestation (CS10-12) but, at this stage, ACE⁺ cells have a limited hematopoietic potential *ex vivo* (Sinka *et al*, 2012). At CS13 the hemogenic population is enriched within CD34⁺ACE⁺CD45^{neg} cells in the AGM (Jokubaitis *et al*, 2008). Coherently, the Tavian's lab observed that ACE expression overlapped with the one of RUNX1 in the DA of CS13 human embryos (Figure 18 a). Similarly to RUNX1 (North *et al*, 1999; Nottingham *et al*, 2007), ACE expression is not limited to the endothelial layer but spreads to the sub-aortic mesenchyme. At 34 days of gestation (CS15), ACE is expressed in the endothelial layer of the DA but also within the emerging hematopoietic clusters (Sinka *et al*, 2012).

To evaluate ACE as a marker of hPSC-derived HE, we tested its expression in hPSC-derived WNT-dependent hematopoietic cultures (Sturgeon *et al*, 2014). We observed that ACE (BB9) tracks the majority of the CD34⁺ population (Figure 18 b). Therefore, ACE cannot be considered as selective marker of hPSC-derived HE.

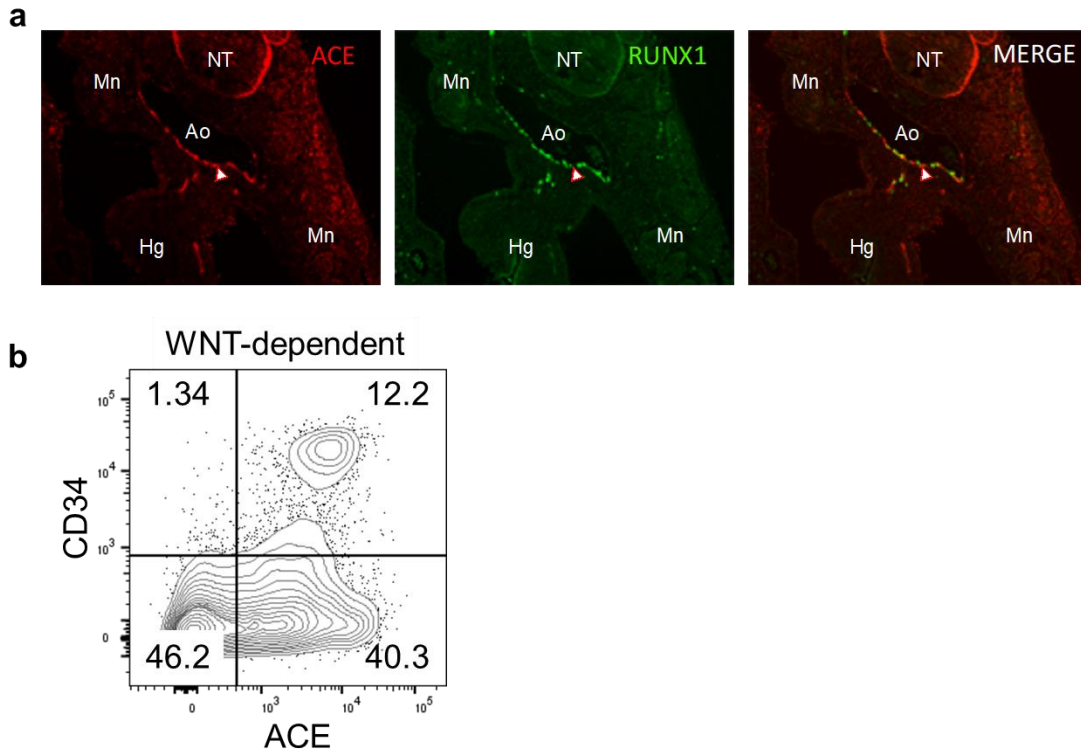


Figure 18 – ACE tracks RUNX1⁺ cells in the AGM of CS13 human embryos but does not enrich hPSC-derived HE

a) Transverse section of a CS13 human embryos, that includes the AGM region, immunostained with ACE (left panel), RUNX1 (middle panel) and merged picture (right panel); *n*=3 independent. NT, neural tube; Mn, mesonephros; Ao, aorta; Hg, hindgut; b) Representative plot of CD34 and ACE expression at day 8 of hPSC-derived WNT-dependent hematopoietic culture. Gated on SSC/FSC/Live, *n*=2, independent.

In the attempt to identify a selective HE marker, we performed transcriptomic analysis of CD34⁺ACE⁺CD45^{neg} cells that include the hemogenic population (referred to as ACE⁺) and CD34⁺ACE⁺CD45^{neg} non-hemogenic endothelial cells (referred to as ACE^{neg}) isolated from the AGM of four CS12-13 human embryos (28-32 days of gestation). The four human embryos will be referred to as E1, E2, E3, E4. Differential gene expression analysis identified 785 differentially expressed genes (DEGs) between ACE^{neg} (E1_ ACE^{neg}, E2_ ACE^{neg}, E3_ ACE^{neg}, E4_ ACE^{neg}) samples when compared to ACE⁺ (E1_ ACE⁺, E2_ ACE⁺, E3_ ACE⁺, E4_ ACE⁺) ones. In detail, 345 genes resulted as upregulated in ACE^{neg} samples and 440 downregulated (Figure 19

a). Using unsupervised hierarchical clustering by k-means and principal component analysis (PCA) on the DEGs, ACE^{neg} samples clustered together when compared to ACE⁺ samples (Figure 19 b) confirming the unique nature of both populations.

At the population level, both ACE⁺ and ACE^{neg} samples express high levels of endothelial genes (*CD34*, *CDH5*, *PECAM1*, *TEK*). However, ACE⁺ show an enrichment for genes classically associated with arterial cells (*GJA5*, *DLL4*, *CXCR4*, *HEY2*) and HECs (*MYB*, *GFI1*, *CD44*) (Figure 19 c). Therefore, the transcriptional analysis highlighted that ACE⁺ endothelium enriches a population that expresses genes involved in HE activity compared to ACE^{neg} cells. In addition, ACE⁺ samples include cells with an arterial-like phenotype. Despite *ACE* transcript is expressed at low level, it is enriched in ACE⁺ samples, confirming the quality of the sorting and the reliability of the transcriptomic data.

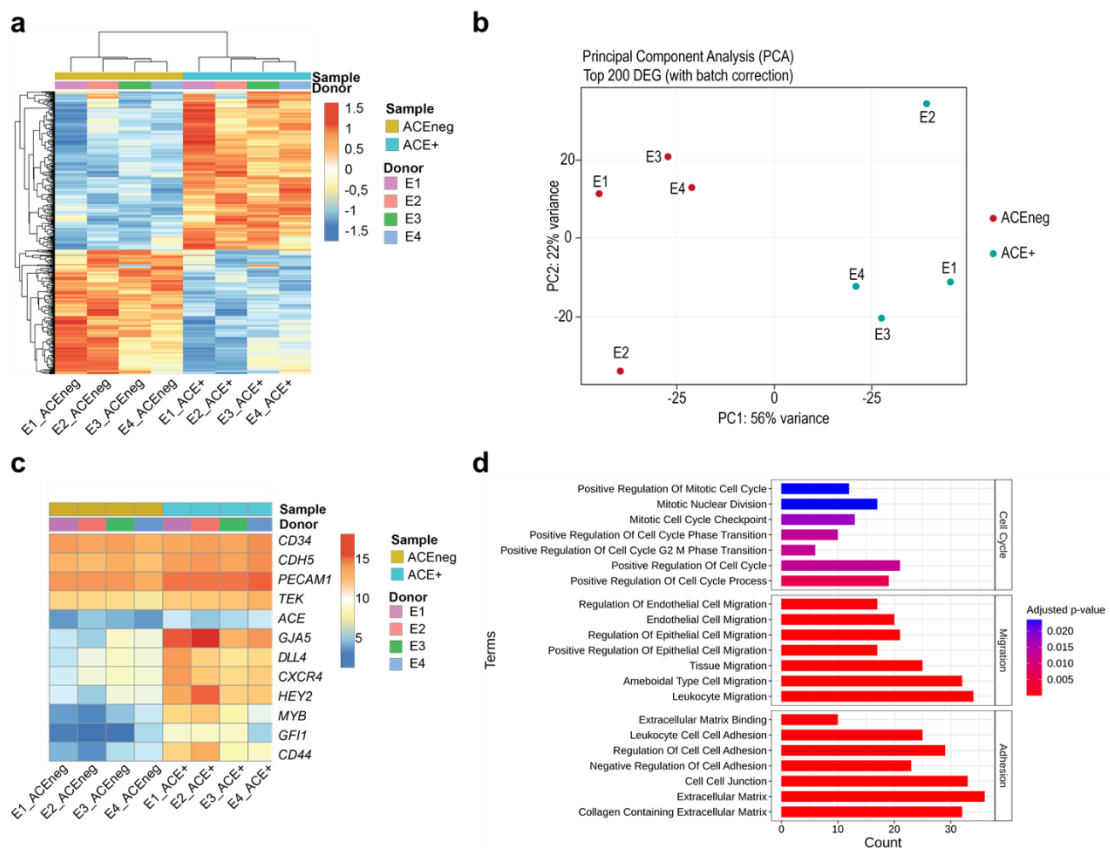


Figure 19 – ACE-expressing cells enrich the expression of arterial and hematopoietic genes.

a) Heatmap of the DEGs obtained from the comparison of ACE^{neg} (E1_ACE^{neg}, E2_ACE^{neg}, E3_ACE^{neg}, E4_ACE^{neg}) against ACE⁺ (E1_ACE⁺, E2_ACE⁺, E3_ACE⁺, E4_ACE⁺) samples obtained from the four CS13 human embryos (E1, E2, E3, E4). The *rlog* gene expression values

are shown in rows. Tiles are colored according to up (red) or down (blue) regulation. b) Heatmap showing the expression of selected endothelial (*CD34*, *CDH5*, *PECAM*, *TEK*), arterial (*GJA5*, *DLL4*, *CXCR4*, *HEY2*) and hemogenic (*ACE*, *MYB*, *GFI1*, *CD44*) genes within ACE^+ ($E1_ACE^+$, $E2_ACE^+$, $E3_ACE^+$, $E4_ACE^+$) or ACE^{neg} ($E1_ACE^{neg}$, $E2_ACE^{neg}$, $E3_ACE^{neg}$, $E4_ACE^{neg}$) samples obtained from four CS13 human embryos ($E1$, $E2$, $E3$, $E4$). The $rlog$ gene expression values are shown in rows. Tiles are colored according to up (red) or down (blue) regulation. c) Barplot showing significant enriched functional Gene Ontology (GO) terms (adjusted p -value < 0.05) of the differentially expressed genes from the comparison between ACE^+ versus ACE^{neg} samples. The barplot shows enriched terms grouped by custom categories: cell cycle in downregulated genes and migration and adhesion in upregulated genes.

Starting from the DEGs list, we performed a Gene Set Enrichment Analysis (GSEA) using the Gene Ontology (GO) and Molecular Signatures Database (MSigDB) gene sets to identify the presence of enriched functional categories. In particular, we observed ACE^+ cells are associated with migration, cell-cell and extra-cellular matrix related GO terms in line with the remodeling occurring during the EHT process (Figure 19 d) (Lie-A-Ling *et al*, 2014). On the contrary, ACE^+ cells are negatively associated with cell-cycle-related GO-terms, suggesting that at a population level they are undergoing an active arterialization process which requires cell growth suppression (Luo *et al*, 2021). In summary, ACE -expressing cells within the AGM of CS1fr3-14 human embryos show an enriched expression of arterial genes and pivotal genes involved in hematopoietic development.

To identify specific HE markers, we focused our attention on differentially expressed genes coding for cell surface proteins enriched in ACE^+ cells compare to ACE^{neg} population. Among them, *FCGR2B*, ranked as the third cell-surface gene enriched in ACE^+ cells, caught our attention (Figure 20 a, b). *FCGR2B* (isoform B of the Fc γ receptor 2 or CD32B) is an immunoglobulin G (IgG) low affinity receptor, part of the immunoglobulin superfamily, that primarily binds the Fc portion of IgG (Nimmerjahn & Ravetch, 2008). The human FCGR super-family is divided in three classes (FCGR1, FCGR2 and FCGR3) according to their molecular weight, cell-surface expression, and IgG affinity. The FCGR2 family includes two activator receptors, CD32A and CD32C and an inhibitory receptor, CD32B. They share a high amino-acidic identity (roughly 85%) and the same extracellular binding domain while differing mainly in the cytoplasmic domain in which the formers contain the immunoreceptor tyrosine-based activation motif (ITAM) and the latter the immunoreceptor tyrosine-based inhibitory motif (ITIM) (Ravetch & Lanier, 2000; Nimmerjahn & Ravetch, 2006). CD32B is widely distributed on hematopoietic cells and its activation by IgG-antigen complex binding regulates the release of inflammatory cytokines, the antibody production, and the cell-mediated antibody-dependent cytotoxicity

(Nimmerjahn & Ravetch, 2008). CD32B is not only expressed on immune cells but also on other highly specialized endothelial cells, such as human endothelial cells such as liver sinusoidal endothelial cells (LSEC) (Strauss *et al*, 2017) and human placental endothelial cells (Mishima *et al*, 2007; Takizawa *et al*, 2005). On LSEC, CD32B activation is involved in regulating molecules exchange from blood (Ganesan *et al*, 2012), endocytosis (Ishikawa *et al*, 2019) and clearance of immune complexes (Liu *et al*, 2008). More relevant to hematopoietic development, Fc receptors are expressed on murine EMPs that originate from the HE during the second extra-embryonic hematopoietic wave (McGrath *et al*, 2015). Considering these observations, we hypothesized that FCGR2B may distinguish HE from non-hemogenic endothelial cells.

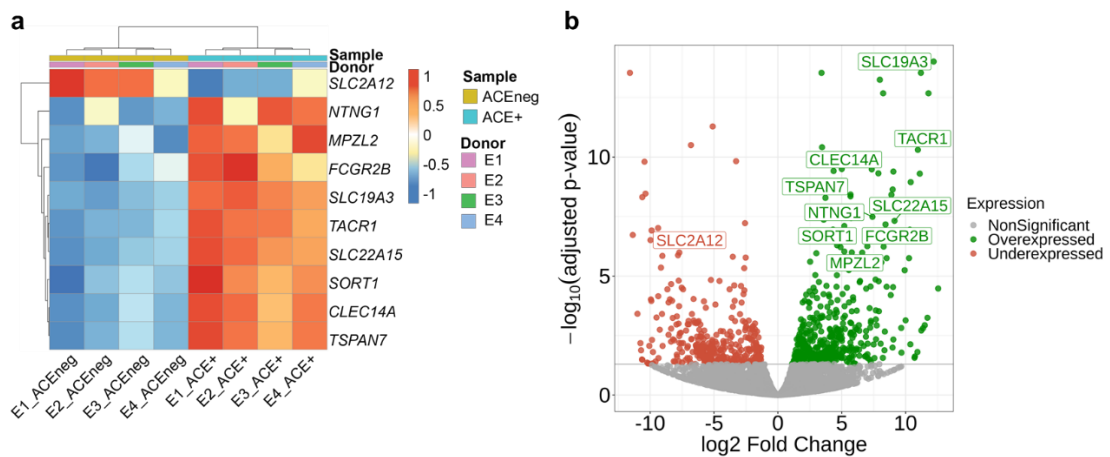


Figure 20 – Top 10 differentially expressed genes on HEC versus EC

a) Heatmap and b) Volcano plot representing the top 10 differentially expressed surface genes comparing ACE⁺ and ACE^{neg} cells isolated from the AGM of four CS13-CS14 human embryos (E1, E2, E3, E4). a) In the heatmap, the row-scaled rlog gene expression values are shown. b) In the volcano plot, the \log_2 fold change is shown on the x-axis and the adjusted p-value ($-\log_{10}$) on the y-axis.

First, Manuela Tavian and collaborators evaluated the expression of CD32 (FUN2 clone that recognizes isoforms CD32A and CD32B) on CD34⁺ endothelial cells within extra-embryonic (YS) and intra-embryonic (AGM, VA) hematopoietic sites of CS13 human embryos. We observed that CD32 and CD34 are co-expressed on YS blood islands (Figure 21a), site of *de novo* generation of hematopoietic cells (Haar & Ackerman, 1971; Sasaki & Matsumura, 1986; Bielinska *et al*, 1996; Tavian *et al*, 2001). We then looked into the embryo proper and observed that a subset of endothelial cells residing in the ventral wall of the DA as well as the emerging IAHCs

co-express CD32, CD34, and ACE by immunohistochemistry (Figure 21 b, c). Interestingly, CD32 expression is not restricted to the aortic endothelium but also spans over the connected VA (Figure 21 b), other known hematopoietic site at this embryonic stage (Tavian *et al*, 2001).

In conclusion, CD32 is expressed by CD34⁺ endothelial cells at the time of hematopoietic cell emergence in both extra- and intra-embryonic sites. Remarkably, CD34⁺ endothelial cells positive for CD32 also express other factors known to distinguish the HE population, as ACE and RUNX1. Given this peculiar pattern of CD32 expression in regions with active hematopoiesis, we functionally tested whether CD32 could serve as a specific HE marker.

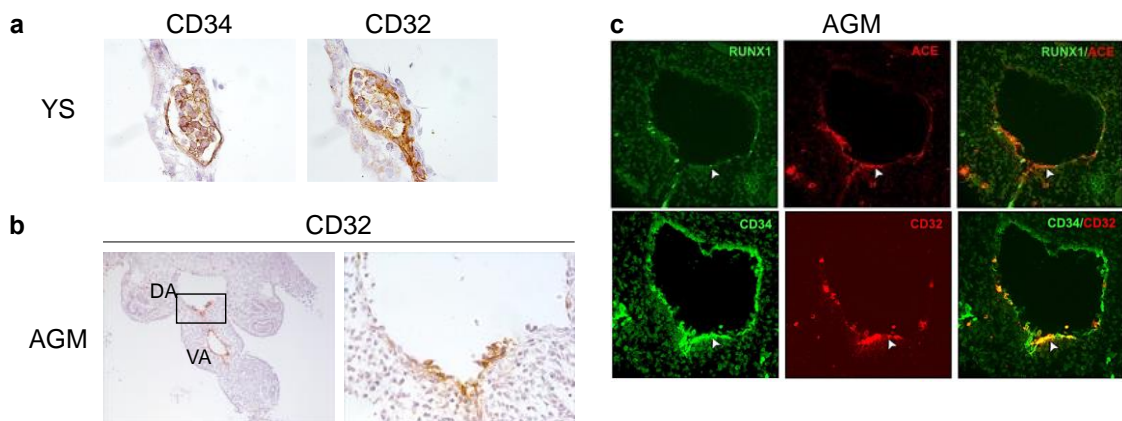


Figure 21 – CD32 is expressed in extra- and intra-embryonic hematopoietic sites of CS13 human embryos

a) Immunohistochemistry of CD34 (left panel) and CD32 (right panel) within YS endothelial and hematopoietic structures of CS13 human embryos. Representative plots, $n=3$, independent. b) Cross-sections through AGM of CS13 human embryo. Immunohistochemistry of CD32. On the right, high magnification of the IAHCs emerging from the ventral side of the DA. Representative plots of $n=3$, independent. c) Transverse sections of the DA of CS13 human embryos. Immunofluorescence staining: upper panel, RUNX1 (green) and ACE (red); lower panel, CD34 (green) and CD32 (red). Single channels are shown on the left, merged picture on the right. Representative plots, $n=3$, independent.

3.2 CD32 distinguishes a population with hemogenic fate in CS13 human embryos

To evaluate CD32 as human HE marker, we performed functional analysis on AGM and YS samples dissected from CS13 human embryos. We obtained dissected AGM and corresponding YS of two human embryos *via* the UK Human Developmental Biology Resource (HDBR) Consortium from Newcastle University, International Centre for Life. First, we assessed CD32 expression within CD34⁺CD43^{neg}CD45^{neg}

endothelial cells derived from YS and AGM by flow cytometry using the same anti-human CD32 clone (FUN2) as in Figure 21. In line with the RNA sequencing data, the histological and immunofluorescence analysis, a sub-population of $CD34^+CD43^{neg}CD45^{neg}$ cells in the AGM expresses CD32. In addition, the majority of $CD34^+CD43^{neg}CD45^{neg}$ YS cells express CD32 (Figure 22 a, b).

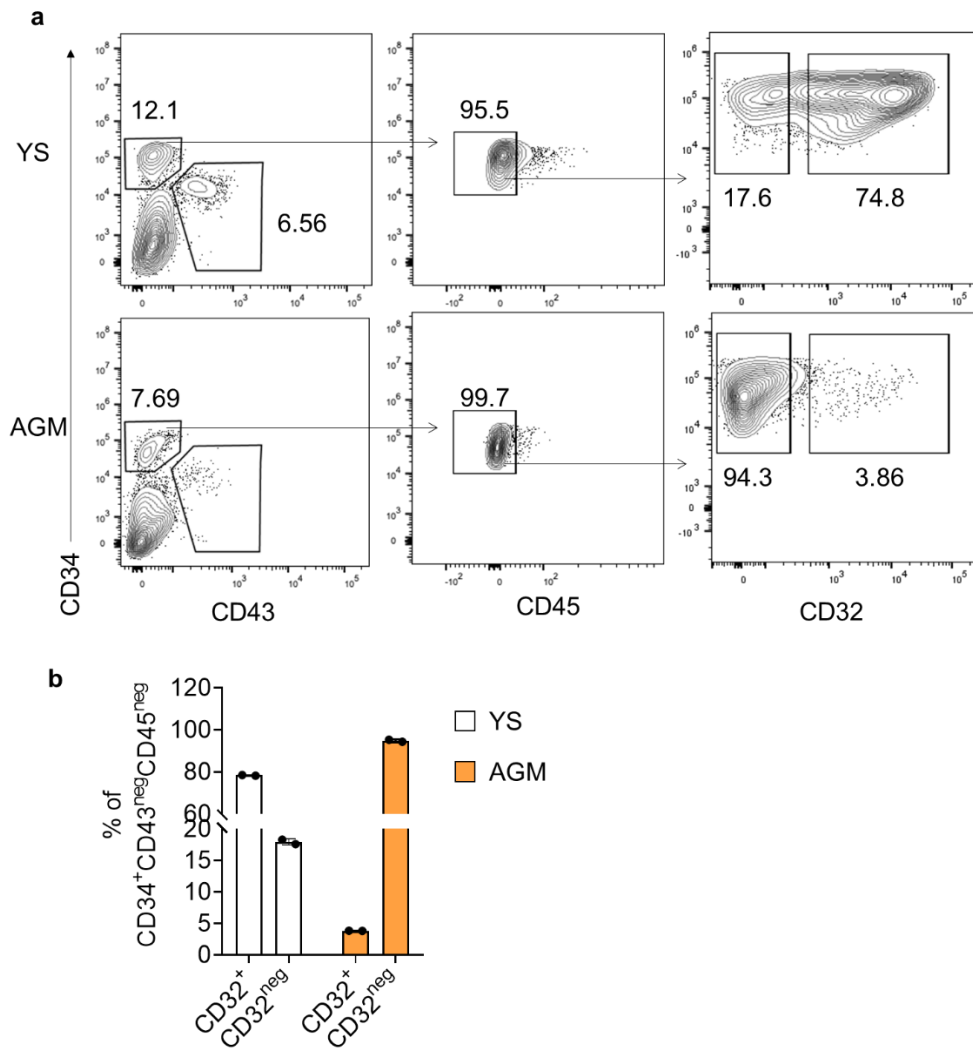


Figure 22 – Flow cytometry analysis of CD32 expression in CS13 human embryo

a) Representative plots showing the gating strategy and CD34, CD43, CD45, CD32 expression in the YS (upper panel) and AGM (bottom panel) of CS13 human embryos. From the left, expression of CD34 and CD43. $CD43^+$ cells are isolated as positive control. $CD32^{neg}$ and $CD32^+$ are isolated from $CD34^+CD43^{neg}CD45^{neg}$ cells (right panel). All populations are gated on SSC/FSC/Live cells. b) Bar plot showing the frequencies of $CD34^+CD43^{neg}CD45^{neg}CD32^{neg/+}$ cells isolated from the YS (white bars) and AGM (orange bars) of $n=2$, independent, CS13 human embryonic samples.

We next sought to understand whether CD34⁺CD32⁺CD43^{neg}CD45^{neg} (abbreviated as CD32⁺) cells enriched HE cells compared to CD34⁺CD32^{neg}CD43^{neg}CD45^{neg} (abbreviated as CD32^{neg}) cells. Therefore, both CD32 fractions were isolated by FAC-sorting, and cultured to evaluate their hematopoietic multilineage potential. In addition, from both sites we isolated CD43⁺ cells as positive control of already-committed hematopoietic progenitors.

To evaluate the lymphoid potential, we cultured the cells for 14-21 days on OP9DLL1 stroma in a cytokine-rich medium that support the specification of either T- or NK-cells as previously reported (Kennedy *et al*, 2012; Sturgeon *et al*, 2014; Dege *et al*, 2020). Of note, the co-culture on OP9 stromal cells overexpressing Notch ligands such as DLL1 or DLL4 represents the existing gold standard for assessing T cells development *in vitro*. However, co-culture on murine stromal cells allows human progenitor to progress along the T-lymphoid lineage up to double positive CD4⁺CD8⁺ stage albeit preventing any further specification to CD8 or CD4 single positive, cytotoxic or helper T-cell due to the inability of the system to recapitulate the thymic positive selection, which is mediated by MHC class I/II and is therefore specie-specific (Sturgeon *et al*, 2014; Kennedy *et al*, 2012). When 150 cells of either CD32⁺ or CD32^{neg} were seeded, both fractions could give rise to CD45⁺CD56^{neg}CD4⁺CD8⁺ T cell- and CD45⁺CD56^{neg} NK cell- progenitors, without any major difference. As expected, CD43⁺ cells also differentiate into T cell or NK progenitors under same culture conditions (Figure 23 a, b).

To evaluate which of the CD32 fractions could generate erythro-myeloid progenitors, we co-cultured CD32⁺, CD32^{neg} and CD43⁺ cells on irradiated OP9DLL1 stroma for 5 days to promote the hematopoietic differentiation. Then, we assayed the derivative output in methylcellulose supplemented with human hematopoietic cytokines (Kennedy *et al*, 2012). Remarkably, the frequency of CFCs derived from CD32⁺ cells isolated from both YS and AGM, exceeded that from CD32^{neg} population of more than 6-fold. In all the samples the majority of colonies consist of burst forming units-erythroid (BFU-E, 87% in CD32⁺, 80% CD32^{neg} and 97% in CD43⁺ sample), whereas colony forming units-macrophages (CFU-M, 6% in CD32⁺, 12% CD32^{neg} and 1% in CD43⁺ sample) and colony forming units-granulocyte-macrophages (CFU-GM, 7% in CD32⁺, 8% CD32^{neg} and 1% in CD43⁺ sample) were less represented. Overall, the CFC assay showed that the CD32⁺ endothelium has higher erythro-myeloid clonogenic potential than the CD32^{neg} counterpart (Figure 24 a).

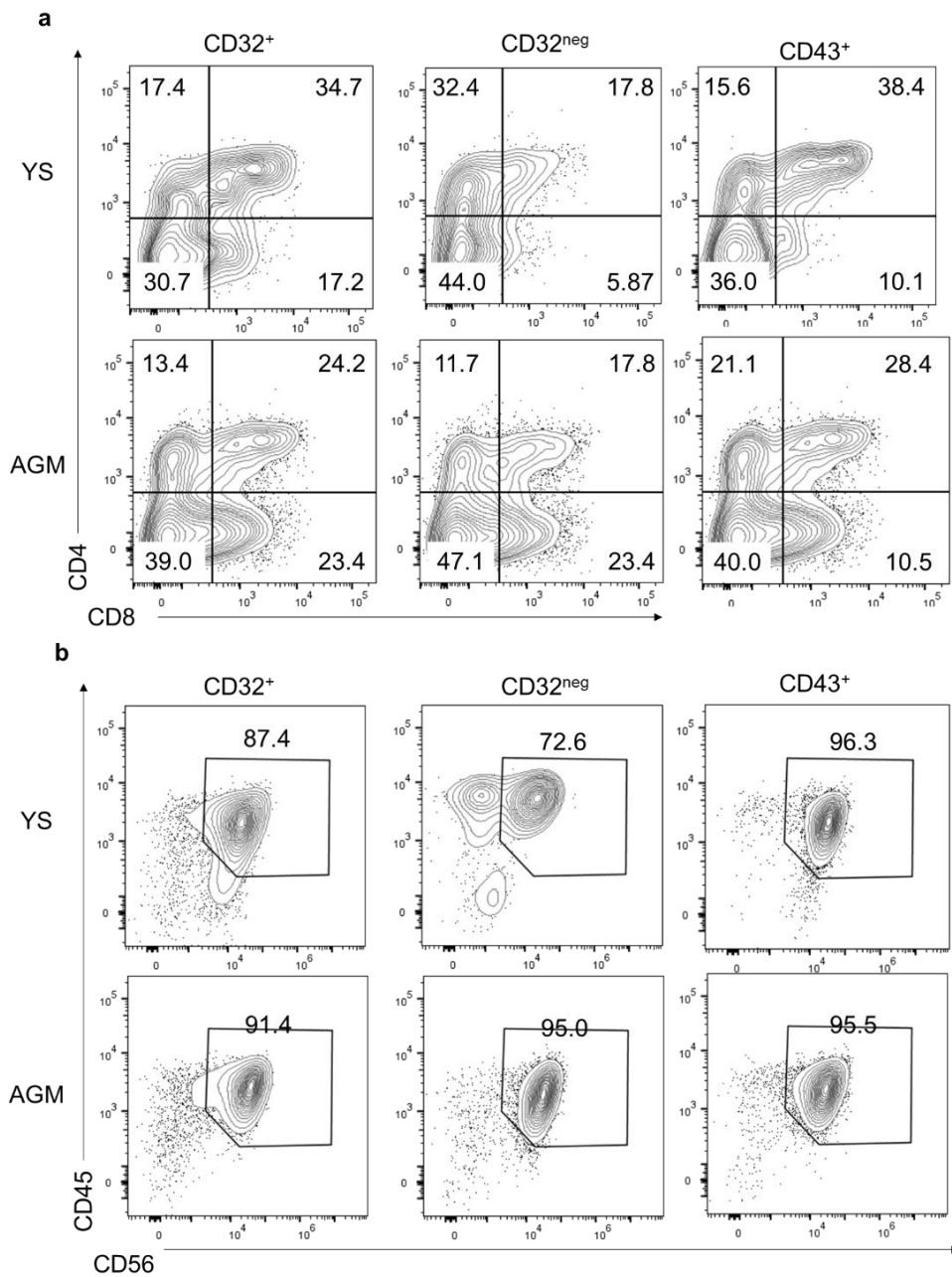


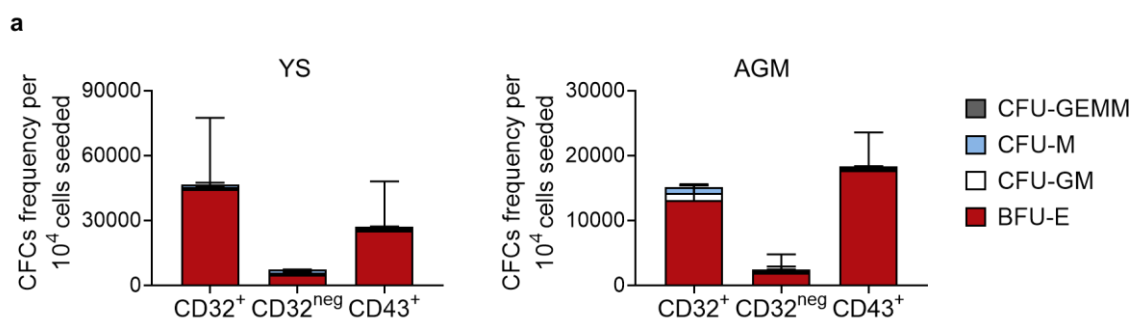
Figure 23 – CD32^{+/neg} endothelial populations show lymphoid potential in ex vivo cultures

a) Representative plots showing CD45⁺CD56^{neg}CD4⁺CD8⁺ T lymphoid progenitors derived from CD32⁺ (left column), CD32^{neg} (middle column) endothelial cells and CD34⁺CD43⁺ hematopoietic progenitors (right column) isolated from the YS (upper panel) or the AGM (lower panel) of CS13 human embryos. b) Representative plots showing CD45⁺CD56⁺ NK lymphoid progenitors derived from CD32⁺ (left column), CD32^{neg} (middle column) endothelial cells and CD34⁺CD43⁺ hematopoietic progenitors (right column) isolated from the YS (upper panel) or the AGM (lower panel) of CS13 human embryos.

To exclude the contamination of already committed hematopoietic progenitors within the CD32⁺ and CD32^{neg} endothelial fractions, we seeded a portion of the cells on

methylcellulose cultures directly after sorting. Unfortunately, this was not possible for CD32⁺ cells isolated from the AGM of one of the two CS13 human embryos due to the low number of sorted cells. In addition, we similarly cultured isolated CD43⁺ hematopoietic progenitors as positive control. By direct methylcellulose plating, we observed that both CD32^{+/neg} populations isolated from either YS or AGM contains hematopoietic progenitors with clonogenic potential (Figure 24 b). However, the frequency of CFC from CD32^{+/neg} samples was drastically reduced. For instance, CD32⁺ cells show a 15-fold decrease in CFC frequency compare to methylcellulose plating after OP9DLL1 co-culture. The presence of hematopoietic progenitors might be caused by a cross-contamination between samples. Indeed, the limited number of cells prevented us to perform a purity control of the sort. On the other hand, the same number of CD43⁺ cells directly plated on methylcellulose generated too many colonies that could not be properly counted.

Unfortunately, the rare availability of human embryos prevented us to perform the experiment again. Should we receive new embryos in the future, we will repeat it with a more stringent gating strategy to avoid the contamination of early hematopoietic progenitors within the CD32^{+/neg} populations. In addition, we will perform limiting dilution assay to assess whether that CD32⁺ endothelial fraction is enriched for cells with lymphoid potential compared to the CD32^{neg}. In conclusion, our data support the hypothesis of CD32 marks the HE in CS13 human embryos, regardless of the location.



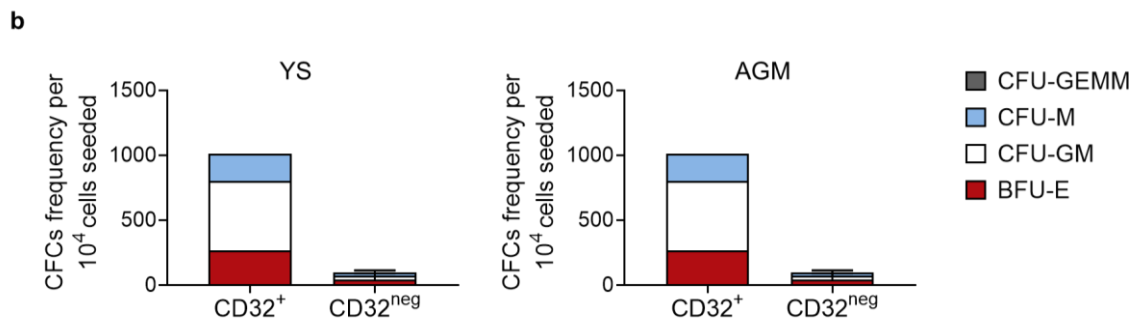


Figure 24 – CD32⁺endothelial cells display clonogenic potential

a, b) Bar plots showing the CFCs frequency derived from CD32⁺ or CD32^{neg} populations isolated from YS (left panel) or AGM (right panel) of CS13 human embryos. CD43⁺ were seeded as positive control a). Cells were seeded in methylcellulose after 5 days of co-culture with OP9DLL1 stromal cells a) or directly after sort b). The bar plots show the average result of n=2 experiments, independent. A unique replicate is shown in b), CD32⁺ cells isolated from the AGM.

3.3 CD32 is expressed in hPSC-derived HE

Our results showed that CD32 identifies a subset of endothelial cells with robust hematopoietic potential in CS13 human embryos. To better characterize CD32 as HE marker, we evaluated the expression in hPSC-derived HE. In addition to their tremendous potential applications for regenerative medicine, hPSCs represent thus far one of the most powerful tools to study human embryonic development since human embryos are rare and difficult to obtain. hPSCs allow to recapitulate extra-embryonic or intra-embryonic-like hematopoiesis *via* the stage-specific manipulation of the Wnt and Notch pathway (see Introduction, paragraph 1.11) (Sturgeon *et al*, 2014; Ditadi *et al*, 2015). In particular, the isolation of CD34⁺CD43^{neg}CD184^{neg}CD73^{neg} cells from hPSC-derived differentiating cultures include a population with hemogenic potential, further enriched by isolating CD34⁺CD43^{neg}CD184^{neg}CD73^{neg}DLL4^{neg} cells (referred to as DLL4^{neg}) (Ditadi *et al*, 2015).

We monitored CD32 expression within WNT-independent extra-embryonic-like or WNT-dependent intra-embryonic-like HE population. In both conditions, we could identify four different populations according to CD32 and DLL4 expression (Figure 25 a). The percentages of the four CD34⁺CD43^{neg}CD183^{neg}CD73^{neg}CD32^{+/neg}DLL4^{+/neg} sub-fractions (herein referred to as CD32⁺DLL4^{neg}, CD32^{neg}DLL4^{neg}, CD32^{neg}DLL4⁺, CD32⁺DLL4⁺) varied across the

experiments. The most abundant population in all the experiments was the CD32^{neg}DLL4^{neg} (WNT-independent: 53.6-75.3%; WNT-dependent: 42.7-74.9%). The CD32⁺DLL4^{neg} population ranged between 4,86%-17,9% and 4,31%-21,9% in WNT-independent or WNT-dependent hematopoietic cultures respectively. We detected similar frequencies for the CD32^{neg}DLL4⁺ fraction (WNT-independent: 7.2-18.8%; WNT-dependent: 4.99-32.3%). The less represented subpopulation was CD32⁺DLL4⁺ that was barely detectable in WNT-independent (0.18-1.29%) and WNT-dependent (0.45-5.85%) hematopoietic cultures (Figure 25 b). These preliminary observations confirmed that CD32 is expressed within the hPSC-derived endothelial fraction known to contain the HE.

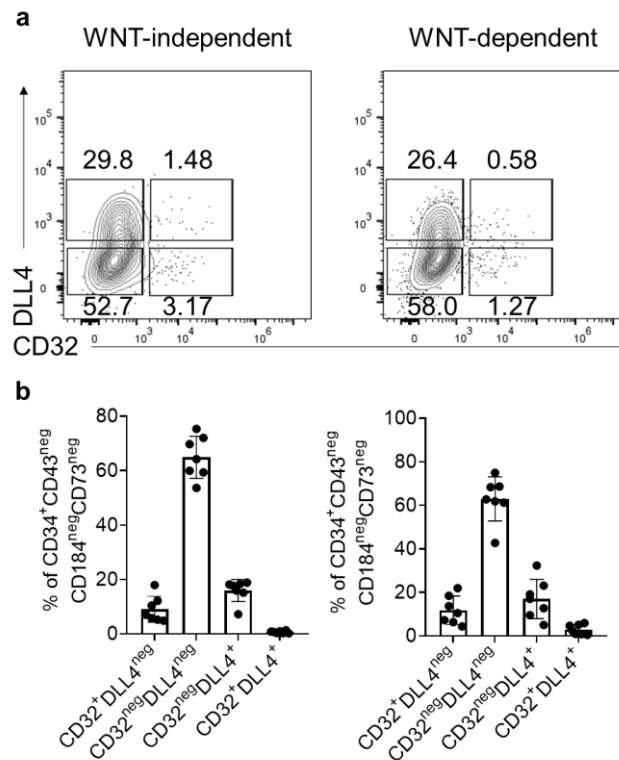


Figure 25 – CD32 is expressed within the hPSC-derived WNT-dependent or WNT-independent CD34⁺CD43^{neg}CD184^{neg}CD73^{neg}DLL4^{neg} population.

a) Representative plots showing CD32 and DLL4 expression gated on SSC/FSC/Live/CD34⁺CD43^{neg}CD184^{neg}CD73^{neg} cells. Four different populations are highlighted with rectangular gates: CD32⁺DLL4^{neg} (bottom right), CD32^{neg}DLL4^{neg} (bottom left), CD32^{neg}DLL4⁺ (upper left), CD32⁺DLL4⁺ (upper right). b) Left panel: bar plot showing the frequencies of the four sub-fractions gated on CD34⁺CD43^{neg}CD184^{neg}CD73^{neg} cells derived from WNT-independent hematopoietic cultures (n=7, independent, mean ± standard deviation (SD)). Right panel: bar plot showing the frequencies of the four HE sub-fractions gated on CD34⁺CD43^{neg}CD184^{neg}CD73^{neg} cells derived from WNT-dependent hematopoietic cultures (n=7, independent, mean ± SD).

3.4 CD32⁺DLL4^{neg} cells generate erythroid and myeloid progenitors

To evaluate and quantify whether the four endothelial sub-populations harbor hematopoietic potential and therefore contain HE, we FAC-sorted the CD32⁺DLL4^{neg}, CD32^{neg}DLL4^{neg}, CD32^{neg}DLL4⁺, CD32⁺DLL4⁺ fractions at day 8 of either WNT-independent or WNT-dependent hematopoietic differentiation (Figure 26 a). Then, we plated the cells for 5 days on irradiated OP9DLL1 stromal cells to promote the hematopoietic differentiation and we tested the colony forming cell (CFC) potential afterwards.

Consistently with previous results, the DLL4^{neg} fraction is enriched for cells harboring hematopoietic potential in both WNT-independent and WNT-dependent hematopoietic cultures. Interestingly, in both cultures, CD32⁺DLL4^{neg} population generated more clonogenic progenitors compared to the CD32^{neg}DLL4^{neg} (Figure 26 b). In detail, CD32⁺DLL4^{neg} generated 3700 CFCs (\pm SD: 2435) on average (including the different lineages) compared to 572 CGCs (\pm SD: 517.5) of CD32^{neg}DLL4^{neg} in WNT-independent hematopoietic culture. The CD32^{neg}DLL4⁺, CD32⁺DLL4⁺ did not yield any clonogenic progenitor.

Similarly, the CFC frequency was higher in cells generated from CD32⁺DLL4^{neg} fraction in WNT-dependent hematopoietic culture, that generated 3213 CFCs (\pm SD: 2084) compared to the 863 (\pm SD: 1367) obtained when plating progenitors generated from CD32^{neg}DLL4^{neg} cells. While the CD32⁺DLL4⁺ fraction never displayed hematopoietic activity, the CD32^{neg}DLL4⁺ fraction generated few hematopoietic progenitors able to form erythroid or myeloid colonies (97 ± 113.7) in two out of four experiments, possibly due to a low sorting purity and cross-contamination between the different fractions. However, the low number of cells isolated from each fraction prevented us to check the sorting purity.

To verify that CD32 could track HE in differentiating cultures using multiple hPSC lines, we repeated the experiment using the H9 human embryonic stem cell (hESC) line. When cultured in WNT-dependent condition, H9 gave rise to CD32⁺DLL4^{neg} cells capable to generate erythroid and myeloid progenitors at higher frequency than the other CD34⁺CD43^{neg}CD73^{neg}CD184^{neg} sub-fractions (Figure 26 b), in accordance with what was previously shown. In detail, CD32⁺DLL4^{neg} generated 3300 CFCs (\pm SD: 558.5) while CD32^{neg}DLL4^{neg} cells 545.4 (\pm SD: 376.1). The two DLL4⁺ endothelial sub-population did not originate any blood cell type.

In conclusion, our results showed that under hPSC-derived WNT-independent or -dependent hematopoietic cultures, the hematopoietic potential is restricted almost exclusively to DLL4^{neg} cells. Within this fraction the expression of CD32 identify cells increased erythro-myeloid potential. In the next experiments we decided to exclude the CD32^{neg}DLL4⁺ and CD32⁺DLL4⁺ fractions as those did not display robust hematopoietic activity.

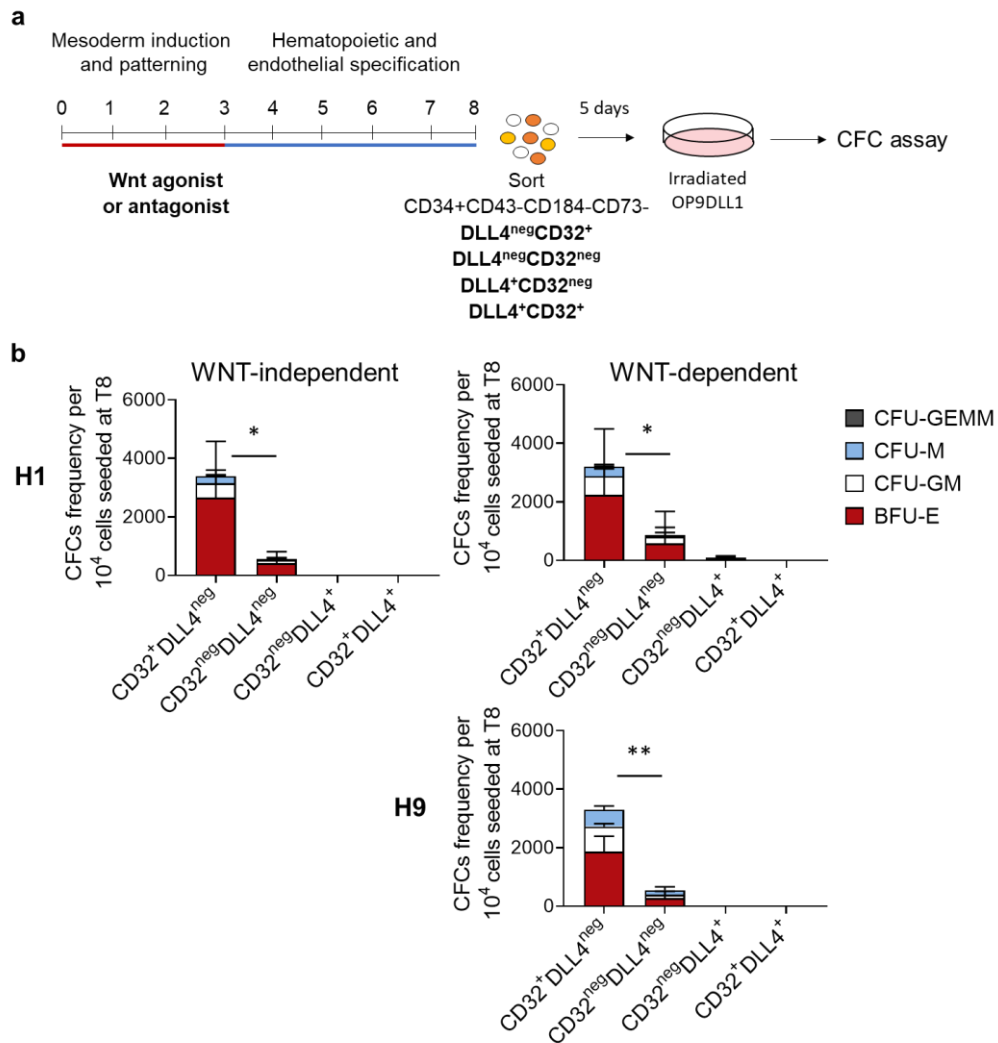


Figure 26 – hPSC-derived CD32⁺ endothelial cells give rise to erythroid and myeloid progenitors

a) Scheme of the hPSC-derived WNT-dependent or WNT-independent hematopoietic differentiation. At day 8 of differentiation, CD34⁺CD43^{neg}CD184^{neg}CD73^{neg}CD32^{+/neg}DLL4^{+/neg} cells were isolated by FAC-Sorting. The isolated populations are referred to as CD32⁺DLL4^{neg}, CD32^{neg}DLL4^{neg}, CD32^{neg}DLL4⁺, CD32⁺DLL4⁺. Isolated cells were cultured for 5 days on irradiated OP9/DLL1 stroma and then plated on methylcellulose to assess their erythroid and myeloid hematopoietic potential (CFC assay). b) CFC assay from CD32⁺DLL4^{neg}, CD32^{neg}DLL4^{neg}, CD32^{neg}DLL4⁺, CD32⁺DLL4⁺ sub-populations from WNT-independent (performed in H1 hESC line: top left, n=6, mean ± SD, one-tail paired student T test

considering the total number of colonies, $p=0.0111$) or WNT-dependent hematopoietic cultures. The latter was performed from H1 or H9 hESC lines. H1: top right, $n=4$, mean \pm SD, one-tail paired student T test considering the total number of colonies $p=0.0155$. H9: bottom left, $n=3$ one-tail paired T test considering the total number of colonies $p=0.0092$).

3.5 CD32⁺DLL4^{neg} cells are enriched for NK lymphoid progenitors in WNT-independent hematopoietic culture

To further characterize the hematopoietic potential of CD32⁺DLL4^{neg} and CD32^{neg}DLL4^{neg} cells, we evaluated their ability to generate T and NK lymphoid progenitors. NK lymphoid cells have multiple developmental origins. Both extra-embryonic (Dege *et al*, 2020; Tavian *et al*, 2001) and intra-embryonic HSC-independent and -dependent (Kondo *et al*, 1997; Sturgeon *et al*, 2014; Dege *et al*, 2020) hematopoietic programs are endowed with NK potential. To characterize the NK potential of WNT-independent hematopoietic cultures, we isolated CD32⁺DLL4^{neg} and CD32^{neg}DLL4^{neg} fractions and seeded the sorted cells on OP9DLL1 stroma in a cytokine-rich culture media to stimulate NK-lymphoid differentiation (Dege *et al*, 2020). After 14 days, we analyzed by FACS analysis the presence of CD45⁺ hematopoietic cells displaying expression of CD56, a classical marker of the NK lineage. Both CD32⁺DLL4^{neg} and CD32^{neg}DLL4^{neg} cells support the differentiation into CD56⁺ NK cells (Figure 27 a, b). However, CD32⁺DLL4^{neg} cells yielded significantly more NK-cells than the CD32^{neg}DLL4^{neg} fraction (Figure 27 b). The increased NK output can be explained by either an increased initial frequency of progenitors with NK potential and/or higher proliferation of NK cells in culture. To test the first hypothesis, we set out to determine the frequency of progenitors with NK potential in both CD32⁺DLL4^{neg} and CD32^{neg}DLL4^{neg} populations by performing a limiting dilution assay (LDA) (Figure 27 c, d, e). In detail, we seeded a range of different cell numbers per well (1, 5, 10, 25, 30, 50, 100) on a 96 well coated with OP9DLL1 and analyze the presence of CD45⁺CD56⁺ cells by FACS after 21 days (Figure 27 c, d). The frequency of NK lymphocytes was calculated by using ELDA, a software application for limiting dilution analysis (Hu & Smyth, 2009) (Figure 27 d). ELDA calculated that 1 out of 15 CD32⁺DLL4^{neg} cells gives rise to NK cell while only 1 out of 244 from CD32^{neg}DLL4^{neg} cells, *i.e.* a 16-fold enrichment in cells expressing CD32 (Figure 27 e).

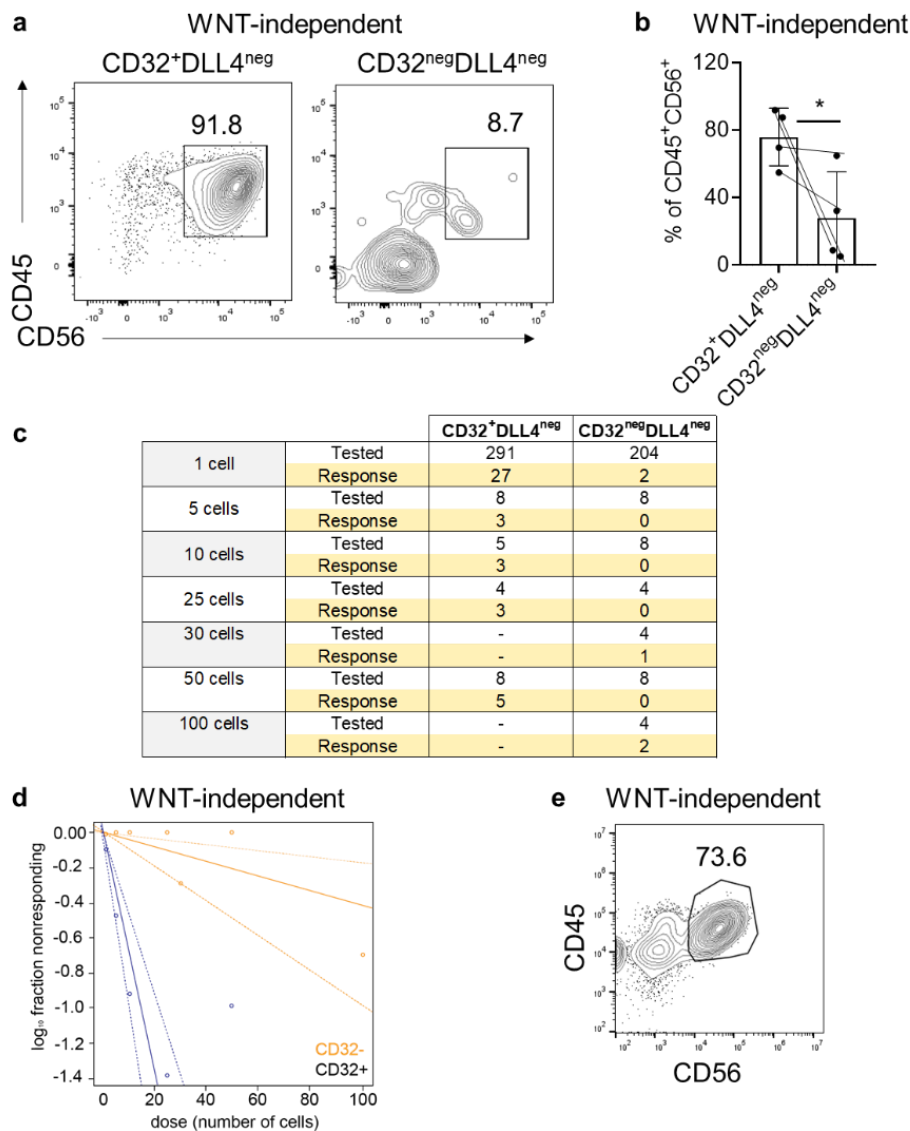


Figure 27 – hPSC-derived CD32⁺endothelial cells give rise to NK lymphoid progenitors in WNT-independent hematopoietic cultures

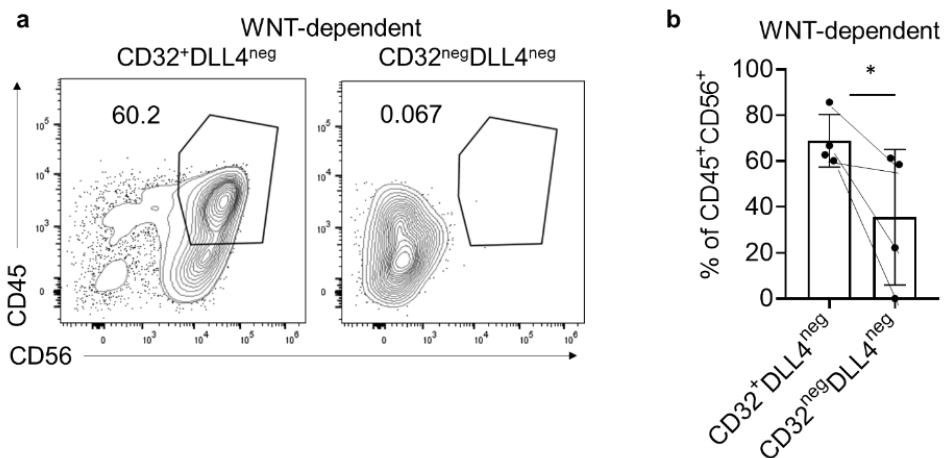
a) Representative plots of CD45⁺CD56⁺ NK lymphocytes emerged from CD32⁺DLL4^{neg} (left) and CD32^{neg}DLL4^{neg} (right) cells from WNT-independent hematopoietic cultures. b) Bar plot showing the frequency (mean ± SD) of CD45⁺CD56⁺ NK generated from CD32⁺DLL4^{neg} and CD32^{neg}DLL4^{neg} cells from WNT-independent hematopoietic cultures in n=3, independent experiment. One-tail paired T test p=0.04881. c-e) Limiting dilution assays of CD32⁺DLL4^{neg} and CD32^{neg}DLL4^{neg} cells obtained from WNT-independent hematopoietic cultures to assess their derived NK potential. c) Table enlisting the number (1, 5, 10, 25, 30, 50 or 100) of CD32^{+/neg}DLL4^{neg} cells seeded on each 96 well coated with OP9/DLL1 stroma at day 8 of differentiation. 30 and 100 cells conditions are missing for the CD32⁺DLL4^{neg} sample. The emergence of NK progenitor cells was calculated by counting the wells that display CD45⁺CD56⁺ NK immuno-phenotype (column "response" in the table) by FACS analysis. The total number of seeded cells is enlisted in the "tested" row. d) Extreme limiting dilution analysis (ELDA) of NK cell potential derived from CD32⁺DLL4^{neg} (blue) and CD32^{neg}DLL4^{neg} (orange) cells (<http://bioinf.wehi.edu.au/software/elda/>). Number of tested conditions and of seeded cells are enlisted in c). n=3, independent. e) Representative plot of CD45⁺CD56⁺ NK cells generated in a well seeded with one CD32⁺DLL4^{neg} cell at day 8. Gated on SSC/FSC/Live.

3.6 CD32⁺DLL4^{neg} cells give rise to NK and T lymphoid progenitors in WNT-dependent hematopoietic culture

Given our promising results, we investigated the NK lymphoid potential of CD32⁺DLL4^{neg} and CD32^{neg}DLL4^{neg} populations in WNT-dependent hematopoietic cultures. NK progenitor cells could be generated from both CD32⁺DLL4^{neg} and CD32^{neg}DLL4^{neg} populations. However, increased frequency of NK-progenitor cells differentiated from CD32⁺DLL4^{neg} cells (68% compared to 35.5% generated from CD32^{neg}DLL4^{neg}) (Figure 28 a, b).

Rather than NK, T lymphoid progenitors constitute the defining lymphoid lineage of WNT-dependent intra-embryonic hematopoiesis. Therefore, we isolated CD32⁺DLL4^{neg} and CD32^{neg}DLL4^{neg} sub-populations at day 8 of differentiation and co-cultured the cells on OP9DLL4 stroma to favor the T-lymphoid differentiation. Remarkably, CD45⁺CD8⁺CD4⁺CD56^{neg} T lymphocytes emerge exclusively from CD32⁺DLL4^{neg} cells, while the CD32^{neg}DLL4^{neg} fraction is devoid of T cell potential (Figure 28 c, d). In conclusion, our results show that CD32⁺DLL4^{neg} cells derive T and NK lymphocytes at higher frequency than the corresponding CD32^{neg}DLL4^{neg}.

Since CD32⁺DLL4^{neg} cells show enrichment in multi-lineage hematopoietic potential, these results support the hypothesis that the expression of CD32 can be used as selective positive marker to isolate HE populations in both extra- and intra-embryonic hematopoietic programs.



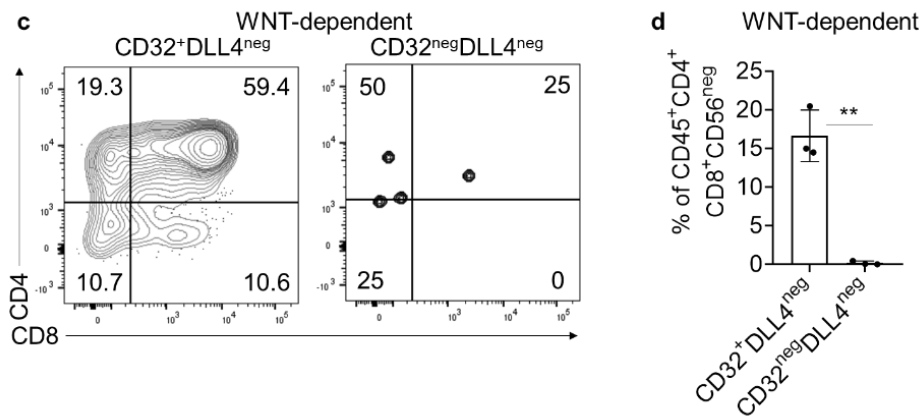


Figure 28 – hPSC-derived $CD32^+$ endothelial cells give rise to NK and T lymphoid progenitors in WNT-dependent hematopoietic cultures

a) Representative plots of $CD45^+CD56^+$ NK cells generated from $CD32^+DLL4^{neg}$ (left) and $CD32^{neg}DLL4^{neg}$ (right) cells in WNT-dependent hematopoietic cultures (gated on SSC/FSC/Live). b) Bar plot indicating the frequency (mean \pm SD) of $CD45^+CD56^+$ NK cells generated from $CD32^+DLL4^{neg}$ (left) and $CD32^{neg}DLL4^{neg}$ from WNT-dependent hematopoietic cultures in $n=3$, independent experiment. One-tail paired T test $p=0.03537$. c) Representative plots of $CD45^+CD56^{neg}CD4^+CD8^+$ T-cells generated from $CD32^+DLL4^{neg}$ and $CD32^{neg}DLL4^{neg}$ cells from WNT-dependent hematopoietic cultures. Gated on SSC/FSC/Live/ $CD45^+CD56^{neg}$ b) Bar plots showing the percentages of $CD45^+CD4^+CD8^+CD56^{neg}$ T-cells ratioed on the percentages of $CD45^+CD56^{neg}$ cells ($n=3$, independent, mean \pm SD, paired one-tailed T test, $p=0.0073$).

3.7 Clonal analysis of $CD32^+DLL4^{neg}$ hemogenic potential

Our data showed that $CD32^+DLL4^{neg}$ cells show an enriched hemogenic potential compared to $CD32^{neg}DLL4^{neg}$ cells in WNT-dependent hematopoietic cultures. The data presented thus far show that CD32 is a valuable marker for the enrichment of HE cells, but we have no clue about its specificity or its selectivity compared to other already reported HE markers.

To evaluate the specificity of CD32 as HE marker and estimate the frequency of HE cells within the $CD32^+DLL4^{neg}$ and $CD32^{neg}DLL4^{neg}$ populations, we performed single-cell clonal EHT assay, as previously described (Ditadi *et al*, 2015). We isolated single $CD32^+DLL4^{neg}$ and $CD32^{neg}DLL4^{neg}$ cell on a Matrigel coated 96-well at day 8 of hPSC-derived WNT-dependent hematopoietic differentiation. We cultured the cells for 7 days in a cytokine-rich medium to promote hematopoietic commitment. Then, we quantified those clones that generated round hematopoietic-like or adherent non-hematopoietic-like cells (Figure 29 a). To evaluate the cellular features of the selected clones, we collected round hematopoietic-like or adherent non-hematopoietic-like colonies and analyzed the expression of the pan-hematopoietic cell-surface marker CD45 by FACS analysis (Figure 29b). Of note, all the clones that generate rounded

hematopoietic-like cells express CD45 while the adherent non-hematopoietic-like cells were exclusively CD45^{neg}. In addition, CD45⁺ and CD45^{neg} cells have not been observed in the same well, highlighting that the two lineages are mutually exclusive and a hemogenic endothelial cell can derive only one cell type as previously reported (Swiers *et al*, 2013; Ditadi *et al*, 2015). We quantified that within CD32⁺DLL4^{neg} cells that showed clonogenic potential (112 out of 576 cells seeded including all the three independent experiments), 89% ±8.05 generated CD45⁺ hematopoietic cells (total of 98 out of 112 cells comprehensive of the three independent experiments). On the other hand, the CD32^{neg}DLL4^{neg} cells with clonogenic potential (78 of 574 total cells seeded in the three independent experiment) generate only 33% ±25.16 CD45⁺ clones (20 out of 574 cells seeded) while the majority (58 out of 574 cells seeded) consists non-hematopoietic clones (Figure 29 c, f). This first result confirmed that CD32⁺DLL4^{neg} enriches the frequency of HE in respect to CD32^{neg}DLL4^{neg} generating 89% ±8.05 or 33% ±25.16 of hematopoietic clones respectively.

We compared the isolation of HE cells using either CD32 or CD44, another known HE marker, conserved in human and mouse species (Watt *et al*, 2000; Oatley *et al*, 2020). First of all, we evaluated the expression of CD44 in hPSC-based WNT-dependent hematopoietic cultures. Similarly to ACE expression (Figure 18 b), CD34⁺ cells co-express CD44, indicating that CD44 largely marks endothelial cells without specifically immuno-phenotyping HE (Figure 30 a, left panel). However, within subset of CD34⁺CD43^{neg}CD184^{neg}CD73^{neg} cells that includes cells with HE features, four different sub-populations could be identified according to CD44 and DLL4 expression (referred to as CD44⁺DLL4^{neg}, CD44^{neg}DLL4^{neg}, CD44^{neg}DLL4⁺, CD44⁺DLL4⁺) (Figure 30 a, right panel). Therefore, we isolated the four fractions to address their hematopoietic potential by CFC assay. Also in this case, DLL4⁺ populations are devoid of hematopoietic potential, confirming what previously reported (Ditadi *et al*, 2015) and shown (Figure 26 b). Moreover, CD44⁺DLL4^{neg} cells significantly enrich derived erythroid-myeloid progenitors (total number of CFC: 3300±558.5) compared to the CD44^{neg}DLL4^{neg} sub-population (545±376.1) (Figure 30 b). As such, we confirm that CD44 expression can be used to enrich endothelial populations with hematopoietic potential.

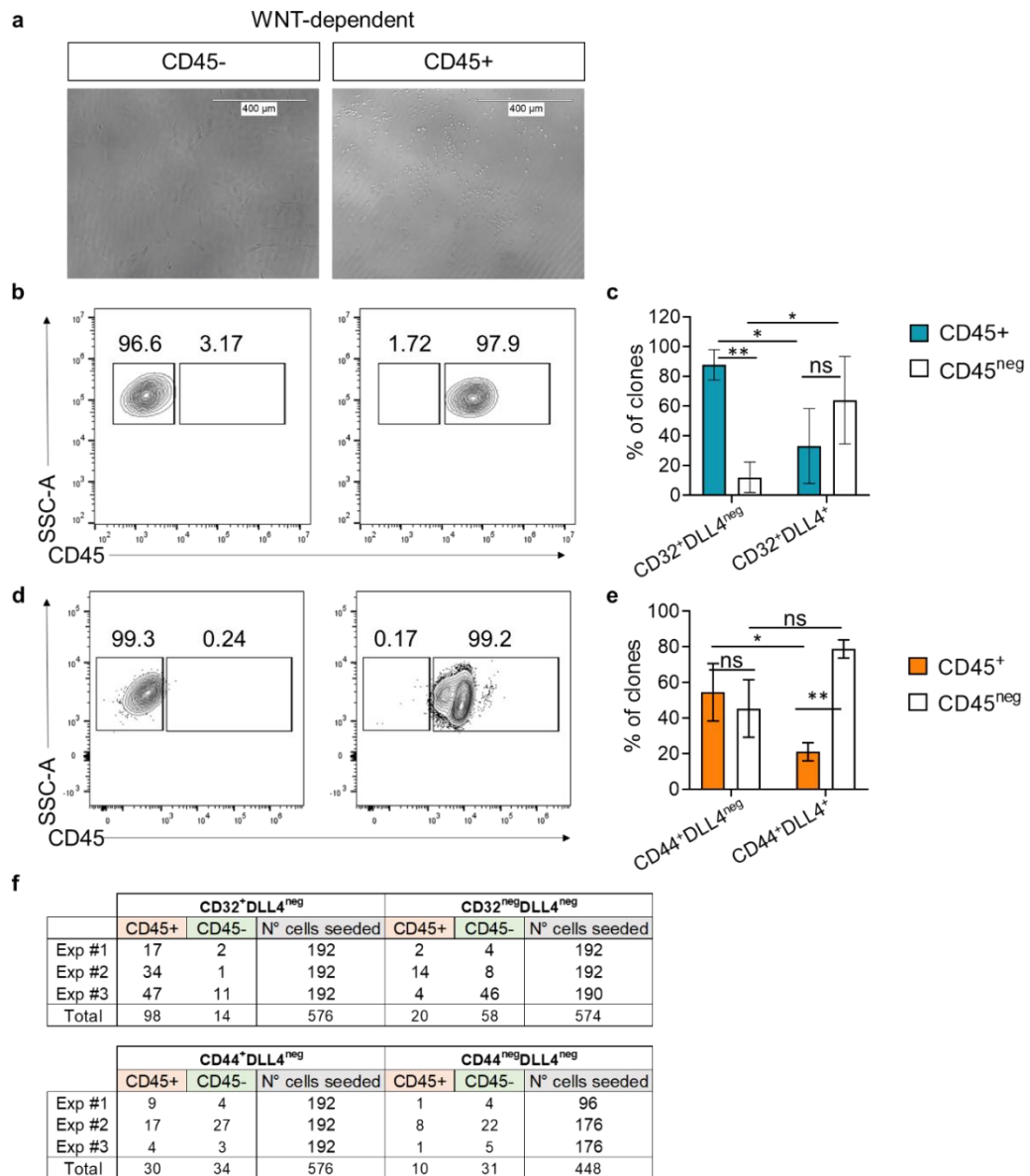


Figure 29 – Quantification of the frequency of HE cells within hPSC-derived CD32⁺ endothelial population

a) Photo-micrographs of an adherent-non-hematopoietic-like clone (left) and rounded-hematopoietic-like clone (right) obtained from CD32⁺DLL4^{neg} differentiated in WNT-dependent hematopoietic cultures. The clones obtained either from b) CD32⁺DLL4^{neg} or d) CD44⁺DLL4^{neg} population were analyzed for CD45 expression at FACS to confirm their hematopoietic or non-hematopoietic identity. c) Bar plot of CD45⁺ or CD45^{neg} clones generated from CD32⁺DLL4^{neg} or CD32^{neg}DLL4^{neg} cells. Showed mean ± SD, n=3 independent experiments, one-tailed paired student T test. ** p=0.0068905 (CD45⁺ or CD45^{neg} clones generated from CD32⁺DLL4^{neg}); ns p=0.2153; * p=0.0148625 (CD45⁺ or CD45^{neg} clones generated from CD32⁺DLL4^{+/neg}); * p=0.0215213 (CD45^{neg} clones generated from CD32^{+/neg}DLL4^{neg}). e) Bar plot of CD45⁺ or CD45^{neg} clones generated from CD44⁺DLL4^{neg} or CD44^{neg}DLL4^{neg} cells. Showed mean ± SD, n=3 independent experiments, ns p=0.3392985 (CD45⁺ or CD45^{neg} clones generated from CD44⁺DLL4^{neg}); ns p=0.0521105 (CD45⁺ clones generated from CD44^{+/neg}DLL4^{neg}); ns p=0.0521105 (CD45^{neg} clones generated from

$CD44^{+}/negDLL4^{neg}$; * $p=0.049132$ ($CD45^{+}$ clones generated from $CD44^{+}/negDLL4^{neg}$); ** $p=0.0050955$ ($CD45^{+}$ or $CD45^{neg}$ clones generated from $CD44^{+}/negDLL4^{neg}$).

As performed for $CD32^{+}/negDLL4^{neg}$ populations, we analyzed the hematopoietic potential of $CD44^{+}DLL4^{neg}$ or $CD44^{neg}DLL4^{neg}$ cells at clonal level. Also in this case, the hematopoietic or non-hematopoietic progeny was distinguishable by morphology and confirmed by FACS analysis (Figure 29 c). Among $CD44^{+}DLL4^{neg}$ cells with clonogenic potential (64 out of 576 cells seeded as comprehensive of the three experiments performed), 55% ± 15 generate hematopoietic colonies (a total of 30 out of 576 cells seeded) and 45% ± 15 non-hematopoietic cells (a total of 34 out of 576 cells seeded). Therefore, $CD44^{+}DLL4^{neg}$ cells generate hematopoietic or non-hematopoietic progeny without a statistically significant difference. However, $CD44^{+}DLL4^{neg}$ population displays an enriched hematopoietic potential when compared to the $CD44^{neg}DLL4^{neg}$. Indeed, the clonogenic $CD44^{neg}DLL4^{neg}$ cells (41 out of 448 seeded in total of three independent experiment) generate only 21% ± 5 $CD45^{+}$ clones (10 out of 448) whereas the 79% ± 5 (consists of non-hematopoietic clones (31 out of 448) (Figure 29 e, f). In conclusion, $CD44^{+}DLL4^{neg}$ population includes higher frequency of HE cells compared to the counterpart not expressing CD44. However, CD44 cannot be considered as selective HE marker since it does not enrich the HE towards cells without any hematopoietic fate. On the other hand, single cell analysis indicates that CD32 is a reliable marker for hPSC-derived HE, whose specificity is superior to the one of CD44, often used to identify human HECs.

The low clonogenic potential of either $CD32^{+}/negDLL4^{neg}$ or $CD44^{+}/negDLL4^{neg}$ suggests that the populations include other cellular types not fully supported by the adopted culture conditions and/or that single-cell cultures enhance cellular distressed following manipulation. In addition, the low clonogenicity may be the result of a sub-optimal single cell sorting efficiency.

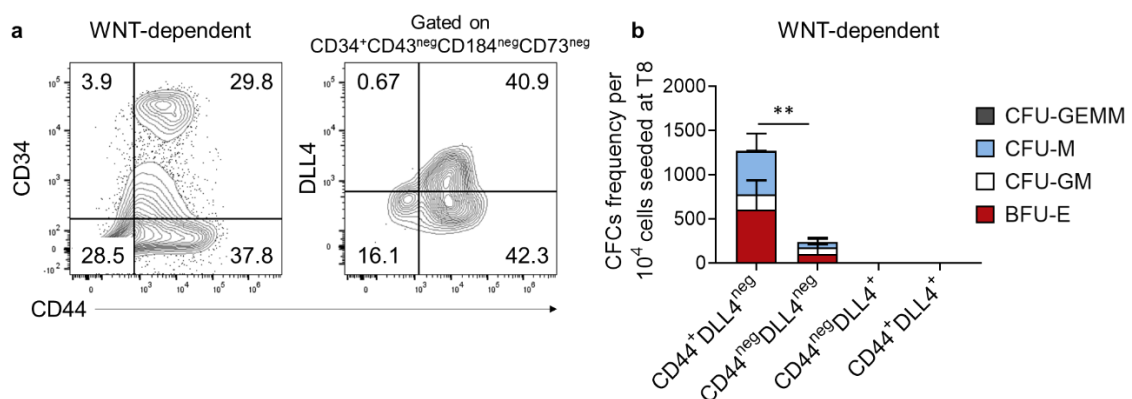


Figure 30 – Analysis of CD44 as hPSC-derived HE marker

a) Representative plots of CD44 expression at day 8 of hPSC-derived WNT-dependent hematopoietic differentiation. Left panel, CD44 and CD34. Gated on SSC/FSC/Live. Right panel, CD44 and DLL4 gated on SSC/FSC/Live/CD34⁺CD43^{neg}CD184^{neg}CD73^{neg}: four different subpopulations are identified by CD44 and DLL4 expression. These populations have been sorted to perform CFC assay b) after 5 days of OP9DLL1 co-culture; n=3, independent, mean ± SD, one-tailed paired student T test p=0.0098.

3.8 Evaluating CD32 as HE marker in mouse

As previously described, murine EMPs emerge from the second wave of hematopoietic development from the HE and are characterized by the expression of CD16/32 on their surface (McGrath *et al*, 2015). Considering the result on human embryonic and hPSC-derived HE, we speculated whether CD32 or other Fc receptors can enrich for the fraction of endothelial cells with hemogenic potential also in mouse. In fact, available single-cell RNA-sequencing (scRNA-seq) transcriptomic analysis showed that *FcγR3* (CD16) is expressed in a population with HE features in E6.5-E8.5 (Pijuan-Sala *et al*, 2019) or E9.5-E10.5 (Pijuan-Sala *et al*, 2019; Zhu *et al*, 2020) murine embryos (Figure 31 a, b) while *FcγR2* (CD32) is not detected.

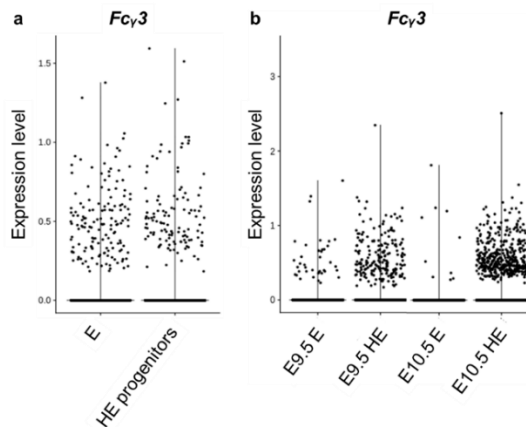


Figure 31 – *Fcγr3* is expressed in endothelial populations of E6.5-E9.5 mouse embryos

Violin plot showing the normalized expression values of *Fcγr3* gene in a) endothelial (E) and HE progenitor cells as assigned by computational methods and enriched in E8.25-E8.5 murine embryonic cells (Pijuan-Sala *et al*, 2019). b) Expression level of *Fcγr3* in E9.5 and E10.5 embryos. HE and endothelial (E) cells were defined as: *Ter119^{neg}CD41^{neg}CD45^{neg}Kit^{neg}Runx1:GFP^{neg}CD31⁺CD144⁺ESAM⁺* (E) and *Ter119^{neg}CD41^{neg}CD45^gCD45^{neg}Kit^{neg/low}Runx1:GFP⁺CD31⁺CD144⁺ESAM⁺* (HE) (Zhu *et al* 2020).

We dissected AGM and YS tissues of E10.5-E11 murine embryos, a comparable developmental stage to the human embryos we previously analyzed

(Figure 5). Using a mouse CD16/32 (FCGR3/FCGR2) antibody we observed that CD16/32 expression demarcates two sub-populations within the CD144⁺CD31⁺CD45^{neg}CD43^{neg} endothelial fraction (Figure 32 a, b) known to display HE potential in mouse (Nishikawa *et al*, 1998b). Therefore, we isolated the CD144⁺CD31⁺CD16/32⁺CD45^{neg}CD43^{neg} (referred to as CD16/32⁺) and the CD144⁺CD31⁺CD16/32^{neg}CD45^{neg}CD43^{neg} (referred to as CD16/32^{neg}) populations from E10.5-E11 AGM and YS (Figure 32 a, b). Then, we seeded the isolated cells on OP9DLL1 stroma in a cytokine-rich medium to allow their hematopoietic differentiation. After 7 days, we evaluated the frequency of hematopoietic cells in the culture analyzing the expression of the pan-hematopoietic marker CD45 and the erythroid marker TER119 by FACS. In fact, all the hematopoietic cells express CD45 on their surface except for erythroid cells (TER119⁺) after the enucleation, final differentiation step to the development of mature erythrocytes (Fraser *et al*, 2006). As such, the analysis of both markers is necessary to comprehensively evaluate the hematopoietic compartment. While YS-derived CD16/32⁺ population shows an increased, albeit not significant, trend of hematopoietic output compared to the CD16/32^{neg} counterpart, the hematopoietic yield in the AGM is comparable or even skewed in favor of the CD16/32^{neg} fraction (Figure 32 c, d). Of note, *Fcgr2* is not expressed in the sorted CD16/32⁺ population while *Fcgr3* is (Figure 32 e), confirming what we observed with the analysis of the public datasets of murine embryonic hematopoietic progenitors (Figure 31). In conclusion, our experiments suggest that Fc receptors should be carefully evaluated as HE markers in different species. In fact, despite our results in mouse models do not strictly parallel the data in humans, murine CD16 might enrich YS HSC-independent hematopoiesis. For this, we will perform further experiments as LDA to calculate the frequency of HE progenitors with the CD16/32^{+/neg} endothelial fraction. On the other hand, the hematopoietic potential does not segregate to any of the fraction of interest in the AGM. However, we might take into consideration that *ex vivo* cultures prevent the complete recapitulation of the temporal aspect of *in vivo* maturation. In fact, CD16/CD32^{neg} cells might mature into CD16/32⁺ *in vivo*, before giving rise to blood.

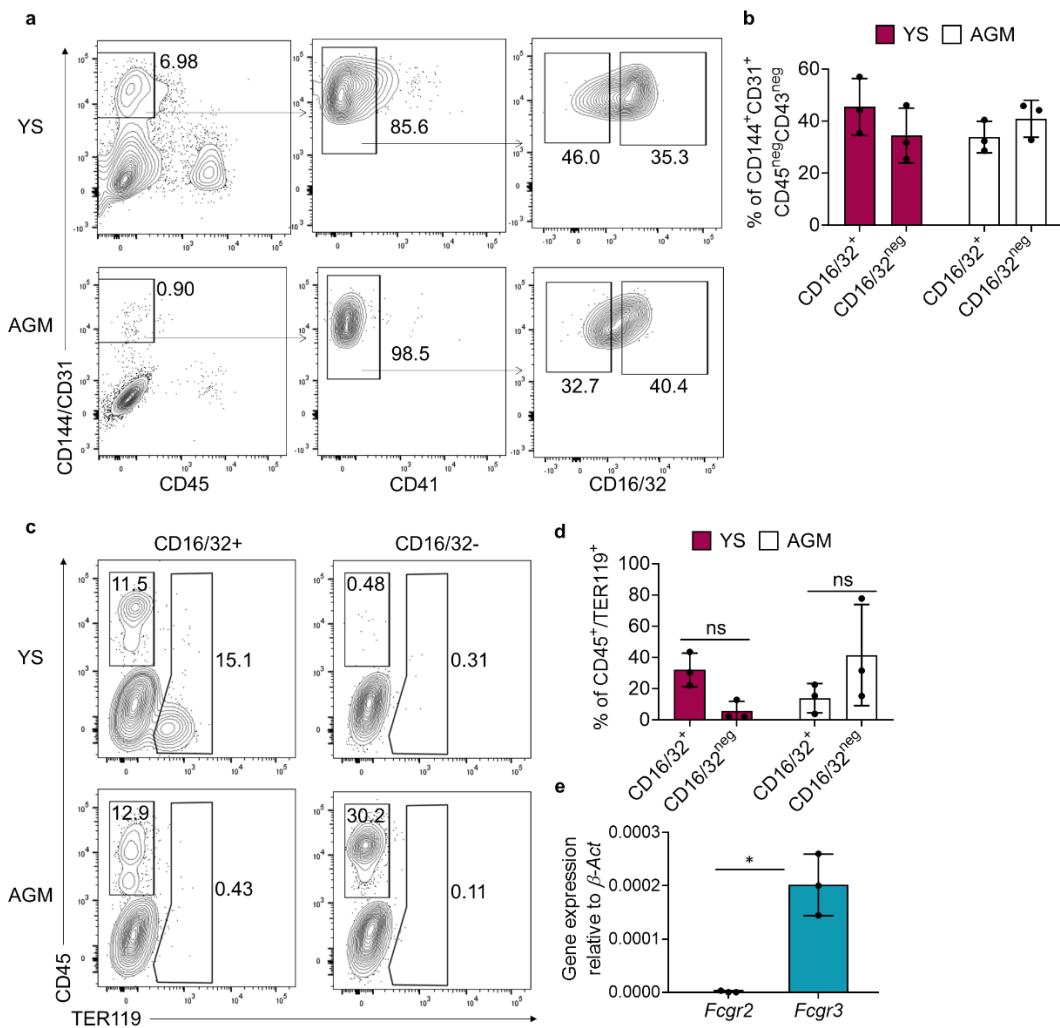


Figure 32 - Evaluating CD16/32 as HE marker in mouse embryos

a) Representative plots showing CD16/32 expression within CD144⁺CD31⁺CD45^{neg}CD43^{neg} cells in AGM and YS dissected from E10.5-E11.0 murine embryos. The highlighted gates correspond to the sorting strategy. Cells are gated on SSC/FSC/Live (left panel), SSC/FSC/Live/CD144⁺CD45^{neg} (middle panel), SSC/FSC/Live/CD144⁺CD41^{neg} (right panel). b) Bar plots highlighting the percentages of CD144⁺CD31⁺CD16/32⁺CD45^{neg}CD43^{neg} (referred to as CD16/32⁺) and CD144⁺CD31⁺CD16/32^{neg}CD45^{neg}CD43^{neg} (referred to as CD16/32^{neg}) cells in YS (purple) and AGM (white) of E10.5-E11.0 murine embryos in n=3, independent, mean \pm SD. c, d) Hematopoietic output derived from sorted CD16/32⁺ and CD16/32^{neg} fractions after 7 days of co-culture on OP9DLL1: c) representative plots of YS- (upper panel) and AGM-derived (bottom panel) hematopoietic (CD45⁺) cells and erythroid cells (TER119⁺CD45⁺) emerging from CD16/32⁺ (on the left) or CD16/32^{neg} (on the right) populations; gated on SSC/FSC/Live d) Bar plot showing the hematopoietic output of CD16/32⁺/^{neg} populations isolated from YS (purple) or AGM (white) of E10.5-E11.0 mouse embryos; n=3, independent, mean \pm SD, one-tailed paired T test p=0.05337 (YS), p=0.1862 (AGM). e) Bar plot of the gene expression analysis of murine Fcgr2b and Fcgr3 (blue) within the CD16/32⁺ sorted fraction of the AGM. Gene expression is relative to murine β -actin; n=3, independent, mean \pm SD, one tailed paired T test p=0.01521.

4. Discussion

One of the major aims of our lab is to faithfully recapitulate human embryonic development from hPSCs. In fact, the successful generation of the different blood types *in vitro*, particularly HSCs, would allow the autologous transplantation for the treatment of congenital BM disorders. In addition, hPSC-derived disease modeling might be instrumental to dissect several hematological diseases. Currently, hPSC differentiation protocols have been refined to yield multipotent progenitors showing characteristic of intra-embryonic hematopoiesis such as NOTCH-dependency. However, we are still unable to generate HSC from these HE cells. We believe that the precise identification of the HE cells will allow to compare the *in vitro* hPSC-derived HE with the one isolated from human embryos. Thus, we would identify the missing factors, whose manipulation will allow to finally generate HSC *in vitro*. Moreover, it will allow to determine the differences between HE that emerge within distinct hematopoietic programs during human embryonic development and identify the molecular factors that regulate their distinct potential.

In collaboration with Manuela Tavian's lab in Strasbourg, we took advantage of ACE expression in CD34⁺ endothelial cells to demarcate cells with hematopoietic potential in the developing human embryo (Jokubaitis *et al*, 2008). Of note, ACE does not similarly define endothelial cells with hemogenic potential in CD34⁺CD43^{neg}CD73^{neg}CD184^{neg} cells, which comprise HE cells in hPSC-based differentiating cultures. In fact, ACE is expressed by virtually all the CD34⁺ cells obtained by WNT-dependent intra-embryonic-like hematopoietic culture. Thus, it cannot distinguish the HE from other vascular endothelial cells.

Although ACE does not selectively label the hPSC-derived HE, ACE expression in the human embryonic dorsal aorta tracks with RUNX1⁺ cells at CS13 (Figure 18 a) (Jokubaitis *et al*, 2008). Thus far, RUNX1 is the most conserved and reliable marker of the HE (North *et al*, 1999; Ciau-Uitz *et al*, 2000; Burns *et al*, 2002; Kalev-Zylinska *et al*, 2002; Bollerot *et al*, 2005; Gering & Patient, 2005), functionally involved in the EHT (North *et al*, 1999; Yokomizo *et al*, 2001; Lacaud *et al*, 2002; North *et al*, 2002; Yokomizo *et al*, 2008; Chen *et al*, 2009; Kissa & Herbomel, 2010; Bertrand *et al*, 2010a; Boisset *et al*, 2010; Tober *et al*, 2013; Padrón-Barthe *et al*, 2014; Potts *et al*, 2014; Frame *et al*, 2016; Eliades *et al*, 2016). Therefore, we isolated CD34⁺ACE⁺CD45^{neg} cells (ACE⁺) from the AGM region of four embryos staged between day 28 and 32 (CS13-14) and performed whole-transcriptomic analysis. We

isolated and analyzed the corresponding CD34⁺ACE^{neg}CD45^{neg} (ACE^{neg}) fraction as control endothelial population devoid of hemogenic potential. To identify specific HE markers, we restricted the analysis to differentially expressed cell-surface genes. Among them, we identified *FCGR2B* (that encode for the isoform B of Fc receptor CD32) as one of the top cell-surface gene enriched in ACE⁺ compared to ACE^{neg} endothelium. Remarkably, CD32 is expressed in CD34⁺ endothelial cells of YS blood islands, in the endothelial layer of DA, and at the branching point between the DA and VA in the AGM of CS13 human embryos. These sites are known to contain a high frequency of endothelial cells with hemogenic potential at this stage (Tavian *et al*, 1996, 1999; Watt *et al*, 2000; Oberlin *et al*, 2002; Ivanovs *et al*, 2011; Easterbrook *et al*, 2019). Moreover, CD32 marks the IAHCs as well as the underlining endothelial cells in the DA including some CD34⁺RUNX1⁺ cells. To functionally validate CD32 as HE marker, we isolated CD34⁺CD43^{neg}CD45^{neg}CD32^{+/neg} cells from the AGM and the YS. Regardless of their location, CD32⁺ and CD32^{neg} fractions showed T- and NK-lymphoid potential. However, the CD32⁺ population more robustly generated clonogenic progenitors with erythro-myeloid potential.

Differently from ACE, CD32 is a reliable marker to isolate hPSC-derived HE with multilineage potential from both WNT-independent- extra-embryonic-like and WNT-dependent- intra-embryonic-like hematopoietic cultures. In both cultures, we confirmed that the hematopoietic potential segregates almost exclusively to CD34⁺CD32⁺CD73^{neg}CD184^{neg}DLL4^{neg} cells (referred to CD32⁺DLL4^{neg}) as they generate significantly more erythro-myeloid clonogenic progenitors in both H1 and H9 hESC lines. As mentioned in the introduction, further experiments will prove whether this population upregulates Notch signaling (*i.e.* acquiring DLL4 expression) while transitioning to hematopoiesis. Furthermore, we evaluated the lymphoid potential specific of each hematopoietic program. In particular, the EMP wave generates NK lymphoid progenitors while T-lymphoid potential is rare and limited as we observed by LDA in mouse embryos. In WNT-independent hematopoietic culture, NK-lymphoid progenitors derive from both CD32^{+/neg}DLL4^{neg} fractions. However, LDA revealed a 16-fold enrichment in CD32⁺DLL4^{neg} subset. On the contrary, intra-embryonic hematopoiesis gives rise to both NK and T-lymphoid cells. Remarkably, T-lymphoid potential is mostly restricted to the CD32⁺DLL4^{neg} population obtained by WNT-dependent hematopoietic cultures. Likewise, CD32⁺DLL4^{neg} enriches the NK potential in WNT-dependent hematopoietic cultures. We speculate that the residual hematopoietic potential of CD32^{neg}DLL4^{neg} fraction is due to the co-existence of cells at different maturation stage within the *in vitro* cultures. In fact, embryonic

development is a highly dynamic process, and we can speculate that CD32^{neg}DLL4^{neg} cells further mature to CD32⁺DLL4^{neg} HE cells at the early stages of our hematopoietic assays.

In addition, we compared the specificity of CD32 as hPSC-derived HE marker against CD44, another cell-surface protein known to enrich the HE population in mouse embryos (Watt *et al*, 2000; Zeng *et al*, 2019; Oatley *et al*, 2020). In addition, single cell RNA sequencing analysis highlighted that CD44⁺ aortic endothelial population of CS13 human embryos segregates the expression of genes involved in the EHT (*i.e.* *RUNX1*) (Zeng *et al*, 2019). According to the reported expression of CD44 in arterial endothelial cells (Watt *et al*, 2000; Oatley *et al*, 2020), CD44 marks most of WNT-dependent CD34⁺ cells. However, the CD44⁺ fraction within CD34⁺CD43^{neg}CD73^{neg}CD184^{neg}DLL4^{neg} population is enriched for HE. To compare the specificity of CD32 and CD44 as HE marker, we performed single cell EHT assay. The clonal analysis revealed that 89.2% of CD32⁺DLL4^{neg} cells that formed a clone generate CD45⁺ hematopoietic cells. The remaining 10.8% generate non-hematopoietic progeny. As previously observed, hematopoietic and non-hematopoietic clones never originate from the same CD32⁺DLL4^{neg} cell (Swiers *et al*, 2013; Ditadi *et al*, 2015). In contrast, CD44⁺DLL4^{neg} fraction contains less HE population compared to CD32⁺DLL4^{neg} cells. In fact, single CD44⁺DLL4^{neg} cell generates hematopoietic and non-hematopoietic in equal proportion. In conclusion, the single cell analysis indicates that CD32 is a reliable marker for hPSC-derived HE, whose specificity is superior to the one of CD44, often used to identify human HECs. Of note, CD44 plays a functional role during the EHT in murine embryos. On the other hand, we still need to understand whether the HE marker CD32 is also involved in hematopoietic emergence from human HE. Interestingly, CD44 and the isoform B of CD32 (FcγRIIB) share a peculiar expression and function on another specific endothelial subtype: the liver sinusoidal endothelial cells (LSEC). Here, they act as scavenger receptors involved in the clearance of waste molecules from the blood (Bhandari *et al*, 2021).

To speculate whether CD32 has a function in the EHT, we evaluated the available information about the cell-surface molecule. CD32 is an integral membrane glycoprotein that belongs to the family of receptors that bind the Fc portion of Ig (FCGR1, FCGR2A, FCGR2B, FCGR2C, FCGR3). CD32B (FCGR2B) extracellular domain is 95% homologous to the one of the isoforms CD32A and C (Hibbs *et al*, 1988; Qiu

et al, 1990). Therefore, the analysis of the expression pattern of the three isoforms has been complicated before the recent development of specific monoclonal antibodies for CD32A/CD32C and CD32B (Su *et al*, 2007; Veri *et al*, 2007; Ramsland *et al*, 2011). CD32B is the only isoform that contains ITIM-based inhibitory motif within the cytoplasmic domain that distinguishes its role from the other activating FcGRs. The activation of CD32B induces the phosphorylation of the tyrosine within the ITIM motif by Lyn (Malbec *et al*, 1998) thus promoting the phosphorylation and recruitment of inositol phosphatases SHIP1, 2 that hydrolyzes phosphatidylinositol (3,4,5)-trisphosphate (PIP₃). PIP₃ activates downstream protein, as the kinase Akt (Ma *et al*, 2019), by binding their PH domain.

In humans, CD32B has two major isoforms the CD32B1 and CD32B2 that differ for the inclusion of C1 exon in the former (Brooks *et al*, 1989; Qiu *et al*, 1990). The two isoforms are expressed on different cellular types. For instance, B cells mainly express CD32B1 in which C1 exon tethers the receptor on the cell membrane. On the other hand, CD32B2 is mainly expressed on myeloid cells. The absence of C1 exons allows the rapid internalization of the receptor on the expressing cell types thereby modulating its function. In general, CD32B1 function is the best characterized. It acts as immune checkpoint on the surface of B cells, controlling the action of activating-type Fc receptors.

In agreement with his role as immuno-regulator, CD32B expression is positively regulated by IL6 and IL10 while pro-inflammatory agents as TNF α and INF γ negatively regulate its expression (Guyre *et al*, 1983; Shushakova *et al*, 2002; Velde *et al*, 1992). Notably, IL6, TNF α and INF γ are also involved in the emergence of HSCs from the aortic layer in the AGM region (Espín-Palazón *et al*, 2014; Sawamiphak *et al*, 2014; Tie *et al*, 2019). Therefore, a tight regulation of the inflammatory signals might be involved in the transition from an endothelial to a hematopoietic fate. To understand the role of CD32, we are going to perform loss of function experiments using a drug-based or a genetic approach. First, we want to block CD32B activation by means of a Lyn peptide inhibitor (drug-based approach). In fact, the inhibition of the Lyn-mediated phosphorylation of the ITIM motif will prevent the signaling transduction activated by the ligand-receptor coupling. However, Lyn kinase is involved in several cellular process (Ingley, 2012). To avoid such aspecific and confounding effect, we plan to genetically knock-out the expression of the gene using base editing nucleases. In fact, Fc receptors share high degree of sequence homology

thus resulting in low-efficiency and off-targeted Cas9-mediated genome editing. On the contrary, base editors induce single point mutations into genomic DNA without the creation of double-stranded DNA breaks (DSBs) (Rees & Liu, 2018), allowing us to more efficiently knock-out CD32B.

In addition, dissecting the putative ligands of CD32B on the HE might unravel its potential role during the EHT. The main reported ligands of FCGR are IgG-immune complexes (IgG1-4 in humans) which bind to the receptors with different affinity. FCGR2 and 3 bind to the broad spectrum of IgG with low-affinity whereas FCGR1 is the only with high IgG affinity (100-1000-fold higher than the others) but preferential binding for IgG1 and IgG3. The binding of IgG immune complexes to CD32B promotes the activation of the receptor and the conventional inhibitory signaling. The immune complex engagement on the receptor might also induce the co-ligation with ITAM-containing receptors expressed on the cell surface (*i.e.* Dectin1, BCR, TCR) thereby regulating their activation or expression by endocytosis (Hunter *et al*, 1998; Malbec *et al*, 1998; Karsten *et al*, 2012). However, during human embryonic development, IgGs start to be produced at 12 weeks of gestation (Moro *et al*, 1990) and maternal IgGs are transferred to the fetus by transplacental delivery from the second trimester of pregnancy (Kristoffersen & Matre, 1996; Mimoun *et al*, 2020). In addition, *Rag1* and *Rag2*-deficient and NOD.Cg-Prkdcscid Il2rgtm1Wjl/SzJ (NSG) immunocompromised mice lack any B cells, hence IgG. However, they are viable and show no hematopoietic abnormalities. Therefore, IgGs are unlikely the ligand that mediates the putative role of CD32B on extra-embryonic and intra-embryonic HE.

In addition to IgG, FCGRs bind the acute phase reactant C-reactive protein (CRP), a member of the pentraxin family of proteins (Bharadwaj *et al*, 1999; Stein *et al*, 2000; Sundgren *et al*, 2011; Temming *et al*, 2021). In the adult, CRP is mainly produced by the liver in response to different stimuli as inflammation and infection. In addition, CRP expression is detectable in adult adipose and stromal cells (Ouchi *et al*, 2003; Memoli *et al*, 2007). Other sources of CRP are endothelial cells, particularly when stimulated with macrophage conditioned medium (Venugopal *et al*, 2005) or electronegative low-density lipoprotein (Chu *et al*, 2013). However, CRP expression in the embryo starts in the FL at E11.5. Therefore, CRP is unlikely the mediator of a putative CD32B function on HE cells.

Another alternative ligand of CD32B is the multifunctional protein fibrinogen-like protein 2 (FGL2) also known as fibroleukin (Liu *et al*, 2008). FGL2 belongs to the fibrinogen-related protein superfamily because of the high homology with fibrinogen β and γ chains (fibrinogen related domain, FRED), conserved in fibrinogen family members (Parr *et al*, 1995). FRED domain is required to promote fibrinogen interaction with intercellular adhesion molecule 1 (ICAM-1) expressed on the endothelium. The fibrinogen binding to vascular receptors has been demonstrated to initiate leukocyte adhesion to the endothelium and trans-endothelial migration, thus mediating early stages of immune inflammatory response (Languino *et al*, 1993, 1995). Therefore, FGL2-CD32B interaction might be involved in cell-cell interaction modification required to the EHT. The *Fgl2*-null murine model shows developmental defects and high rate of early embryonic lethality between E4.5 and E9.5 (Clark *et al*, 2004; Foerster *et al*, 2007) or neonatal lethality (Mu *et al*, 2007). FGL2 is highly conserved in human, mouse, and rat (Rüegg & Pytela, 1995; Levy *et al*, 2000; Yuwaraj *et al*, 2001; Rychlik *et al*, 2003) and exists in two different forms, a membrane-bound (mFGL2) and a soluble protein (sFGL2) (Yuwaraj *et al*, 2001). The two forms share the FRED domain, responsible of the immunosuppressive activity of sFGL2 (Chan *et al*, 2003), despite it remains poorly elucidated. To date, activated cytotoxic and regulatory T lymphocytes have been described as the major producers of sFGL2 so its involvement as CD32B ligand on the HE is unlikely (Rüegg & Pytela, 1995; Marazzi *et al*, 1998; Shalev *et al*, 2008; Yang *et al*, 2013). Contrarily to sFGL2, mFGL2 has not a reported role in the regulation of the immune response but shows prothrombinase activity and related pro-inflammatory effect (Levy *et al*, 2000; Marsden *et al*, 2003; Clark *et al*, 2004; Melnyk *et al*, 2011; Liu *et al*, 2012). mFGL2 is expressed as transmembrane protein (Liu *et al*, 2010; Yuwaraj *et al*, 2001; Chen *et al*, 2011b; Yang *et al*, 2013) on endothelial cells, epithelial cells, macrophages, and dendritic cells. In addition, the first expression of mFGL2 starts at E6.5 in the mouse embryo and remains constitutively expressed during embryonic development, although the expression dynamically changes (Clark *et al*, 2004). Transcriptomic analysis of CS7 (gastrulation stage) (Tyser *et al*, 2021), CS11, CS13 human embryos (Zeng *et al*, 2019; Tyser *et al*, 2021) highlighted that *FGL2* is expressed in cells with putative HE fate. The expression of FGL2 on endothelial cells might suggest its functional role as adhesion protein. In this context, the binding FGL2-CD32 might be required to accomplish the morphological changes needed for the EHT. To test this, we will perform protein-protein interaction screenings as two-hybrid system, crosslinking and immunoprecipitation and eventually mass-spectrometry that will shed the light on the identity of CD32 ligands when expressed on HE.

Since the HE is a central and evolutionary-conserved element for the generation of blood cells during development, we postulate that the putative function of CD32B in HE specification or maturation will likely be conserved between species, possibly involving other FCGRs. On this regard, it must be noted that the biology of FCGRs differs significantly between mouse and human. For instance, CD32B is the only FCGR2 isoform expressed in murine model. On the other hand, the same family in humans also includes the ITAM-based CD32A, C. Thus, the role of CD32B in controlling the action of activating-type Fc receptors upon co-aggregation is limited in mouse while widely experienced in humans (Malbec *et al*, 1998; Sato & Ochi, 1998; Brauweiler *et al*, 2001; Huang *et al*, 2003; Karsten *et al*, 2012). On the other hand, mouse *FcyRIIB* has three splicing variants, *FcyRIIB1*, *B1'*, *B2* differently from the two in human. Although the sequences of human and mouse *CD32B* homologs are highly conserved, the amino acid differences in their splicing variants have not been functionally characterized. In addition, cellular expression can also vary between humans and mice.

Our data performed on E10.5-E11 murine embryos indicate already discrepancies between human and murine FCGRs expression in the developing hematopoietic system. In fact, we observed that *FcyRII* is not expressed within CD144⁺CD31⁺CD45^{neg}CD43^{neg} endothelial population isolated from AGM or YS whereas *FcyRIII* (CD16) is. Interestingly, available transcriptomic analysis performed on E6.5-E8.5 murine embryos confirmed that hemato-endothelial progenitors express *FcyRIII* but not *FcyRII* (Pijuan-Sala *et al*, 2019; Zhu *et al*, 2020). We evaluated whether CD144⁺CD31⁺CD45^{neg}CD43^{neg}CD16/32^{+/neg} (referred to as CD16/32⁺ or CD16/32^{neg}) populations isolated from E10.5-E11 AGM or YS samples have different hemogenic potential *ex vivo*. We isolated the two fractions by FAC-sorting and assessed their potential by co-culture on OP9DLL1 stroma. Neither the AGM- nor the YS- derived CD16/32^{pos/neg} fractions showed a significant enrichment of hematopoietic frequency. However, the YS CD16/32⁺ fraction showed a trend of enriched hematopoietic output in terms of total hematopoietic progeny (CD45⁺) and committed erythroid cells (CD45^{neg}Ter119⁺). Therefore, either CD16/32 does not mark the HE in mouse, we are capturing a wrong developmental window and/or cells do acquire CD16/32 the expression during the *ex vivo* culture. In order to draw meaningful conclusion, LDA and other experiments are required. However our preliminary results suggest that CD16 expression enriches for endothelial cells with hematopoietic potential in the YS and as such it might be considered as extra-embryonic HE marker. However, the activation of CD16 relies on an ITAM-based

activating signal, opposite to CD32B. This would complicate the understanding of their function in the specification or maturation of HE in mouse or human embryos. Nevertheless, little is known on whether murine CD16 and human CD32B share common mechanisms of activation and/or signal transduction. Regardless, if in the mouse embryo CD16 will be validated as an HE marker for YS hematopoiesis, particular attention will need to be paid to the careful dissection of HSC-dependent and HSC-independent intra-embryonic hematopoietic program. In particular, defining whether CD16 expression discriminates only extra- vs intra-embryonic HE cells, or more globally HSC-non-competent vs HSC-competent HE cells. Such careful dissection of the developmental programs will need to be performed in the human model as well, since thus far most of our functional experiments have been performed using the hPSC model that does not yield HSC yet.

The precise isolation of HE, both from *in vitro* cultures as well as developing human embryos, will also help dissecting the missing steps for generating HSCs in a dish, one of the major goals of our lab. In fact, we are currently unable to specify cells towards an HSC fate. Culture conditions supporting HSC specification even from cells derived from human embryos are lacking (Ivanovs *et al*, 2014; Easterbrook *et al*, 2019) and the signals that cell-autonomously coax human HE cells to mature into HSC are currently unknown. Studies in other animal models have shown that signaling pathways involved in the process are inflammation (Guyre *et al*, 1983; Shushakova *et al*, 2002; Velde *et al*, 1992), blood flow (Rhodes *et al*, 2008; Lux *et al*, 2008; Adamo *et al*, 2009; North *et al*, 2009) and RA signaling activation (Chanda *et al*, 2013; Dou *et al*, 2016). In particular, RA signaling is critical for the generation of HSCs from HE cells. However, the activation of the RA signaling on hPSC-derived WNT-dependent HE did not support the emergence of HSCs (Yu *et al*, 2010; Rönn *et al*, 2015; Dou *et al*, 2016). While our experiments have now identified an RA-dependent HE population capable of contribute transiently to multilineage hematopoiesis *in vivo*, RAd HE-derivatives are still lacking the long-term self-renewing property of HSCs. We hypothesize that the activation of further specific signaling(s) might be required to allow long-term engrafting HSC emergence from RAd HE *in vitro*. Inflammatory signaling, biophysical forces stemming from the onset of blood flow (sheer and circumferential stress) as well as additional RA signaling are amongst the first pathways we will investigate. On the other hand, we cannot exclude that the RAd HE gives rise to another hematopoietic wave devoid of HSC potential, increasing the complexity of HSC-independent hematopoiesis. Regardless, further

analysis is required to discriminate whether the HE potential remains enriched in the CD32⁺DLL4^{neg} fraction also in the RAd HE.

In conclusion, our hPSC-based tool allows to model the hematopoietic development *in vitro* and to dissect the mechanisms underlying the emergence of blood cells. In addition, it allows to evaluate markers to discriminate the HE population *in vitro*. Notably, the *in vitro* analysis corresponds to *in vivo* or *ex vivo* evidence.

We believe that recapitulating the ontogeny of the HE and characterizing its identity throughout the different embryonic hematopoietic waves is crucial to provide a complete view of developmental hematopoiesis. The characterization of the transcriptomic and genomic accessibility landscape of hPSC-derived CD32⁺ HE might help us to discriminate the signaling pathways and transcriptional factors involved in the specification of the hematopoietic fate during different hematopoietic programs. In this way, the immuno-phenotypical definition of the HE would help to define program-specific protocols to efficiently recapitulate the emergence of peculiar hematopoietic progenitors *in vitro* with consequent clinical and therapeutical relevance. In fact, the use of CD32 in combination with other endothelial markers will allow to greatly enrich for cells with hematopoietic potential from a broad range of hPSC lines, including those that do not differentiate efficiently to the hematopoietic lineages using current protocols. This will also be extremely helpful to the production of hPSC-derived blood therapeutics, even HSC-independent hematopoietic cell types, like lymphoid cells for immunotherapy as well as microglia and tissue resident macrophages for regenerative medicine applications.

5. Materials and methods

5.1 Human embryonic tissues

Human embryonic samples were obtained after elective medical termination of pregnancy. Each patient signed an informed consent to approve the research use of the samples. The study was approved by Ospedale San Raffaele Ethical Committee (TIGET-HPCT protocol) or French National Ethic Committee (CEEI/IRB 21-854). The developmental stage was established using the Carnegie classification (Tavian *et al*, 2004). Samples were either used immediately as fresh tissues (*ex vivo* and RNA sequencing analysis) or fixed in PBS supplemented with 4% para-formaldehyde (Sigma-Aldrich), embedded in Optimal Cutting Temperature (OCT) compound and stored at -80°C (immunohistochemistry and immunofluorescence).

Human embryonic tissues (CS13) employed for *ex vivo* hematopoietic cultures were collected by human developmental biology resource (HDBR), Newcastle University, Newcastle, United Kingdom. The human embryonic tissues were dissociated for 50 minutes at 37°C with 10mg/ml Collagenase/Dispase (Sigma-Aldrich, 10269638001) in PBS with Ca^{2+} and Mg^{2+} , supplemented with 7% heat-inactivated fetal bovine serum (FBS, Hyclone), 100 IU/ml penicillin (Invitrogen), 100 $\mu\text{g}/\text{ml}$ streptomycin (Invitrogen) and 10 $\mu\text{g}/\text{ml}$ DNase I (Calbiochem, 260913) and filtered through a 40 μm cell strainer (Falcon, 352235), similarly to what was previously described (Ivanovs *et al*, 2011).

Human embryonic tissues (CS13-CS14) analyzed by RNA sequencing were processed in Manuela Tavian's laboratory, Inserm, Strasbourg, France. Single-cell suspensions were obtained after incubation in medium containing 0.23% w/v collagenase Type I (Worthington Biochemical Corporation, NC9482366) for 30' at 37°C and filtered through a 70 μm cell strainer (70 μm , BD Biosciences).

5.2 Immunohistochemistry and immunofluorescence

Immunohistochemistry and immunofluorescence experiments were exclusively performed in Manuela Tavian's Lab, Inserm, Strasbourg, France. The techniques employed have been previously described in (Sinka *et al*, 2012). The sections were cut at 5 μm , incubated with primary antibodies overnight at 4°C . Biotinylated secondary antibodies were added the next day for 1 hour at room temperature (RT).

A third staining was performed for 1 hour at RT adding fluorochrome-labeled or peroxidase-labeled streptavidin (Immunotech). Peroxidase activity was assessed by the addition of PBS supplemented with 0.03% hydrogen peroxide, 0.025% 3,3-diaminobenzidine (Sigma-Aldrich). Low amounts of antigens (CD32, ACE) were revealed by Tyramide signal amplification (TSA) biotin and fluorescence amplification systems (Akoya, Biosciences). When 3,3-diaminobenzidine was used on slides, they were counterstained with Gill's hematoxylin (Sigma-Aldrich), mounted in XAM neutral medium (BDH Laboratory Supplies), analyzed and imaged using an Optiphot 2 microscope (Nikon). Stained sections were mounted in Mowiol containing 4',6-diamino-2-phenylindole dihydrochloride. An isotype-matched negative control was performed for each immunostaining. Immunofluorescent staining was observed on a DMR/HCS fluorescence microscope (Leica DMS) and pictures were acquired using Metavue software (Molecular Devices). The anti-human uncoupled primary antibodies used are listed: uncoupled CD34 (QBEnd/10. Beckman), anti-human ACE (BB9, BD Biosciences, 557813), anti-human CD32 (Biolegend, 303202) and rabbit anti-human/mouse Runx1 (Abcam, ab23980). Secondary biotinylated antibodies were: goat anti-mouse IgG (Jackson Immuno Research) and goat anti-rabbit IgG antibody (Jackson Immuno Research). Double-immunofluorescence staining used Alexa688-labeled anti-mouse antibody (Life Technologies Invitrogen) coupled to fluorescence amplification with the TSA Fluorescent Plus System.

5.3 RNA sequencing data analysis

Raw single-end reads quality control was determined using FastQC tool (<http://www.bioinformatics.babraham.ac.uk/projects/fastqc>) and read trimming was performed using Trim Galore software (<https://doi.org/10.5281/zenodo.5127899>) to remove residual adapters and low-quality sequences. Trimmed reads were aligned against the human reference genome (GRCh38) using STAR (Dobin *et al*, 2013) with standard input parameters, and only uniquely mapped reads were considered for downstream analyses. Reads were assigned to genes with the featureCounts tool (Liao *et al*, 2014), using the GENCODE primary assembly v.34 gene transfer file (GTF) as reference annotation for the genomic features. Transcript count matrices were then processed by the R/Bioconductor differential gene expression analysis packages DESeq2 (Love *et al*, 2014) following standard workflows. In particular, a paired analysis was set up, modeling gene counts using the following design formula:

~donor + condition. Genes with adjusted p-values less than 0.05 were considered differentially expressed.

Lists of differentially expressed genes were analyzed for functional enrichment analysis. Enrichment p-values were corrected for multiple testing using FDR. Gene Set Enrichment Analysis (GSEA) was performed considering different the Gene Ontology and Molecular Signatures Database using clusterProfiler (Wu *et al*, 2021) (v 3.8.1, <http://bioconductor.org/packages/release/bioc/html/clusterProfiler.html>) by pre-ranking genes according to Log2 Fold Change values. Enriched terms with an adjusted p-value < 0.05 were considered statistically significant. Volcano plots were generated using the ggplot2 R package (<https://ggplot2.tidyverse.org>) and have been used to display RNA-seq results plotting the statistical significance (adjusted P-value) versus the magnitude of change (fold change). Heatmaps were generated using the pheatmap R package (<https://CRAN.R-project.org/package=pheatmap>). Surface genes were extracted using the surfaceome database (Bausch-Fluck *et al*, 2018) (<http://wlab.ethz.ch/surfaceome/>).

5.3.1 Public single-cell RNA-seq datasets visualization

Single-cell RNA-seq dataset from (Pijuan-Sala *et al*, 2019) was downloaded using the MouseGastrulationData R package, whereas the dataset from was downloaded from (Zhu *et al*, 2020) the Gene Expression Omnibus (GEO) database (<https://www.ncbi.nlm.nih.gov/geo/query/acc.cgi?acc=GSE137116>). Raw counts and cells metadata were retrieved and a Seurat object was created for both the datasets using the CreateSeuratObject function from the Seurat R package (Stuart *et al*, 2019) (v 3.2.2, <https://cran.r-project.org/web/packages/Seurat/index.html>). Then, expression values were log-normalized using the NormalizeData function and were visualized using the VlnPlot function from the same R package.

5.4 Murine embryonic fibroblasts

Murine embryonic fibroblasts (MEF) were isolated from Swiss Webster E13.5 embryos. Cells were expanded for five passages and irradiated at 30 Gy. The culture medium before or after the irradiation consists of IMDM (Invitrogen, 12200069) supplemented with 2.54 g of Sodium Bicarbonate (Life Technologies), 15% FBS (Hyclone), 100 IU/ml penicillin (Invitrogen), 100 µg/ml streptomycin (Invitrogen),

1% glutamine (Invitrogen) and 400 μ M 1-Thioglycerol solution (Sigma-Aldrich, M6145). After irradiation, 250000 cells/well were plated on a 6-well plate coated with 1 ml/well 0.1% gelatin (Sigma-Aldrich, G1890-100G) 15' in advance and aspirated right before use.

5.5 Human embryonic stem cells

The use of human embryonic stem cells (hESC) was approved by the Ospedale San Raffaele Ethical Committee, included in the TIGET-HPCT protocol. H1, H9 or HES2 hESCs were grown on irradiated MEF feeders in DMEM/F12 medium (Corning, L022046-10092CVR) supplemented with 25% of KnockOut™ Serum Replacement (Gibco, 10828028), 100 IU/ml penicillin (Invitrogen), 100 μ g/ml streptomycin (Invitrogen), 1% glutamine, 0.1% β -Mercaptoethanol, 0.7% of MEM Non-Essential Amino Acids Solution (Thermo Fisher, 11140035). 0.1 μ l/ml Ciprofloxacin HCl (Sigma-Aldrich, PHR1044-1G) and 20-30 ng/ml human recombinant basic fibroblast growth factor (bFGF, R&D, 233-FB-500/CF) were added to hES medium right before usage. Fresh medium was added every day to the cells in culture. After 4-5 days from thawing, hESCs were detached by adding 0.5 ml/well of pre-heated 0.25% Trypsin-EDTA (Thermo Fisher, 25-200-056) for 1' at room temperature. Then, Trypsin-EDTA was aspirated, and eventual residues stopped by "Wash medium" (DMEM-F12 supplemented with 5% KSR, 25 mM HCl) supplemented with 10% FBS and 10 μ l/ml DNase I. Cells were additionally dissociated by scraping, collected and centrifuged at 1000 rpm for 5'. Eventually cells were plated on new MEF for additional 4-5 days of expansion. Before differentiation, cells were split 1:2 onto Matrigel (Corning, 356230) coated 6-wells for 24-48 hours to deplete feeders. Cells were maintained and expanded at 37°C, 21% O₂, 5% CO₂.

5.6 Hematopoietic differentiation

After the feeder depletion step, hESCs were dissociated by TrypLE (Thermo Fisher Scientific, 12605010) and scraping, similarly to the procedure observed during cell expansion. Cells were collected in "Wash medium" supplemented with 10 μ l/ml DNase I, centrifuged at 1000 rpm for 5' and resuspended at 250000-400000 cells/ml and plated into 6-wells plates coated with 5% polyheme solution (Sigma-Aldrich, P3932) to avoid cell adhesion. The differentiation was performed at 37°C, 5% O₂, 5% CO₂. For the first three days of differentiation (*i.e.* mesoderm induction and

patterning), the base medium consists of 75:25 mixture of IMDM:Ham's F-12 supplemented with BSA to a final concentration of 0.05% w/v. To induce the hematopoietic and endothelial specification, we used a Stempro-34 base medium (Life Technologies, 10639011). The base media were supplemented with 1% glutamine, 50 µg/ml ascorbic acid, 150 µg/ml transferrin, 400 µM 1-Thioglycerol solution (Sigma-Aldrich, M6145). In addition, the differentiation medium was changed and supplemented with specific cytokines and small molecules to induce WNT-dependent and -independent hematopoiesis as previously reported (Ditadi & Sturgeon, 2016).

5.6.1 Aldefluor assay

To evaluate the regulation of Notch, AhR and TGFβ in the specification of a RA-responsive mesoderm, we treated hESC-based differentiation cultures at day 2 by supplementing the differentiation medium with 10 µM GSI (Tocris Bioscience, 2627), 1 µM SR 1 (Cayman Chemical Company, 10625), 0.3 µM SB 431542 (Cayman Chemical Company, 13031) or 1-10 ng/ml of Activin A (Miltenyi Biotech, 130-115-010). ALDH assay was performed at day 3 of hematopoietic differentiation (36 hours after the small molecules treatment) according to the manufacturer's instruction (Stemcell Technologies, 01705).

5.6.2 Mesoderm isolation and RA treatment

KDR⁺CD235^{neg}CD184^{+/neg} cells were isolated by FAC-sorting at day 3 of WNT-dependent differentiation and reaggregated at 300000 cells/ml in a low-adherence 24-well plate in day 3 differentiation medium as described in (Ditadi & Sturgeon, 2016). Cells were grown at 37°C, 5% O₂, 5% CO₂. After 6 hours, cells were fed with additional T3 medium supplemented ATRA (Sigma, R2625) to obtain a final concentration of 1nM or an equal volume of DMSO. The derived CD34⁺CD43^{neg} cells were sorted at day 8 of differentiation.

5.7 OP9DLL4 or OP9DLL1 co-culture for T and NK lineage differentiation

OP9 cells expressing human DLL4 or murine DLL1 were generated as previously described (Kennedy *et al*, 2012). OP9DLL4/DLL1 cells were maintained in Alpha

Minimum Essential Medium (Alpha-MEM, Thermo Fisher, 12000063) supplemented with 2.2 g/L sodium bicarbonate (Corning, 61-065-RO), 10% FBS (Hyclone), 100 IU/ml penicillin (Invitrogen), 100 µg/ml streptomycin (Invitrogen), 1% glutamine (Invitrogen). The cells were cultured at 37°C, 21% O₂, 5% CO₂ on 10 cm-Petri dishes and divided every 2-3 days at a confluence of 80%.

5.8 T- and NK lineage differentiation

To test the T- or the NK- cell potential, 150-500 candidate cells isolated by FAC-sorting were seeded on OP9DLL4/DLL1-coated 24-well plates. 60000 OP9DLL4/DLL1 cells/well were seeded on 24-well the day before. OP9DLL1 were used for the experiments performed on human embryonic samples. On the other hand, hPSC-derived cells isolated at day 8 of differentiation were seeded on OP9DLL4 stroma. For both T- and NK- cell differentiations, the cells were cultured in Alpha MEM (Thermo Fisher, 12000063) supplemented with 2.2 g/L sodium bicarbonate (Corning, 61-065-RO), 20% FBS (HyClone), 100 IU/ml penicillin (Invitrogen), 100 µg/ml streptomycin (Invitrogen), 1% glutamine (Invitrogen) and 400 µM 1-Thioglycerol solution (Sigma-Aldrich, M6145)) supplemented with lineage specific cytokines.

For T lineage differentiation, T-cell specific cytokines were added to "Alpha MEM base medium": 5 ng/ml IL7 (130-095-362), 5ng/ml FLT3l (130-096-479), 50 ng/ml SCF (130-096-696) (only for the first 5 days of differentiation). All cytokines were purchased from Miltenyi Biotech. The cells were split every 4-5 days and plated on freshly seeded OP9DLL4/Dll1. T-lymphoid output was assayed by FACS analysis after 21-24 days of differentiation.

For NK-specific differentiation, the cells were seeded on OP9Dl1 stroma in "Alpha MEM base medium" supplemented with 5 ng/ml IL7, 5ng/ml FLT3l, 10 ng/ml IL15 (130-95-765), 30 ng/ml IL3 (130-095-070. only for the first 7 days of differentiation). Cytokines were purchased from Miltenyi Biotech. The cells maintained for 14 days on the same stromal cells. Every 7 days, the culture was supplemented with fresh medium. The differentiation was prolonged to 21 days for LDA assays in which 1, 5, 10, 25, 30, 50 or 100 cells were directly seeded on OP9DLL1-coated 96-well during FAC-Sorting. NK-lymphoid output was assayed by FACS analysis.

5.9 Colony forming cell assay

OP9DLL1/OP9DLL4 cells were irradiated at 30 Gy. 120000 cells/well were seeded on a 24-well plate the day prior to use. FAC-Sorted cells were seeded on irradiated OP9DLL1/OP9DLL4 in Alpha-MEM (Alpha-MEM, ThermoFisher, 12000063) supplemented with 20% FBS (HyClone), 100 IU/ml penicillin (Invitrogen), 100 µg/ml streptomycin (Invitrogen), 1% glutamine (Invitrogen), 30 ng/ml TPO (130-095-747), 10 ng/ml BMP4 (314-BP-MTO), 50 ng/ml SCF (130-096-696), 25 ng/ml IGF1 (130-093-887), 10 ng/ml IL11 (130-103-439), 10 ng/ml FLT3L (130-096-479), 4 U/ml EPO (100-64). After five days, cells in suspension were collected while adherent cells were detached by 0.25% Trypsin-EDTA for 3' at 37°C. Trypsin-EDTA was stopped by adding Alpha-MEM supplemented with 10% FBS (Hyclone). Cells were filtered through a 40 µm filter and centrifuged at 1000 rpm for 5'. The cell pellet was resuspended in 100 µl of medium and seeded on methylcellulose medium (Stemcell Technologies, H4034). WNT-independent hematopoietic cultures were seeded on methylcellulose supplemented with 150 µg/ml transferrin (R&D, 2914-HT), 50 ng/ml TPO, 10 ng/ml VEGF (MAB3572), 50 ng/ml IL3 (130-095-070), SCF 100 ng/ml, 10 ng/ml IL6 (130-093-934), 50 ng/ml IGF1, 5 ng/ml IL11, 4 U/ml EPO, GM-CSF 1 ng/ml (130-093-864), 6 µM SB 431542 (Cayman Chemical Company, 13031). WNT-dependent hematopoietic cultures were seeded on methylcellulose supplemented with 150 µg/ml transferrin, 50 ng/ml TPO, 10 ng/ml VEGF, 10 ng/ml IL6 (130-093-934), 50 ng/ml IGF1, 5 ng/ml IL11, 4 U/ml EPO. Colonies' number and morphology was evaluated after fifteen days by light microscopy. All the cytokines were purchased by Miltenyi biotech except for EPO, Peprotech, BMP4 and VEGF, R&D.

5.10 Multilineage clonal assay

Single CD34⁺CD43^{neg}CD184^{neg}CD73^{neg}DLL4^{+/neg}CD32^{+/neg}/CD44^{+/neg} cells were seeded into a Matrigel-coated (Corning, 356230)- well of 96-well plate during the sorting procedure. The cells were seeded in Stempro media (Life Technologies, 10639011), complemented with 1% glutamine, 50 µg/ml ascorbic acid, 150 µg/ml transferrin, 400 µM 1-Thioglycerol solution (Sigma-Aldrich, M6145), 30 ng/ml TPO, 10 ng/ml VEGF (R&D, MAB3572), 5 ng/ml bFGF (R&D, 233-FB-500/CF), 30 ng/ml IL3 (130-095-070), SCF (130-096-696), 50 ng/ml IGF1 (130-093-887), 10 ng/ml IL6 (130-093-934), 5 ng/ml IL11 (130-103-439), 4 U/ml EPO (Peprotech, 100-64). Hematopoietic and non-hematopoietic clones were evaluated by light microscopy and

FACS analysis after 10 days of culture. Cytokines were obtained from Miltenyi Biotech except when differently reported.

5.11 Mouse embryonic tissues

All procedures involving mice were in compliance with the Animal Care and Use Committee of the Ospedale San Raffaele (IACUC 841) and communicated to the Ministry of Health and local authorities according to the Italian law. Mice were housed with free access to food and water and maintained in a 12-hour light–dark cycle. Pregnant CD-1 mice were obtained by Charles River Laboratories and sacrificed at E9.5-E10.5 by CO₂ narcosis. The uterus was collected into a petri dish with PBS supplemented with 10% FBS and cut into single embryo units with scissors and forceps. Single embryo units were further dissected to remove the outer uterine muscular membranes and to expose the YS and the embryo proper. First, YS was gently separated from the embryo proper by cutting at the origin of the vitelline vessel. For P-Sp/AGM isolation, the caudal part was isolated from the rest of the embryo and somites were removed by using thin needle-syringes. The isolated tissues were kept on ice during the procedure. Samples were dissociated for 15' at 37°C with 0.1% Collagenase type I (Sigma-Aldrich, SCR103) in PBS with Ca²⁺ and Mg²⁺ supplemented with 5% FBS. Then, samples were dissociated by gentle manual pipetting.

5.12 Murine xenografts

0.5-5x10⁵ CD34⁺CD43^{neg} cells isolated from DMSO- or ATRA-treated hPSC-based hematopoietic differentiation cultures were intra-hematically injected into neonatal NSG mice. Peripheral blood (PB) and BM aspirates were collected every 4 weeks to assess the xenograft persistence. PB was collected by retroorbital vein. BM aspirate was obtained from the injected femur under deep anesthesia, by inserting a 29G needle syringe into the distal femur shaft. Both BM and PB samples treated with ACK lysis buffer (0.15 M NH₄CL, 0.01 M KHCO₃, 1x10⁻⁴ M Na₂EDTA) to properly lyse red blood cells. Mice were sacrificed by CO₂ four months post-transplantation. After sacrifice, BM were harvested, and blood cells collected by flushing it using a 29G needle syringe. The collected cells were treated with ACK as above. The animal studies were performed as indicated in the IACUC 841/710 communicated to Ministry

of Health and local authorities and approved by the Animal Care and Use Committee of the Ospedale San Raffaele and the Italian law.

5.13 Multilineage assay from murine samples

Candidate cells ($0.5-10 \times 10^3$) were cultured on 24-well plate containing OP9 cells expressing Delta-like 1 (OP9DLL1) in α -MEM supplemented with 100 ug/ml penicillin-streptomycin (Invitrogen), 20% FBS (Hyclone), mouse (m) SCF 50ng/ml (130-101-697), mTPO 50ng/ml (130-096-301), mGM-CSF 3ng/ml (315-03), mIL3 30 ng/ml (130-099-511), mIL6 5 ng/ml (130-096-685), mFLT3 10 ng/ml (130-097-372), mIL7 5 ng/ml (130-108-957), EPO 2U/ml (100-64). All cytokines were purchased from Miltenyi but mGM-CSF and EPO, Peprotech. After five days co-cultures were transferred onto fresh OP9DLL1 cells by vigorous pipetting and passaging through a 40 μ M cell strainer. Cells were analyzed by flow cytometry at day 11. 1, 3, 10. 30. 100 cells were sorted directly onto individual wells of a 96-well plate containing OP9DII1 cells and cultured as above.

5.14 Gene expression analysis by quantitative real-time PCR

Total RNA was prepared using ReliaPrep RNA Miniprep Systems (Promega, Z6012) and retro-transcribed using random hexamers and Oligo(dT) with ImProm-II Reverse Transcription System (Promega, A3800), according to the manufacturer's instructions. Real-time quantitative PCR (qPCR) was performed on a Viiia 7 Real-Time PCR System (Thermo Fisher). The samples were analyzed in technical replicate on FrameStar FastPlate 96 (4titude, cat. 4ti-0910/C) using Fast SYBR Green Master Mix (Thermo Fisher Scientific, cat. 4385617). Expression levels were normalized to the housekeeping gene β -actin. The oligonucleotides used are: mFCGR2b FW CGGTGACACTGACATGCGAA, RV ATGGTGACAGGCTTGGACTGG; mFCGR3 FW ATGGTGACACTGATGTGCGAAG, RV CTGAGGGGTCTGGAGCAGCA; m β -actin FW AGGTGACAGCATTGCTTCTGTG, RV CTCAGACCTGGGCCATTCAGAAT.

5.15 Cell staining, flow cytometry and cell sorting

Samples for FACS analysis or cell sorting were incubated with antibody mixes for 15-30' at 4°C The staining The antibodies employed are listed in the table included in

paragraph 5.17. Dead cells were excluded using 7AAD during staining or collected in a solution of 7-aminoactinomycin D (2 µg/ml) before sorting. Cells were sorted with FACSARIA II (BD). Sorting gates were set using appropriate fluorescence minus one (FMO) and single staining controls. FACS-analysis were performed either at FACS Canto, (BD Biosciences) or Cytoflex S (Beckman Coulter).

5.16 Ethical statement

All the procedures involving mouse models were performed according to the protocols acknowledge by the Animal Care and Use Committee of the Ospedale San Raffaele (IACUC 841). The Ministry of Health and local authorities were duly informed according to the Italian law. The mouse animal models share significant genetic similarities with humans and represent the specie with the lowest neurological development. Therefore, they have been employed through the study when no suitable alternative exists and to research purpose only, embracing the policy of the 3 Rs: reduction, refinement and replacement. In details, the experiments were designed to minimize the number of animals used but to achieve statistically significant scientific results (reduction). The number of animals needed was calculated in advance, to avoid the use of excessive number of mice and redundant experiments. All the experimental procedures were designed to reduce animal distress and suffering (refinement). Food and water were *at libitum* available and routinary changed. The number of mice per cage were set to five to limit animal distress. Before sacrifice, the animals were anesthetized using Isoflurane. The euthanasia was performed by CO₂ narcosis. Whenever possible, the use of animals was replaced by *in vitro* hPSC-based systems (replacement).

The use of hESC to accomplish this work was approved by Ospedale San Raffaele Ethical Committee, included in the TIGET-HPCT protocol.

The human embryonic tissues employed in this thesis were obtained by informed consent after elective termination of pregnancy. The tissues used for *ex vivo* analysis were collected by Human Developmental Biology Resource (HDBR), Newcastle University, Newcastle, United Kingdom. The use of human embryonic material was approved by the Ospedale San Raffaele Ethical Committee (protocol TIGET-HPCT) or French National Ethics Committee (CEEI/IRB 21-854).

Overall, the use of human material in the laboratory followed the international regulations, as the Declaration of Helsinki and the Belmont Report, updated throughout the years according to the scientific advancement.

5.17 Table 1: Antibodies list

Anti-mouse antibodies	Fluorofore	Brand	Catalogue number	Dilution
anti-IgG1	PE	Southern Biotechnology	1070-05	1:1000
CD117	APC H7	BD	560250	1:200
CD11B	PE VIO 770	Miltenyi	130-113-808	2:100
CD16/32	PE	Miltenyi	130-120-295	2:100
CD16/32	PE Cyanine 7	eBioscience	25-0161-82	5:100
CD4	APC	BD	553051	1:200
CD41	PE	BD	561850	2:100
CD41	VIOBLUE	Miltenyi	130-105-870	2:100
CD45	BV605	BD	563053	2:100
CD45	VIOBLUE	Miltenyi	130-110-802	2:100
CD8A	APC VIO 770	Miltenyi	130-109-250	1:200
Ly6G	FITC	Miltenyi	130-120-820	2:100
Sca1	FITC	Miltenyi	130-116-490	2:100
Ter119	PE	BD	553673	2:100
CD16/CD32 Rat anti Mouse	-	BD	553142	1:100
	7AAD	BD	559925	1:100
Anti-human antibodies				
ACE (BB9)	-	BD	557813	2:100
CD184	BV421	BD	562448	1:100
CD235a	APC	BD	563666	2:100
CD235a	PE Cyanine 7	BD	563666	2:100
CD32	PE	BD	303206	2:100
CD34	APC	Beckman Coulter	IM2472	2:100
CD34	PE Cyanine 7	Biologend	343616	1:400
CD34	PE Cyanine 7	eBioscience	25034942	1:400
CD4	PE Cy7	BD	560649	2:100
CD43	FITC	BD	555475	10:100
CD44	PE	Miltenyi	130-113-342	2:100
CD45	APC Cyanine 7	Biologend	368516	1:100
CD45	FITC	Beckman Coulter	A07782	2:100
CD45	BV421	BioLegend	304032	2:100
CD5	PE	BioLegend	300607	5:100
CD56	BV421	BD	740076	3:100
CD7	APC	BD	561604	2:100
CD73	BV421	BD	562430	3:100
CD8	PE	Biologend	31051	2:100
DLL4	APC	Biologend	346508	1:100
KDR	Biotin	Miltenyi	130-120-479	2:100
KDR	Biotin	R&D	MAB3572	5:100
Streptavidin	APC	BD	554067	2:100
Streptavidin	PE	BD	554061	1:200
Fcr Blocking reagent human	-	Miltenyi	130-059-901	20:100

6 Appendix to main results (I)

6.1 Mesodermal activation of RA pathway triggers a distinct WNT-dependent hematopoietic wave from hPSCs

The main goal of this thesis is to unravel the embryonic hematopoietic development and characterize the heterogeneity of the HE population across the different embryonic hematopoietic waves. As discussed, while different hematopoietic waves originate from the HE, the hematopoietic output of these programs is profoundly different. In particular, only the HE generated during the last, intra-embryonic hematopoietic wave harbors the potential to generate HSCs (Dzierzak & Bigas, 2018). In the previous chapter we have discussed the identification of a specific marker to track and study HE cells. Herein we will present our efforts to specify HSCs from hPSCs. We hypothesized that the current failure in generating HSCs *in vitro* reflects an incorrect hematopoietic specification. For this, we focused on the signaling pathways that may differ between HSC-dependent and HSC-independent HE populations that emerge intra-embryonically.

RA signaling is essential for HSC emergence (Chanda *et al*, 2013; Goldie *et al*, 2008) and suppresses the extra-embryonic hematopoiesis in zebrafish and mouse model (Jong *et al*, 2010). However, the current hPSC-based *in vitro* models lack any RA source during hematopoietic differentiation. Previous experiments manipulating the RA signaling on hPSC-derived WNT-dependent HE failed to yield HSC-like progeny (Yu *et al*, 2010; Rönn *et al*, 2015; Dou *et al*, 2016). However, the enforced overexpression of seven transcription factors (*ERG*, *HOXA5*, *HOXA9*, *HOXA10*, *LCOR*, *RUNX1* and *SPI1*) allows the HSC emergence from hPSC-derived WNT-dependent HE (Sugimura *et al*, 2017). Notably, the seven transcription factors include three RA direct target genes (*HOXA5*, *HOXA9*, *HOXA10*) (Dou *et al*, 2016) and the ligand dependent corepressor (*LCOR*) that modulate RAR/RXR-mediated transcriptional activation of RA responsive genes (Fernandes *et al*, 2003). Therefore, we hypothesized that RA signaling might play an important role in the specification of HSC-competent HE cells throughout the activation of a stemness program in HE cells *via* the regulation of homeobox (*HOX*) genes expression. In fact, *HOXA* genes are a conserved family of transcription factors involved in the specification of cell identity in early development and known to be expressed in WNT-dependent HE in both human and murine AGM (Ng *et al*, 2016; Kennedy *et al*, 2012; Gao *et al*, 2018).

The production of RA from the physiological precursor ROH consists of a series of oxidative reactions. Among these, RALDH2 (encoded by *ALDH1A2*) catalyzes the irreversible conversion of retinaldehyde to ATRA during embryogenesis (Niederreither & Dollé, 2008) (Introduction: paragraph 1.9). To investigate the RA signaling requirement during hematopoiesis, we took advantage of the Aldefluor assay, that, as previously described, allows to monitor the activity of ALDH enzymes, including RALDH2, during hPSC-based *in vitro* hematopoietic differentiation. Since RA has a fundamental role in regulating the mesodermal patterning during the early development of different systems (Duester, 2008), we initially checked ALDH expression at mesodermal level (day 3 of hPSC-derived hematopoietic differentiation). Surprisingly, we found that ALDHs are selectively activated in WNT-dependent $KDR^+CD235(GYPA)^{neg}$ but not in WNT-independent KDR^+CD235^+ mesoderm cells, suggesting RA signaling might play a role in WNT-dependent mesoderm specification (Figure 33 a). To better characterize the mesodermal populations, our collaborators in Christopher Sturgeon Lab, Icahn School of Medicine at Mount Sinai, New York, performed a single cell RNA sequencing on day 3 differentiation cultures obtained during WNT-dependent or WNT-independent differentiations (Figure 34). In agreement with what previously shown by FACS analysis (Figure 33 a), WNT-independent KDR^+GYPA^+ cells had virtually no *ALDH1A2* expression but express high levels of *CYP26a*, the enzyme that catabolizes RA (Figure 34 a, b). On the contrary, *ALDH1A2* was robustly expressed by WNT-dependent KDR^+ cells (Figure 34 b). To identify candidate RA-responsive subset of cells, our collaborators in Christopher Sturgeon Lab performed differential gene expression analysis between WNT-dependent $KDR^+ALDH1A2^+$ vs $KDR^+ALDH1A2^{neg}$ populations, which revealed *CXCR4* (that encodes for CXCR4 or CD184) as a candidate cell surface marker (Figure 34 b). Flow cytometry analysis confirmed that CD184 is expressed within KDR^+ cells obtained at day 3 of WNT-dependent hematopoietic culture. In contrast, day 3 WNT-independent KDR^+ cells show significantly lower CD184 expression (Figure 33 b). In addition, ALDH activity measured via Aldefluor segregated to the KDR^+CD184^+ WNT-dependent mesoderm (Figure 33 c). These results hint at a possible role of RA signaling in the specification of a RA-dependent (RA_d) HE from WNT-dependent CD184⁺ mesoderm.

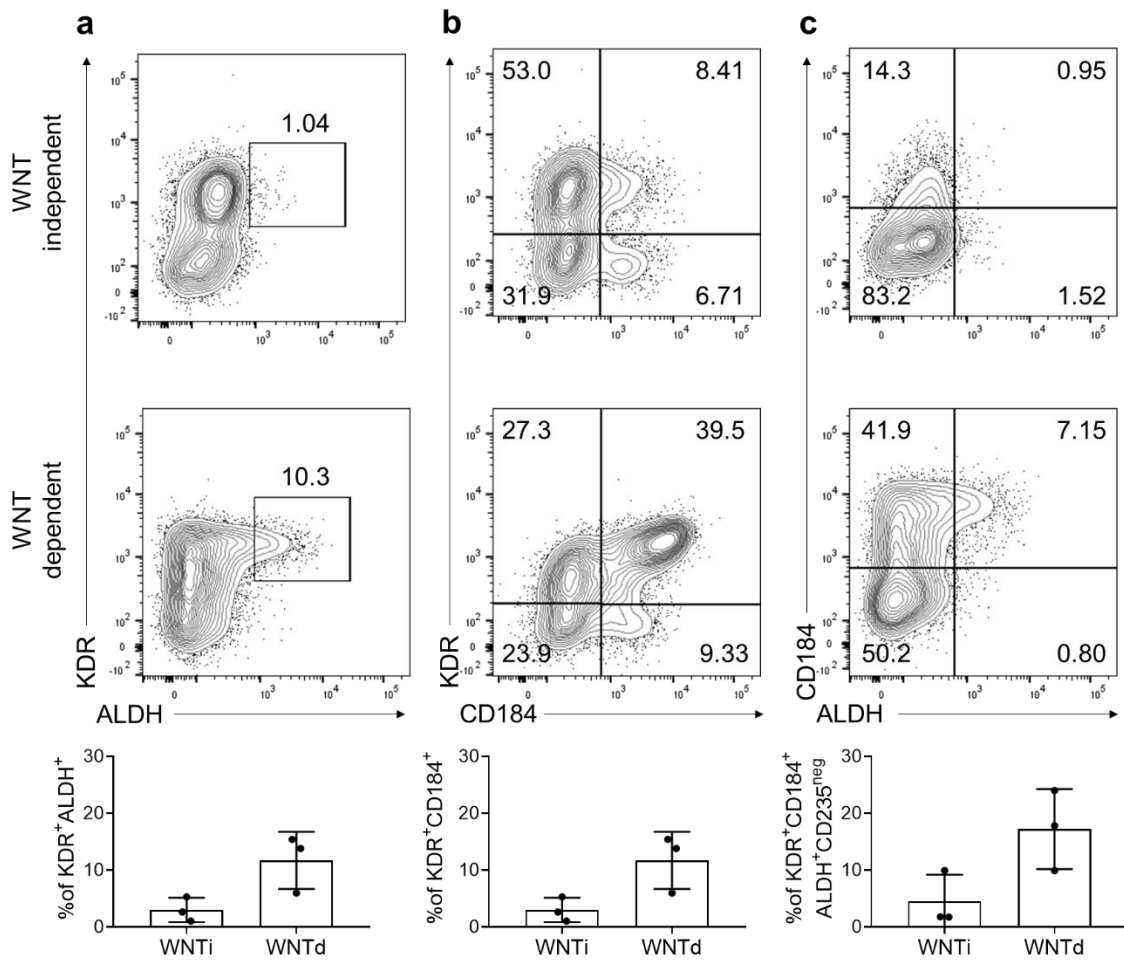


Figure 33 – WNT-dependent CD184⁺mesoderm shows ALDH activity

Representative plots of WNT-independent (upper panel) and WNT-dependent (bottom panel) mesoderm at day 3 of hPSC-derived EB differentiation. a) ALDH activity is restricted to WNT-dependent KDR⁺ cells and barely present in WNT-independent hematopoietic cultures. Gated on SSC/FSC/Live. n=3, independent as shown in the bar plot underneath. b) WNT-dependent mesoderm is subdivided in two subpopulations according to CD184 expression. CD184 is expressed to a less extent in WNT-independent KDR⁺ cells as shown in the bar plot below. Gated on SSC/FSC/Live. n=3, independent. c) ALDH activity is restricted to the WNT-dependent KDR⁺CD184⁺ mesoderm. Gated on SSC/FSC/Live/KDR⁺CD235^{neg}, n=3, independent as shown in the bar plot below. WNTi: WNT-independent; WNTd: WNT-dependent.

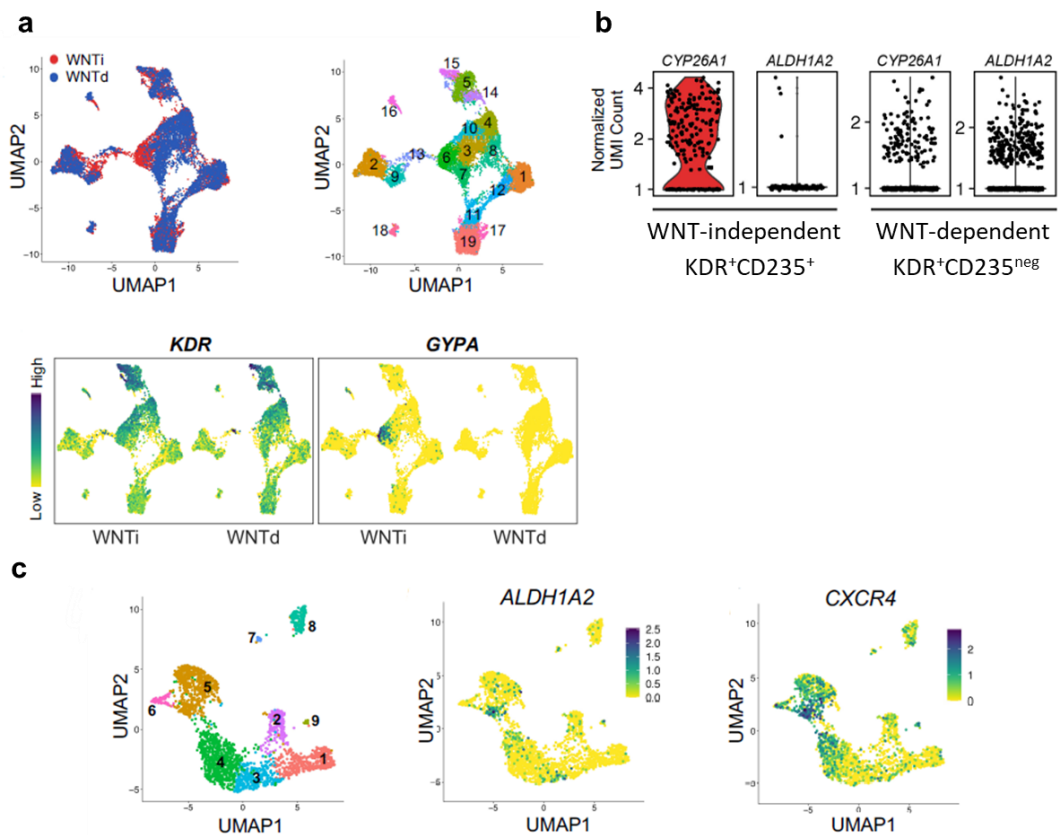


Figure 34 – scRNA-seq analysis of WNT-independent and WNT-dependent cultures at day 3 of differentiation

a) Top panels, UMAP plots of sample origin (left panel) and transcriptional distinct clusters within WNT-independent or WNT-dependent differentiation cultures at day 3 (right panel). Lower panel, expression of KDR and GYPA genes within WNT-independent (WNTi, on the left) and WNT-dependent (WNTd, on the right) differentiation cultures. Cluster 6 contains mostly WNTi cells and expresses GYPA at 2.9-fold higher than the rest of the dataset. b) Violin plots for CYP26A1 and ALDH1A2 expression within WNT-independent KDR⁺GYPA⁺ and WNT-dependent KDR⁺GYPA^{neg} cells, as indicated. UMI: unique molecular identifier. c) UMAP plots visualizing clusters of WNTd KDR⁺ cells (left panel) further subset by the expression of ALDH1A2 (middle panel) and CXCR4 (right panel). CXCR4 is enriched 2.5-fold (adj. *p* val. = 4×10^{-14615}) within ALDH1A2⁺ cells.

To dissect whether these two WNT-dependent mesodermal sub-populations differentially contribute to hematopoietic development, we isolated KDR⁺CD184^{neg}CD235^{neg} (referred to as CD184^{neg}) and KDR⁺CD184⁺CD235^{neg} (referred to as CD184⁺) cells by FAC-sorting. Remarkably, both populations give rise to CD34⁺CD43^{neg} endothelial population (Figure 35). However, only the CD184^{neg} mesoderm harbored HE activity with multilineage hematopoietic potential, giving rise to erythro-myeloid and T-lymphoid cells (Figure 36 a, b). In contrast, CD184⁺ population did not show any hematopoietic potential (Figure 36 a, b). Considering that ALDH activity was enriched in the CD184⁺ mesoderm, we hypothesized that this population may require RA signaling activation for HE specification. If so, the

CD34⁺CD43^{neg} population derived from CD184⁺ mesoderm would lack hematopoietic potential in the absence of exogenous sources of RA. The treatment of freshly isolated CD184⁺ populations with ATRA did not alter the generation of CD34⁺CD43^{neg} population (Figure 35). Strikingly, the RA-treatment of CD184⁺ mesoderm specified endothelial population that harbored multilineage hematopoietic potential (Figure 36 a, b). While RA triggers the hemogenic activity from CD184⁺ mesoderm, it does not affect the hematopoietic potential derived from the CD184^{neg} mesodermal counterpart (referred to as RA-independent, RAi). Of note, the RA-mediated effect on CD184⁺ mesoderm was reproducible on different cells lines (Figure 36 a). Our results suggest that CD184⁺ and CD184^{neg} mesodermal cells specify distinct HE populations within WNT-dependent hematopoietic differentiation cultures.

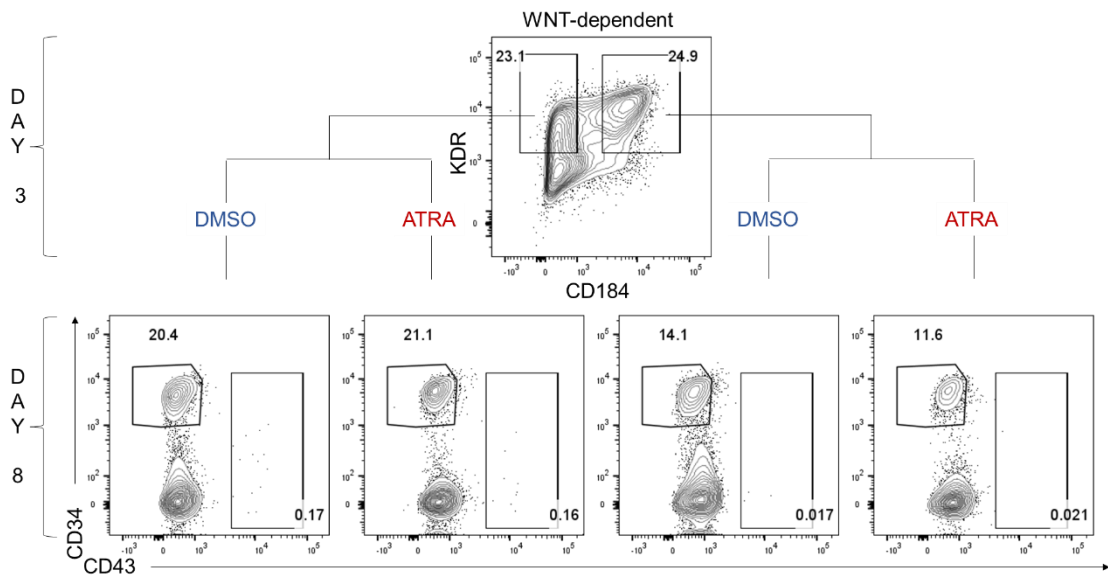


Figure 35 – CD184^{+/neg} mesodermal populations generate CD34⁺CD43^{neg} endothelial cells

Representative plots, sorting strategy and experimental layout. From the top, gating strategy for the isolation of KDR⁺CD184^{neg} and KDR⁺CD184⁺ cells at day 3 of WNT-dependent hematopoietic differentiation (Gated on SSC/FSC/Live/CD235^{neg}). The sorted populations were treated either with DMSO or ATRA and cultured until day 8 of hematopoietic differentiation. At day 8, CD34⁺CD43^{neg} cells were isolated from the different samples (middle panel, gated on SSC/FSC/Live). N=2, independent.

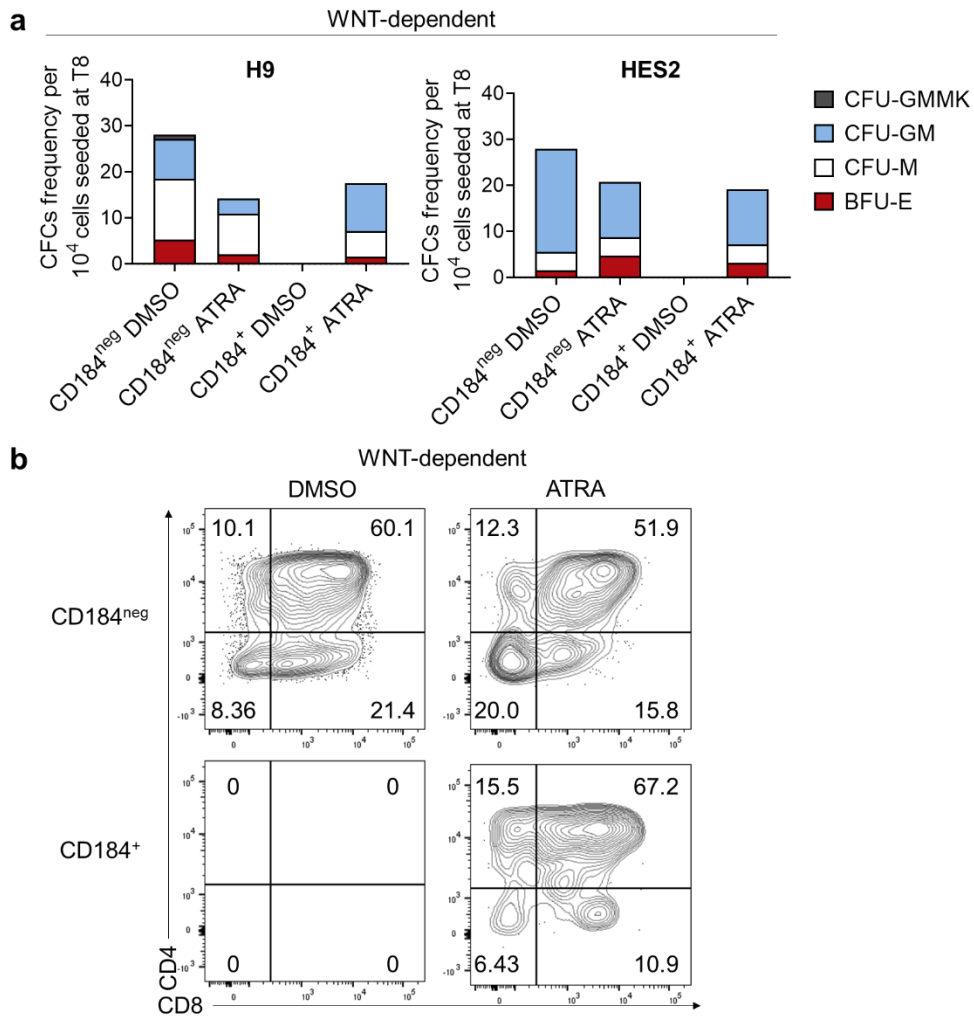


Figure 36 – RA-treatment of CD184⁺ mesoderm allows the emergence of RA^d hemogenic potential

Isolated WNT-dependent CD184^{+/neg} mesoderm was treated with DMSO/ATRA as shown in Figure 35. The CD184⁺- derived CD34⁺CD43^{neg} cells show a) erythroid and myeloid (on the left: H9 line, N=2, independent; on the right: HES2 line, N=1) or b) T-lymphoid progenitors only after RA-treatment (H9 line, representative plots of N=2, independent. Gated on SSC/FSC/Live/CD45⁺CD56^{neg}). On the other hand, CD184^{neg} mesoderm give rise to hematopoietic progenitors regardless to DMSO or RA-treatment.

As additional functional characterization of RA^d HE, we treated bulk WNT-dependent cultures with either DMSO or ATRA to induce RAⁱ or RA^d hematopoiesis, respectively. Then, we isolated CD34⁺CD43^{neg} cells and assessed their ability to engraft into sub-lethally irradiated immunocompromised recipients. Together with our collaborators, we evaluated the short- and long-term contribution to hematopoiesis from 6 to 14 weeks after transplant by looking at their hematopoietic progeny at the injection site, the bone marrow (BM) of the femur, and as circulating

hematopoietic cells (peripheral blood, PB). As expected, CD34⁺CD43^{neg} cells derived from DMSO-treated mesoderm lack any engrafting ability (referred to as RAi in Figure 37). However, CD34⁺CD43^{neg} cells derived from RA-treated hematopoietic cultures (referred to as RAd in Figure 37) gave rise to a transient human hematopoietic (CD45⁺) population, detectable in the BM niche and in the PB until 8-10 weeks post-transplantation (Figure 37 a, b). Despite the frequency of human chimerism remains low and decreases over time, engrafting cells show multilineage potential, giving rise to CD33⁺ myeloid cells and CD19⁺ B-lymphoid lineage (Figure 37 c).

In conclusion, these results indicate that RA signaling activation at mesodermal level is fundamental to the emergence of CD34⁺ cells that generate a transient multilineage hematopoietic engraftment *in vivo* that functionally distinguishes them from RAi CD34⁺ cells. The presented data are collected in the manuscript "Identification of a retinoic acid-dependent hemogenic endothelial progenitor from human pluripotent stem cells" now under review at Nature Cell Biology.

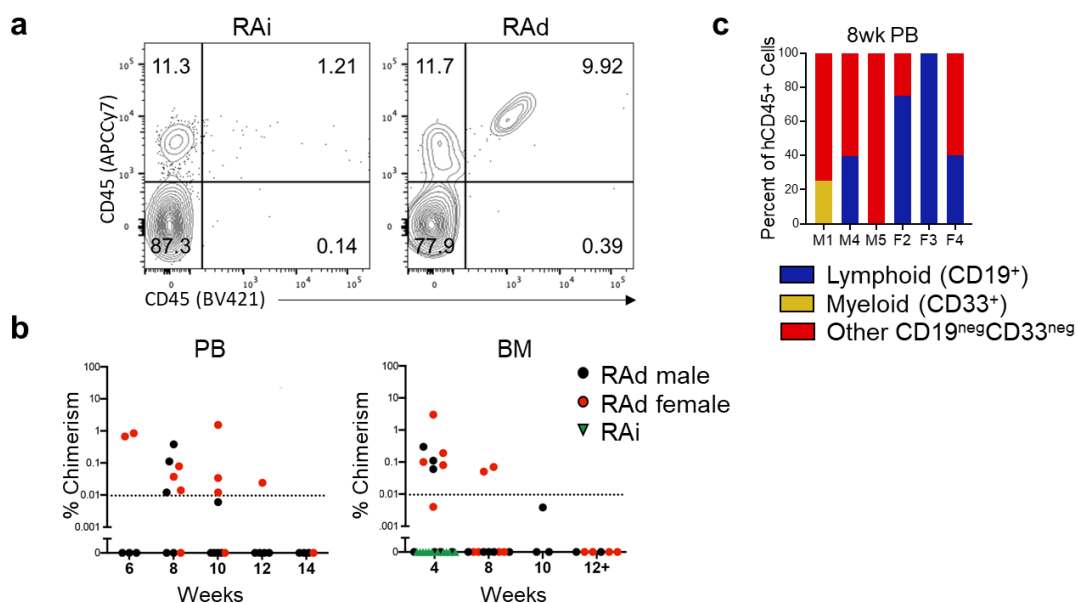


Figure 37 – RA signaling activation at mesodermal level generates CD34⁺ cells with engrafting potential

a) Representative plots of hematopoietic progenitors derived from the BM of sub-lethally irradiated immunocompromised mice 4 weeks after the injection. Mice have been injected with hPSC-derived CD34⁺CD43^{neg} cells obtained from DMSO-treated (RAi, left panel) or ATRA-treated (RAd, right panel) mesodermal cells. b) Frequency of human hematopoietic progenitors in the PB (left panel) or BM (right panel) of sub-lethally irradiated immunocompromised mice. hPSC-derived CD34⁺CD43^{neg} cells obtained from RAd (black and red circles) or RAi (green triangles) WNT-dependent hematopoietic cultures have been injected into male or female adult mice and their repopulation potential have been assessed after 4 to 14 weeks. c) Frequency

of hematopoietic contribution of engrafting RAd HE in irradiated immunocompromised mice. Blue: lymphoid ($CD45^+CD19^+$); yellow: myeloid ($CD45^+CD33^+$); red: other hematopoietic lineages ($CD45^+CD19^{neg} CD33^{neg}$). M: male; F: female.

With this compelling data in our hands, we sought to understand the mechanisms that regulate the emergence of a WNT-dependent RAd mesoderm. Therefore, we analyzed putative pathways that might regulate the specification of a RA-responsive mesoderm, in particular the expression of CD184 and ALDH. We focused our attention on the aryl hydrocarbon receptor (AHR), Transforming growth factor-beta ($TGF\beta$) and Notch pathways. Indeed, CD184 has been shown to be a direct target of Notch pathway (Yamamizu *et al*, 2013) and binding sites for AHR are present on the *Aldh1a2* promoter (Wang *et al*, 2001). In addition, the AHR pathway regulates the expression of *ALDH1A2* (Simones & Shepherd, 2011; Franchini *et al*, 2019) and, together with the Notch signaling influences CD184 expression in cancer cells (Dubrovskaya *et al*, 2012; Williams *et al*, 2008; Xie *et al*, 2013). On the other hand, $TGF\beta$ signaling modulates ALDHs activity (Katsuno *et al*, 2012; Bae *et al*, 2016; Nishida *et al*, 2018).

We evaluated the effect of the inhibition/antagonism of each of the three pathways by treating the cells at day 2 of differentiation, time of WNT-dependent mesodermal patterning. We analyzed the mesodermal commitment after 36 hours. The inhibition of Notch signaling occurred via gamma-secretase inhibitor (GSI) whereas StemRegenin 1 (SR1) was used to antagonize the AHR. In addition, SB 431542 was used to selectively inhibit the $TGF\beta$ type I receptor and, contrarily, different concentration (1 ng/ml, 10 ng/ml) of Activin A, a member of $TGF\beta$ superfamily, were used to activate the signaling. While the administration of SB 431542 and GSI decreased the frequency of KDR^+CD184^+ population with active ALDHs, SR1 and high concentration of Activin A boost the same population (Figure 38 a, b). Collectively, these results showed that the emergence of WNT-dependent $CD184^+ALDH^+$ mesodermal subpopulation is negatively regulated by the AHR signaling but positively controlled by Notch and $TGF\beta$. In future, we plan to perform functional *in vitro* and *in vivo* experiments to confirm that the increased $KDR^+CD184^+ALDH^+$ population induces a parallel increase of RAd HE with multilineage and engrafting potential. Moreover, we will confirm that the enhanced ALDH activity in SR1- or ACT10- treated conditions is due to a higher expression of *ALDH1A2* within the $KDR^+CD184^+ALDH^+$ populations and no other ALDHs.

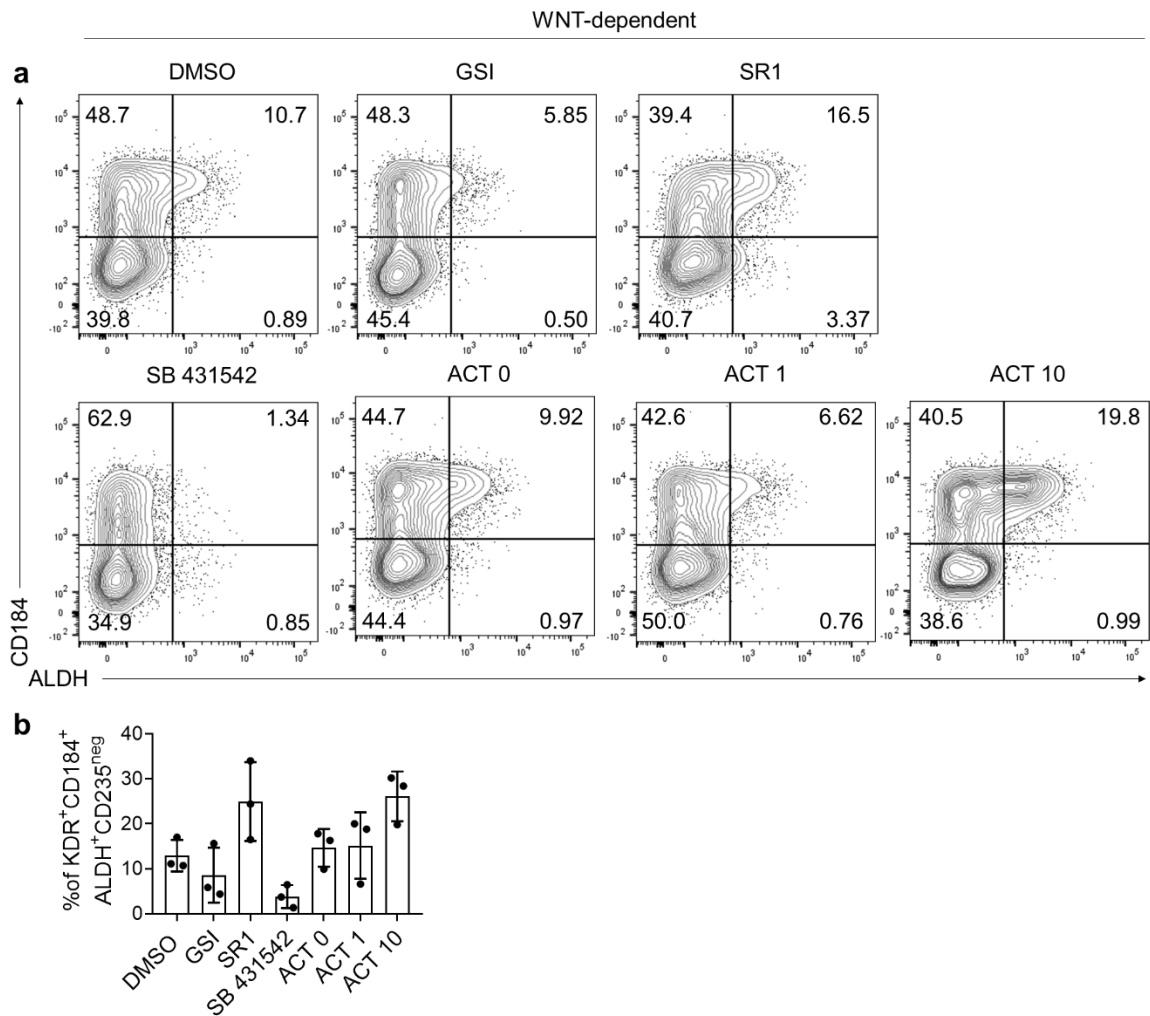


Figure 38 – Modulation of TGF β , Notch and AHR signaling pathways influence ALDH activity within WNT-dependent CD184⁺ mesoderm.

a) Representative plots of WNT-dependent mesoderm at day 3 of hPSC-derived differentiation. At the time of mesodermal patterning (day 2), cells were treated with DMSO as control condition, the Notch inhibitor GSI and the AHR antagonist SR1 (upper panel, from the left to the right). Moreover, cells were treated with the TGF β inhibitor SB 431542 and the TGF β family member Activin A (0, 1, 10 refer to the ng/ml used in each culture condition). Gated on SSC/FSC/Live/KDR⁺CD235^{neg}. N=3, independent as shown in the bar plot in b).

7. Appendix to main results (II)

7.1 Immuno-phenotypic EMPs display lymphoid potential in E9.5 murine YS

In mouse, YS hematopoiesis consists of two temporally distinct but successive extra-embryonic waves. While the first YS hematopoietic wave mainly generates primitive hematopoietic cells (Palis *et al*, 1999; Tober *et al*, 2008), the second gives rise to progenitors with broader hematopoietic potential, generating myeloid, erythroid and lymphoid cells (Yoder *et al*, 1997; Palis *et al*, 1999, 2001; Chen *et al*, 2011a; Kobayashi *et al*, 2014; Dege *et al*, 2020). In particular, the ontogeny of YS T-lymphoid potential is still discussed. Scientists have shown that T lymphocytes emerge from bipotent T-lymphoid-myeloid-primed progenitors (LMPP) that arise in the murine YS at E9.5 (Adolfsson *et al*, 2005; Månsson *et al*, 2007). Others challenged the lympho-myeloid-restricted YS hematopoiesis and support that LMPPs also have megakaryocyte-erythroid potential *in vivo* (Forsberg *et al*, 2006; Boyer *et al*, 2011; Böiers *et al*, 2013). Nevertheless, the T-cell potential of EMP, one of the most abundant hematopoietic progenitors of the second hematopoietic program, has never been addressed. In fact, EMP-derived lymphoid potential was assessed by co-culture with OP9 stroma (McGrath *et al*, 2015). OP9 co-cultures are permissive to B but not T cell differentiation since they lack the expression of high levels of Notch ligands of the Delta family that trigger the activation of Notch signaling required for T cells differentiation (Schmitt *et al*, 2004).

To dissect whether EMPs display T lymphoid potential, we isolated $\text{KIT}^+\text{CD41}^+\text{CD16/32}^+\text{SCA1}^{\text{neg}}$ cells from E9.5 YS by FAC-Sorting (Figure 39 a). We co-cultured $\text{KIT}^+\text{CD41}^+\text{CD16/32}^+\text{SCA1}^{\text{neg}}$ progenitors on OP9DLL1 stroma for 11 days after which we analyzed erythroid (TER119^+), myeloid ($\text{CD45}^+\text{CD11b}^+$ and/or LY6G^+) and lymphoid ($\text{CD45}^+\text{CD4}^+\text{CD8}^+$) output. As expected, YS-derived $\text{Kit}^+\text{CD41}^+\text{CD16/32}^+\text{SCA1}^{\text{neg}}$ progenitors generate cells belonging to the erythroid and myeloid lineages. Strikingly, at the population level, E9.5 EMPs also give rise $\text{CD45}^+\text{CD4}^+\text{CD8}^+$ T cells (Figure 39 b). Of note, as previously reported, we confirmed that $\text{Kit}^+\text{CD41}^+\text{CD16/32}^+$ progenitors lack B cell potential, as the not-EMP $\text{Kit}^+\text{CD41}^+\text{CD16/32}^{\text{neg}}$ fraction generate $\text{CD45}^+\text{CD19}^+\text{B220}^{\text{low/neg}}$ B cells when cultured on OP9 cells (Figure 39 c) (Yoder *et al*, 1997; Adolfsson *et al*, 2005; Forsberg *et al*, 2006; Kobayashi *et al*, 2014; Böiers *et al*, 2013).

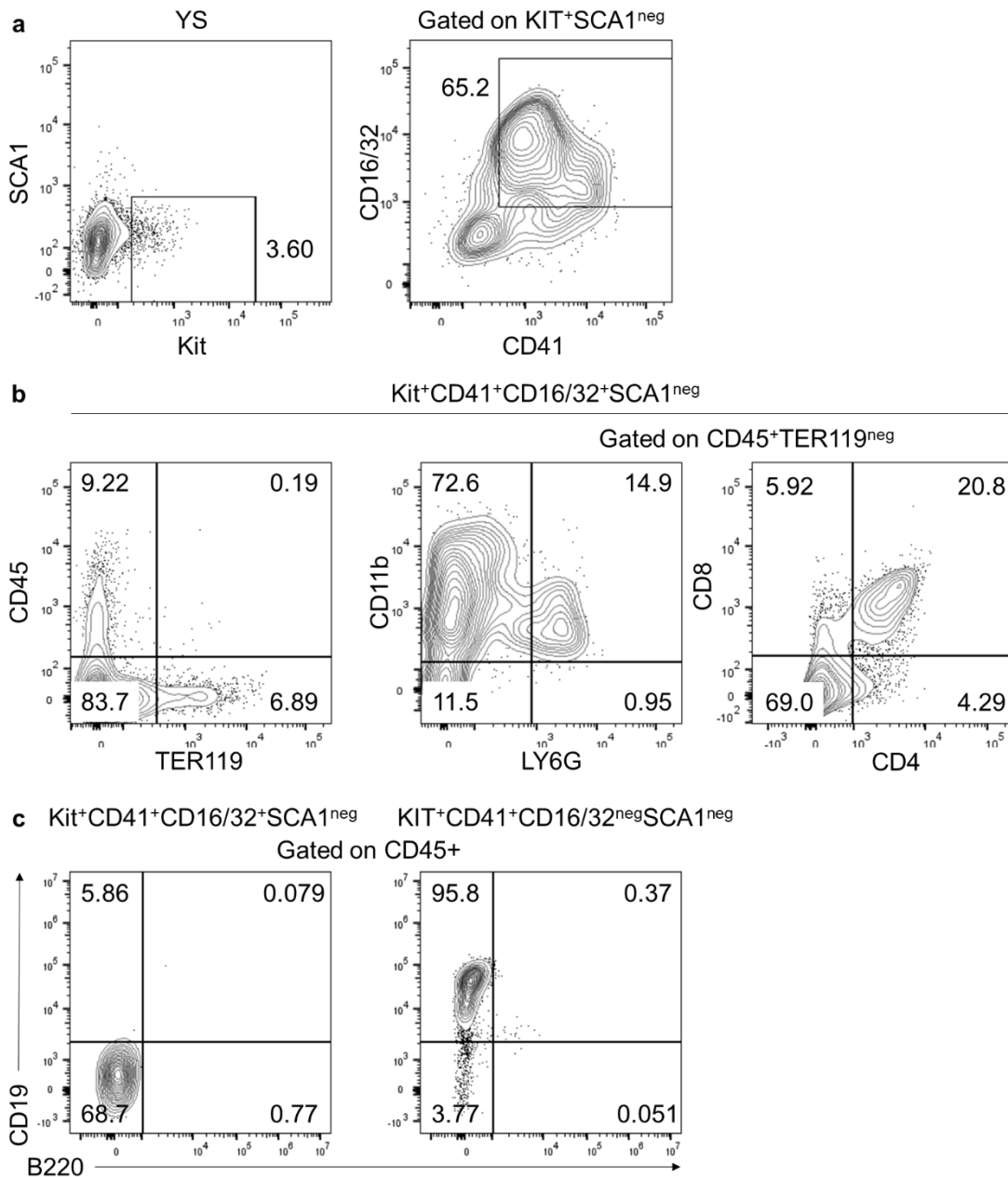


Figure 39 – YS E9.5 Kit⁺CD41⁺CD16/32⁺SCA1^{neg} (EMP) cells display erythroid, myeloid, and T-lymphoid potential

a) Representative plots of the gating strategy used to isolate KIT⁺CD41⁺CD16/32⁺SCA1^{neg} progenitors, n=4, independent. b) Isolated E9.5 KIT⁺CD41⁺CD16/32⁺SCA1^{neg} progenitor cells, cultured on OP9DLL1 stroma for 11 days, generate TER119⁺ erythroid progenitors (left panel, gated on SSC/FSC/Live), CD45⁺CD11b⁺ and/or LY6G⁺ myeloid progenitors (middle panel, gated on SSC/FSC/Live/CD45⁺TER119^{neg}) and CD45⁺CD4⁺CD8⁺ T lymphoid progenitors (right panel, gated on SSC/FSC/Live/CD45⁺TER119^{neg}) n=4, independent. c) Unlike KIT⁺CD41⁺CD16/32^{neg}SCA1^{neg} progenitors isolated from E9.5 YS, KIT⁺CD41⁺CD16/32⁺SCA1^{neg} do not show B cell potential. Gated on SSC/FSC/Live/CD45⁺ N=3, independent.

We next asked whether T-cells are generated at a clonal level by progenitors harboring also myeloid and erythroid potential and therefore whether the $KIT^+CD41^+CD16/32^+SCA1^{neg}$ fraction contains multipotent progenitors. We therefore performed single cell clonal analysis and LDA by single-cell sorting on 96-multiwells coated with OP9DLL1 stromal cells. Our analysis showed that 1 in 144 $KIT^+CD41^+CD16/32^+SCA1^{neg}$ cell has T lymphoid potential with a frequency of 1,8% in single cell clones (8 clones out of 859 analyzed) (Figure 40 a). Index sorting analysis confirmed that clonal cells that derive T lymphoid progenitors reside in the $KIT^+CD41^+CD16/32^+SCA1^{neg}$ population (Figure 40 b). $KIT^+CD41^+CD16/32^+SCA1^{neg}$ progenitors with T lymphoid potential also generate myeloid (5 of the 8 clones with T lymphoid potential), erythroid (2 of the 8 clones) or erythroid and myeloid (1 of the 8 clones) cells (Figure 40 c). Of cells devoid of lymphoid potential, most developed uni-lineage output, either erythroid (77%) or myeloid (6,8%) progenitors. with 14,6% showing a bi-lineage erythroid and myeloid fate. Since it was recently showed that phenotypic EMPs contain cells displaying NK-lymphoid potential(Dege *et al*, 2020), our results clearly indicates that the second hematopoietic program emerging in the YS generates multipotent progenitors (MPP), thus comprising both EMP and lymphoid hematopoiesis.

Our results contribute to resolve the emergence of lymphoid lineages, in particular regarding the origin of HSC-independent YS T lymphoid progenitors, which is still currently debated (Yoder *et al*, 1997; Adolfsson *et al*, 2005; Forsberg *et al*, 2006; Kobayashi *et al*, 2014; Böiers *et al*, 2013). In parallel to our experiments, our collaborators in Gordon Keller Lab, at the University Health Network in Toronto, have described a method for generating the equivalent of the murine EMPs from hPSCs and showed that hPSC-derived EMP-like progenitors also display T lymphoid potential (Atkins *et al*, 2021). The results here presented are included in the manuscript "Modeling human yolk sac hematopoiesis with pluripotent stem cells", published on Journal of Experimental Medicine on 2021, December 20th (Atkins *et al*, 2021).

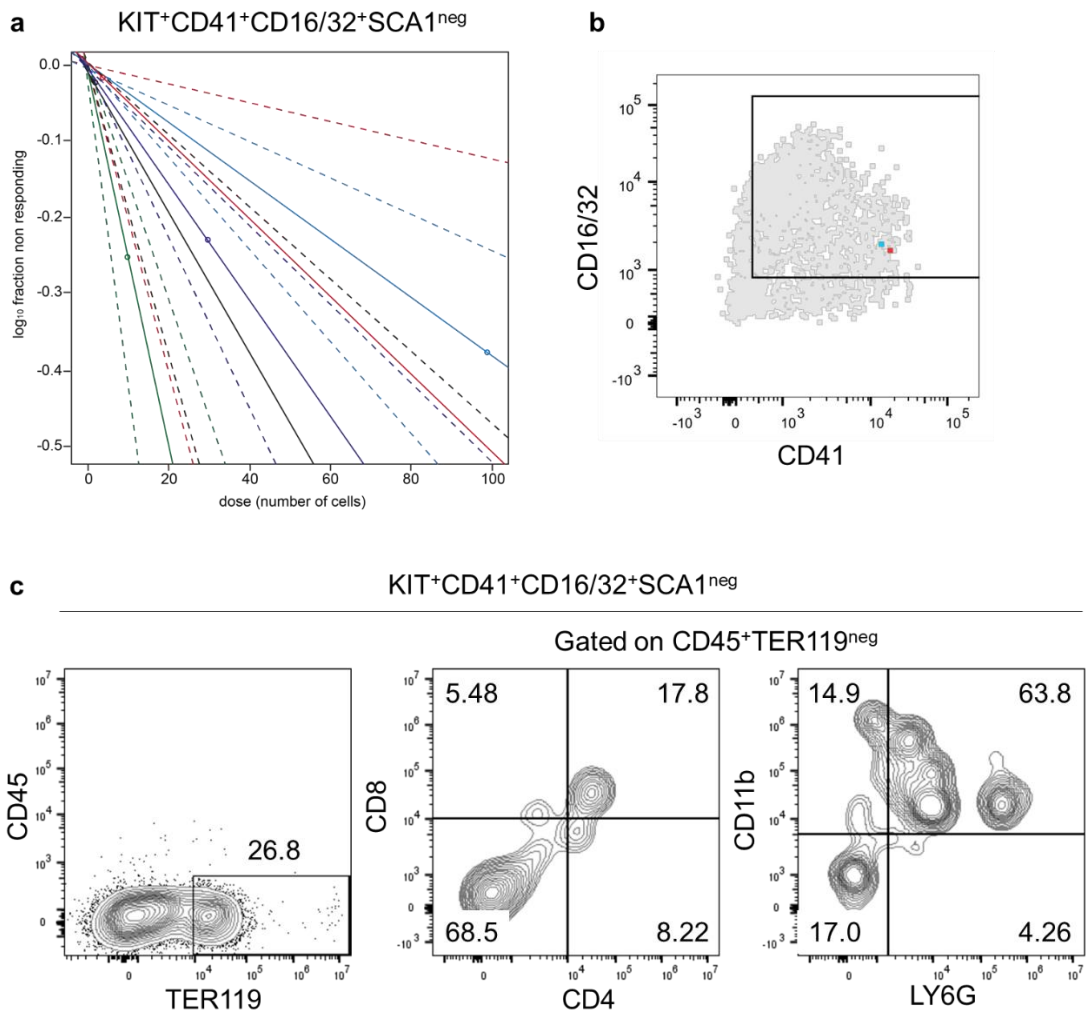


Figure 40 – Clonal analysis of T lymphoid potential within E9.5 $KIT^+CD41^+CD16/32^+SCA1^{neg}$ population

a) Frequency of $CD45^+CD4^+CD8^+$ T lymphoid progenitors derived from $KIT^+CD41^+CD16/32^+SCA1^{neg}$ E9.5 YS population in $n=3$, independent. The frequency was calculated by ELDA (<http://bioinf.wehi.edu.au/software/elda/>). b) Representative plot highlighting the E9.5 YS $KIT^+CD41^+CD16/32^+SCA1^{neg}$ cells with multipotent (blue) or erythrolymphoid (red) potential. Gated on $SSC/FSC/Live/KIT^+SCA1^{neg}$. c) Representative plots of $TER119^+$ (left panel, gated on $SSC/FSC/Live$), $CD4^+CD8^+$ (middle panel, gated on $SSC/FSC/Live/CD45^+TER119^{neg}$) or $CD11b^+LY6G^+$ (right panel, gated on $SSC/FSC/Live/CD45^+TER119^{neg}$) cells derived from a single E9.5 YS $KIT^+CD41^+CD16/32^+SSC1^{neg}$ progenitor cell sorted on OP9DLL1 stromal cells and analyzed after 11 days. $N=3$, independent.

8. References

- Ackermann M, Liebhaber S, Klusmann J & Lachmann N (2015) Lost in translation: pluripotent stem cell-derived hematopoiesis. *Embo Mol Med* 7: 1388–1402
- Adamo L, Naveiras O, Wenzel PL, McKinney-Freeman S, Mack PJ, Gracia-Sancho J, Suchy-Dacey A, Yoshimoto M, Lensch MW, Yoder MC, *et al* (2009) Biomechanical forces promote embryonic haematopoiesis. *Nature* 459: 1131–1135
- Adolfsson J, Månsson R, Buza-Vidas N, Hultquist A, Liuba K, Jensen CT, Bryder D, Yang L, Borge O-J, Thoren LAM, *et al* (2005) Identification of Flt3+ Lympho-Myeloid Stem Cells Lacking Erythro-Megakaryocytic Potential A Revised Road Map for Adult Blood Lineage Commitment. *Cell* 121: 295–306
- Akashi K, Traver D, Miyamoto T & Weissman IL (2000) A clonogenic common myeloid progenitor that gives rise to all myeloid lineages. *Nature* 404: 193–197
- Arnautova I & Kleinman HK (2010) In vitro angiogenesis: endothelial cell tube formation on gelled basement membrane extract. *Nat Protoc* 5: 628–635
- Arora N, Wenzel PL, McKinney-Freeman SL, Ross SJ, Kim PG, Chou SS, Yoshimoto M, Yoder MC & Daley GQ (2014) Effect of Developmental Stage of HSC and Recipient on Transplant Outcomes. *Dev Cell* 29: 621–628
- Atkins MH, Scarfò R, McGrath KE, Yang D, Palis J, Ditadi A & Keller GM (2021) Modeling human yolk sac hematopoiesis with pluripotent stem cells. *J Exp Med* 219: e20211924
- Azzoni E, Frontera V, McGrath KE, Harman J, Carrelha J, Nerlov C, Palis J, Jacobsen SEW & Bruijn MF (2018) Kit ligand has a critical role in mouse yolk sac and aorta-gonad-mesonephros hematopoiesis. *Embo Rep* 19
- Bae SC, Ogawa E, Maruyama M, Oka H, Satake M, Shigesada K, Jenkins NA, Gilbert DJ, Copeland NG & Ito Y (1994) PEBP2 alpha B/mouse AML1 consists of multiple isoforms that possess differential transactivation potentials. *Mol Cell Biol* 14: 3242–3252
- Bae W-J, Lee S-H, Rho Y-S, Koo B-S & Lim Y-C (2016) Transforming growth factor β 1 enhances stemness of head and neck squamous cell carcinoma cells through activation of Wnt signaling. *Oncol Lett* 12: 5315–5320
- Baron CS, Kester L, Klaus A, Boisset J-C, Thambyrajah R, Yvernogeu L, Kouskoff V, Lacaud G, Oudenaarden A van & Robin C (2018) Single-cell transcriptomics reveal the dynamic of haematopoietic stem cell production in the aorta. *Nat Commun* 9: 2517
- Baron CS & Oudenaarden A van (2019) Unravelling cellular relationships during development and regeneration using genetic lineage tracing. *Nat Rev Mol Cell Bio* 20: 753–765

- Baron MH (2005) Early patterning of the mouse embryo: Implications for hematopoietic commitment and differentiation. *Exp Hematol* 33: 1015–1020
- Batsivari A, Rybtsov S, Souilhol C, Binagui-Casas A, Hills D, Zhao S, Travers P & Medvinsky A (2017) Understanding Hematopoietic Stem Cell Development through Functional Correlation of Their Proliferative Status with the Intra-aortic Cluster Architecture. *Stem Cell Rep* 8: 1549–1562
- Bausch-Fluck D, Goldmann U, Müller S, Oostrum M van, Müller M, Schubert OT & Wollscheid B (2018) The in silico human surfaceome. *P Natl Acad Sci Usa* 115: E10988–E10997
- Beaudin AE, Boyer SW, Perez-Cunningham J, Hernandez GE, Derderian SC, Jujjavarapu C, Aaserude E, MacKenzie T & Forsberg EC (2016) A Transient Developmental Hematopoietic Stem Cell Gives Rise to Innate-like B and T Cells. *Cell Stem Cell* 19: 768–783
- Bee T, Ashley ELK, Bickley SRB, Jarratt A, Li P-S, Sloane-Stanley J, Göttgens B & Bruijn MFTR de (2009a) The mouse Runx1 +23 hematopoietic stem cell enhancer confers hematopoietic specificity to both Runx1 promoters. *Blood* 113: 5121–5124
- Bee T, Liddiard K, Swiers G, Bickley SRB, Vink CS, Jarratt A, Hughes JR, Medvinsky A & Bruijn MFTR de (2009b) Alternative Runx1 promoter usage in mouse developmental hematopoiesis. *Blood Cells Mol Dis* 43: 35–42
- Bee T, Swiers G, Muroi S, Pozner A, Nottingham W, Santos AC, Li P-S, Taniuchi I & Bruijn MFTR de (2010) Nonredundant roles for Runx1 alternative promoters reflect their activity at discrete stages of developmental hematopoiesis. *Blood* 115: 3042–3050
- Benedito R, Roca C, Sörensen I, Adams S, Gossler A, Fruttiger M & Adams RH (2009) The Notch Ligands Dll4 and Jagged1 Have Opposing Effects on Angiogenesis. *Cell* 137: 1124–1135
- Bernstein KE & Berk BC (1993) The Biology of Angiotensin II Receptors. *Am J Kidney Dis* 22: 745–754
- Bertrand JY, Chi NC, Santoso B, Teng S, Stainier DYR & Traver D (2010a) Haematopoietic stem cells derive directly from aortic endothelium during development. *Nature* 464: 108–111
- Bertrand JY, Cisson JL, Stachura DL & Traver D (2010b) Notch signaling distinguishes 2 waves of definitive hematopoiesis in the zebrafish embryo. *Blood* 115: 2777–2783
- Bertrand JY, Giroux S, Golub R, Klaine M, Jalil A, Boucontet L, Godin I & Cumano A (2005) Characterization of purified intraembryonic hematopoietic stem cells as a tool to define their site of origin. *P Natl Acad Sci Usa* 102: 134–139
- Bertrand JY, Kim AD, Teng S & Traver D (2008) CD41+ cmyb+ precursors colonize the zebrafish pronephros by a novel migration route to initiate adult hematopoiesis. *Development* 135: 1853–1862

- Bertrand JY & Traver D (2009) Hematopoietic cell development in the zebrafish embryo. *Curr Opin Hematol* 16: 243–248
- Bhandari S, Larsen AK, McCourt P, Smedsrød B & Sørensen KK (2021) The Scavenger Function of Liver Sinusoidal Endothelial Cells in Health and Disease. *Front Physiol* 12: 757469
- Bielinska M, Narita N, Heikinheimo M, Porter SB & Wilson DB (1996) Erythropoiesis and vasculogenesis in embryoid bodies lacking visceral yolk sac endoderm. *Blood* 88: 3720–30
- Bigas A & Espinosa L (2012) Hematopoietic stem cells: to be or Notch to be. *Blood* 119: 3226–3235
- Bohnsack BL, Lai L, Dolle P & Hirschi KK (2004) Signaling hierarchy downstream of retinoic acid that independently regulates vascular remodeling and endothelial cell proliferation. *Gene Dev* 18: 1345–1358
- Böiers C, Carrelha J, Lutteropp M, Luc S, Green JCA, Azzoni E, Woll PS, Mead AJ, Hultquist A, Swiers G, *et al* (2013) Lymphomyeloid Contribution of an Immune-Restricted Progenitor Emerging Prior to Definitive Hematopoietic Stem Cells. *Cell Stem Cell* 13: 535–548
- Boisset J-C, Cappellen W van, Andrieu-Soler C, Galjart N, Dzierzak E & Robin C (2010) In vivo imaging of haematopoietic cells emerging from the mouse aortic endothelium. *Nature* 464: 116–120
- Boisset J-C, Clapes T, Klaus A, Papazian N, Onderwater J, Mommaas-Kienhuis M, Cupedo T & Robin C (2015) Progressive maturation toward hematopoietic stem cells in the mouse embryo aorta. *Blood* 125: 465–469
- Bollerot K, Romero S, Dunon D & Jaffredo T (2005) Core binding factor in the early avian embryo: cloning of Cbf β and combinatorial expression patterns with Runx1. *Gene Expr Patterns* 6: 29–39
- Boyer SW, Schroeder AV, Smith-Berdan S & Forsberg EC (2011) All Hematopoietic Cells Develop from Hematopoietic Stem Cells through Flk2/Flt3-Positive Progenitor Cells. *Cell Stem Cell* 9: 64–73
- Bradley T & Metcalf D (1966) THE GROWTH OF MOUSE BONE MARROW CELLS IN VITRO. *Aust J Exp Biol Med* 44: 287–300
- Brauweiler A, Tamir I, Marschner S, Helgason CD & Cambier JC (2001) Partially Distinct Molecular Mechanisms Mediate Inhibitory Fc γ RIIB Signaling in Resting and Activated B Cells. *J Immunol* 167: 204–211
- Breier G, Breviario F, Caveda L, Berthier R, Schnürch H, Gotsch U, Vestweber D, Risau W & Dejana E (1996) Molecular cloning and expression of murine vascular endothelial-cadherin in early stage development of cardiovascular system. *Blood* 87: 630–41

- Brooks DG, Qiu WQ, Luster AD & Ravetch JV (1989) Structure and expression of human IgG FcRII(CD32). Functional heterogeneity is encoded by the alternatively spliced products of multiple genes. *J Exp Medicine* 170: 1369–1385
- Brown LA, Rodaway ARF, Schilling TF, Jowett T, Ingham PW, Patient RK & Sharrocks AD (2000) Insights into early vasculogenesis revealed by expression of the ETS-domain transcription factor Fli-1 in wild-type and mutant zebrafish embryos. *Mech Develop* 90: 237–252
- Brückner K, Perez L, Clausen H & Cohen S (2000) Glycosyltransferase activity of Fringe modulates Notch–Delta interactions. *Nature* 406: 411–415
- Bruijn M de & Dzierzak E (2017) Runx transcription factors in the development and function of the definitive hematopoietic system. *Blood* 129: 2061–2069
- Bruijn MFTR de, Ma X, Robin C, Ottersbach K, Sanchez M-J & Dzierzak E (2002) Hematopoietic Stem Cells Localize to the Endothelial Cell Layer in the Midgestation Mouse Aorta. *Immunity* 16: 673–683
- Bruijn MFTR de, Speck NA, Peeters MCE & Dzierzak E (2000) Definitive hematopoietic stem cells first develop within the major arterial regions of the mouse embryo. *Embo J* 19: 2465–2474
- Burns CE, DeBlasio T, Zhou Y, Zhang J, Zon L & Nimer SD (2002) Isolation and characterization of runxa and runxb, zebrafish members of the runt family of transcriptional regulators. *Exp Hematol* 30: 1381–1389
- Burns CE, Traver D, Mayhall E, Shepard JL & Zon LI (2005) Hematopoietic stem cell fate is established by the Notch–Runx pathway. *Gene Dev* 19: 2331–2342
- Butko E, Distel M, Pouget C, Weijts B, Kobayashi I, Ng K, Mosimann C, Poulain FE, McPherson A, Ni C-W, *et al* (2015) Gata2b is a restricted early regulator of hemogenic endothelium in the zebrafish embryo. *Development* 142: 1050–1061
- Cai Z, Bruijn M de, Ma X, Dortland B, Luteijn T, Downing JR & Dzierzak E (2000) Haploinsufficiency of AML1 Affects the Temporal and Spatial Generation of Hematopoietic Stem Cells in the Mouse Embryo. *Immunity* 13: 423–431
- Cao G, Savani RC, Fehrenbach M, Lyons C, Zhang L, Coukos G & DeLisser HM (2006) Involvement of Endothelial CD44 during in Vivo Angiogenesis. *Am J Pathology* 169: 325–336
- Chadwick K, Wang L, Li L, Menendez P, Murdoch B, Rouleau A & Bhatia M (2003) Cytokines and BMP-4 promote hematopoietic differentiation of human embryonic stem cells. *Blood* 102: 906–915
- Challen GA & Goodell MA (2010) Runx1 isoforms show differential expression patterns during hematopoietic development but have similar functional effects in adult hematopoietic stem cells. *Exp Hematol* 38: 403–416
- Chan CWY, Kay LS, Khadaroo RG, Chan MWC, Lakatoo S, Young KJ, Zhang L, Gorczynski RM, Cattral M, Rotstein O, *et al* (2003) Soluble Fibrinogen-Like Protein 2/Fibroleukin Exhibits Immunosuppressive Properties: Suppressing T Cell

- Proliferation and Inhibiting Maturation of Bone Marrow-Derived Dendritic Cells. *J Immunol* 170: 4036–4044
- Chanda B, Ditadi A, Iscove NN & Keller G (2013) Retinoic Acid Signaling Is Essential for Embryonic Hematopoietic Stem Cell Development. *Cell* 155: 215–227
- Chen MJ, Li Y, De Obaldia ME, Yang Q, Yzaguirre AD, Yamada-Inagawa T, Vink CS, Bhandoola A, Dzierzak E & Speck NA (2011a) Erythroid/Myeloid Progenitors and Hematopoietic Stem Cells Originate from Distinct Populations of Endothelial Cells. *Cell Stem Cell* 9: 541–552
- Chen MJ, Yokomizo T, Zeigler BM, Dzierzak E & Speck NA (2009) Runx1 is required for the endothelial to haematopoietic cell transition but not thereafter. *Nature* 457: 887–891
- Chen Y, Wu S, Guo G, Fei L, Guo S, Yang C, Fu X & Wu Y (2011b) Programmed Death (PD)-1-Deficient Mice Are Extremely Sensitive to Murine Hepatitis Virus Strain-3 (MHV-3) Infection. *Plos Pathog* 7: e1001347
- Choi K, Kennedy M, Kazarov A, Papadimitriou JC & Keller G (1998) A common precursor for hematopoietic and endothelial cells. *Dev Camb Engl* 125: 725–32
- Christensen JL, Wright DE, Wagers AJ & Weissman IL (2004) Circulation and Chemotaxis of Fetal Hematopoietic Stem Cells. *Plos Biol* 2: e75
- Ciau-Uitz A, Walmsley M & Patient R (2000) Distinct Origins of Adult and Embryonic Blood in Xenopus. *Cell* 102: 787–796
- Clark DA, Foerster K, Fung L, He W, Lee L, Mendicino M, Markert UR, Gorczynski RM, Marsden PA & Levy GA (2004) The fgl2 prothrombinase/fibroleukin gene is required for lipopolysaccharide-triggered abortions and for normal mouse reproduction. *Mhr Basic Sci Reproductive Medicine* 10: 99–108
- Clarke RL, Yzaguirre AD, Yashiro-Ohtani Y, Bondue A, Blanpain C, Pear WS, Speck NA & Keller G (2013) The expression of Sox17 identifies and regulates haemogenic endothelium. *Nat Cell Biol* 15: 502–510
- Collins LS & Dorshkind K (1987) A stromal cell line from myeloid long-term bone marrow cultures can support myelopoiesis and B lymphopoiesis. *J Immunol Baltim Md 1950* 138: 1082–7
- Corada M, Orsenigo F, Morini MF, Pitulescu ME, Bhat G, Nyqvist D, Breviaro F, Conti V, Briot A, Iruela-Arispe ML, *et al* (2013) Sox17 is indispensable for acquisition and maintenance of arterial identity. *Nat Commun* 4: 2609
- Corbel C & Salaün J (2002) α IIB Integrin Expression during Development of the Murine Hemopoietic System. *Dev Biol* 243: 301–311
- Costa G, Kouskoff V & Lacaud G (2012) Origin of blood cells and HSC production in the embryo. *Trends Immunol* 33: 215–223
- Crosse EI, Gordon-Keylock S, Rybtsov S, Binagui-Casas A, Felchle H, Nnadi NC, Kirschner K, Chandra T, Tamagno S, Webb DJ, *et al* (2020) Multi-layered Spatial

- Transcriptomics Identify Secretory Factors Promoting Human Hematopoietic Stem Cell Development. *Cell Stem Cell* 27: 822-839.e8
- Cuadros MA, Martin C, Coltey P, Almendros A & Navascués J (1993) First appearance, distribution, and origin of macrophages in the early development of the avian central nervous system. *J Comp Neurol* 330: 113–129
- Cumano A, Dieterlen-Lievre F & Godin I (1996) Lymphoid Potential, Probed before Circulation in Mouse, Is Restricted to Caudal Intraembryonic Splanchnopleura. *Cell* 86: 907–916
- Cumano A, Ferraz JC, Klaine M, Santo JPD & Godin I (2001) Intraembryonic, but Not Yolk Sac Hematopoietic Precursors, Isolated before Circulation, Provide Long-Term Multilineage Reconstitution. *Immunity* 15: 477–485
- Daane JM & Downs KM (2011) Hedgehog signaling in the posterior region of the mouse gastrula suggests manifold roles in the fetal-umbilical connection and posterior morphogenesis. *Dev Dynam* 240: 2175–2193
- DAGA A, TIGHE JANE & CALABI F (1992) Leukaemia/Drosophila homology. *Nature* 356: 484–484
- Dantschakoff W (1908) Untersuchungen über die Entwicklung des Blutes und Bindegewebes bei den Vögeln. *Anatomische Hefte* 37: 471–587
- Dege C, Fegan KH, Creamer JP, Berrien-Elliott MM, Luff SA, Kim D, Wagner JA, Kingsley PD, McGrath KE, Fehniger TA, *et al* (2020) Potently Cytotoxic Natural Killer Cells Initially Emerge from Erythro-Myeloid Progenitors during Mammalian Development. *Dev Cell* 53: 229-239.e7
- Dieterlen-Lievre F (1975) On the origin of haemopoietic stem cells in the avian embryo: an experimental approach. *J Embryol Exp Morph* 33: 607–19
- Ditadi A & Sturgeon CM (2016) Directed differentiation of definitive hemogenic endothelium and hematopoietic progenitors from human pluripotent stem cells. *Methods* 101: 65–72
- Ditadi A, Sturgeon CM & Keller G (2016) A view of human haematopoietic development from the Petri dish. *Nat Rev Mol Cell Biology* 18: 56–67
- Ditadi A, Sturgeon CM, Tober J, Awong G, Kennedy M, Yzaguirre AD, Azzola L, Ng ES, Stanley EG, French DL, *et al* (2015) Human definitive haemogenic endothelium and arterial vascular endothelium represent distinct lineages. *Nat Cell Biol* 17: 580–591
- Dobin A, Davis CA, Schlesinger F, Drenkow J, Zaleski C, Jha S, Batut P, Chaisson M & Gingeras TR (2013) STAR: ultrafast universal RNA-seq aligner. *Bioinformatics* 29: 15–21
- Dou DR, Calvanese V, Sierra MI, Nguyen AT, Minasian A, Saarikoski P, Sasidharan R, Ramirez CM, Zack JA, Crooks GM, *et al* (2016) Medial HOXA genes demarcate haematopoietic stem cell fate during human development. *Nat Cell Biol* 18: 595–606

- D'Souza SL, Elefanty AG & Keller G (2005) SCL/Tal-1 is essential for hematopoietic commitment of the hemangioblast but not for its development. *Blood* 105: 3862–3870
- Dubrovskaja A, Hartung A, Bouchez LC, Walker JR, Reddy VA, Cho CY & Schultz PG (2012) CXCR4 activation maintains a stem cell population in tamoxifen-resistant breast cancer cells through AhR signalling. *Brit J Cancer* 107: 43–52
- Duester G (2008) Retinoic Acid Synthesis and Signaling during Early Organogenesis. *Cell* 134: 921–931
- Dzierzak E & Bigas A (2018) Blood Development: Hematopoietic Stem Cell Dependence and Independence. *Cell Stem Cell* 22: 639–651
- Easterbrook J, Rybtsov S, Gordon-Keylock S, Ivanovs A, Taoudi S, Anderson RA & Medvinsky A (2019) Analysis of the Spatiotemporal Development of Hematopoietic Stem and Progenitor Cells in the Early Human Embryo. *Stem Cell Rep* 12: 1056–1068
- Edbauer D, Winkler E, Regula JT, Pesold B, Steiner H & Haass C (2003) Reconstitution of γ -secretase activity. *Nat Cell Biol* 5: 486–488
- Eich C, Arlt J, Vink CS, Kartalaei PS, Kaimakis P, Mariani SA, Linden R van der, Cappellen WA van & Dzierzak E (2018) In vivo single cell analysis reveals Gata2 dynamics in cells transitioning to hematopoietic fate. *J Exp Medicine* 215: 233–248
- Eilken HM, Nishikawa S-I & Schroeder T (2009) Continuous single-cell imaging of blood generation from haemogenic endothelium. *Nature* 457: 896–900
- Eliades A, Wareing S, Marinopoulou E, Fadlullah MZH, Patel R, Grabarek JB, Plusa B, Lacaud G & Kouskoff V (2016) The Hemogenic Competence of Endothelial Progenitors Is Restricted by Runx1 Silencing during Embryonic Development. *Cell Reports* 15: 2185–2199
- Elsaid R, Meunier S, Burlen-Defranoux O, Soares-da-Silva F, Perchet T, Iturri L, Freyer L, Vieira P, Pereira P, Golub R, et al (2020) A wave of embryonic bipotent T/lymphoid tissue inducer progenitors regulates the maturation of medullary thymic epithelial cells. *Biorxiv*: 791103
- Espín-Palazón R, Stachura DL, Campbell CA, García-Moreno D, Del Cid N, Kim AD, Candel S, Meseguer J, Mulero V & Traver D (2014) Proinflammatory Signaling Regulates Hematopoietic Stem Cell Emergence. *Cell* 159: 1070–1085
- Fadlullah MZ, Neo WH, Lie-a-ling M, Thambyrajah R, Patel R, Mevel R, Aksoy I, Khoa ND, Savatier P, Fontenille L, et al (2021) Murine AGM single-cell profiling identifies a continuum of hemogenic endothelium differentiation marked by ACE. *Blood*
- Fernandes I, Bastien Y, Wai T, Nygard K, Lin R, Cormier O, Lee HS, Eng F, Bertos NR, Pelletier N, et al (2003) Ligand-Dependent Nuclear Receptor Corepressor LCoR Functions by Histone Deacetylase-Dependent and -Independent Mechanisms. *Mol Cell* 11: 139–150

- Flynn KM, Michaud M, Canosa S & Madri JA (2013) CD44 regulates vascular endothelial barrier integrity via a PECAM-1 dependent mechanism. *Angiogenesis* 16: 689–705
- Foerster K, He W, Manuel J, Bartczak A, Liu M, Markert UR, Levy GA & Clark DA (2007) LPS-Induced Occult Loss in Mice Requires FGL2. *Am J Reprod Immunol* 58: 524–529
- FORD CE, HAMERTON JL, BARNES DWH & LOUTIT JF (1956) Cytological Identification of Radiation-Chimæras. *Nature* 177: 452–454
- Forsberg EC, Serwold T, Kogan S, Weissman IL & Passegué E (2006) New Evidence Supporting Megakaryocyte-Erythrocyte Potential of Flk2/Flt3+ Multipotent Hematopoietic Progenitors. *Cell* 126: 415–426
- Frame JM, Fegan KH, Conway SJ, McGrath KE & Palis J (2016) Definitive Hematopoiesis in the Yolk Sac Emerges from Wnt-Responsive Hemogenic Endothelium Independently of Circulation and Arterial Identity. *Stem Cells* 34: 431–444
- Franchini AM, Myers JR, Jin G-B, Shepherd DM & Lawrence BP (2019) Genome-Wide Transcriptional Analysis Reveals Novel AhR Targets That Regulate Dendritic Cell Function during Influenza A Virus Infection. *Immunohorizons* 3: 219–235
- Fraser ST, Isern J & Baron MH (2006) Maturation and enucleation of primitive erythroblasts during mouse embryogenesis is accompanied by changes in cell-surface antigen expression. *Blood* 109: 343–352
- Fraser ST, Ogawa M, Yokomizo T, Ito Y, Nishikawa S & Nishikawa S (2003) Putative intermediate precursor between hematogenic endothelial cells and blood cells in the developing embryo. *Dev Growth Differ* 45: 63–75
- Fraser ST, Ogawa M, Yu RT, Nishikawa S, Yoder MC & Nishikawa S-I (2002) Definitive hematopoietic commitment within the embryonic vascular endothelial-cadherin+ population. *Exp Hematol* 30: 1070–1078
- Fryer CJ, Lamar E, Turbachova I, Kintner C & Jones KA (2002) Mastermind mediates chromatin-specific transcription and turnover of the Notch enhancer complex. *Gene Dev* 16: 1397–1411
- Fujita Y, Nishimura M, Taniwaki M, Abe T & Okuda T (2001) Identification of an Alternatively Spliced Form of the Mouse AML1/RUNX1 Gene Transcript AML1c and Its Expression in Early Hematopoietic Development. *Biochem Biophys Res Commun* 281: 1248–1255
- Ganesan LP, Kim J, Wu Y, Mohanty S, Phillips GS, Birmingham DJ, Robinson JM & Anderson CL (2012) FcγRIIb on Liver Sinusoidal Endothelium Clears Small Immune Complexes. *J Immunol* 189: 4981–4988
- Gao L, Tober J, Gao P, Chen C, Zhu Q, Tan K & Speck NA (2018) RUNX1 and the endothelial origin of blood. *Exp Hematol* 68: 2–9

- Gao X, Johnson KD, Chang Y-I, Boyer ME, Dewey CN, Zhang J & Bresnick EH (2013) Gata2 cis-element is required for hematopoietic stem cell generation in the mammalian embryo. *J Exp Med* 210: 2833–2842
- Garcia-Porrero JA, Godin IE & Dieterlen-Lièvre F (1995) Potential intraembryonic hemogenic sites at pre-liver stages in the mouse. *Anat Embryol* 192: 425–435
- Gekas C, Dieterlen-Lièvre F, Orkin SH & Mikkola HKA (2005) The Placenta Is a Niche for Hematopoietic Stem Cells. *Dev Cell* 8: 365–375
- Gentek R, Ghigo C, Hoeffel G, Bulle MJ, Msallam R, Gautier G, Launay P, Chen J, Ginhoux F & Bajénoff M (2018) Hemogenic Endothelial Fate Mapping Reveals Dual Developmental Origin of Mast Cells. *Immunity* 48: 1160-1171.e5
- Gering M & Patient R (2005) Hedgehog Signaling Is Required for Adult Blood Stem Cell Formation in Zebrafish Embryos. *Dev Cell* 8: 389–400
- Ginhoux F, Greter M, Leboeuf M, Nandi S, See P, Gokhan S, Mehler MF, Conway SJ, Ng LG, Stanley ER, *et al* (2010) Fate Mapping Analysis Reveals That Adult Microglia Derive from Primitive Macrophages. *Science* 330: 841–845
- Giroux S, Kaushik A-L, Capron C, Jalil A, Kelaidi C, Sablitzky F, Dumenil D, Albagli O & Godin I (2007) Iyl-1 and tal-1/scl, two genes encoding closely related bHLH transcription factors, display highly overlapping expression patterns during cardiovascular and hematopoietic ontogeny. *Gene Expr Patterns* 7: 215–226
- Glittenberg M, Pitsouli C, Garvey C, Delidakis C & Bray S (2006) Role of conserved intracellular motifs in Serrate signalling, cis-inhibition and endocytosis. *Embo J* 25: 4697–4706
- Goldie LC, Lucitti JL, Dickinson ME & Hirschi KK (2008) Cell signaling directing the formation and function of hemogenic endothelium during murine embryogenesis. *Blood* 112: 3194–3204
- Gordon-Keylock S, Sobiesiak M, Rybtsov S, Moore K & Medvinsky A (2013) Mouse extraembryonic arterial vessels harbor precursors capable of maturing into definitive HSCs. *Blood* 122: 2338–2345
- Griffioen AW, Coenen MJH, Damen CA, Hellwig SMM, Weering DHJ van, Vooy W, Blijham GH & Groenewegen G (1997) CD44 Is Involved in Tumor Angiogenesis; an Activation Antigen on Human Endothelial Cells. *Blood* 90: 1150–1159
- Growney JD, Shigematsu H, Li Z, Lee BH, Adelsperger J, Rowan R, Curley DP, Kutok JL, Akashi K, Williams IR, *et al* (2005) Loss of Runx1 perturbs adult hematopoiesis and is associated with a myeloproliferative phenotype. *Blood* 106: 494–504
- Guyre PM, Morganelli PM & Miller R (1983) Recombinant immune interferon increases immunoglobulin G Fc receptors on cultured human mononuclear phagocytes. *J Clin Invest* 72: 393–397
- Haar JL & Ackerman GA (1971) A phase and electron microscopic study of vasculogenesis and erythropoiesis in the yolk sac of the mouse. *Anatomical Rec* 170: 199–223

- Haas JD, Ravens S, Düber S, Sandrock I, Oberdörfer L, Kashani E, Chennupati V, Föhse L, Naumann R, Weiss S, *et al* (2012) Development of Interleukin-17-Producing $\gamma\delta$ T Cells Is Restricted to a Functional Embryonic Wave. *Immunity* 37: 48–59
- Hart A, Melet F, Grossfeld P, Chien K, Jones C, Tunnacliffe A, Favier R & Bernstein A (2000) Fli-1 Is Required for Murine Vascular and Megakaryocytic Development and Is Hemizygotously Deleted in Patients with Thrombocytopenia. *Immunity* 13: 167–177
- Heitzler P, Bourouis M, Ruel L, Carteret C & Simpson P (1996) Genes of the Enhancer of split and achaete-scute complexes are required for a regulatory loop between Notch and Delta during lateral signalling in *Drosophila*. *Dev Camb Engl* 122: 161–71
- Hellström M, Phng L-K, Hofmann JJ, Wallgard E, Coultas L, Lindblom P, Alva J, Nilsson A-K, Karlsson L, Gaiano N, *et al* (2007) Dll4 signalling through Notch1 regulates formation of tip cells during angiogenesis. *Nature* 445: 776–780
- Herbomel P, Thisse B & Thisse C (2001) Zebrafish Early Macrophages Colonize Cephalic Mesenchyme and Developing Brain, Retina, and Epidermis through a M-CSF Receptor-Dependent Invasive Process. *Dev Biol* 238: 274–288
- Hibbs ML, Bonadonna L, Scott BM, McKenzie IF & Hogarth PM (1988) Molecular cloning of a human immunoglobulin G Fc receptor. *Proc National Acad Sci* 85: 2240–2244
- Hirai H, Ogawa M, Suzuki N, Yamamoto M, Breier G, Mazda O, Imanishi J & Nishikawa S-I (2003) Hemogenic and nonhemogenic endothelium can be distinguished by the activity of fetal liver kinase (Flk)-1 promoter/enhancer during mouse embryogenesis. *Blood* 101: 886–893
- Holmes R & Zúñiga-Pflücker JC (2009) The OP9-DL1 System: Generation of T-Lymphocytes from Embryonic or Hematopoietic Stem Cells In Vitro. *Cold Spring Harb Protoc* 2009: pdb.prot5156
- Hu Y & Smyth GK (2009) ELDA: Extreme limiting dilution analysis for comparing depleted and enriched populations in stem cell and other assays. *J Immunol Methods* 347: 70–78
- Huang Z, Hunter S, Kim M, Indik ZK & Schreiber AD (2003) The effect of phosphatases SHP-1 and SHIP-1 on signaling by the ITIM- and ITAM-containing Fc γ receptors Fc γ RIIB and Fc γ RIIA. *J Leukocyte Biol* 73: 823–829
- Huber TL, Kouskoff V, Fehling HJ, Palis J & Keller G (2004) Haemangioblast commitment is initiated in the primitive streak of the mouse embryo. *Nature* 432: 625–630
- Hunter S, Indik ZK, Kim M-K, Cauley MD, Park J-G & Schreiber AD (1998) Inhibition of Fc γ Receptor-Mediated Phagocytosis by a Nonphagocytic Fc γ Receptor. *Blood* 91: 1762–1768

- Iacovino M, Chong D, Szatmari I, Hartweck L, Rux D, Caprioli A, Cleaver O & Kyba M (2011) HoxA3 is an apical regulator of haemogenic endothelium. *Nat Cell Biol* 13: 72–78
- Ichikawa M, Asai T, Saito T, Yamamoto G, Seo S, Yamazaki I, Yamagata T, Mitani K, Chiba S, Hirai H, *et al* (2004) AML-1 is required for megakaryocytic maturation and lymphocytic differentiation, but not for maintenance of hematopoietic stem cells in adult hematopoiesis. *Nat Med* 10: 299–304
- Ikuta K & Weissman IL (1992) Evidence that hematopoietic stem cells express mouse c-kit but do not depend on steel factor for their generation. *Proc National Acad Sci* 89: 1502–1506
- Ingley E (2012) Functions of the Lyn tyrosine kinase in health and disease. *Cell Commun Signal Ccs* 10: 21–21
- Ishikawa T, Yokoyama H, Matsuura T & Fujiwara Y (2019) Fc gamma RIIb expression levels in human liver sinusoidal endothelial cells during progression of non-alcoholic fatty liver disease. *Plos One* 14: e0211543
- Iso T, Kedes L & Hamamori Y (2003) HES and HERP families: Multiple effectors of the notch signaling pathway. *J Cell Physiol* 194: 237–255
- Ivanovs A, Rybtsov S, Anderson RA, Turner ML & Medvinsky A (2014) Identification of the Niche and Phenotype of the First Human Hematopoietic Stem Cells. *Stem Cell Rep* 2: 449–456
- Ivanovs A, Rybtsov S, Ng ES, Stanley EG, Elefanty AG & Medvinsky A (2017) Human haematopoietic stem cell development: from the embryo to the dish. *Development* 144: 2323–2337
- Ivanovs A, Rybtsov S, Welch L, Anderson RA, Turner ML & Medvinsky A (2011) Highly potent human hematopoietic stem cells first emerge in the intraembryonic aorta-gonad-mesonephros region. *J Exp Medicine* 208: 2417–2427
- Jaffe L, Robertson EJ & Bikoff EK (1991) Distinct patterns of expression of MHC class I and beta 2-microglobulin transcripts at early stages of mouse development. *J Immunol Baltim Md 1950* 147: 2740–9
- Jaffredo T, Bollerot K, Sugiyama D, Gautier R & Drevon C (2003) Tracing the hemangioblast during embryogenesis: developmental relationships between endothelial and hematopoietic cells. *Int J Dev Biol* 49: 269–277
- Jaffredo T, Gautier R, Eichmann A & Dieterlen-Lièvre F (1998) Intraaortic hemopoietic cells are derived from endothelial cells during ontogeny. *Dev Camb Engl* 125: 4575–83
- Jokubaitis VJ, Sinka L, Driessen R, Whitty G, Haylock DN, Bertoncetto I, Smith I, Péault B, Tavian M & Simmons PJ (2008) Angiotensin-converting enzyme (CD143) marks hematopoietic stem cells in human embryonic, fetal, and adult hematopoietic tissues. *Blood* 111: 4055–4063

- Jong JLO de, Davidson AJ, Wang Y, Palis J, Opara P, Pugach E, Daley GQ & Zon LI (2010) Interaction of retinoic acid and scl controls primitive blood development. *Blood* 116: 201–209
- Joutel A, Corpechot C, Ducros A, Vahedi K, Chabriat H, Mouton P, Alamowitch S, Domenga V, Cécillion M, Maréchal E, *et al* (1996) Notch3 mutations in CADASIL, a hereditary adult-onset condition causing stroke and dementia. *Nature* 383: 707–710
- Julien E, Biasch K, Omar RE, Freund J, Gachet C, Lanza F & Tavian M (2021) Renin-angiotensin system is involved in embryonic emergence of hematopoietic stem/progenitor cells. *Stem Cells* 39: 636–649
- Jung HS, Uenishi G, Park MA, Liu P, Suknuntha K, Raymond M, Choi YJ, Thomson JA, Ong IM & Slukvin II (2021) SOX17 integrates HOXA and arterial programs in hemogenic endothelium to drive definitive lympho-myeloid hematopoiesis. *Cell Reports* 34: 108758
- Kabrun N, Bühring HJ, Choi K, Ullrich A, Risau W & Keller G (1997) Flk-1 expression defines a population of early embryonic hematopoietic precursors. *Dev Camb Engl* 124: 2039–48
- Kalev-Zylinska ML, Horsfield JA, Flores MVC, Postlethwait JH, Vitas MR, Baas AM, Crosier PS & Crosier KE (2002) Runx1 is required for zebrafish blood and vessel development and expression of a human RUNX1-CBF2T1 transgene advances a model for studies of leukemogenesis. *Dev Camb Engl* 129: 2015–30
- Kamachi Y, Ogawa E, Asano M, Ishida S, Murakami Y, Satake M, Ito Y & Shigesada K (1990) Purification of a mouse nuclear factor that binds to both the A and B cores of the polyomavirus enhancer. *J Virol* 64: 4808–4819
- Kao H-Y, Ordentlich P, Koyano-Nakagawa N, Tang Z, Downes M, Kintner CR, Evans RM & Kadesch T (1998) A histone deacetylase corepressor complex regulates the Notch signal transduction pathway. *Gene Dev* 12: 2269–2277
- Karsten CM, Pandey MK, Figge J, Kilchenstein R, Taylor PR, Rosas M, McDonald JU, Orr SJ, Berger M, Petzold D, *et al* (2012) Anti-inflammatory activity of IgG1 mediated by Fc galactosylation and association of FcγRIIB and dectin-1. *Nat Med* 18: 1401–1406
- Kartalaei PS, Yamada-Inagawa T, Vink CS, Pater E de, Linden R van der, Marks-Bluth J, Slood A van der, Hout M van den, Yokomizo T, Schaick-Solernó ML van, *et al* (2015) Whole-transcriptome analysis of endothelial to hematopoietic stem cell transition reveals a requirement for Gpr56 in HSC generation. *J Exp Medicine* 212: 93–106
- Katsuno Y, Ehata S, Yashiro M, Yanagihara K, Hirakawa K & Miyazono K (2012) Coordinated expression of REG4 and aldehyde dehydrogenase 1 regulating tumorigenic capacity of diffuse-type gastric carcinoma-initiating cells is inhibited by TGF-β. *J Pathology* 228: 391–404

- Kawaguchi R, Yu J, Honda J, Hu J, Whitelegge J, Ping P, Wiita P, Bok D & Sun H (2007) A Membrane Receptor for Retinol Binding Protein Mediates Cellular Uptake of Vitamin A. *Science* 315: 820–825
- Keller G (2005) Embryonic stem cell differentiation: emergence of a new era in biology and medicine. *Gene Dev* 19: 1129–1155
- Kennedy M, Awong G, Sturgeon CM, Ditadi A, LaMotte-Mohs R, Zúñiga-Pflücker JC & Keller G (2012) T lymphocyte potential marks the emergence of definitive hematopoietic progenitors in human pluripotent stem cell differentiation cultures. *Cell Reports* 2: 1722–35
- Kennedy M, D'Souza SL, Lynch-Kattman M, Schwantz S & Keller G (2006) Development of the hemangioblast defines the onset of hematopoiesis in human ES cell differentiation cultures. *Blood* 109: 2679–2687
- Khandekar M, Brandt W, Zhou Y, Dagenais S, Glover TW, Suzuki N, Shimizu R, Yamamoto M, Lim K-C & Engel JD (2007) A Gata2 intronic enhancer confers its pan-endothelia-specific regulation. *Development* 134: 1703–1712
- Kim I, He S, Yilmaz OH, Kiel MJ & Morrison SJ (2006) Enhanced purification of fetal liver hematopoietic stem cells using SLAM family receptors. *Blood* 108: 737–744
- Kim I, Saunders TL & Morrison SJ (2007) Sox17 Dependence Distinguishes the Transcriptional Regulation of Fetal from Adult Hematopoietic Stem Cells. *Cell* 130: 470–483
- Kim I, Yilmaz OH & Morrison SJ (2005) CD144 (VE-cadherin) is transiently expressed by fetal liver hematopoietic stem cells. *Blood* 106: 903–905
- Kinder SJ, Tsang TE, Quinlan GA, Hadjantonakis AK, Nagy A & Tam PP (1999) The orderly allocation of mesodermal cells to the extraembryonic structures and the anteroposterior axis during gastrulation of the mouse embryo. *Dev Camb Engl* 126: 4691–701
- Kingsley PD, Malik J, Fantauzzo KA & Palis J (2004) Yolk sac-derived primitive erythroblasts enucleate during mammalian embryogenesis. *Blood* 104: 19–25
- Kissa K & Herbomel P (2010) Blood stem cells emerge from aortic endothelium by a novel type of cell transition. *Nature* 464: 112–115
- Kobayashi M, Shelley WC, Seo W, Vemula S, Lin Y, Liu Y, Kapur R, Taniuchi I & Yoshimoto M (2014) Functional B-1 progenitor cells are present in the hematopoietic stem cell-deficient embryo and depend on Cbfb for their development. *P Natl Acad Sci Usa* 111: 12151–6
- Kondo M, Weissman IL & Akashi K (1997) Identification of Clonogenic Common Lymphoid Progenitors in Mouse Bone Marrow. *Cell* 91: 661–672
- Koushik SV, Wang J, Rogers R, Moskophidis D, Lambert NA, Creazzo TL & Conway SJ (2001) Targeted inactivation of the sodium-calcium exchanger (Ncx1) results in the lack of a heartbeat and abnormal myofibrillar organization. *Faseb J* 15: 1209–1211

- Krebs LT, Shutter JR, Tanigaki K, Honjo T, Stark KL & Gridley T (2004) Haploinsufficient lethality and formation of arteriovenous malformations in Notch pathway mutants. *Gene Dev* 18: 2469–2473
- Krebs LT, Xue Y, Norton CR, Shutter JR, Maguire M, Sundberg JP, Gallahan D, Closson V, Kitajewski J, Callahan R, *et al* (2000) Notch signaling is essential for vascular morphogenesis in mice. *Gene Dev* 14: 1343–52
- Kristiansen TA, Gyllenbäck EJ, Zriwil A, Björklund T, Daniel JA, Sitnicka E, Soneji S, Bryder D & Yuan J (2016) Cellular Barcoding Links B-1a B Cell Potential to a Fetal Hematopoietic Stem Cell State at the Single-Cell Level. *Immunity* 45: 346–57
- Kristoffersen EK & Matre R (1996) Co-localization of the neonatal Fcγ receptor and IgG in human placental term syncytiotrophoblasts. *Eur J Immunol* 26: 1668–1671
- Kumano K, Chiba S, Kunisato A, Sata M, Saito T, Nakagami-Yamaguchi E, Yamaguchi T, Masuda S, Shimizu K, Takahashi T, *et al* (2003) Notch1 but Not Notch2 Is Essential for Generating Hematopoietic Stem Cells from Endothelial Cells. *Immunity* 18: 699–711
- Kumaravelu P, Hook L, Morrison AM, Ure J, Zhao S, Zuyev S, Ansell J & Medvinsky A (2002) Quantitative developmental anatomy of definitive haematopoietic stem cells/long-term repopulating units (HSC/RUs): role of the aorta-gonad-mesonephros (AGM) region and the yolk sac in colonisation of the mouse embryonic liver. *Dev Camb Engl* 129: 4891–9
- Labastie MC, Cortés F, Roméo PH, Dulac C & Péault B (1998) Molecular identity of hematopoietic precursor cells emerging in the human embryo. *Blood* 92: 3624–35
- Lacaud G, Carlsson L & Keller G (1998) Identification of a Fetal Hematopoietic Precursor with B Cell, T Cell, and Macrophage Potential. *Immunity* 9: 827–838
- Lacaud G, Gore L, Kennedy M, Kouskoff V, Kingsley P, Hogan C, Carlsson L, Speck N, Palis J & Keller G (2002) Runx1 is essential for hematopoietic commitment at the hemangioblast stage of development in vitro. *Blood* 100: 458–466
- Lai EC (2004) Notch signaling: control of cell communication and cell fate. *Development* 131: 965–973
- Lai L, Bohnsack BL, Niederreither K & Hirschi KK (2003) Retinoic acid regulates endothelial cell proliferation during vasculogenesis. *Development* 130: 6465–6474
- Lakhan R & Rathinam CV (2021) Deficiency of Rbpj Leads to Defective Stress-Induced Hematopoietic Stem Cell Functions and Hif Mediated Activation of Non-canonical Notch Signaling Pathways. *Frontiers Cell Dev Biology* 8: 622190
- Lancrin C, Mazan M, Stefanska M, Patel R, Lichtinger M, Costa G, Vargel Ö, Wilson NK, Möröy T, Bonifer C, *et al* (2012) GFI1 and GFI1B control the loss of endothelial identity of hemogenic endothelium during hematopoietic commitment. *Blood* 120: 314–322

- Lancrin C, Sroczynska P, Stephenson C, Allen T, Kouskoff V & Lacaud G (2009) The haemangioblast generates haematopoietic cells through a haemogenic endothelium stage. *Nature* 457: 892–895
- Languino LR, Duperray A, Joganic KJ, Fornaro M, Thornton GB & Altieri DC (1995) Regulation of leukocyte-endothelium interaction and leukocyte transendothelial migration by intercellular adhesion molecule 1-fibrinogen recognition. *Proc National Acad Sci* 92: 1505–1509
- Languino LR, Plescia J, Duperray A, Brian AA, Plow EF, Geltosky JE & Altieri DC (1993) Fibrinogen mediates leukocyte adhesion to vascular endothelium through an ICAM-1-dependent pathway. *Cell* 73: 1423–1434
- Laurenti E & Göttgens B (2018) From haematopoietic stem cells to complex differentiation landscapes. *Nature* 553: 418–426
- Lawson KA, Meneses JJ & Pedersen RA (1991) Clonal analysis of epiblast fate during germ layer formation in the mouse embryo. *Dev Camb Engl* 113: 891–911
- Lawson ND, Scheer N, Pham VN, Kim CH, Chitnis AB, Campos-Ortega JA & Weinstein BM (2001) Notch signaling is required for arterial-venous differentiation during embryonic vascular development. *Dev Camb Engl* 128: 3675–83
- Lawson ND, Vogel AM & Weinstein BM (2002) sonic hedgehog and vascular endothelial growth factor Act Upstream of the Notch Pathway during Arterial Endothelial Differentiation. *Dev Cell* 3: 127–136
- Lee LK, Ghorbanian Y, Wang W, Wang Y, Kim YJ, Weissman IL, Inlay MA & Mikkola HKA (2016) LYVE1 Marks the Divergence of Yolk Sac Definitive Hemogenic Endothelium from the Primitive Erythroid Lineage. *Cell Reports* 17: 2286–2298
- Levy GA, Liu M, Ding J, Yuwaraj S, Leibowitz J, Marsden PA, Ning Q, Kovalinka A & Phillips MJ (2000) Molecular and Functional Analysis of the Human Prothrombinase Gene (HFGL2) and Its Role in Viral Hepatitis. *Am J Pathology* 156: 1217–1225
- Li C & Johnson G (1995) Murine hematopoietic stem and progenitor cells: I. Enrichment and biologic characterization. *Blood* 85: 1472–1479
- Li Z, Chen MJ, Stacy T & Speck NA (2006) Runx1 function in hematopoiesis is required in cells that express Tek. *Blood* 107: 106–110
- Liao Y, Smyth GK & Shi W (2014) featureCounts: an efficient general purpose program for assigning sequence reads to genomic features. *Bioinformatics* 30: 923–930
- Lie-A-Ling M, Marinopoulou E, Li Y, Patel R, Stefanska M, Bonifer C, Miller C, Kouskoff V & Lacaud G (2014) RUNX1 positively regulates a cell adhesion and migration program in murine hemogenic endothelium prior to blood emergence. *Blood* 124: e11–e20
- Ling K-W, Ottersbach K, Hamburg JP van, Oziemlak A, Tsai F-Y, Orkin SH, Ploemacher R, Hendriks RW & Dzierzak E (2004) GATA-2 Plays Two Functionally Distinct Roles during the Ontogeny of Hematopoietic Stem Cells. *J Exp Medicine* 200: 871–882

- Liu H, Shalev I, Manuel J, He W, Leung E, Crookshank J, Liu MF, Diao J, Cattral M, Clark DA, *et al* (2008) The FGL2-FcγRIIB pathway: A novel mechanism leading to immunosuppression. *Eur J Immunol* 38: 3114–3126
- Liu Y, Xu L, Zeng Q, Wang J, Wang M, Xi D, Wang X, Yang D, Luo X & Ning Q (2012) Downregulation of FGL2/prothrombinase delays HCCLM6 xenograft tumour growth and decreases tumour angiogenesis. *Liver Int* 32: 1585–1595
- Liu Y, Xu S, Xiao F, Xiong Y, Wang X, Gao S, Yan W & Ning Q (2010) The FGL2/fibroleukin prothrombinase is involved in alveolar macrophage activation in COPD through the MAPK pathway. *Biochem Bioph Res Co* 396: 555–561
- Lizama CO, Hawkins JS, Schmitt CE, Bos FL, Zape JP, Cautivo KM, Pinto HB, Rhyner AM, Yu H, Donohoe ME, *et al* (2015) Repression of arterial genes in hemogenic endothelium is sufficient for haematopoietic fate acquisition. *Nat Commun* 6: 7739
- Love MI, Huber W & Anders S (2014) Moderated estimation of fold change and dispersion for RNA-seq data with DESeq2. *Genome Biol* 15: 550
- Luo W, Garcia-Gonzalez I, Fernández-Chacón M, Casquero-Garcia V, Sanchez-Muñoz MS, Mühleder S, Garcia-Ortega L, Andrade J, Potente M & Benedito R (2021) Arterialization requires the timely suppression of cell growth. *Nature* 589: 437–441
- Lux CT, Yoshimoto M, McGrath K, Conway SJ, Palis J & Yoder MC (2008) All primitive and definitive hematopoietic progenitor cells emerging before E10 in the mouse embryo are products of the yolk sac. *Blood* 111: 3435–3438
- Ma Q, Zhu C, Zhang W, Ta N, Zhang R, Liu L, Feng D, Cheng H, Liu J & Chen Q (2019) Mitochondrial PIP3-binding protein FUNDC2 supports platelet survival via AKT signaling pathway. *Cell Death Differ* 26: 321–331
- Malbec O, Fong DC, Turner M, Tybulewicz VL, Cambier JC, Fridman WH & Daëron M (1998) Fc epsilon receptor I-associated lyn-dependent phosphorylation of Fc gamma receptor IIB during negative regulation of mast cell activation. *J Immunol Baltim Md 1950* 160: 1647–58
- Månsson R, Hultquist A, Luc S, Yang L, Anderson K, Kharazi S, Al-Hashmi S, Liuba K, Thorén L, Adolfsson J, *et al* (2007) Molecular Evidence for Hierarchical Transcriptional Lineage Priming in Fetal and Adult Stem Cells and Multipotent Progenitors. *Immunity* 26: 407–419
- Marazzi S, Blum S, Hartmann R, Gundersen D, Schreyer M, Argraves S, Fliedner V von, Pytela R & Rüegg C (1998) Characterization of human fibroleukin, a fibrinogen-like protein secreted by T lymphocytes. *J Immunol Baltim Md 1950* 161: 138–47
- Marsden PA, Ning Q, Fung LS, Luo X, Chen Y, Mendicino M, Ghanekar A, Scott JA, Miller T, Chan CWY, *et al* (2003) The Fgl2/fibroleukin prothrombinase contributes to immunologically mediated thrombosis in experimental and human viral hepatitis. *J Clin Invest* 112: 58–66

- McCright B, Gao X, Shen L, Lozier J, Lan Y, Maguire M, Herzlinger D, Weinmaster G, Jiang R & Gridley T (2001) Defects in development of the kidney, heart and eye vasculature in mice homozygous for a hypomorphic Notch2 mutation. *Dev Camb Engl* 128: 491–502
- MCCULLOCH EA & TILL JE (1960) The radiation sensitivity of normal mouse bone marrow cells, determined by quantitative marrow transplantation into irradiated mice. *Radiat Res* 13: 115–25
- McGarvey AC, Rybtsov S, Souilhol C, Tamagno S, Rice R, Hills D, Godwin D, Rice D, Tomlinson SR & Medvinsky A (2017) A molecular roadmap of the AGM region reveals BMPER as a novel regulator of HSC maturation. *J Exp Medicine* 214: 3731–3751
- McGrath K & Palis J (2008) Chapter 1 Ontogeny of Erythropoiesis in the Mammalian Embryo. *Curr Top Dev Biol* 82: 1–22
- McGrath KE, Frame JM, Fegan KH, Bowen JR, Conway SJ, Catherman SC, Kingsley PD, Koniski AD & Palis J (2015) Distinct Sources of Hematopoietic Progenitors Emerge before HSCs and Provide Functional Blood Cells in the Mammalian Embryo. *Cell Reports* 11: 1892–1904
- McGrath KE, Frame JM, Fromm GJ, Koniski AD, Kingsley PD, Little J, Bulger M & Palis J (2011) A transient definitive erythroid lineage with unique regulation of the β -globin locus in the mammalian embryo. *Blood* 117: 4600–4608
- McGrath KE, Koniski AD, Maltby KM, McGann JK & Palis J (1999) Embryonic Expression and Function of the Chemokine SDF-1 and Its Receptor, CXCR4. *Dev Biol* 213: 442–456
- Medvinsky A & Dzierzak E (1996) Definitive Hematopoiesis Is Autonomously Initiated by the AGM Region. *Cell* 86: 897–906
- Medvinsky AL, Samoylina NL, Müller AM & Dzierzak EA (1993) An early pre-liver intraembryonic source of CFU-S in the developing mouse. *Nature* 364: 64–67
- Melnyk M, Shalev I, Zhang J, Bartczak A, Gorczynski R, Selzner N, Inman R, Marsden P, Phillips M, Clark D, *et al* (2011) The prothrombinase activity of FGL2 contributes to the pathogenesis of experimental arthritis. *Scand J Rheumatol* 40: 269–278
- Mikkola HKA, Fujiwara Y, Schlaeger TM, Traver D & Orkin SH (2003) Expression of CD41 marks the initiation of definitive hematopoiesis in the mouse embryo. *Blood* 101: 508–516
- Mikkola HKA & Orkin SH (2006) The journey of developing hematopoietic stem cells. *Development* 133: 3733–3744
- Millauer B, Wizigmann-Voos S, Schnürch H, Martinez R, Møller NPH, Risau W & Ullrich A (1993) High affinity VEGF binding and developmental expression suggest Flk-1 as a major regulator of vasculogenesis and angiogenesis. *Cell* 72: 835–846

- Miller J, Horner A, Stacy T, Lowrey C, Lian JB, Stein G, Nuckolls GH & Speck NA (2002) The core-binding factor β subunit is required for bone formation and hematopoietic maturation. *Nat Genet* 32: 645–649
- Mimoun A, Delignat S, Peyron I, Daventure V, Lecerf M, Dimitrov JD, Kaveri SV, Bayry J & Lacroix-Desmazes S (2020) Relevance of the Materno-Fetal Interface for the Induction of Antigen-Specific Immune Tolerance. *Front Immunol* 11: 810
- Minegishi N, Ohta J, Yamagiwa H, Suzuki N, Kawauchi S, Zhou Y, Takahashi S, Hayashi N, Engel JD & Yamamoto M (1999) The Mouse GATA-2 Gene is Expressed in the Para-Aortic Splanchnopleura and Aorta-Gonads and Mesonephros Region. *Blood* 93: 4196–4207
- Mishima T, Kurasawa G, Ishikawa G, Mori M, Kawahigashi Y, Ishikawa T, Luo S-S, Takizawa T, Goto T, Matsubara S, *et al* (2007) Endothelial Expression of Fc Gamma Receptor IIb in the Full-term Human Placenta. *Placenta* 28: 170–174
- Miyoshi H, Shimizu K, Kozu T, Maseki N, Kaneko Y & Ohki M (1991) t(8;21) breakpoints on chromosome 21 in acute myeloid leukemia are clustered within a limited region of a single gene, AML1. *Proc National Acad Sci* 88: 10431–10434
- Monteiro R, Pinheiro P, Joseph N, Peterkin T, Koth J, Repapi E, Bonkhofer F, Kirmizitas A & Patient R (2016) Transforming Growth Factor β Drives Hemogenic Endothelium Programming and the Transition to Hematopoietic Stem Cells. *Dev Cell* 38: 358–370
- Monvoisin A, Alva JA, Hofmann JJ, Zovein AC, Lane TF & Iruela-Arispe ML (2006) VE-cadherin-CreERT2 transgenic mouse: A model for inducible recombination in the endothelium. *Dev Dynam* 235: 3413–3422
- Morgan TH (1917) The Theory of the Gene. *Am Nat* 51: 513–544
- Moro I, Iwase T, Komiyama K, Kusama K, Saito I, Asano M & Takahashi T (1990) Advances in Mucosal Immunology, Proceedings of the Fifth International Congress of Mucosal Immunology. 459–460
- Motoike T, Markham DW, Rossant J & Sato TN (2003) Evidence for novel fate of Flk1+ progenitor: Contribution to muscle lineage. *Genesis* 35: 153–159
- Mu J, Qu D, Bartczak A, Phillips MJ, Manuel J, He W, Kosciak C, Mendicino M, Zhang L, Clark DA, *et al* (2007) Fgl2 deficiency causes neonatal death and cardiac dysfunction during embryonic and postnatal development in mice. *Physiol Genomics* 31: 53–62
- Müller AM, Medvinsky A, Strouboulis J, Grosveld F & Dzierzakt E (1994) Development of hematopoietic stem cell activity in the mouse embryo. *Immunity* 1: 291–301
- Murray PDF (1932) The development in vitro of the blood of the early chick embryo. *Proc Royal Soc Lond Ser B Contain Pap Biological Character* 111: 497–521
- Naito M, Takahashi K & Nishikawa S (1990) Development, Differentiation, and Maturation of Macrophages in the Fetal Mouse Liver. *J Leukocyte Biol* 48: 27–37

- Nakajima-Takagi Y, Osawa M, Oshima M, Takagi H, Miyagi S, Endoh M, Endo TA, Takayama N, Eto K, Toyoda T, *et al* (2013) Role of SOX17 in hematopoietic development from human embryonic stem cells. *Blood* 121: 447–458
- Nandi A, Estess P & Siegelman MH (2000) Hyaluronan Anchoring and Regulation on the Surface of Vascular Endothelial Cells Is Mediated through the Functionally Active Form of CD44*. *J Biol Chem* 275: 14939–14948
- Ng CEL, Yokomizo T, Yamashita N, Cirovic B, Jin H, Wen Z, Ito Y & Osato M (2010) A Runx1 Intronic Enhancer Marks Hemogenic Endothelial Cells and Hematopoietic Stem Cells. *Stem Cells* 28: 1869–1881
- Ng ES, Azzola L, Bruveris FF, Calvanese V, Phipson B, Vlahos K, Hirst C, Jokubaitis VJ, Yu QC, Maksimovic J, *et al* (2016) Differentiation of human embryonic stem cells to HOXA+ hemogenic vasculature that resembles the aorta-gonad-mesonephros. *Nat Biotechnol* 34: 1168–1179
- Niederreither K & Dollé P (2008) Retinoic acid in development: towards an integrated view. *Nat Rev Genet* 9: 541–553
- Niederreither K, McCaffery P, Dräger UC, Chambon P & Dollé P (1997) Restricted expression and retinoic acid-induced downregulation of the retinaldehyde dehydrogenase type 2 (RALDH-2) gene during mouse development. *Mech Develop* 62: 67–78
- Niederreither K, Subbarayan V, Dollé P & Chambon P (1999) Embryonic retinoic acid synthesis is essential for early mouse post-implantation development. *Nat Genet* 21: 444–448
- Niki M, Okada H, Takano H, Kuno J, Tani K, Hibino H, Asano S, Ito Y, Satake M & Noda T (1997) Hematopoiesis in the fetal liver is impaired by targeted mutagenesis of a gene encoding a non-DNA binding subunit of the transcription factor, polyomavirus enhancer binding protein 2/core binding factor. *Proc National Acad Sci* 94: 5697–5702
- Nimmerjahn F & Ravetch JV (2006) Fcγ Receptors: Old Friends and New Family Members. *Immunity* 24: 19–28
- Nimmerjahn F & Ravetch JV (2008) Fcγ receptors as regulators of immune responses. *Nat Rev Immunol* 8: 34–47
- Nishida J, Miyazono K & Ehata S (2018) Decreased TGFBR3/betaglycan expression enhances the metastatic abilities of renal cell carcinoma cells through TGF-β-dependent and -independent mechanisms. *Oncogene* 37: 2197–2212
- Nishikawa SI, Nishikawa S, Hirashima M, Matsuyoshi N & Kodama H (1998a) Progressive lineage analysis by cell sorting and culture identifies FLK1+VE-cadherin+ cells at a diverging point of endothelial and hemopoietic lineages. *Dev Camb Engl* 125: 1747–57
- Nishikawa S-I, Nishikawa S, Kawamoto H, Yoshida H, Kizumoto M, Kataoka H & Katsura Y (1998b) In Vitro Generation of Lymphohematopoietic Cells from Endothelial Cells Purified from Murine Embryos. *Immunity* 8: 761–769

- North T, Gu TL, Stacy T, Wang Q, Howard L, Binder M, Marín-Padilla M & Speck NA (1999) *Cbfa2* is required for the formation of intra-aortic hematopoietic clusters. *Dev Camb Engl* 126: 2563–75
- North TE, Bruijn MFTR de, Stacy T, Talebian L, Lind E, Robin C, Binder M, Dzierzak E & Speck NA (2002) *Runx1* Expression Marks Long-Term Repopulating Hematopoietic Stem Cells in the Midgestation Mouse Embryo. *Immunity* 16: 661–672
- North TE, Goessling W, Peeters M, Li P, Ceol C, Lord AM, Weber GJ, Harris J, Cutting CC, Huang P, *et al* (2009) Hematopoietic Stem Cell Development Is Dependent on Blood Flow. *Cell* 137: 736–748
- Nostro MC, Cheng X, Keller GM & Gadue P (2008) Wnt, Activin, and BMP Signaling Regulate Distinct Stages in the Developmental Pathway from Embryonic Stem Cells to Blood. *Cell Stem Cell* 2: 60–71
- Nottingham WT, Jarratt A, Burgess M, Speck CL, Cheng J-F, Prabhakar S, Rubin EM, Li P-S, Sloane-Stanley J, Kong-a-San J, *et al* (2007) *Runx1*-mediated hematopoietic stem-cell emergence is controlled by a *Gata/Ets/SCL*-regulated enhancer. *Blood* 110: 4188–4197
- Nüsslein-Volhard C & Wieschaus E (1980) Mutations affecting segment number and polarity in *Drosophila*. *Nature* 287: 795–801
- Oatley M, Bölükbası ÖV, Svensson V, Shvartsman M, Ganter K, Zirngibl K, Pavlovich PV, Milchevskaya V, Foteva V, Natarajan KN, *et al* (2020) Single-cell transcriptomics identifies CD44 as a marker and regulator of endothelial to haematopoietic transition. *Nat Commun* 11: 586
- Oberlin E, Tavian M, Blazsek I & Péault B (2002) Blood-forming potential of vascular endothelium in the human embryo. *Dev Camb Engl* 129: 4147–57
- Ogawa E, Inuzuka M, Maruyama M, Satake M, Naito-Fujimoto M, Ito Y & Shigesada K (1993) Molecular Cloning and Characterization of PEBP2 β , the Heterodimeric Partner of a Novel *Drosophila runt*-Related DNA Binding Protein PEBP2 α . *Virology* 194: 314–331
- Ogilvy S, Metcalf D, Gibson L, Bath ML, Harris AW & Adams JM (1999) Promoter elements of *vav* drive transgene expression in vivo throughout the hematopoietic compartment. *Blood* 94: 1855–63
- Okochi M, Steiner H, Fukumori A, Tanii H, Tomita T, Tanaka T, Iwatsubo T, Kudo T, Takeda M & Haass C (2002) Presenilins mediate a dual intramembranous γ -secretase cleavage of Notch-1. *Embo J* 21: 5408–5416
- Okuda T, Deursen J van, Hiebert SW, Grosveld G & Downing JR (1996) AML1, the Target of Multiple Chromosomal Translocations in Human Leukemia, Is Essential for Normal Fetal Liver Hematopoiesis. *Cell* 84: 321–330
- Org T, Duan D, Ferrari R, Montel-Hagen A, Handel BV, Kerényi MA, Sasidharan R, Rubbi L, Fujiwara Y, Pellegrini M, *et al* (2015) *Scl* binds to primed enhancers in

mesoderm to regulate hematopoietic and cardiac fate divergence. *Embo J* 34: 759–777

Osawa M, Hanada K, Hamada H & Nakauchi H (1996) Long-Term Lymphohematopoietic Reconstitution by a Single CD34-Low/Negative Hematopoietic Stem Cell. *Science* 273: 242–245

Ottersbach K & Dzierzak E (2005) The Murine Placenta Contains Hematopoietic Stem Cells within the Vascular Labyrinth Region. *Dev Cell* 8: 377–387

Ozato K, Wan YJ & Orrison BM (1985) Mouse major histocompatibility class I gene expression begins at midsomite stage and is inducible in earlier-stage embryos by interferon. *Proc National Acad Sci* 82: 2427–2431

Padrón-Barthe L, Temiño S, Campo CV del, Carramolino L, Isern J & Torres M (2014) Clonal analysis identifies hemogenic endothelium as the source of the blood-endothelial common lineage in the mouse embryo. *Blood* 124: 2523–2532

Paik EJ & Zon LI (2010) Hematopoietic development in the zebrafish. *Int J Dev Biol* 54: 1127–1137

Palis J (2014) Primitive and definitive erythropoiesis in mammals. *Front Physiol* 5: 3

Palis J (2017) Interaction of the Macrophage and Primitive Erythroid Lineages in the Mammalian Embryo. *Front Immunol* 7: 669

Palis J, Chan RJ, Koniski A, Patel R, Starr M & Yoder MC (2001) Spatial and temporal emergence of high proliferative potential hematopoietic precursors during murine embryogenesis. *Proc National Acad Sci* 98: 4528–4533

Palis J, McGrath KE & Kingsley PD (1995) Initiation of hematopoiesis and vasculogenesis in murine yolk sac explants. *Blood* 86: 156–63

Palis J, Robertson S, Kennedy M, Wall C & Keller G (1999) Development of erythroid and myeloid progenitors in the yolk sac and embryo proper of the mouse. *Dev Camb Engl* 126: 5073–84

Parr RL, Fung L, Reneker J, Myers-Mason N, Leibowitz JL & Levy G (1995) Association of mouse fibrinogen-like protein with murine hepatitis virus-induced prothrombinase activity. *J Virol* 69: 5033–5038

Pater E de, Kaimakis P, Vink CS, Yokomizo T, Yamada-Inagawa T, Linden R van der, Kartalaei PS, Camper SA, Speck N & Dzierzak E (2013) Gata2 is required for HSC generation and survival. *J Exp Med* 210: 2843–2850

Peeters M, Ling K-W, Oziemlak A, Robin C & Dzierzak E (2005) Multipotential hematopoietic progenitor cells from embryos developed in vitro engraft unconditioned W41/W41 neonatal mice. *Haematologica* 90: 734–9

Pick M, Azzola L, Mossman A, Stanley EG & Elefanty AG (2007) Differentiation of Human Embryonic Stem Cells in Serum-Free Medium Reveals Distinct Roles for Bone Morphogenetic Protein 4, Vascular Endothelial Growth Factor, Stem Cell

- Factor, and Fibroblast Growth Factor 2 in Hematopoiesis. *Stem Cells* 25: 2206–2214
- Pijuan-Sala B, Griffiths JA, Guibentif C, Hiscock TW, Jawaid W, Calero-Nieto FJ, Mulas C, Ibarra-Soria X, Tyser RCV, Ho DLL, *et al* (2019) A single-cell molecular map of mouse gastrulation and early organogenesis. *Nature* 566: 490–495
- Pimanda JE, Ottersbach K, Knezevic K, Kinston S, Chan WYI, Wilson NK, Landry J-R, Wood AD, Kolb-Kokocinski A, Green AR, *et al* (2007) Gata2, Fli1, and Scl form a recursively wired gene-regulatory circuit during early hematopoietic development. *Proc National Acad Sci* 104: 17692–17697
- Porcher C, Swat W, Rockwell K, Fujiwara Y, Alt FW & Orkin SH (1996) The T Cell Leukemia Oncoprotein SCL/tal-1 Is Essential for Development of All Hematopoietic Lineages. *Cell* 86: 47–57
- Porcheri C, Golan O, Calero-Nieto FJ, Thambyrajah R, Ruiz-Herguido C, Wang X, Catto F, Guillén Y, Sinha R, González J, *et al* (2020) Notch ligand Dll4 impairs cell recruitment to aortic clusters and limits blood stem cell generation. *Embo J* 39: e104270
- Potts KS, Sargeant TJ, Markham JF, Shi W, Biben C, Josefsson EC, Whitehead LW, Rogers KL, Liakhovitskaia A, Smyth GK, *et al* (2014) A lineage of diploid platelet-forming cells precedes polyploid megakaryocyte formation in the mouse embryo. *Blood* 124: 2725–2729
- Pozner A, Goldenberg D, Negreanu V, Le S-Y, Elroy-Stein O, Levanon D & Groner Y (2000) Transcription-Coupled Translation Control of AML1/RUNX1 Is Mediated by Cap- and Internal Ribosome Entry Site-Dependent Mechanisms. *Mol Cell Biol* 20: 2297–2307
- Qiu WQ, Bruin D de, Brownstein BH, Pearse R & Ravetch JV (1990) Organization of the Human and Mouse Low-affinity FcγR Genes: Duplication and Recombination. *Science* 248: 732–735
- Ramsland PA, Farrugia W, Bradford TM, Sardjono CT, Esparon S, Trist HM, Powell MS, Tan PS, Cendron AC, Wines BD, *et al* (2011) Structural Basis for FcγRIIa Recognition of Human IgG and Formation of Inflammatory Signaling Complexes. *J Immunol* 187: 3208–3217
- Ravetch JV & Lanier LL (2000) Immune Inhibitory Receptors. *Science* 290: 84–89
- Rees HA & Liu DR (2018) Base editing: precision chemistry on the genome and transcriptome of living cells. *Nat Rev Genet* 19: 770–788
- Rhodes KE, Gekas C, Wang Y, Lux CT, Francis CS, Chan DN, Conway S, Orkin SH, Yoder MC & Mikkola HKA (2008) The Emergence of Hematopoietic Stem Cells Is Initiated in the Placental Vasculature in the Absence of Circulation. *Cell Stem Cell* 2: 252–263
- Robb L, Lyons I, Li R, Hartley L, Köntgen F, Harvey RP, Metcalf D & Begley CG (1995) Absence of yolk sac hematopoiesis from mice with a targeted disruption of the scl gene. *Proc National Acad Sci* 92: 7075–7079

- Robert-Moreno A, Espinosa L, Pompa JL de la & Bigas A (2005) RBPjk-dependent Notch function regulates Gata2 and is essential for the formation of intra-embryonic hematopoietic cells. *Development* 132: 1117–1126
- Robert-Moreno À, Guiu J, Ruiz-Herguido C, López ME, Inglés-Esteve J, Riera L, Tipping A, Enver T, Dzierzak E, Gridley T, *et al* (2008) Impaired embryonic haematopoiesis yet normal arterial development in the absence of the Notch ligand Jagged1. *Embo J* 27: 1886–1895
- Rönn RE, Guibentif C, Moraghebi R, Chaves P, Saxena S, Garcia B & Woods N-B (2015) Retinoic Acid Regulates Hematopoietic Development from Human Pluripotent Stem Cells. *Stem Cell Rep* 4: 269–281
- Rüegg C & Pytela R (1995) Sequence of a human transcript expressed in T-lymphocytes and encoding a fibrinogen-like protein. *Gene* 160: 257–262
- Rybtsov S, Batsivari A, Bilotkach K, Paruzina D, Senserrich J, Nerushev O & Medvinsky A (2014) Tracing the Origin of the HSC Hierarchy Reveals an SCF-Dependent, IL-3-Independent CD43– Embryonic Precursor. *Stem Cell Rep* 3: 489–501
- Rybtsov S, Ivanovs A, Zhao S & Medvinsky A (2016) Concealed expansion of immature precursors underpins acute burst of adult HSC activity in foetal liver. *Development* 143: 1284–1289
- Rybtsov S, Sobiesiak M, Taoudi S, Souilhol C, Senserrich J, Liakhovitskaia A, Ivanovs A, Frampton J, Zhao S & Medvinsky A (2011) Hierarchical organization and early hematopoietic specification of the developing HSC lineage in the AGM region. *J Exp Med* 208: 1305–1315
- Rychlik DF, Chien EK, Wolff D, Phillippe S & Phillippe M (2003) Cloning and Tissue expression of the Tissue Prothrombinase Fgl-2 in the Sprague-Dawley Rat. *J Soc Gynecol Investigation Jsgj* 10: 67–73
- Sabin FR (2002) Preliminary Note on the Differentiation of Angioblasts and the Method by Which They Produce Blood-Vessels, Blood-Plasma and Red Blood-Cells As Seen in the Living Chick. *J Hematoth Stem Cell* 11: 5–7
- Sadler & Langman TW& (2004) J. Langman’s Medical Embryology.
- Sánchez M-J, Holmes A, Miles C & Dzierzak E (1996) Characterization of the First Definitive Hematopoietic Stem Cells in the AGM and Liver of the Mouse Embryo. *Immunity* 5: 513–525
- Sandell LL, Sanderson BW, Moiseyev G, Johnson T, Mushegian A, Young K, Rey J-P, Ma J, Staehling-Hampton K & Trainor PA (2007) RDH10 is essential for synthesis of embryonic retinoic acid and is required for limb, craniofacial, and organ development. *Gene Dev* 21: 1113–1124
- Sandrock I, Reinhardt A, Ravens S, Binz C, Wilharm A, Martins J, Oberdörfer L, Tan L, Lienenklaus S, Zhang B, *et al* (2018) Genetic models reveal origin, persistence and non-redundant functions of IL-17-producing $\gamma\delta$ T cells. *J Exp Medicine* 215: 3006–3018

- Sasaki K & Matsumura G (1986) Haemopoietic cells of yolk sac and liver in the mouse embryo: a light and electron microscopical study. *J Anat* 148: 87–97
- Sasaki K, Yagi H, Bronson RT, Tominaga K, Matsunashi T, Deguchi K, Tani Y, Kishimoto T & Komori T (1996) Absence of fetal liver hematopoiesis in mice deficient in transcriptional coactivator core binding factor beta. *Proc National Acad Sci* 93: 12359–12363
- Sato K & Ochi A (1998) Superclustering of B cell receptor and Fc gamma RIIB1 activates Src homology 2-containing protein tyrosine phosphatase-1. *J Immunol Baltim Md 1950* 161: 2716–22
- Sawamiphak S, Kontarakis Z & Stainier DYR (2014) Interferon Gamma Signaling Positively Regulates Hematopoietic Stem Cell Emergence. *Dev Cell* 31: 640–653
- Schier AF & Shen MM (2000) Nodal signalling in vertebrate development. *Nature* 403: 385–389
- Schlaeger TM, Mikkola HKA, Gekas C, Helgadottir HB & Orkin SH (2005) Tie2Cre-mediated gene ablation defines the stem-cell leukemia gene (SCL/tal1)-dependent window during hematopoietic stem-cell development. *Blood* 105: 3871–3874
- Schmitt TM, Pooter RF de, Gronski MA, Cho SK, Ohashi PS & Zúñiga-Pflücker JC (2004) Induction of T cell development and establishment of T cell competence from embryonic stem cells differentiated in vitro. *Nat Immunol* 5: 410–417
- Schroeter EH, Kisslinger JA & Kopan R (1998) Notch-1 signalling requires ligand-induced proteolytic release of intracellular domain. *Nature* 393: 382–386
- Serrano AG, Gandillet A, Pearson S, Lacaud G & Kouskoff V (2010) Contrasting effects of Sox17- and Sox18-sustained expression at the onset of blood specification. *Blood* 115: 3895–3898
- Shalev I, Liu H, Kosciak C, Bartczak A, Javadi M, Wong KM, Maknoja A, He W, Liu MF, Diao J, *et al* (2008) Targeted Deletion of fgl2 Leads to Impaired Regulatory T Cell Activity and Development of Autoimmune Glomerulonephritis. *J Immunol* 180: 249–260
- Shushakova N, Skokowa J, Schulman J, Baumann U, Zwirner J, Schmidt RE & Gessner JE (2002) C5a anaphylatoxin is a major regulator of activating versus inhibitory FcγRs in immune complex-induced lung disease. *J Clin Invest* 110: 1823–1830
- Simic M, Manosalva I, Spinelli L, Gentek R, Shayan RR, Siret C, Girard-Madoux M, Wang S, Fabritus L de, Verschoor J, *et al* (2020) Distinct Waves from the Hemogenic Endothelium Give Rise to Layered Lymphoid Tissue Inducer Cell Ontogeny. *Cell Reports* 32: 108004
- Siminovitch L, McCulloch EA & Till JE (1963) The distribution of colony-forming cells among spleen colonies. *J Cell Compar Physl* 62: 327–336
- Simones T & Shepherd DM (2011) Consequences of AhR Activation in Steady-State Dendritic Cells. *Toxicol Sci* 119: 293–307

- Sinka L, Biasch K, Khazaal I, Péault B & Tavian M (2012) Angiotensin-converting enzyme (CD143) specifies emerging lympho-hematopoietic progenitors in the human embryo. *Blood* 119: 3712–3723
- Soriano P (1999) Generalized lacZ expression with the ROSA26 Cre reporter strain. *Nat Genet* 21: 70–71
- Spangrude GJ, Heimfeld S & Weissman IL (1988) Purification and Characterization of Mouse Hematopoietic Stem Cells. *Science* 241: 58–62
- Spyropoulos DD, Pharr PN, Lavenburg KR, Jackers P, Papas TS, Ogawa M & Watson DK (2000) Hemorrhage, Impaired Hematopoiesis, and Lethality in Mouse Embryos Carrying a Targeted Disruption of the Fli1 Transcription Factor †. *Mol Cell Biol* 20: 5643–5652
- Squarzoni P, Oller G, Hoeffel G, Pont-Lezica L, Rostaing P, Low D, Bessis A, Ginhoux F & Garel S (2014) Microglia Modulate Wiring of the Embryonic Forebrain. *Cell Reports* 8: 1271–1279
- Sroczyńska P, Lancrin C, Kouskoff V & Lacaud G (2009) The differential activities of Runx1 promoters define milestones during embryonic hematopoiesis. *Blood* 114: 5279–5289
- Stadtfeld M & Graf T (2004) Assessing the role of hematopoietic plasticity for endothelial and hepatocyte development by non-invasive lineage tracing. *Development* 132: 203–213
- Strauss O, Phillips A, Ruggiero K, Bartlett A & Dunbar PR (2017) Immunofluorescence identifies distinct subsets of endothelial cells in the human liver. *Sci Rep-uk* 7: 44356
- Struhl G & Adachi A (1998) Nuclear Access and Action of Notch In Vivo. *Cell* 93: 649–660
- Stuart T, Butler A, Hoffman P, Hafemeister C, Papalexi E, Mauck WM, Hao Y, Stoeckius M, Smibert P & Satija R (2019) Comprehensive Integration of Single-Cell Data. *Cell* 177: 1888-1902.e21
- Sturgeon CM, Ditadi A, Awong G, Kennedy M & Keller G (2014) Wnt signaling controls the specification of definitive and primitive hematopoiesis from human pluripotent stem cells. *Nat Biotechnol* 32: 554–561
- Su K, Yang H, Li X, Li X, Gibson AW, Cafardi JM, Zhou T, Edberg JC & Kimberly RP (2007) Expression Profile of FcγRIIb on Leukocytes and Its Dysregulation in Systemic Lupus Erythematosus. *J Immunol* 178: 3272–3280
- Suchting S, Freitas C, Noble F le, Benedito R, Bréant C, Duarte A & Eichmann A (2007) The Notch ligand Delta-like 4 negatively regulates endothelial tip cell formation and vessel branching. *Proc National Acad Sci* 104: 3225–3230
- Sugimura R, Jha DK, Han A, Soria-Valles C, Rocha EL da, Lu Y-F, Goettel JA, Serrao E, Rowe RG, Malleshaiah M, et al (2017) Haematopoietic stem and progenitor cells from human pluripotent stem cells. *Nature* 545: 432–438

- Sugiyama D, Ogawa M, Hirose I, Jaffredo T, Arai K & Tsuji K (2003) Erythropoiesis from acetyl LDL incorporating endothelial cells at the pre-liver stage. *Blood* 101: 4733–4738
- Swiers G, Baumann C, O'Rourke J, Giannoulatou E, Taylor S, Joshi A, Moignard V, Pina C, Bee T, Kokkaliaris KD, *et al* (2013) Early dynamic fate changes in haemogenic endothelium characterized at the single-cell level. *Nat Commun* 4: 2924
- Szilvassy SJ, Humphries RK, Lansdorp PM, Eaves AC & Eaves CJ (1990) Quantitative assay for totipotent reconstituting hematopoietic stem cells by a competitive repopulation strategy. *Proc National Acad Sci* 87: 8736–8740
- Takahashi K, Yamamura F & Naito M (1989) Differentiation, Maturation, and Proliferation of Macrophages in the Mouse Yolk Sac: A Light-Microscopic, Enzyme-Cytochemical, Immunohistochemical, and Ultrastructural Study. *J Leukocyte Biol* 45: 87–96
- Takizawa T, Anderson CL & Robinson JM (2005) A Novel FcγR-Defined, IgG-Containing Organelle in Placental Endothelium. *J Immunol* 175: 2331–2339
- Tammela T, Zarkada G, Wallgard E, Murtomäki A, Suchting S, Wirzenius M, Waltari M, Hellström M, Schomber T, Peltonen R, *et al* (2008) Blocking VEGFR-3 suppresses angiogenic sprouting and vascular network formation. *Nature* 454: 656–660
- Taoudi S, Gonneau C, Moore K, Sheridan JM, Blackburn CC, Taylor E & Medvinsky A (2008) Extensive Hematopoietic Stem Cell Generation in the AGM Region via Maturation of VE-Cadherin+CD45+ Pre-Definitive HSCs. *Cell Stem Cell* 3: 99–108
- Taoudi S & Medvinsky A (2007) Functional identification of the hematopoietic stem cell niche in the ventral domain of the embryonic dorsal aorta. *Proc National Acad Sci* 104: 9399–9403
- Taoudi S, Morrison AM, Inoue H, Gribi R, Ure J & Medvinsky A (2005) Progressive divergence of definitive haematopoietic stem cells from the endothelial compartment does not depend on contact with the foetal liver. *Development* 132: 4179–4191
- Tavian M, Baron MH & Péault B (2004) Developmental Hematopoiesis, Methods and Protocols. *Methods Mol Medicine* 105: 413–424
- Tavian M, Coulombel L, Luton D, Clemente HS, Dieterlen-Lièvre F & Péault B (1996) Aorta-associated CD34+ hematopoietic cells in the early human embryo. *Blood* 87: 67–72
- Tavian M, Hallais MF & Péault B (1999) Emergence of intraembryonic hematopoietic precursors in the pre-liver human embryo. *Dev Camb Engl* 126: 793–803
- Tavian M, Robin C, Coulombel L & Péault B (2001) The Human Embryo, but Not Its Yolk Sac, Generates Lympho-Myeloid Stem Cells. *Immunity* 15: 487–495

- Telfer JC & Rothenberg EV (2001) Expression and Function of a Stem Cell Promoter for the Murine CBFa2 Gene: Distinct Roles and Regulation in Natural Killer and T Cell Development. *Dev Biol* 229: 363–382
- Tian Y, Xu J, Feng S, He S, Zhao S, Zhu L, Jin W, Dai Y, Luo L, Qu JY, *et al* (2017) The first wave of T lymphopoiesis in zebrafish arises from aorta endothelium independent of hematopoietic stem cells. *J Exp Med* 214: 3347–3360
- Tie R, Li H, Cai S, Liang Z, Shan W, Wang B, Tan Y, Zheng W & Huang H (2019) Interleukin-6 signaling regulates hematopoietic stem cell emergence. *Exp Mol Medicine* 51: 1–12
- Timmerman LA, Grego-Bessa J, Raya A, Bertrán E, Pérez-Pomares JM, Díez J, Aranda S, Palomo S, McCormick F, Izpisua-Belmonte JC, *et al* (2004) Notch promotes epithelial-mesenchymal transition during cardiac development and oncogenic transformation. *Gene Dev* 18: 99–115
- Tober J, Koniski A, McGrath KE, Vemishetti R, Emerson R, Mesy-Bentley KKL de, Waugh R & Palis J (2006) The megakaryocyte lineage originates from hemangioblast precursors and is an integral component both of primitive and of definitive hematopoiesis. *Blood* 109: 1433–1441
- Tober J, McGrath KE & Palis J (2008) Primitive erythropoiesis and megakaryopoiesis in the yolk sac are independent of c-myb. *Blood* 111: 2636–2639
- Tober J, Yzaguirre AD, Piwarzyk E & Speck NA (2013) Distinct temporal requirements for Runx1 in hematopoietic progenitors and stem cells. *Development* 140: 3765–3776
- Tsai F-Y, Keller G, Kuo FC, Weiss M, Chen J, Rosenblatt M, Alt FW & Orkin SH (1994) An early haematopoietic defect in mice lacking the transcription factor GATA-2. *Nature* 371: 221–226
- Tsuji K & Noda M (2000) Identification and Expression of a Novel 3'-Exon of Mouse Runx1/Pebp2aB/Cbfa2/AML1 Gene. *Biochem Bioph Res Co* 274: 171–176
- Turpen JB, Knudson CM & Hoefen PS (1981) The early ontogeny of hematopoietic cells studied by grafting cytogenetically labeled tissue anlagen: Localization of a prospective stem cell compartment. *Dev Biol* 85: 99–112
- Tyser RCV, Mahammadov E, Nakanoh S, Vallier L, Scialdone A & Srinivas S (2021) Single-cell transcriptomic characterization of a gastrulating human embryo. *Nature* 600: 285–289
- Uenishi GI, Jung HS, Kumar A, Park MA, Hadland BK, McLeod E, Raymond M, Moskvin O, Zimmerman CE, Theisen DJ, *et al* (2018) NOTCH signaling specifies arterial-type definitive hemogenic endothelium from human pluripotent stem cells. *Nat Commun* 9: 1828
- Ueno H & Weissman IL (2006) Clonal Analysis of Mouse Development Reveals a Polyclonal Origin for Yolk Sac Blood Islands. *Dev Cell* 11: 519–533

- Urness LD, Sorensen LK & Li DY (2000) Arteriovenous malformations in mice lacking activin receptor-like kinase-1. *Nat Genet* 26: 328–331
- Van Handel B, Montel-Hagen A, Sasidharan R, Nakano H, Ferrari R, Boogerd CJ, Schredelseker J, Wang Y, Hunter S, Org T, *et al* (2012) Scl Represses Cardiomyogenesis in Prospective Hemogenic Endothelium and Endocardium. *Cell* 150: 590–605
- Velde AA te, Malefijt R de W, Huijbens RJ, Vries JE de & Figdor CG (1992) IL-10 stimulates monocyte Fc gamma R surface expression and cytotoxic activity. Distinct regulation of antibody-dependent cellular cytotoxicity by IFN-gamma, IL-4, and IL-10. *J Immunol Baltim Md 1950* 149: 4048–52
- Veri M, Gorlatov S, Li H, Burke S, Johnson S, Stavenhagen J, Stein KE, Bonvini E & Koenig S (2007) Monoclonal antibodies capable of discriminating the human inhibitory Fcγ-receptor IIB (CD32B) from the activating Fcγ-receptor IIA (CD32A): biochemical, biological and functional characterization. *Immunology* 121: 392–404
- Vogeli KM, Jin S-W, Martin GR & Stainier DYR (2006) A common progenitor for haematopoietic and endothelial lineages in the zebrafish gastrula. *Nature* 443: 337–339
- Wakimoto K, Yanaka K, Kuro-o M, Yao A, Iwamoto T, Yanaka N, Kita S, Nishida A, Azuma S, Toyoda Y, *et al* (2000) Targeted disruption of Na⁺/Ca²⁺ exchanger gene leads to cardiomyocyte apoptosis and defects in heart beat. *J Biol Chem* 275: 36991–36998
- Walmsley M, Ciau-Uitz A & Patient R (2002) Adult and embryonic blood and endothelium derive from distinct precursor populations which are differentially programmed by BMP in *Xenopus*. *Development* 129: 5683–5695
- Wang Q, Stacy T, Binder M, Marin-Padilla M, Sharpe AH & Speck NA (1996a) Disruption of the Cbfa2 gene causes necrosis and hemorrhaging in the central nervous system and blocks definitive hematopoiesis. *Proc National Acad Sci* 93: 3444–3449
- Wang Q, Stacy T, Miller JD, Lewis AF, Gu T-L, Huang X, Bushweller JH, Bories J-C, Alt FW, Ryan G, *et al* (1996b) The CBFβ Subunit Is Essential for CBFα2 (AML1) Function In Vivo. *Cell* 87: 697–708
- Wang S, Wang Q, Crute BE, Melnikova IN, Keller SR & Speck NA (1993) Cloning and characterization of subunits of the T-cell receptor and murine leukemia virus enhancer core-binding factor. *Mol Cell Biol* 13: 3324–3339
- Wang X, Sperkova Z & Napoli JL (2001) Analysis of Mouse Retinal Dehydrogenase Type 2 Promoter and Expression. *Genomics* 74: 245–250
- Wang Y & Nakayama N (2009) WNT and BMP signaling are both required for hematopoietic cell development from human ES cells. *Stem Cell Res* 3: 113–125
- Watt SM, Butler LH, Tavian M, Bühring HJ, Rappold I, Simmons PJ, Zannettino AC, Buck D, Fuchs A, Doyonnas R, *et al* (2000) Functionally defined CD164 epitopes

are expressed on CD34(+) cells throughout ontogeny but display distinct distribution patterns in adult hematopoietic and nonhematopoietic tissues. *Blood* 95: 3113–24

- White RJ, Nie Q, Lander AD & Schilling TF (2007) Complex Regulation of *cyp26a1* Creates a Robust Retinoic Acid Gradient in the Zebrafish Embryo. *Plos Biol* 5: e304
- Williams CK, Segarra M, Sierra MDLL, Sainson RCA, Tosato G & Harris AL (2008) Regulation of CXCR4 by the Notch Ligand Delta-like 4 in Endothelial Cells. *Cancer Res* 68: 1889–1895
- Willison K (1990) The mouse Brachyury gene and mesoderm formation. *Trends Genet* 6: 104–106
- Wilson A, Laurenti E, Oser G, Wath RC van der, Blanco-Bose W, Jaworski M, Offner S, Dunant CF, Eshkind L, Bockamp E, *et al* (2008) Hematopoietic Stem Cells Reversibly Switch from Dormancy to Self-Renewal during Homeostasis and Repair. *Cell* 135: 1118–1129
- Wingert RA, Selleck R, Yu J, Song H-D, Chen Z, Song A, Zhou Y, Thisse B, Thisse C, McMahon AP, *et al* (2007) The *cdx* Genes and Retinoic Acid Control the Positioning and Segmentation of the Zebrafish Pronephros. *Plos Genet* 3: e189
- Wood HB, May G, Healy L, Enver T & Morriss-Kay GM (1997) CD34 expression patterns during early mouse development are related to modes of blood vessel formation and reveal additional sites of hematopoiesis. *Blood* 90: 2300–11
- Wu L, Aster JC, Blacklow SC, Lake R, Artavanis-Tsakonas S & Griffin JD (2000) MAML1, a human homologue of *Drosophila* Mastermind, is a transcriptional co-activator for NOTCH receptors. *Nat Genet* 26: 484–489
- Wu T, Hu E, Xu S, Chen M, Guo P, Dai Z, Feng T, Zhou L, Tang W, Zhan L, *et al* (2021) clusterProfiler 4.0: A universal enrichment tool for interpreting omics data. *Innovation* 2: 100141
- Xie J, Wang W, Si J-W, Miao X-Y, Li J-C, Wang Y-C, Wang Z-R, Ma J, Zhao X-C, Li Z, *et al* (2013) Notch signaling regulates CXCR4 expression and the migration of mesenchymal stem cells. *Cell Immunol* 281: 68–75
- Xue Y, Gao X, Lindsell CE, Norton CR, Chang B, Hicks C, Gendron-Maguire M, Rand EB, Weinmaster G & Gridley T (1999a) Embryonic Lethality and Vascular Defects in Mice Lacking the Notch Ligand Jagged1. *Hum Mol Genet* 8: 723–730
- Xue Y, Gao X, Lindsell CE, Norton CR, Chang B, Hicks C, Gendron-Maguire M, Rand EB, Weinmaster G & Gridley T (1999b) Embryonic Lethality and Vascular Defects in Mice Lacking the Notch Ligand Jagged1. *Hum Mol Genet* 8: 723–730
- Yamada Y, Pannell R, Forster A & Rabbitts TH (2000) The oncogenic LIM-only transcription factor Lmo2 regulates angiogenesis but not vasculogenesis in mice. *Proc National Acad Sci* 97: 320–324

- Yamaguchi TP, Dumont DJ, Conlon RA, Breitman ML & Rossant J (1993) flk-1, an flt-related receptor tyrosine kinase is an early marker for endothelial cell precursors. *Dev Camb Engl* 118: 489–98
- Yamamizu K, Matsunaga T, Uosaki H, Fukushima H, Katayama S, Hiraoka-Kanie M, Mitani K & Yamashita JK (2013) Convergence of Notch and β -catenin signaling induces arterial fate in vascular progenitors. *J Cell Biology* 202: 179–179
- Yang C, Chen Y, Guo G, Li H, Cao D, Xu H, Guo S, Fei L, Yan W, Ning Q, *et al* (2013) Expression of B and T lymphocyte attenuator (BTLA) in macrophages contributes to the fulminant hepatitis caused by murine hepatitis virus strain-3. *Gut* 62: 1204
- Yatim A, Benne C, Sobhian B, Laurent-Chabalier S, Deas O, Judde J-G, Lelievre J-D, Levy Y & Benkirane M (2012) NOTCH1 Nuclear Interactome Reveals Key Regulators of Its Transcriptional Activity and Oncogenic Function. *Mol Cell* 48: 445–458
- Yoder MC & Hiatt K (1997) Engraftment of Embryonic Hematopoietic Cells in Conditioned Newborn Recipients. *Blood* 89: 2176–2183
- Yoder MC, Hiatt K, Dutt P, Mukherjee P, Bodine DM & Orlic D (1997) Characterization of Definitive Lymphohematopoietic Stem Cells in the Day 9 Murine Yolk Sac. *Immunity* 7: 335–344
- Yokomizo T & Dzierzak E (2010) Three-dimensional cartography of hematopoietic clusters in the vasculature of whole mouse embryos. *Development* 137: 3651–3661
- Yokomizo T, Hasegawa K, Ishitobi H, Osato M, Ema M, Ito Y, Yamamoto M & Takahashi S (2008) Runx1 is involved in primitive erythropoiesis in the mouse. *Blood* 111: 4075–4080
- Yokomizo T, Ogawa M, Osato M, Kanno T, Yoshida H, Fujimoto T, Fraser S, Nishikawa S, Okada H, Satake M, *et al* (2001) Requirement of Runx1/AML1/PEBP2 α B for the generation of haematopoietic cells from endothelial cells. *Genes Cells* 6: 13–23
- Yoshida H, Hayashi S-I, Kunisada T, Ogawa M, Nishikawa S, Okamura H, Sudo T, Shultz LD & Nishikawa S-I (1990) The murine mutation osteopetrosis is in the coding region of the macrophage colony stimulating factor gene. *Nature* 345: 442–444
- Yoshimoto M, Montecino-Rodriguez E, Ferkowicz MJ, Porayette P, Shelley WC, Conway SJ, Dorshkind K & Yoder MC (2011) Embryonic day 9 yolk sac and intra-embryonic hemogenic endothelium independently generate a B-1 and marginal zone progenitor lacking B-2 potential. *P Natl Acad Sci Usa* 108: 1468–73
- Yoshimoto M, Porayette P, Glosson NL, Conway SJ, Carlesso N, Cardoso AA, Kaplan MH & Yoder MC (2012) Autonomous murine T-cell progenitor production in the extra-embryonic yolk sac before HSC emergence. *Blood* 119: 5706–14
- Yu C, Liu Y, Miao Z, Yin M, Lu W, Lv Y, Ding M & Deng H (2010) Retinoic acid enhances the generation of hematopoietic progenitors from human embryonic stem cell-derived hemato-vascular precursors. *Blood* 116: 4786–4794

- Yu P, Pan G, Yu J & Thomson JA (2011) FGF2 Sustains NANOG and Switches the Outcome of BMP4-Induced Human Embryonic Stem Cell Differentiation. *Cell Stem Cell* 8: 326–334
- Yuwaraj S, Ding J, Liu M, Marsden PA & Levy GA (2001) Genomic Characterization, Localization, and Functional Expression of FGL2, the Human Gene Encoding Fibroleukin: A Novel Human Procoagulant. *Genomics* 71: 330–338
- Zeng Y, He J, Bai Z, Li Z, Gong Y, Liu C, Ni Y, Du J, Ma C, Bian L, *et al* (2019) Tracing the first hematopoietic stem cell generation in human embryo by single-cell RNA sequencing. *Cell Res* 29: 881–894
- Zhong TP, Childs S, Leu JP & Fishman MC (2001) Gridlock signalling pathway fashions the first embryonic artery. *Nature* 414: 216–220
- Zhou F, Li X, Wang W, Zhu P, Zhou J, He W, Ding M, Xiong F, Zheng X, Li Z, *et al* (2016) Tracing haematopoietic stem cell formation at single-cell resolution. *Nature* 533: 487–492
- Zhu Q, Gao P, Tober J, Bennett L, Chen C, Uzun Y, Li Y, Howell ED, Mumau M, Yu W, *et al* (2020) Developmental trajectory of prehematopoietic stem cell formation from endothelium. *Blood* 136: 845–856
- Zovein AC, Hofmann JJ, Lynch M, French WJ, Turlo KA, Yang Y, Becker MS, Zanetta L, Dejana E, Gasson JC, *et al* (2008) Fate Tracing Reveals the Endothelial Origin of Hematopoietic Stem Cells. *Cell Stem Cell* 3: 625–636